UNIVERSITY OF CALIFORNIA

SANTA CRUZ

THE APPLICATION OF TRACE METAL ISOTOPE ANALYSIS TO HOMINIDS: RECONSTRUCTING THE BEHAVIOR, DIET, AND PHYSIOLOGY OF WILD CHIMPANZEES

A dissertation submitted in partial satisfaction
of the requirements for the degree of

DOCTOR OF PHILOSOPHY

in

ANTHROPOLOGY

by

Renée Damiana Boucher

September 2024

The Dissertation of Renée Boucher
is approved:

_____
Professor Vicky M. Oelze, Chair

_____
Professor Paul L. Koch

_____
Professor Lars Fehren-Schmitz

_____
Peter Biehl
Vice Provost and Dean of Graduate Studies

Table of Contents

List of Figures

List of Tables

Abstract

Renee D. Boucher

The application of trace metal isotope analysis to hominids: Reconstructing the behavior, diet, and physiology of wild chimpanzees

Isotopes have been widely used by biological anthropologists to indicate migration, diet, trophic position, and habitat use in a variety of organisms. In biological anthropology, the analysis of strontium isotope ratios ($^{87}Sr/^{86}Sr$) are an established method to trace mobility and migration, whereas initial work on the stable isotope ratios of zinc ($\delta^{66}Zn$), iron ($\delta^{56}Fe$), and copper ($\delta^{65}Cu$) has revealed patterns related to diet, trophic position, as well as physiological differences between the sexes, respectively. These trace metals are readily analyzed in the inorganic matrix of bone and teeth, bioapatite which allows us to analyze sex-related differences in dispersal patterns, diet or trophic position, and reproductive physiology.

This dissertation focuses on chimpanzees (*Pan troglodytes*), a large bodied and highly social non-human primate, which are genetically similar to humans, but vary drastically in life history and diet, leading to population-level differences in survivorship, fertility, and health. This makes chimpanzees a highly relevant model of the last common ancestor before our split with early humans. We employ the stable isotope ratios of trace metals (Sr, Zn, Fe, Cu) to examine dispersal, origin, age, sex, and diet in wild populations of chimpanzees. Specifically, this project establishes a reference dataset to address interspecific variation in ontogeny, reproductive biology and diet during the evolutionary transition from hominins to modern humans.

Dedication

For my sister, Annalyse Therese Boucher (1991-2023).

A radiant ray of sunshine, she will always be an inspiration to me. She is a driving force, who always emphasized that no matter your disability, you can achieve anything you dream of in this world. She is a reminder of the dire need to improve present health care practices, especially in diagnosing and properly supporting women who suffer from reproductive health diseases and disorders. Women who have endometriosis have a higher likelihood of developing opioid addictions due to the lack of substantial treatment programs for chronic pain in the United States. It is imperative that we work harder to develop refined methods for addressing women's health concerns to ensure women suffering from these conditions receive the support that they need.

Acknowledgements

This dissertation is the product of many years of research, oftentimes winding and awry. The support of my amazing friends, family, colleagues, and advisers has made this journey feasible. This year has been more difficult than any other year in my life, and it is the unwavering support of friends, family and colleagues that has kept me from succumbing to darkness. Without the encouragement and progress reminders from my friends and family, this dissertation would not be possible.

I would like to thank my sisters, Stephanie and Annalyse, who have always been my strongest support system and have continually encouraged my completion of this degree. Without Stephanie's guidance, I would not have even considered pursuing a doctoral degree in the first place. I would also like to thank my perpetual life partner, Martha Ugwu, who is a queen and the first to don a ski mask and a baseball bat, going to all ends to remind me of my potential. I would especially like to thank my partner, Eric White, who always finds ways to make me feel lighter and encourages me to be better. I also thank my brother, Dr. Ethan Iverson, who has provided substantial guidance and support during this Ph.D. I would like to acknowledge my maternal grandfather, James Madar, my father, Damian Boucher, and my sister, Annalyse, because they showed me the wonders of the outdoors and the immense history that each national or state park holds, kindling my interest in archaeology, ecology, and human evolution.

I want to acknowledge my mother, Terri Madar-Jennings, who has been a constant role model. She is a pillar of strength, reminding me that one woman can

accomplish many things and that there is no limit to what you can achieve. Her unyielding positivity has kept me optimistic during graduate school, and I am always thankful for her gratitude. I am grateful that both parents have always kindled my interest in archaeology and encouraged me to pursue a doctoral degree.

I would like to thank Dr. Hylke de Jong and Dr. Erin Vogel for their continued mentorship and support of my intellectual development throughout my higher education. In particular, I would like to thank Dr. Erin Vogel for always being my mentor and by far, my strongest ally. I also thank Dr. Vicky Oelze, Dr. Paul Koch, and Dr. Lars Fehren-Schmitz for their excellent supervision, patience, support, and advice, which have contributed substantially to the completion of many grant proposals, presentations, research articles, and this hefty dissertation. Without the immense dedication of Vicky and Paul's time, all of these accomplishments would not be possible.

I want to thank Dr. Jacob Setera, Dr. Brian Dreyer, Dr. Jan Bolting, Dr. Simon Blotevogel, Dr. Marta Costas-Rodriguez, Dr. Klervia Jaouen, Dr. Linda Godfrey, and Dr. Hannah Lusk for their immense support with the analytical chemistry and mass spectrometry aspect of this project. Without their guidance, supervision, and advice, many questions would still be lingering. The many hours of conversation in the lab, on Zoom, through the interwebs, and on the telephone enriched my knowledge of method development, analytical chemistry, and mass spectrometry. With the investment from all of you, much more was able to be accomplished on this dissertation than ever imaginable.

I would like to thank Dr. Emily Schach, who has always been a supportive adviser in many of the courses that I have been a teaching assistant and is always a burst of color and light within the Anthropology Department. I would also like to thank Kirk Lange, as he has been a wealth of information during my graduate studies, often answering and addressing all of my questions regarding the logistics of graduate school, as well as providing quarterly stickers and letting me into my office when I oftentimes lock myself out. I also want to acknowledge Fred Deakin and Kayla Ott, who have also always been around the department to let me into my office when I accidentally lock myself out (or forget my work keys), and especially, Fred Deakin who has supported me during graduate school since 2019, acting as the interim Graduate Advisor. Lastly, I would like to thank Paul Sosbee, who has provided substantial technical support during my graduate studies. I am eternally grateful to all of them for their support in the pursuit of my Ph.D. in Biological Anthropology.

CHAPTER 1: Introduction

The study of human and human ancestors elucidates the lifeways of extinct species, demonstrating the wealth of information incorporated into one's bones during their life. There are many ways to analyze bone in deep time, but for the following projects, we focus on isotope analysis. Isotope analysis involves the study of two or more isotopes of a given element in the matrix of interest, here, we are focusing on bone and tooth enamel. Isotopes are versions of an element that have the same number of protons, but a different number of neutrons, which causes slight differences in mass. These differences in mass can be detected by an instrument, such as a mass spectrometer, and then their respective isotope ratios can be analyzed.

The relationship between two isotopes, or the isotope ratio, can change through a process called isotope fractionation, where the proportion of one isotope to the other changes after passing through a barrier or phase. This process is typically mass-dependent, meaning whether an isotope passes through the barrier or not is dependent on its mass. Lighter isotopes can move faster through barriers and can experience a preference by certain molecules due to a kinetic effect. On the contrary, heavy isotopes may be preferred because they have the ability to form stronger bonds, although they move slower through phases. As a result of this preference, a different isotope ratio may be observed dependent on the tissue type sampled within an individual's body. We will focus on the isotope analysis of trace metals, specifically strontium (Sr), iron (Fe), copper (Cu), and zinc (Zn).

Trace metals are elements that can be found at low levels in body tissues, and this includes transition metals, such as Fe, Cu, and Zn, which are critical in many chemical reactions in the body. The isotope ratios of Fe, Cu, and Zn are stable, meaning that isotope fractionation is caused by chemical reactions that occur within the body. Sr, on the other hand, is radiogenic and the change that is observed in the environment is caused by the radioactive decay of rubidium (Rb) in bedrock and is affected by many different processes (see chapter 2).

In this dissertation, we will focus on two tissue types: bone and dental enamel. Bone is a relatively porous, cryptocrystalline structures, whereas dental enamel is dense and highly mineralized (Bourgon et al., 2020; Jaouen, 2018; Jaouen & Pons, 2016; Reynard & Balter, 2014). The inorganic mineral portion of bone and enamel is composed of hydroxyapatite [$(Ca_{10}(PO_4)_6(OH)_2$], which we will refer to as bioapatite. Elements with a similar atomic structure to Calcium (the Ca in hydroxyapatite) can be incorporated into the bioapatite mineral during tissue formation (Bentley, 2006; Bourgon et al., 2020; Dean et al., 2018; Price et al., 2002). Therefore, with an atomic structure like Ca, the elements, Sr and Zn is incorporated as a trace element in the bioapatite mineral in bones and teeth (Bentley, 2006; Bourgon et al., 2020; Dean et al., 2018; Price et al., 2002). Similarly, due to their key roles in oxygen transport and enzymes, the elements Fe and Cu are important components in serum and blood, which irrigates bone. Hence, Fe and Cu, along with their isotopic compositions are recorded in bone (Balter et al., 2013; Jaouen et al., 2012; Jaouen & Pons, 2016).

The application of trace metal isotope analysis to explore dispersal patterns, diet, trophic position, and sex-related differences in physiology in non-human primates is still in its infancy. However, given the genetic similarities of great apes to our shared last common ancestor, the applications of trace metals to well-studied long term study populations of wild primates enables the hypothesis-testing of evolutionary hypotheses in modern samples. The diminished preservation of early human ancestor skeletal remains limits our ability to answer questions regarding how the behavior and physiology of modern humans evolved. Therefore, in the following chapters, we discuss the potential of using modern populations of great apes to ask key questions about the evolution of dispersal patterns, meat consumption and menstruation.

The proposed research will be the first the apply trace metal isotope analysis to better understand the behavior, diet and physiology in wild primates for future applications to ancestral humans. In Chapter 2, we use Sr isotopes to explore dispersal in four communities of wild chimpanzees. As part of this project, we present the first Sr isoscape of Taï National Park, and then identify the possible origins of several females that were part of the North community when the Taï Chimpanzee Project was established in 1979. We demonstrate that when studying historic and modern migration patterns of chimpanzees, and by extension any other species that migrates, the integration of $^{87}Sr/^{86}Sr$ analysis offers crucial geographical information, which can significantly reduce the potential origin locales when attempting to identify possible migrants.

In Chapter 3, we use zinc stable isotopes to explore dietary differences between the sexes in wild chimpanzees. This is the first study to analyze zinc stable isotopes in chimpanzee food items within the Taï Chimpanzee Project study area as well as the Taï chimpanzees themselves. In this chapter, we explore if zinc isotope ratios are a better proxy for protein consumption than nitrogen stable isotopes in environmental contexts with poor preservation. To address this question, we use zinc isotope ratios and assess the quantity of meat consumption relative to an individual's position in the Taï ecosystem's food web. As such, this chapter illustrates that zinc isotope analysis can reliably indicate low levels of meat consumption in tooth enamel with direct applications to the study of the paleodiets of early hominin taxa. Specifically, this encourages exploring when meat consumption became a more substantial part of the human diet. We also assess if zinc stable isotopes are a useful proxy for breastfeeding by analyzing zinc stable isotopes in the enamel of chimpanzee molars, which form at different ages than humans.

In Chapter 4, we analyze iron and copper stable isotopes in a museum-curated collection of chimpanzees and bonobos. This project expands on previous work that explored sex-related differences in humans and rhesus macaques (Boucher et al., 2021). In this study, we assess if menstrual blood loss is a primary factor controlling the sex differences that have been observed in humans and rhesus macaques, but not mice (Boucher et al., 2021; Jaouen et al., 2012; Moynier et al., 2022). In order to address these questions, we first adapt the Fe and Cu isolation protocol to be more suitable for bone, or more specifically bioapatite samples as well as more cost-

effective and time efficient. Then, we explore how iron and copper isotope ratios vary in a minimally menstruating primate, such as the chimpanzee and bonobo. We demonstrate that iron and copper stable isotopes can be reliably measured in the bone of chimpanzees and bonobos, opening the possibility of using great apes as models for hominins with minimal menstruation. However, further consideration of female reproductive investment, estrous cycling and diet is needed to discern the origin of sex-related differences in iron and copper metabolism in primates.

The three main chapters (Chapter 2, Chapter 3, and Chapter 4) of this dissertation have either been published in (chapter 2, (Boucher et al., 2024)), submitted to (chapter 3), or are in preparation for submission to peer-reviewed journals (chapter 4). In this dissertation, these papers have been reformatted from their original to fulfill the dissertation formatting requirements at the University of California Santa Cruz Graduate Division.

CHAPTER 2: Strontium isotopes track female dispersal in Taï chimpanzees

Authors: Renee D. Boucher, Roman M. Wittig[,3], Sylvain R. T. Lemoine, Aleksey Maro[5], Xueye Wang[,6], Paul L. Koch[7], Vicky M. Oelze[1]

[1] Department of Anthropology, University of California, Santa Cruz, CA 95064, USA
[2]Institute of Cognitive Sciences, UMR5229 CNRS, 67 Boulevard Pinel, 69675 Bron cedex, France
[3]Taï Chimpanzee Project, CSRS, 01 BP 1303, Abidjan, Côte d'Ivoire
[4]Department of Archaeology, University of Cambridge, Cambridge, UK
[5] Department of Integrative Biology, University of California, Berkeley, CA 94720, USA
[6] Center for Archaeological Science, Sichuan University, Chengdu 610064, China
[7]Department of Earth and Planetary Sciences, University of California, Santa Cruz, CA 95064, USA

Note: Published in American Journal for Biological Anthropology, 2024. Formatting has been modified from origin article to fit dissertation guidelines. Permission to include this article has been granted by all co-authors and signed permission letter submitted to ProQuest.

Reference: Boucher, R. D., Wittig, R. M., Lemoine, S., Maro, A., Wang, X., Koch, P. L., & Oelze, V. M. (2024). Strontium isotopes track female dispersal in Taï chimpanzees. American Journal of Biological Anthropology. doi:10.1002/ajpa.24981

2.1. Introduction

Dispersal in chimpanzees

Natal dispersal upon reproductive maturity is common in many social animals, with one or both sexes leaving their natal community to seek novel mating opportunities, leading to a sex-biased dispersal pattern (Clutton-Brock & Lukas, 2012; Johnson & Gaines, 1990; Lawson Handley & Perrin, 2007; Li & Kokko, 2019). In chimpanzees (*Pan troglodytes*), typically only nulliparous females disperse (Goodall, 1986; Lee & Strier, 2015; Nishida, 2011; Parr & de Waal, 1999). Male chimpanzees are patrilocal, so they generally remain in their natal community for their lifetime (Inoue, Inoue-Murayama, Vigilant, Takenaka, & Nishida, 2008;

Lehmann & Boesch, 2008, 2009; Moore, Langergraber, & Vigilant, 2015). While there are some reports of females remaining in natal communities, female dispersal is much more likely and is often sustained by regular immigration of nulliparous females into studied communities (Gagneux, Boesch, & Woodruff, 1999; Hammond, Lawson, Handley, Winney, Bruford, & Perrin, 2006; Langergraber et al., 2014; Langergraber et al., 2007; Pusey & Packer, 1986; Walker & Pusey, 2020).

Chimpanzees are a territorial species and generally restrict their activity to a specific area (Boesch, Kohou, Néné, & Vigilant, 2006). The territory of a given social community can shift over time due to fluctuations in the number of adult males or in response to dynamics within the community's dominance hierarchy (Lehmann & Boesch, 2003; Lemoine et al., 2020). Female chimpanzee dispersal between communities can be high risk, due to travel through unknown territory and exposure to predators in unfamiliar feeding grounds (Boesch, 1991; Stumpf, Thompson, Muller, & Wrangham, 2009; Thompson, 2013). In Taï National Park (Côte d'Ivoire), ongoing observational studies as part of the Taï Chimpanzee Project (TCP) have documented the dispersal of female chimpanzees for over 40 years (Boesch and Wittig, 2019; Lemoine et al., 2019). From these studies, it is estimated that most females disperse from their natal community upon sexual maturation, which occurs around ten years of age, as signaled by pronounced sexual swellings (Boesch, 1997; Lemoine et al., 2019). However, some unknown circumstances result in a few staying to reproduce and raising their offspring with members of their natal community (Lemoine et al., 2019). In most dispersal events, predicting how far females travel to

a new community or where they eventually immigrate is difficult. Although there are some rare instances of inter-community migration of females and the arrival of females with infants, more often, female immigrants arrive unpredictably, and it is usually unknown where they emigrated from (Lemoine et al., 2019; Luncz & Boesch, 2014; Vigilant, Hofreiter, Siedel, & Boesch, 2001).Thus, much of what we know of chimpanzee natal dispersal is restricted to rare instances at long-term study sites where female origin and dispersal between different habituated populations may be tracked. Therefore, for most immigrants, researchers do not know how far females are traveling and what additional risks (natural or anthropogenic) they might encounter.

The implications for a refined chimpanzee dispersal model

Understanding female dispersal also has implications for chimpanzee conservation. Western chimpanzees (*Pan troglodytes verus*) have undergone a dramatic population decline over the past two decades and are now considered critically endangered (Kühl et al., 2017). Even Taï National Park, one of the last primary evergreen rainforests in West Africa and a protected refuge for western chimpanzees, was found to have one-tenth of the expected population density of chimpanzees (Campbell, Kuehl, Kouamé, & Boesch, 2008). The rapid decline in western chimpanzees is related to a rising human population that has increased deforestation and poaching, and led to habitat fragmentation (Campbell et al., 2008; Kühl et al., 2017; Marchesi, Marchesi, Fruth, & Boesch, 1995). Habitat fragmentation has been shown to increase the potential for inbreeding depression and subsequent

population extinction (Knight, Chapman, & Hale, 2016). In environments that are impacted by habitat fragmentation, comparative data on female chimpanzee dispersal may be useful in contextualizing dispersal. Knowing how far females travel to find a new community allows us to better understand the risks associated with female dispersal and opens the doorway for expanding protected areas and assessing conservation need. Understanding female reproductive biology, including female dispersal patterns, is imperative for improving conservation efforts of western chimpanzees.

A clearer model of female chimpanzee dispersal can also help us understand how dispersal strategies evolved in our own species' ancestral lineage. Much of what we know about the social evolution of early hominins is limited by what is preserved in the fossil record, and contrasting interpretations of community dynamics and mating systems for hominins make the behavioral and socio-environmental context for early hominins unclear (Hill et al., 2011; Murdock, 1981; Wilkins & Marlowe, 2006). The reconstruction of hominin dispersal patterns using strontium (Sr) isotope analysis has been proposed as a useful proxy for behavioral trends that are not observable from the fossil record, such as philopatry, dispersal, landscape use, and community dynamics (Balter, Braga, Télouk, & Thackeray, 2012; Copeland et al., 2011; Hamilton, Fernandez, & Nelson, 2021). For instance, strontium isotope ($^{87}Sr/^{86}Sr$) ratios and Sr concentrations have been used to show differences in landscape use by early hominins, as well as to contend that early australopiths had a similar home range size, but different dietary breadths than anatomically modern

humans (Balter et al., 2012; Copeland et al., 2011). The use of extant non-human primates has informed many behavioral models and assumptions about fossil hominins, often emphasizing sexual dimorphism of body size (Gordon, Green, & Richmond, 2008; Lovejoy, 2009). Non-human primates, specifically within the genus *Pan*, are often used as analogues for early human dispersal models (Copeland et al., 2011; Lockwood, Menter, Moggi-Cecchi, & Keyser, 2007). Yet given the remaining unknowns about dispersal in chimpanzees, additional sources of information about their origins and distance traveled would enrich the comparative model for apes (Koenig & Borries, 2012) and be useful in contextualizing emerging evidence for early African hominin mobility (Chazan, 2022; Heydari-Guran & Ghasidian, 2020).

Strontium isotope geochemistry

Strontium isotope ($^{87}Sr/^{86}Sr$) analysis is a well-established method for provenance studies, and the $^{87}Sr/^{86}Sr$ ratios in animals are representative of the local environment (weathered bedrock and other sources) that are integrated into skeletal tissues when animals consume plant or animal food (Beard & Johnson, 2000; Bentley, 2006; Price, Burton, & Bentley, 2002). $^{87}Sr/^{86}Sr$ analysis uses the natural abundance of the radiogenic isotope ^{87}Sr, relative to the stable isotope ^{86}Sr, to assess the spatial variation among geological terrains (Bataille, Crowley, Wooller, & Bowen, 2020; Beard & Johnson, 2000; Bentley, 2006; Britton et al., 2020; Capo, Stewart, & Chadwick, 1998; Faure & Powell, 2012; Gosz, Brookins, & Moore, 1983; Hoppe, Koch, & Furutani, 2003; Hurst & Davis, 1981). Variations in $^{87}Sr/^{86}Sr$ measurements

reflect the chemical composition and age of bedrock (Åberg, 1995). The $^{87}Sr/^{86}Sr$ ratio of a given bedrock terrain is determined by the radioactive decay of rubidium (^{87}Rb) to ^{87}Sr, with variations related to its age of formation and the initial abundance of Rb (Bentley, 2006).

Different types of bedrock underlying the soils and bodies of water on a landscape result in different $^{87}Sr/^{86}Sr$ ratios. The weathering of bedrock can release Sr into soils and water that is taken up by plants and animals (Bentley, 2006). Although, different minerals in the rock, with different $^{87}Sr/^{86}Sr$ ratios, may weather at different rates, so soil age or the depth at which plants root (thereby accessing weathered bedrock) can influence the regional environmental baseline, or even isotopic ratios within a region (Crowley et al., 2017). Windborne dust, especially downwind of deserts or previously glaciated terranes (Aarons et al., 2017; Frumkin & Stein, 2004), and sea spray (Whipkey, Capo, Chadwick, & Stewart, 2000) can contribute Sr with isotopic ratios unrelated to the bedrock at a site. The balance of Sr supplied by local weathering versus these airborne sources can also affect the local environmental $^{87}Sr/^{86}Sr$ baseline.

Consequently, it is critical to analyze environmental samples and establish a Sr isotope baseline for any given study area. Bioavailable $^{87}Sr/^{86}Sr$ baselines are typically established by measuring soils, plants, and animal remains across a given study region (Bataille & Bowen, 2012; Bataille et al., 2020). These samples of bioavailable $^{87}Sr/^{86}Sr$ baselines can then be used to create a heat map of the predicted $^{87}Sr/^{86}Sr$ spatial distribution, commonly referred to as a Sr isoscape. The use of Sr

isoscapes has become standard practice, as they enable the prediction of an organism's origin based on the observed $^{87}Sr/^{86}Sr$ ratios in each study area. Measuring plants of varying kind and root depth has been shown to accurately portray bioavailable Sr in an ecosystem (Britton et al., 2020; Oelze et al., 2012).

The use of Sr isoscapes enables $^{87}Sr/^{86}Sr$ analysis to address broad questions related to the mobility and migration of various organisms, including primates (Bentley, 2006; Brennan et al., 2015; Balter et al., 2012; Copeland et al., 2011;Crowley & Godfrey, 2019; Dominy et al., 2020; Fannin et al., 2021; Koch et al., 1995; Sugiyama et al., 2022). However, $^{87}Sr/^{86}Sr$ analysis in primatology has thus far only been used to assess habitat use (Hamilton, Nelson, Fernandez, & Hunt, 2019), and to identify the sex of philopatric and dispersing individuals (Hamilton et al., 2021). In this study, we use $^{87}Sr/^{86}Sr$ analysis of chimpanzee skeletal remains and environmental reference samples from five chimpanzee communities occupying neighboring territories in Taï National Park to assess female chimpanzee immigrant status and mobility within the well sampled North Community. Specifically, we address the following questions:

1) Are there environmental baseline $^{87}Sr/^{86}Sr$ differences across Taï chimpanzee territories?
2) Do $^{87}Sr/^{86}Sr$ ratios differ among chimpanzee members of different Taï chimpanzee communities with distinct territories?

3) Are $^{87}Sr/^{86}Sr$ ratios able to discern the status (natal or immigrant) of Taï chimpanzee females and, if so, what do they reveal about the potential areas of origin for immigrant females from unknown chimpanzee communities?

2.2. Materials

Study site

In 1978, the evergreen tropical rainforest of Taï National Park (TNP, Figure 2.2.1; 5°45'N, 7°7'W), Côte d'Ivoire was registered as a Biosphere Reserve and in 1982 was added to the UNESCO World Heritage List due to its unique fauna, which includes the western chimpanzee (*P. troglodytes verus*) and 11 other primate species (Boesch & Boesch-Achermann, 2000; Guillaumet & Adjanohoun, 1971; Kolongo, Decocq, Yao, Blom, & Van Rompaey, 2006; Mangenot, 1950a, 1950b, 1955). At 5,082 km^2, the park is one of the largest remaining areas of tropical rainforest in West Africa[1]. Taï National Park consists of an ancient sloping peneplain broken by several rocky outcrops of Paleoproterozoic and Archean rock, which stand out from encircling plains as more or less isolated hills, including Mount Niénokoué (396 m) (Kolongo et al., 2006). A large zone of bedrock runs SW to NE across the park, dissected by tributaries that run parallel to it (Collinet, Monteny, & Pouyaud, 1984; Rouw, Vellema, & Blokhuis, 1990; Tagini, 1966, 1972). The TCP study area is largely

[1] According to the *Office Ivorien des Parcs et Réserves* TNP was enlarged in 2018 (http://www.oipr.ci/index.php/parcs-reserves/parcs-nationaux/parcnational-de-tai)

composed of Paleoproterozoic volcanic-sedimentary bedrock, with small outcrops of Archean rock. The Cavally River separates Côte d'Ivoire from Liberia, with Archean bedrock on the Liberian side of the border (Petters, 1991). During December-January, the Harmattan Season dry northeasternly winds deposit Saharan dust across Taï National Park (Stoorvogel, Van Breemen, & Jassen, 1997).

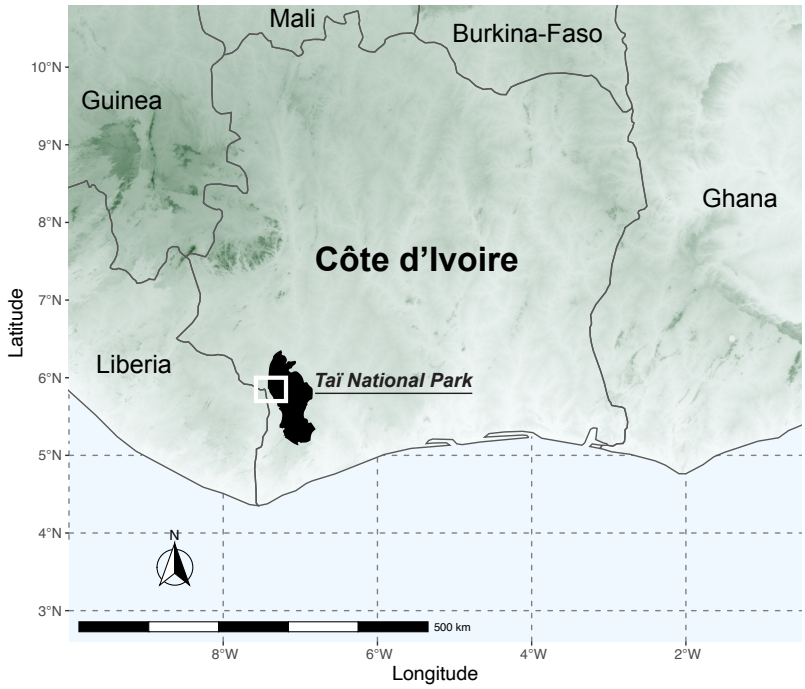

Figure 2.2.1. Topographic map of Côte d'Ivoire.
The study site is demarcated by a white rectangle, within Taï National Park. Dark green corresponds to a higher elevation, whereas light green corresponds to a lower elevation.

Taï chimpanzees

Since 1979, the TCP has operated in a small section on the western side of Taï National Park (400 km^2), successfully habituating five neighboring chimpanzee communities to human observations and research (Boesch & Wittig,

2019;Wittig, and & Boesch, 2019). The habituated communities have been named per their original location within the study area: North community, South community, East community, and Middle community (Boesch & Boesch-Achermann, 2000). In 2014, the Pan African Programme (PanAf) began a census of a fifth community, called Northeast community (originally called Tai-R). In 2015, the TCP began the habituation of Northeast community, and this community has been followed since 2022 (Arandjelovic et al., 2020). Outside of the study area, to the northwest of North community, there is a chimpanzee community designated for ecotourism (Tai-E), which we will refer to as Northwest community (Boesch et al., 2021). Within the TCP study area as of 2019, 467 individuals have been identified, including 257 females, 192 males, and 18 individuals of indeterminate sex (Boesch & Wittig, 2019). Both subadult males and females range with adults of both sexes, using a similar proportion of the home range as their core area, and the individual life histories and genealogies have been well documented (Lehmann and Boesch, 2005).

The Taï chimpanzee skeletal collection is part of the long-term collection of the TCP, housed at the Max Planck Institute for Evolutionary Anthropology in Leipzig, Germany (Boesch et al., 2006; Vigilant et al., 2001). Sampled chimpanzees (Table 2.3.1, n = 34) were born 1954-1997, with TCP demographic data collection beginning in 1980. Before habituation in 1979, North community's territory and size were estimated from focal follows and researcher observation. North camp was established in the central area where North community chimpanzees were first

habituated, and subsequent trails to other chimpanzee communities were built out from there (Lemoine et al., 2019).

Based on researcher observations detailed in the TCP database, sampled individuals were classified as “natal”, “unknown”, or “reference.” The “natal” category comprises resident males as well as females born in North community that had not migrated prior to death (n = 16). North community natal samples include adult (n = 3) and subadult males (n = 7), and subadults females (n = 6) that were born and died in North community’s territory. The natal community is subdivided into pre-1980 (n = 2) and post-1980 (n = 14) to account for a lack of direct observation of North community (and its location) prior to 1980.

The “unknown” sampling category comprises possible immigrants to North community, and therefore includes adult females that were part of North community, but were not observed immigrating, making their origin unclear (n = 11). This community is further subdivided into “pre-1980” (n = 4) and “post-1980” (n = 7), depending on the timing of enamel formation. “Post-1980” includes females that formed tooth enamel when the location of North community (in which they died) is known, but their area of origin is unknown. For unknown females forming tooth enamel “pre-1980”, we do not have direct observations of the location of North community, but we do have samples from males who formed tooth enamel between 1972 and 1980 who can supply a baseline for the community extending back in time. With one exception (NF03, which formed enamel ~1960), all individuals sampled from North community formed enamel when the community occupied its historic

range (1980 to 1999) or in an earlier interval when we can monitor territory with natal community $^{87}Sr/^{86}Sr$ ratios (Table 2.3.1). The historic range from 1980-1987 is estimated from researcher observation, where the territory of North community is generally known to surround North camp. All North community individuals sampled in this study formed enamel within this historic pre-2000 territory of North community (here called North 1).

Lastly, the "reference" sampling category comprises resident males from the other chimpanzee communities in the TCP study area: South (n = 4), East (n = 2), and Middle (n = 1). Since both Northeast community and Northwest community have limited skeletal samples, we did not sample chimpanzees from these territories.

2.3. Methods

Dental sampling

For the 34 Taï chimpanzee samples, skulls were CT-scanned to record morphometric information prior to destructive sampling, and we used this 3D data to determine the best sampling locality on each tooth, avoiding microcracks and dental wear. We mechanically cleaned the sampling area with a diamond-tipped dental drill and then recovered about 50 mg of enamel reaching from the occlusal surface to the cementum-enamel junction, of which ~10 mg was used for subsequent $^{87}Sr/^{86}Sr$ analysis. Abraded enamel was placed in cleaned glass beakers and sonicated in ultrapure acetone to remove dust and exogenous contamination. Cleaned samples

were then removed from the solution, transferred into clean Eppendorf tubes, and air dried in a sterile fume hood.

As tooth enamel forms during a specific developmental time window and does not subsequently remodel (Driessens & Verbeeck, 1990; White, Black, & Folkens, 2011), the dental enamel samples in this study correspond to the following age ranges in years +/- 1 year: *in utero* (m1 and m2), *in utero* to 2.8 (M1), 1.8-5.6 (M2), and 3.6-8 (M3) (Schwartz, Reid, Dean, & Chandrasekera, 2000; Smith, Reid, Dean, Olejniczak, & Martin, 2007; Smith et al., 2010). Lowercase and uppercase letters refer to deciduous and permanent molars, respectively. The $^{87}Sr/^{86}Sr$ ratios measured in deciduous molars, which formed *in utero*, are representative of the maternal body chemistry, given that virtually no placental discrimination of Sr isotopes has been shown (Shagina et al., 2007; Smith et al., 2022). Individual's year of tooth formation (ytf) is extrapolated from the date of birth and tooth type. For example, if an individual was born in 1980, and a third molar is sampled, we can estimate that the enamel formed between 8-9 years of age (from 1988 to 1989). We also include age at death (in years) for the individual (Table 2.3.1). We recognize that all birth dates are estimates based on observation for most individuals sampled, however the relative range for dental tissue formation +/- 1 year should encompass errors in these estimates.

Female chimpanzees reach sexual maturity at around 10 years, often leaving their birth communities in the subsequent years. Therefore, all female permanent teeth used in this study are assumed to represent a pre-dispersal isotope signal from their

birth community's territory (Thompson, 2013). Deciduous premolars represent the $^{87}Sr/^{86}Sr$ range of the territory inhabited by the mother during gestation. Our samples include five deciduous molars, all from individuals with mothers that were North community residents while pregnant, and therefore should reflect the Sr isotope signature for North community's territory.

Table 2.3.1. Summary of Taï chimpanzees sampled (n = 34).
Raw $^{87}Sr/^{86}Sr_{enamel}$ isotope ratios are included to 2 standard errors (SE). "ytf" is defined as the age of tooth formation when Sr accumulation begins. Age (years) represents the age in which the sampled individual died.

ID	Tooth	Sex	Origin	Time of Birth	Age at Death	ytf	Community	$^{87}Sr/^{86}Sr$	2SE
NF03	M2	f	unknown female (pre-1980)	1954‡	39	1956-1961	North	0.71681	0.00001
NF01	M2	f	unknown female (pre-1980)	1969‡	23	1971-1977	North	0.71818	0.00001
NF02	M3	f	unknown female (pre-1980)	1969‡	25	1972-1980	North	0.71703	0.00001
NF09	M3	f	unknown female (pre-1980)	1972‡	27	1975-1980	North	0.71883	0.00001
NF11	M3	f	unknown female (post-1980)	1973‡	28	1976-1984	North	0.72218	0.00001
NF07	M2	f	unknown female (post-1980)	1975‡	19	1977-1983	North	0.72393	0.00001
NF08	M2	f	unknown female (post-1980)	1976‡	22	1978-1984	North	0.72051	0.00001
NF06	M2	f	unknown female (post-1980)	1977‡	16	1979-1985	North	0.72308	0.00001
NF10	M3	f	unknown female (post-1980)	1978‡	27	1981-1989	North	0.73049	0.00001
NF05	M2	f	unknown female (post-1980)	1982‡	12	1983-1988	North	0.72200	0.00001
NF04	M2	f	unknown female (post-1980)	1982‡	11	1984-1990	North	0.72081	0.00001
NF15	M3	f	natal group (post-1980)	1979‡	9	1982-1990	North	0.71639	0.00002
NF14	M2	f	natal group (post-1980)	8/1/84	6	1986-1992	North	0.71765	0.00001
NF13	dm†	f	natal group (post-1980)	9/10/87	5	1987-1987	North	0.72369	0.00001
NF17	M2	f	natal group (post-1980)	6/5/87	11	1989-1997	North	0.71924	0.00001
NF12	M1	f	natal group (post-1980)	2/12/91	3	1990-1993	North	0.71776	0.00001
NF16	M2	f	natal group (post-1980)	11/24/91	10	1993-1999	North	0.71761	0.00001
NM10	M3	m	natal group (pre-1980)	1969‡	25	1972-1980	North	0.72049	0.00001
NM07	M2	m	natal group (pre-1980)	1971‡	13	1973-1979	North	0.72030	0.00001
NM09	M3	m	natal group (post-1980)	1975‡	20	1978-1986	North	0.72179	0.00001
NM08	M3	m	natal group (post-1980)	1980‡	14	1983-1991	North	0.72089	0.00001

NM02	dm†	m	natal group (post-1980)	2/6/89	2	1989-1989	North	0.71901	0.00002
NM04	dm†	m	natal group (post-1980)	12/10/90	5	1990-1990	North	0.72016	0.00001
NM01	dm†	m	natal group (post-1980)	11/3/92	0.06	1992-1992	North	0.71826	0.00001
NM06	M2	m	natal group (post-1980)	9/21/91	10	1992-1997	North	0.71810	0.00001
NM05	M2	m	natal group (post-1980)	10/7/91	8	1993-1999	North	0.71960	0.00002
NM03	dm†	m	natal group (post-1980)	8/31/97	2	1997-1997	North	0.72076	0.00001
SM03	M3	m	non-North group reference	1959‡	40	1962-1970	South	0.72137	0.00001
SM01	M1	m	non-North group reference	1979	19	1979-1983	South	0.72086	0.00001
SM02	M3	m	non-North group reference	1989	25	1992-2000	South	0.72028	0.00001
SM04	M3	m	non-North group reference	1991	ad	1994-2002	South	0.72029	0.00001
EM02	M2	m	non-North group reference	NA	ad	NA	East	0.71662	0.00001
EM01	M3	m	non-North group reference	1993‡	14	1996-2004	East	0.71686	0.00001
MM01	M2	m	non-North group reference	1983‡	19	1985-1989	Middle	0.72187	0.00001

†Deciduous molars, lowercase letters correspond to deciduous dentition, and uppercase letters correspond to permanent dentition

‡Time of birth is estimated, as it was not witnessed by researcher

Environmental sampling for Sr isoscape

To create a bioavailable Sr isoscape for the TCP study area, we sampled leaves of various chimpanzee plant foods from the TCP-established chimpanzee territories (n = 14) and used additional leaf samples (n = 5) from plants as part of a previous study in the surrounding TCP area (Lowry, Wittig, Pittermann, & Oelze, 2021) (Table 2.3.2, Figure 2.4.1). In addition, we used data from nut (*Parinari excelsa*) and snail (*Lissachatina fulica*) shell fragments, which had been analyzed within the framework of a large-scale Sr isoscape project (n = 16, Wang et al., in review). Territory location and population density data collection began in 1984, detailing the temporal territory shifts of the TCP-habituated chimpanzee communities, and informed the environmental sampling of the historic range. An additional collection of ranging data began in the early 1990s, with records of exact

GPS coordinates starting in 2013, informing the modern range of the North community (Wittig and Boesch, 2019).The environmental samples were binned by TCP-established community territories and their orientation within the study area (Figure 2.4.1): North, Northwest (Tai-E), Northeast (Tai-R, Pan African Programme), South, East, and Middle. Environmental samples collected as part of this study were georeferenced with a handheld GPS device, dried on site, stored in falcon tubes with silica and transferred to the Primate Ecology and Molecular Anthropology lab at the University of California, Santa Cruz for analysis under import permits #PCIP-20-00092, -20-00377 and -21-00166.

Around the year 2000, the territory of North community shifted westward, due in part to a reduction in the number of adult males, and in part to pressure from Northeast community, which is known to have expanded westward around this time (see Figures 2.9.3 to 2.9.6). To account for this shift in territory location and population density, the sampling area for North Community is subdivided into two temporal groupings (see Figure 2.4.1), one “historic” North 1 (1980-1999) and one “modern” North 2 (2000- present). For both, highest presence density based on long-term focal follow data from the TCP database is the assumed territory for each grouping. North 1 represents the historical territory range from 1980 to 1999, when the territory was primarily restricted to the trails around North camp, with the main road constituting a border with a neighboring community with which North community had regular intercommunity encounters. North 2 represents 2000 to present when the territory shifted further west of the main road, away from North

camp and the original trails, which aligns with the current ranging of North community. No chimpanzees were sampled from the modern population; therefore, the North 2 territory represents a potential location that individuals could have emigrated from. Northwest is an eco-tourism area that is northwest of North community and is not a TCP-defined study area, therefore there is no data on territory location shifts or population density.

The territory shifts of the South, East, and Middle communities were not under study during the period that North community's territory shifted, as these communities were habituated later. However, based on direct researcher observations, we can report some more subsequent shifts in territorial locale. From 2014, South community, situated south of North community, has expanded their territory further southward, resulting in the expansion of the trail system (Boesch & Wittig, 2019; Lemoine et al., 2019). Since habituation, East community, located east of South community, is reported to have one of the largest territories, and is not known to have shifted its territory location (Kouakou, Boesch, & Kuehl, 2011). During the study period, Middle community, situated between North and South communities did not shift its territory, however, as Middle community is no longer observed after experiencing a significant decline in numbers, it is unclear what the present territory is.

Table 2.3.2. Summary of environmental samples establishing the $^{87}Sr/^{86}Sr$ baseline for the different Taï chimpanzee territories (n = 35).

No	Territory	Species	sample type	latitude	longitude	$^{87}Sr/^{86}Sr$	2SE	source
257	North 1	*Afzelia bella*	plant	5.8702	-7.3384	0.71952	0.00001	this study

1104	North 1	*Lissachatina fulica*	snail shell	5.8863	-7.3162	0.71534	0.00001	this study
507	North 1	*Sterculia oblonga*	plant	5.8771	-7.3336	0.71765	0.00002	this study
514	North 1	*Sterculia oblonga*	plant	5.8708	-7.3299	0.71661	0.00002	this study
319	North 2	*Dialium aubrevillei*	plant	5.8710	-7.3478	0.73460	0.00001	this study
445	North 2	*Parkia bicolor*	plant	5.8760	-7.3467	0.72757	0.00001	this study
1096	North 2	*Lissachatina fulica*	snail shell	5.8871	-7.3407	0.72632	0.00001	Wang et al., in review
1097	Northwest	*Lissachatina fulica*	snail shell	5.9267	-7.3571	0.72205	0.00001	Wang et al., in review
1098	Northwest	*Lissachatina fulica*	snail shell	5.9055	-7.3596	0.72219	0.00001	Wang et al., in review
1099	Northwest	*Lissachatina fulica*	snail shell	5.9053	-7.3399	0.72811	0.00001	Wang et al., in review
1100	Northwest	*Lissachatina fulica*	snail shell	5.9326	-7.3790	0.72233	0.00001	Wang et al., in review
1101	Northwest	*Lissachatina fulica*	snail shell	5.8960	-7.3570	0.72602	0.00002	Wang et al., in review
1102	Northwest	*Lissachatina fulica*	snail shell	5.9132	-7.3617	0.72207	0.00001	Wang et al., in review
1129	Northwest	*Lissachatina fulica*	snail shell	5.9181	-7.3703	0.7248	0.00001	Wang et al., in review
1289	Northwest	*Coula edulis*	nut shell	5.9309	-7.3640	0.72166	0.00001	Wang et al., in review
1306	Northwest	*Coula edulis*	nut shell	5.9312	-7.3466	0.72986	0.00001	Wang et al., in review
1103	Northeast	*Lissachatina fulica*	snail shell	5.8613	-7.3021	0.72102	0.00001	Wang et al., in review
1105	Northeast	*Lissachatina fulica*	snail shell	5.8713	-7.2939	0.72265	0.00001	Wang et al., in review
1106	Northeast	*Lissachatina fulica*	snail shell	5.8535	-7.3119	0.72297	0.00001	Wang et al., in review
1107	Northeast	*Lissachatina fulica*	snail shell	5.8534	-7.3073	0.72035	0.00001	Wang et al., in review
1127	Northeast	*Lissachatina fulica*	snail shell	5.8572	-7.3008	0.72215	0.00001	Wang et al., in review
1645	South	*Musanga cecropioides*	plant	5.8012	-7.3192	0.72185	0.00001	this study
1646	South	*Coula edulis*	plant	5.8180	-7.2992	0.71848	0.00001	this study
1682	South	*Parkia bicolor*	plant	5.8301	-7.3328	0.71106	0.00001	this study
1684	South	*Musanga cecropioides*	plant	5.8156	-7.3249	0.71987	0.00001	this study
1663	South	*Sarcophrynium brachystachyum*	plant	5.8359	-7.3036	0.71753	0.00001	this study
1666	East	*Coula edulis*	plant	5.8430	-7.2766	0.72078	0.00001	this study
1668	East	*Parkia bicolor*	plant	5.8335	-7.2590	0.71394	0.00003	this study
1675	East	*Sterculia oblonga*	plant	5.8240	-7.2842	0.70774	0.00001	this study
1676	East	*Dialium aubrevillei*	plant	5.8139	-7.2792	0.72229	0.00001	this study
1649	Middle	*Coula edulis*	plant	5.8516	-7.3337	0.71655	0.00001	this study
1655	Middle	*Sarcophrynium brachystachyum*	plant	5.8444	-7.3336	0.71344	0.00001	this study
1657	Middle	*Coula edulis*	plant	5.8392	-7.3356	0.71693	0.00001	this study
1654	Middle	*Dialium aubrevillei*	plant	5.8449	-7.3287	0.71842	0.00001	this study
1660	Middle	*Dialium aubrevillei*	plant	5.8399	-7.3260	0.72190	0.00002	this study

$^{87}Sr/^{86}Sr$ analysis

Dried tooth samples were transferred to a clean lab setting where 10 mg was weighed into acid-washed Teflon beakers and digested in 1 ml triple-distilled, concentrated HNO_3 (15.9M) at 120°C and subsequently evaporated to dryness on a hotplate. Dry leaf samples (~1-1.5 g), snail shell (10-15 mg), and nutshell (10-15 mg) were weighed into sonicated porcelain crucibles to be ashed in a muffle furnace at 800°C for 8 hours. The resulting ash (~10mg) was then weighed into clean Teflon beakers and digested in 1ml triple distilled, concentrated HNO_3 at 120°C, which was subsequently evaporated to dryness.

For chromatographic separation of Sr from other elements, we dissolved samples in 1 ml 3M HNO3 for two hours at 120°C along with one procedural blank. We followed the gravity flow column chromatography protocol outlined by Deniel and Pin (2001) modified after Copeland (2008). Briefly, as samples were dissolving, 1 ml 50-100 μm Sr-spec™ resin (Eichrom Technologies) was loaded in Bio-Rad™ gravity-flow chromatography columns, rinsed 2x with 10 ml ultrapure water (18.2MΩ cm) obtained from a Milli-Q Element water purification system, then conditioned with 3 ml of 3M HNO_3. Dissolved samples were carefully loaded onto the columns, drop by drop and then captured and reloaded two additional times to maximize the amount of Sr binding to the resin. After 3 washes with 500 μL 3M HNO_3, the Sr was eluted with 1.5 mL MQ H_2O into a clean Teflon beaker and evaporated to dryness under the presence of 2 drops of phosphoric acid (H_3PO_4), which helps to concentrate the sample while drying.

For measurement of the samples on a TIMS (thermal ionization mass spectrometer, Phoenix62, Isotopx) in the UC Santa Cruz W.M. Keck Isotope Laboratory, we resolved the visible Sr pellet in 1 μL of tantalum chloride ($TaCl_5$) activator, which was then loaded onto degassed rhenium filaments, alongside the international standard, SRM NIST987. Procedural blanks were measured on an Element XR high-resolution ICP-MS in the UC Santa Cruz Plasma Analytical lab to quantify possible cross-contamination or impurity of reagents. Internal precision (in %) and analytical blank concentrations (in ppm) are reported in the results section.

Data Analysis

All analyses and visualizations were created using R, with a significance level of $\alpha = 0.05$ (R Core Development Team, 2022). The full dataset is provided in Table 2.3.1 for all individuals and Table 2.3.2 for all environmental samples.

To assess how $^{87}Sr/^{86}Sr$ differences in chimpanzee enamel and the environment vary in the TCP study area, we conducted the following: (1) established a local isoscape from environmental samples from the territories of four habituated communities (North, South, East, Middle communities), and from two neighboring territories (Northeast and Northwest communities), then assessed if there are significant $^{87}Sr/^{86}Sr$ differences among environmental samples consistent with the territories of chimpanzee communities, (2) assessed if there are $^{87}Sr/^{86}Sr$ differences in chimpanzee enamel samples between communities, and (3) compared the $^{87}Sr/^{86}Sr$ ratios between individuals binned as “unknown” females with females that have a

known natal community, to validate the "unknown" females' origin status (immigrant or native).

(1) Establish a local isoscape from environmental samples

We explored the differences in $^{87}Sr/^{86}Sr$ between the following territories: North 1 (n = 4), North 2 (n = 3), Northeast (n = 4), Northwest (n = 9), South (n = 5), East (n = 4), and Middle (n = 5) (Table 2.3.2). To verify that sample type (plant, nutshell, snail shell) did not cause heteroscedasticity, we assessed the homogeneity of variance between territories (North (North 1-2), Northeast, Northwest, South, East, Middle) using the 'stats' package in R (Bartlett, 1937; R Core Development Team, 2022). To test if there were differences in Sr environmental baselines between TCP-established territories, we fitted two generalized linear mixed models with a beta distribution (GLMMs; Bolker et al., 2009) using the 'glmmTMB' package in R 4.2.1 (Brooks, Bolker, Kristensen, & Maechler, 2022; Magnusson et al., 2017; R Core Development Team, 2022). Mixed model fit was validated using the 'DHARMa' package in R (Hartig & Hartig, 2017). In the hypothesis (full) model, $^{87}Sr/^{86}Sr$ data from environmental samples is predicted by territory, as a fixed effect and sample type (plant, nutshell, snail shell) was included as a random effect. In the null model, $^{87}Sr/^{86}Sr$ data from environmental samples is only predicted by sample type, as the random effect (Table 2.9.1). Since there are small sample sizes for North 1 (n = 4), North 2 (n = 3), and East (n = 4), the Akaike Information Criterion corrected for small sample sizes (AICc). Then, the '*MuMIn*'package was used to compare the full and

null models, and select the model with the best fit, i.e., the model with the lowest AICc scores (Burnham & Anderson, 2004; Barton and Barton, 2015). An estimated marginal means post-hoc analysis was performed to assess the significance of pairwise differences in $^{87}Sr/^{86}Sr$ ranges between territories. Estimated marginal means in log-odds ratio scale were computed and p-values adjusted for multiple comparison by Bonferroni using the 'emmeans' package in R (Lenth, Singmann, Love, Buerkner, & Herve, 2021). Since we have a small sample size per territory ($n < 10$), we also performed a power analysis for each pairwise difference generated by the 'emmeans' package (Kumle, Võ and Draschkow, 2021).

To create a Sr isoscape of the study area, we constructed $^{87}Sr/^{86}Sr$ contour maps with the environmental $^{87}Sr/^{86}Sr$ dataset ($n = 35$) and a Kriging algorithm in the Surfer software package (Figure 2.4.1). Kriging is a geostatistical gridding method that produces maps by interpolating irregularly spaced data points to express the trends within a dataset (Cressie, 1990, 2015; Journel & Journel, 1989; PL & Srivastava, 1989). Although direct researcher observations remark on inselberg outcrops emerging from volcanic tuffs in the TCP study area, a detailed geological map of Taï National Park or the TCP study area is not available. Therefore, we were not able to use random forest modeling to build a local isoscape (Bataille et al., 2018). We can only show predicted $^{87}Sr/^{86}Sr$ trends across the TCP study area in relation to topographic and hydrologic features in the surrounding landscape (Figure 2.4.1).

(2) Are there significant $^{87}Sr/^{86}Sr$ differences in chimpanzee enamel samples between chimpanzee communities?

To validate the environmental baseline and Sr isoscape for the TCP study area, we analyzed $^{87}Sr/^{86}Sr$ ratios in enamel bioapatite from resident chimpanzees (n = 17). The resident chimpanzees are only associated with TCP-established communities included in the sample population, North community (n = 10), South community (n = 4), East community (n = 2), and Middle community (n = 1). Subadult females were omitted, as only males were sampled from the reference communities, to ensure a balanced sample size and prevent overrepresenting North community individuals. The R '*stats*' package was used to compare the theoretical density and distribution of the $^{87}Sr/^{86}Sr$ ratios in enamel bioapatite from resident chimpanzees in TCP established communities. (R Core Development Team, 2022). Since the overall sample size is small for the reference male group (n = 7), we decided to assess the overlap between $^{87}Sr/^{86}Sr$ ratios relative to the North community natal males. First, we used R '*fitdistrplus*' to fit the $^{87}Sr/^{86}Sr$ ratios for post-1980 North community natal males with a beta distribution and calculated the 2.5% (0.718) and 97.5% (0.722) quantiles (Delignette-Muller & Dutang, 2015). Next, we assessed if the $^{87}Sr/^{86}Sr$ ratios of the pre-1980 natal males (n = 2) were different from post-1980 natal males (n = 8) by plotting the $^{87}Sr/^{86}Sr$ ratios of North community pre-1980 natal males onto the theoretical density of post-1980 natal males. Since pre-1980 natal males fell within the quantiles of post-1980 natal males, we included them in this group (n = 10, 1S1) and calculated the new 2.5% (0.717) and 97.5% (0.722) quantiles. Next, we

assessed if the $^{87}Sr/^{86}Sr$ ratios of the other TCP-established communities (South, East, and Middle) fell within the quantiles of the theoretical density of all North community natal males (n = 10).

(3) Do $^{87}Sr/^{86}Sr$ ratios of unknown females correspond to those of natal individuals?

To test if $^{87}Sr/^{86}Sr$ ratios can discern unknown Taï chimpanzee female origin status (natal or immigrant) within North community (n = 27), we compared unknown females from pre-1980 (n = 4) and post-1980 (n = 7) to all native North community residents (n = 16). North Community residents include males (n = 10), and subadult females (n = 6), representing the pre-dispersal population, which we use as a local baseline for North community. To test if there were differences between origin groups (pre-1980 unknown female, post-1980 unknown female, post-1980 natal community), we fitted and validated two GLMMs. For the full model, $^{87}Sr/^{86}Sr$ from enamel samples is predicted by the origin community (natal post-1980, unknown female pre-1980, unknown female post-1980) as a fixed effect. Sample type (dm, M1, M2, M3) is included as a random effect to account for differences in age and tooth formation range. In the null model, $^{87}Sr/^{86}Sr$ data from North community chimpanzee enamel samples are only predicted by sample type, as a random effect. AICc, which is corrected for small sample size was used to compare the full and null models and select the model with the best fit. A post-hoc analysis was run to see the pairwise comparisons between origin groups and determine which origin groups are significantly different in $^{87}Sr/^{86}Sr$ ratios. Since we have a small sample size per origin

group ($n < 20$), we also performed a power analysis for each pairwise difference generated by the 'emmeans' package (Kumle, Võ and Draschkow, 2021). Following a power analysis, we also explore the individual origin of unknown females. To do this, we use the interquartile range (IQR) of North community residents ($n = 16$) multiplied by 1.5 (IQR*1.5) to determine potential outliers, and likely individual immigrants.

2.4. Results

We successfully obtained $^{87}Sr/^{86}Sr$ ratios from all teeth and plant samples. The NIST-987 standard after 7 cycles of data collection had an average ratio of 0.710422 ± 0.00004 (2σ) (McArthur et al., 2001). Internal precision for strontium runs is typically 0.00069% SE. Total procedural blanks for strontium are < 0.0003 ppm.

(1) Establish a local isoscape from environmental samples

$^{87}Sr/^{86}Sr$ ratios for the environmental baseline range from 0.70774 to 0.73460, with precision reported to 2 SE (see Table 2.3.2). To assess the fit of the Sr isoscape (Figure 2.4.1), we used the root-mean-square error (RMSE), where the ordinary kriging resulted in an RMSE value of 0.0048 (22% of the whole $^{87}Sr/^{86}Sr$ data range). There were no significant differences in variance of $^{87}Sr/^{86}Sr$ ratios within TCP established territories (bartlett, $K^2 = 11.1$, $df = 6$, $p > 0.05$). The full model had a lower AICc and GLMMs identified significant differences in $^{87}Sr/^{86}Sr$ between territories, where territory was a fixed effect and sample type was a random effect (summarized in Supporting Informations, Table 2.9.1 to 2.9.2, Figure 2.4.2). There

was a statistically significant difference in $^{87}Sr/^{86}Sr$ for the territories North 2 (Wald-Z Statistic = 5.38, $p < 0.00001$), Northwest (Wald Z-Statistic = 4.29, $p < 0.00001$), and East (Wald Z-Statistic = 115.74, $p < 0.00001$), as well as Northeast (Wald Z-Statistic = 2.58, $p < 0.01$). A post-hoc analysis showed significant pairwise differences between East-North 2 (z-ratio = -5.38, $p < 0.0001$), East-Northwest (z-ratio = -4.19, p = 0.0006, 0.80), Middle-North 2 (z-ratio = -5.11, $p < 0.0001$), Middle-Northwest (z-ratio = -3.83, p = 0.003), North 1-North 2 (z-ratio = -4.96, $p < 0.0001$), North 1-Northwest (z-ratio = -3.64, p = 0.006), North 2-Northeast (z-ratio = 3.27, p = 0.02), North 2-South (z-ratio = 4.98, $p < 0.0001$), and Northwest-South (z-ratio = 3.65, p = 0.005) (estimated marginal means, with a p-value adjustment in Bonferroni method, Table 2.9.2, Figure 2.4.2). However, there was only intermediate to high power for East-Northwest (power = 0.80), Middle-Northwest (power = 0.63), North 1-Northwest (power = 0.66), and North 2-Northeast (power = 0.98). Any intermediate-high power values where there was no significant effect noted in the GLMMs were ignored.

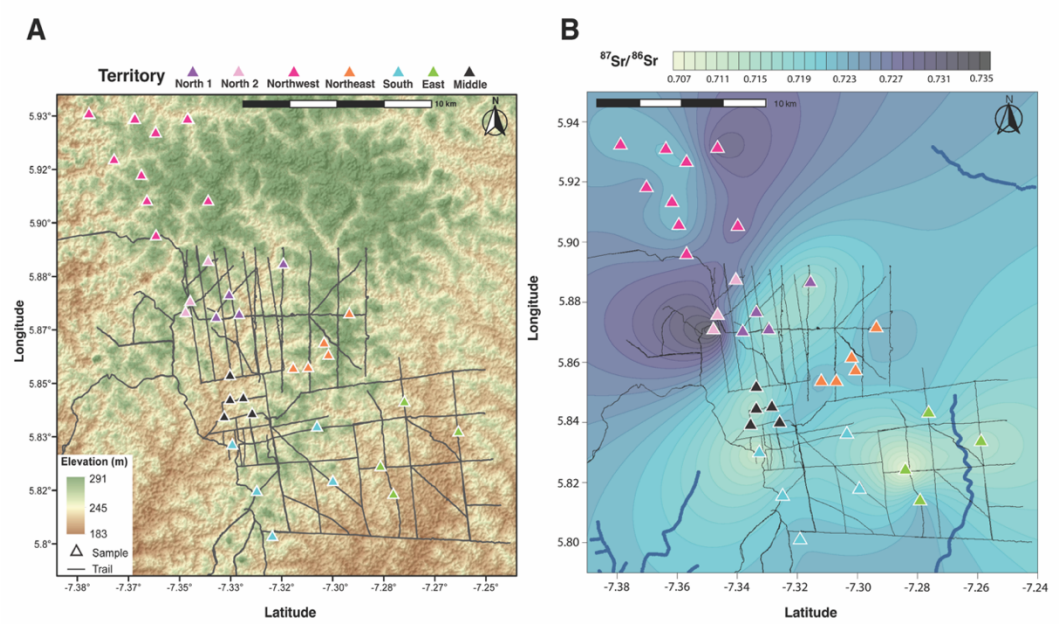

Figure 2.4.1. Map of the environmental sample locations obtained from the TCP study area. **A)** Digital elevation model (DEM) of the TCP study area. Elevation is represented by the color scale, where light green represents higher elevation and brown represents lower elevation in meters (m). **B)** Sr isoscape for the TCP area. Dark blue lines are rivers and streams, as visible on maps, and the overlying contour map is the kriging algorithm interpolation of $^{87}Sr/^{86}Sr$, forming a Sr isoscape of the region. The lighter-contoured regions represent lower Sr isotope ratios, and the darker-contoured regions represent higher Sr isotope ratios. Black lines indicate the trails and the relative extent of the TCP study area. North 1 represents the historic North community's territory from 1980 to 1999 (n = 4), and North 2 represents the modern North community's territory from 2000 to present (n = 3).

(2) Are there significant $^{87}Sr/^{86}Sr$ differences in chimpanzee enamel samples between chimpanzee communities?

$^{87}Sr/^{86}Sr$ ratios for resident male chimpanzees ranged from 0.71662 to 0.72187 (Table 2.3.1, Figure 2.4.2). Since there was a small sample size for reference males, no statistical tests were performed, and we exclusively assess the $^{87}Sr/^{86}Sr$ ratios for the "reference" resident males (n = 7) relative to the North community natal males (n = 10). The mean and median $^{87}Sr/^{86}Sr$ ratios for North community natal males are 0.71993 and 0.72023, respectively. The $^{87}Sr/^{86}Sr$ ratios for resident males from South (n = 4) and Middle (n = 1) communities males fell within the 2.5% (0.717) and 97.5%

(0.722) quantile range of North community natal males (summarized in Supporting Informations, Figure 2.9.2). The $^{87}Sr/^{86}Sr$ ratios for resident males from East community (n = 2) fell outside of the 2.5% (0.717) and 97.5% (0.722) quantile range of North community natal males. This suggests that the $^{87}Sr/^{86}Sr$ ratios for East community males does not overlap with North community natal males, however, due to the small sample size, we are not able to test the statistical significance of this pattern. Within the entire TCP study area, there was an average mismatch of 0.003 between natal males and their respective territories (Figure 2.4.2).

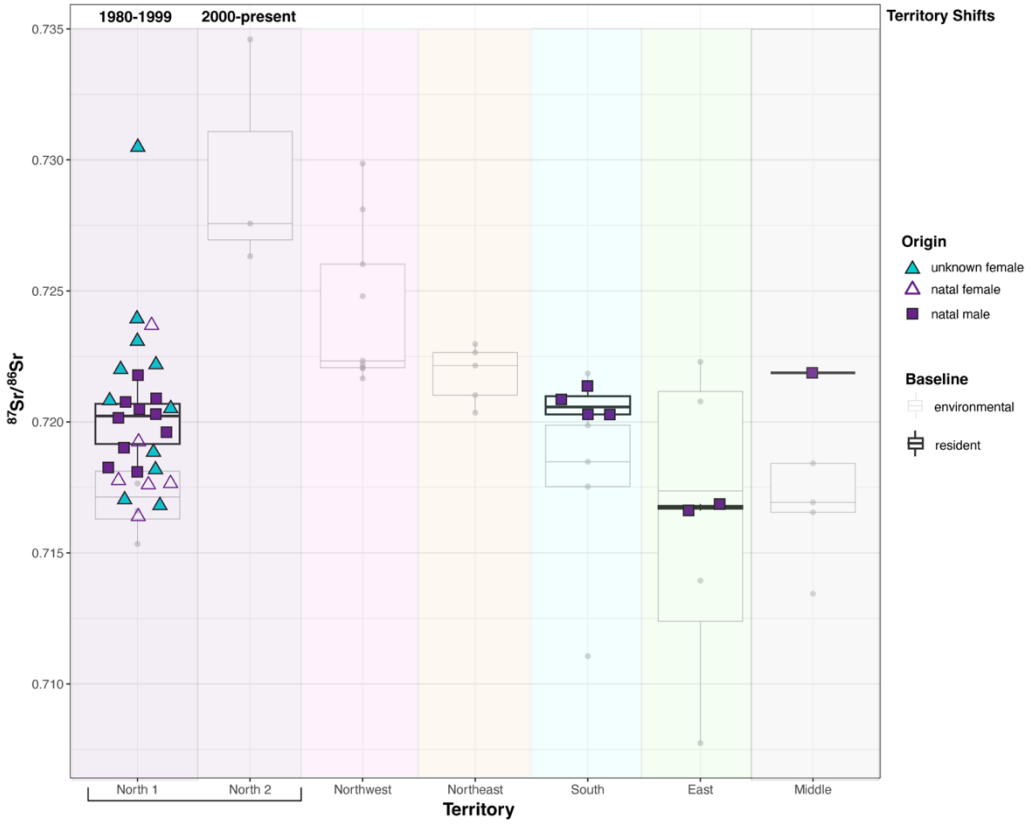

Figure 2.4.2. Boxplot of the environmental variation in $^{87}Sr/^{86}Sr$ by territory.
Boxplot illustrating the environmental variation in $^{87}Sr/^{86}Sr$ by territory, including territories of neighboring chimpanzee communities. For each chimpanzee territory, the black boxplots represent the median, upper, and lower quartiles for the $^{87}Sr/^{86}Sr$ data obtained from resident males. In contrast, grey boxplots represent the $^{87}Sr/^{86}Sr$ baseline obtained from environmental

data. Open triangles are natal subadult females not included in the resident chimpanzee baseline. Cyan triangles designate females of unknown natal status. North comprises individuals that formed tooth enamel before 1980 (n = 6) and after 1980 (n = 21), as well as environmental baseline samples that represent the historical (1980-1999) and modern (2000-present) territory location shifts. The areas Northwest and Northeast are represented only by environmental samples.

(3) Do $^{87}Sr/^{86}Sr$ ratios of unknown females correspond to those of natal individuals?

The $^{87}Sr/^{86}Sr$ ratios for adult females of unknown origin from pre-1980 (n = 4) and post-1980 (n = 7) ranged from 0.71681 to 0.73049 (Table 2.3.1, Figure 2.4.3). The full model had a lower AICc and GLMMs identified significant differences in $^{87}Sr/^{86}Sr$ ratios between adult female origin groups, where origin group was a fixed effect and tooth type was a random effect (Table 2.9.3). Complete model outputs are available in Supporting Information, Table 2.9.3 to 2.9.4 and Figure 2.4.3. The origin community, $^{87}Sr/^{86}Sr$ ratios in unknown female from post-1980 was significantly different from the North natal community (z-ratio = 4.08, $p < 0.000001$; Figure 2.4.3). A post-hoc analysis (estimate marginal means, with a p-value adjustment in Bonferroni method, Table 2.9.4) showed a significant pairwise difference between unknown females and North community residents post-1980 (z-ratio = -4.08, p = 0.0001, power = 0.94), as well as between unknown females post-1980 and pre-1980 (z-ratio = 4.41, $p < 0.0001$, power = 1.00). However, there were no significant differences between unknown females pre-1980 and North community residents post-1980 (z-ratio = 1.47, p = 0.42, power = 0.31).

The IQR*1.5 was 0.71944 $\pm$ 0.004 for North community residents (n = 16). When comparing unknown females (n = 11) to North community residents (0.715-0.723), we found that two out of the eleven unknown females (NF07, NF10) had

$^{87}Sr/^{86}Sr$ ratios that were outside of this range (18%, 0.724-0.730). While nine out of eleven unknown females (NF01, NF02, NF03, NF04, NF05, NF06, NF08, NF09, NF11) were within the $^{87}Sr/^{86}Sr$ ratios IQR*1.5 range (82%, 0.715-0.723) of North community residents (Figure 2.4.3).

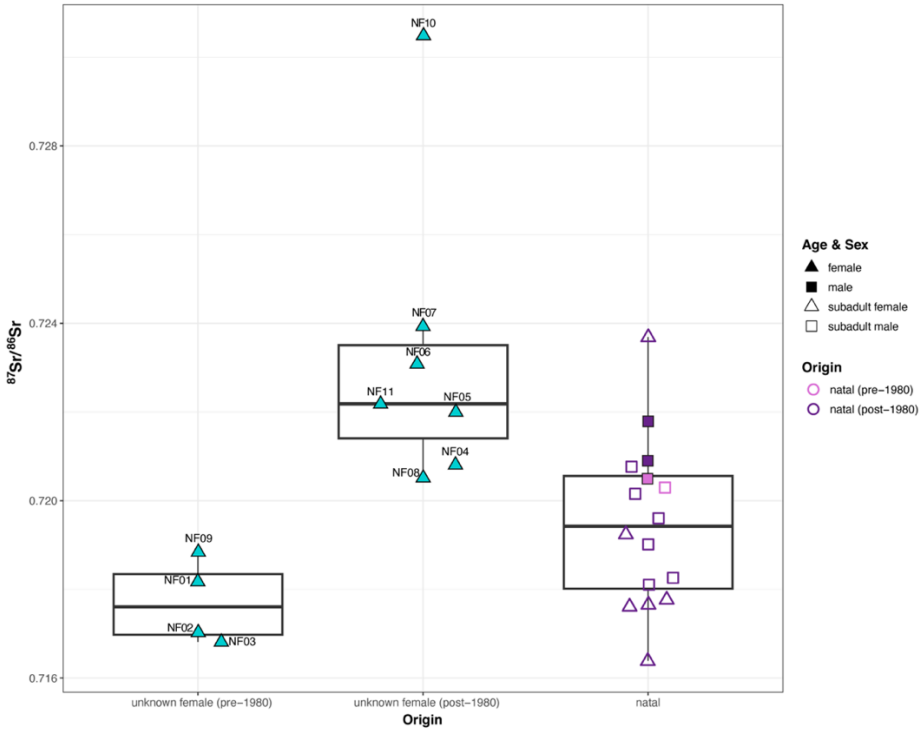

Figure 2.4.3. Boxplots illustrating the $^{87}Sr/^{86}Sr$ variation by origin group.
Boxplots consist of the median, upper, and lower quartiles, representing the interquartile range (IQR). Values beyond the vertical bars ("whiskers") fall beyond 1.5*IQR and are significant outliers. Unknown females comprise individuals that formed tooth enamel "before 1980" (n = 4) and "after 1980" (n = 7). North "natal" comprises individuals that formed tooth enamel before 1980 (n = 2) and after 1980 (n = 14).

2.5. Discussion

In this study, we measured the $^{87}Sr/^{86}Sr$ ratios of chimpanzee enamel from four communities and developed, with locally sourced environmental samples, a local isoscape of their territories (North, South, East, Middle), as well as two neighboring

territories (Northwest, Northeast). We show that the $^{87}Sr/^{86}Sr$ baselines differ between TCP chimpanzee territories and among some Taï chimpanzee communities. We demonstrate that natal males and subadult (pre-dispersal) females can be used to establish a chimpanzee community's $^{87}Sr/^{86}Sr$ baseline. This combined approach allowed us to use $^{87}Sr/^{86}Sr$ ratios to assess which females of unknown origin may have migrated to the TCP-established North Community. However, the exact region that these females could have originated remains unclear and would require more extensive environmental sampling of Taï National Park. There is a general mismatch between the local environmental and resident individual enamel $^{87}Sr/^{86}Sr$ data within each territory, which demands further exploration in the future (Figure 2.4.1).

The TCP study area is highly heterogeneous in $^{87}Sr/^{86}Sr$ ratios (Figure 2.4.1B), which is in line with our observations of general geological heterogeneity in the field but was not supported by the low resolution of geological maps available for this part of Côte d'Ivoire. Within the TCP study area, the environmental $^{87}Sr/^{86}Sr$ ratios range from 0.708 to 0.735, a remarkable range for a relatively small study area of less than 400km^2. However, we do recognize that some variation in $^{87}Sr/^{86}Sr$ ratios could be missed by our relatively small sample size ($n < 10$) for each chimpanzee territory. Even more radiogenic $^{87}Sr/^{86}Sr$ ratios, ranging from 0.724 to 0.767 have been measured approximately 50 to 60 km southeast at the ecotourism site of Djouroutou (Wang et al., in review). This demonstrates that there is immense geological variability within TNP that early geological surveys from the greater park region could not account for (Rouw et al., 1990). It is also noteworthy that the observed

$^{87}Sr/^{86}Sr$ range within the TCP study area aligns with what is reported for Saharan dunes (0.713-0.737), suggesting that there could be a strong influence of the Harmattan season (Stojanowski & Knudson, 2011). Dusts from the Sahara Desert, specifically from the sand dunes in Libya and Chad can have Sr concentrations ranging from 76 to 202 ppm, and Rb concentrations ranging from 53 to 67 ppm (Gross, Palchan, Krom, & Angert, 2016). Therefore, it is possible that within Taï, the $^{87}Sr/^{86}Sr$ variability in plants and the slightly higher $^{87}Sr/^{86}Sr$ ratios for chimpanzee enamel are driven by the seasonal influx of Sahara dust (Frumkin & Stein, 2004). The Harmattan dust typically reaches the TNP in early January and is estimated to deposit around 60-100 kg/ha in the Taï forest (Stoorvogel, Van Breemen, & Jassen, 1997; Wittig, 2018). There was a strong influence of the Harmattan between 1992 and 2009, which overlaps with tooth formation periods of some of the sampled individuals (Table 2.3.1; Schulz-Kornas, Stuhlträger, Clauss, Wittig, & Kupczik, 2019). During the Harmattan, Taï chimpanzees have even been found to respond with less chewing, leading to larger fecal particle size during Harmattan season (Schulz-Kornas et al., 2019). We propose that the seasonal influx of dust during the Harmattan also influences the $^{87}Sr/^{86}Sr$ characteristics of Taï forest, and as a result, could contribute to the isotopic mismatch between resident chimpanzees and their territories.

We found isotopic differences between neighboring chimpanzee territories. For the historic North Community territory, we found that Middle and South Communities overlapped in the isotopic baselines from environmental $^{87}Sr/^{86}Sr$ and chimpanzee enamel $^{87}Sr/^{86}Sr$ ratios, suggesting geological homogeneity across these

territories. When considering the environmental $^{87}Sr/^{86}Sr$ ratios for modern North Community territory (referred to as North 2 in Tables 2.3.1 and S1-S2), there are significant differences in $^{87}Sr/^{86}Sr$ ratios when compared to the territories of historic North Community (referred to as North 1 in Tables 2.3.1, 2.9.1 and 2.9.2), South Community, East Community, Middle Community, and Northeast Community (Table 2.9.2). However, the statistical power was low for the comparisons between the modern North community and East (0.02), Middle (0.01), historic North (0.01), and South (0.29) community's territories (Table 2.9.2). This could suggest the following: (1) there was a high Type II error, since we used the more conservative Bonferroni method, (2) there was high variance among the samples, and (3) the sample size was too small to detect an effect. In spite of this, high statistical power when comparing the Northwest and Northeast territories suggest that these territories are indeed statistically different from the other territories (Table 2.9.2, Figure 2.4.2). The modern North Community appears to be characterized by higher geological heterogeneity than the historic North territory, which could be related to the proximity to the prominent granite outcrops (inselbergs) in the Northwest territory (Figures 2.4.1 to 2.4.2, and 2.9.6). Similarly, in the northwestern northeastern, and western parts of the TCP area, we found more radiogenic $^{87}Sr/^{86}Sr$ baseline ratios (Table 2.9.1 and 2.9.2, Figure 2.4.1), likely driven by inselbergs in these regions (see elevation in Figure 2.4.1A). In contrast, the Middle, East, and South regions are marked by lower $^{87}Sr/^{86}Sr$ ratios (Table 2.9.1 and 2.9.2, Figures 2.4.1 and 2.4.2), which could be related to the influx of extrinsic sediment from the Cavally and Sassandra Rivers (Goldstein

& Jacobsen, 1987). Indeed, water related weathering and erosion, which affect the Sr concentration in river runoff, can result in lower $^{87}Sr/^{86}Sr$ ratios in riparian environments (Capo et al., 1998; Sillen, Hall, Richardson, & Armstrong, 1998).While there are some inselbergs in South, and East territories, we suggest that the environmental $^{87}Sr/^{86}Sr$ ratios are possibly driven by increased weathering related to several small river systems (Figure 2.4.1B and 2.4.2; Luncz et al., 2016). Particularly in East territory, we know of well documented offshoots of the Cavally River, which could influence the distinct pattern in $^{87}Sr/^{86}Sr$ ratios observed in this area (Hamilton, Nelson, Fernandez, & Hunt, 2019; Poszwa, Dambrine, Ferry, Pollier, & Loubet, 2002; Poszwa et al., 2004).

The overall heterogeneity in geology, landscape and the reported $^{87}Sr/^{86}Sr$ ratios allowed us to detect differences between neighboring chimpanzee territories and between resident individuals of these neighboring communities. We found that $^{87}Sr/^{86}Sr$ ratios from resident males in East community (0.716) did not overlap with those from resident males in North community (0.717-0.722, Figure 2.9.5). However, all other chimpanzee reference communities (South and Middle) were within the $^{87}Sr/^{86}Sr$ range of North community resident males (Figure 2.9.5). The unique $^{87}Sr/^{86}Sr$ ratios for East community could be related to the riparian environment in this territory, or the isotopic variation in this community may not have been captured by our small sample size (n = 2). We also found that in North Community, $^{87}Sr/^{86}Sr$ ratios differed between resident males and resident subadult females, where females have lower $^{87}Sr/^{86}Sr$ ratios (Figure 2.4.3). In fact, pre-dispersal subadult females

appear to align better with the environmental baseline for North Community (see Figure 2.4.2). This unexpected sex-difference could possibly be related to diet, with subadult females engaging more in nut-cracking (Boesch & Boesch, 1984). Subadult males do engage in hunting and meat eating, but meat is less than 1% of the overall diet (Boesch & Boesch, 1989; Bertin & Wittig, 2019). Other studies have suggested that meat must make up 90% of a diet before influencing $^{87}Sr/^{86}Sr$ ratios, due to low concentrations of Sr and Ca (Burton & Price, 2002; Burton & Wright, 1995; Runia, 1987). Therefore, we propose that the sex difference could be related to the $^{87}Sr/^{86}Sr$ variation in plants, and more females participating in nut-cracking relative to males.

The combination of the environmental isotope data from the TCP study area and our comparison with resident individuals allowed us to assess the migratory history of several adult females of unknown origin who resided in North Community as adults. First, we show that there is a significant difference in $^{87}Sr/^{86}Sr$ ratios between unknown females pre-1980 (0.717-0.719, n = 4) and post-1980 (0.719-0.730, n = 7). Since unknown females pre-1980 (0.71771) do not overlap with pre-1980 natal males (0.72039), which are shown to align with post-1980 natal males (Figure 2.9.1), it is unclear if this relates to an unknown territory shift in pre-1980 North community residents pre-1980, a sex-difference in diet, or a potential origin locality with similar $^{87}Sr/^{86}Sr$ ratios to the historic North community's territory. The lower variance in $^{87}Sr/^{86}Sr$ ratios for unknown females pre-1980 could also indicate a much smaller population density relative to post-1980. Additionally, since pre-1980 unknown females overlap with East community (Figure 2.4.2), it is possible that the

territory of North community was oriented slightly more east, where there is an area with lower $^{87}Sr/^{86}Sr$ ratios (Figure 2.4.1B). However, additional environmental samples will be needed to confirm this.

From direct observations in the Taï chimpanzees, it is estimated that around 88% of females disperse from their natal territory (Boesch, 1997; Lemoine et al., 2019). For the historically well-studied North Community, we show that females of unknown origin post-1980 (n = 7) are significantly different from resident individuals post-1980. However, due to our small sample size, this could be influenced by two females that have much higher $^{87}Sr/^{86}Sr$ ratios (0.723 and 0.730) than the mean for pre-1980 unknown females (0.71734, n = 3) and post-1980 unknown females (0.72124, n = 6). In spite of this, all unknown females are within the $^{87}Sr/^{86}Sr$ range of the larger TCP study area (Figures 2.4.2 and 2.4.3), suggesting that these females might come from neighboring communities, or the other parts of Taï forest with similar $^{87}Sr/^{86}Sr$ ratios. Our isotope data suggests that only two females (NF07 and NF10) categorized as of unknown origin in North Community indeed did not overlap with the $^{87}Sr/^{86}Sr$ ratios of North territory at the time their teeth formed, nor do they match resident males and subadult females. This suggests they likely migrated to North Community from elsewhere. It is possible that these females could be from areas in the modern North (0.726-0.735), Northwest (0.722-0.729), Northeast (0.720-0.723), or territories that have more radiogenic $^{87}Sr/^{86}Sr$ ratios like those observed for Djouroutou (0.724-0.767, Wang et al., in review). Nine of these females (NF01, NF02, NF03, NF04, NF05, NF06, NF08, NF09, NF11) were within the $^{87}Sr/^{86}Sr$

IQR*1.5 (0.715-0.723) of North community residents, suggesting that they are in line with the median $^{87}Sr/^{86}Sr$ ratio for North Community natives, but it is also possible that they could be from a territory with similar $^{87}Sr/^{86}Sr$ ratios further away. Since there is significant overlap between the historic North Community territory (0.716-0.719) with South Community (0.711-0.722) and Middle Community territory (0.713-0.722), we also suggest that it is possible these nine females are from other TCP-established territories (see Figure 2.4.2). However, without more extensive environmental sampling of the TNP, it is possible there are other areas within TNP that have similar $^{87}Sr/^{86}Sr$ ratios, therefore exact locations of origins are difficult to determine.

2.6. Limitations and further considerations

There are several constraints within the scope of this study, such as the absence of reliable geological maps for our study area, the limited environmental sampling, and the isotopic mismatch between resident chimpanzees and their territories. We recommend the consideration of these limitations in future work that employs $^{87}Sr/^{86}Sr$ analysis in tracking female dispersal in skeletal remains of great apes, as well as the limitations of using $^{87}Sr/^{86}Sr$ ratios to inform early hominin dispersal models.

A main limitation of this study is that there are very little geological data available for TNP and almost none for the TCP study area (Collinet et al., 1984; Kolongo et al., 2006; Rouw et al., 1990). This limited our ability to build a more robust local and regional isoscape using machine learning approaches (e.g. see

Bataille et al. 2020) that could have taken geological and other environmental factors into consideration and allowed us to make predictions on female origins inside and outside of the TCP stduy area. Further, as a result of the limited scope of this study, we primarily sampled the local TCP study area to determine the isotopic variation within and across neighboring chimpanzee territories. More extensive environmental sampling of the larger TNP forest would expand this study's Sr isoscape and allow for a more nuanced interpretation of the possible origins of immigrant females.

We also found lower $^{87}Sr/^{86}Sr$ ratios in environmental samples compared to the respective resident $^{87}Sr/^{86}Sr$ ratios for several chimpanzee communities and their territories (see Figure 2.4.2). These isotopic mismatches could be related to variation in nutrient sources and/or variation in sampled plants' rooting depths (Grimstead, Nugent, & Whipple, 2017). Chimpanzees tend to consume foods from a variety of sources (fruit, leaves, bark, pith, termites, ants, primates) (Bertin & Wittig, 2019), resulting in a mixed dietary $^{87}Sr/^{86}Sr$ signal relative to any single measured plant, which will primarily obtain its $^{87}Sr/^{86}Sr$ ratios from the immediate soil substrate (Wright, 2005). Another possible explanation is that there is variation in rooting depths for the tree species sampled in this study (*Sarcophrynium brachystachyum, Musanga cecropioides, Parkia bicolor, Afzelia bella, Sterculia oblonga, Coula edulis, Dialium aubrevillei*). Overall, trees are described as diverse in $^{87}Sr/^{86}Sr$ ratios due to their variable rooting depths (Poszwa et al., 2004). In primary tropical rainforests however, the humus layer is commonly shallow and rooting depth is overall low. In fact, none of the species sampled are known to exhibit unusually deep root systems

(Koffi et al., 2022). However, foliar Sr levels still might differ in terms of nutrient sourcing, and their ability to sequester Sr from wind-blown dust, such as those that are associated with the Harmattan season discussed above (Grimstead et al., 2017). It is also possible that historical territory shifts occurred and resulted in the mismatch between the resident chimpanzee $^{87}Sr/^{86}Sr$ ratios and the environmental $^{87}Sr/^{86}Sr$ ratios measured from environmental samples in their present-day territories. It is also worth noting that the other chimpanzee communities (South: 1997, Middle: 2000, East: 2005, Northeast: 2015) were habituated much later than North Community (ca. 1985, after Boesch & Wittig, 2019; Lemoine et al., 2019), and therefore territory shifts before tooth enamel formation of resident community members remain unknown and unaccounted for. South Community shifted their territory further south since habituation, which could explain the difference in $^{87}Sr/^{86}Sr$ ratios between their historic and modern territory (Boesch & Wittig, 2019). The single male sampled for Middle Community formed its enamel prior to habituation and it is possible that his community occupied a slightly different territory before they were habituated in 2000.

Hence, when sampling skeletal tissues from chimpanzees to study natal dispersal, the limitations in the recently observed past of the study subjects need to be considered, particularly in long-term research projects with historic skeletal collections, such as the Taï Chimpanzee Project. Ideally, we would be able to measure a pre- and post-dispersal isotope ratio from the same skeleton to identify natal dispersal over larger distances. This could be achieved by sampling early and late forming teeth from the same individual, as is increasingly done in archeological

human populations e.g., (Knipper et al., 2017). However, given that in chimpanzees all teeth form and mineralize well before natal dispersal (< 9 years old), this is not an option. It is possible that bone could capture a post-dispersal isotope signal incorporated over a lifetime, although, bone is prone to Sr contamination (Hoppe et al., 2003), especially in the case of museum curated specimens, which may have been chemically treated for preservation purposes. While sampling teeth and bone could be an option, this would limit research to historic populations.

There are possible alternatives to skeletal tissues for studying the elusive migration of female chimpanzees, such as hair. In humans, the $^{87}Sr/^{86}Sr$ ratios of hair can indicate an individual's geographical origin (Vautour, Poirier, & Widory, 2015), and hair can easily be collected from great ape sleeping nests (Oelze et al., 2011; Oelze, 2016; Oelze et al., 2020). However, isotope ratios in chimpanzee hair can be expected to only record several months of an individual's life (Oelze, 2016). Therefore, hair samples would need to be collected from very recently immigrated females, who are commonly unhabituated, and thereby inaccessible for sampling from researchers. This presents an unfortunate dilemma when considering the future applications of $^{87}Sr/^{86}Sr$ analysis to assess natal dispersal in African great apes, and with that, their use as points of reference when studying early hominin natal dispersal. One solution to this dilemma is the habituation of numerous neighboring chimpanzee communities, which is time and cost intensive, yet increasingly common at long-term field sites. In theory, this would enable direct observations and occasional monitoring of the transition of a habituated female from one community into another, and the

potential to witness the social challenges immigrant females may face in their new social community, as well as the unique cultural transitions she might engage in (Luncz & Boesch, 2014). Another solution is to use multi-proxy isotope profiles (C, N, O, H, S, and Pb) coupled with DNA analysis, which has been useful in identifying individuals and tracking origin in forensic cases (Bartelink & Chesson, 2019). Complementing multi-proxy methods with $^{87}Sr/^{86}Sr$ analysis has the potential to improve our assessment of the migration patterns between multiple chimpanzee communities. When considering historic and modern migration patterns, the integration of $^{87}Sr/^{86}Sr$ analysis offers crucial geographical information, which can significantly reduce the potential origin locales when attempting to identify possible migrants.

2.7. Acknowledgments

We thank the Ministère de l'Enseignement Supérieur et de la Recherche Scientifique of Côte d'Ivoire, the Ministère de Eaux et Forêts of Côte d'Ivoire and the Office Ivorien des Parcs et Réserves for permissions to conduct the study. We are grateful to Christophe Boesch, who founded the field site and started the skeletal collection, to Jean-Jacques Huiblin for curating it, the Centre Suisse de Recherches Scientifiques en Côte d'Ivoire and the staff members of the Taï Chimpanzee Project for their long-term support. The Swiss National Foundation provided core funding for the Taï Chimpanzee Project before 1997 and the Max Planck Society since 1997. We are particularly grateful to Zwedi Tsegai for assisting during sampling and providing CT data, Manuel Trost for preparing the clean lab consumables and space (lab tech

MPI-EVA), Eden Washburn for support with sample preparation, Brian Dreyer for support with the ICP-MS, as well as Terry Blackburn, Gavin Piccione, and Graham Harper Edwards for providing TIMS support.

2.8. References Cited

Aarons, S. M., Aciego, S. M., Arendt, C. A., Blakowski, M. A., Steigmeyer, A., Gabrielli, P., . . . Baccolo, G. (2017). Dust composition changes from Taylor Glacier (East Antarctica) during the last glacial-interglacial transition: A multi-proxy approach. *Quaternary Science Reviews, 162*, 60-71.

Åberg, G. (1995). The use of natural strontium isotopes as tracers in environmental studies. *Water, Air, and Soil Pollution, 79*, 309-322.

Anderson, D., & Burnham, K. (2004). Model selection and multi-model inference. Springer.

Arandjelovic, M., Boesch, C., Campbell, G., Hohmann, G., Junker, J., Kouakou, Y., . . . Möbius, Y. (2020). Pan African Programme: the cultured chimpanzee. *Guidelines for Research and Data Collection*.

Balter, V., Braga, J., Télouk, P., & Thackeray, J. F. (2012). Evidence for dietary change but not landscape use in South African early hominins. *Nature, 489*(7417), 558.

Bartelink, E. J., & Chesson, L. A. (2019). Recent applications of isotope analysis to forensic anthropology. *Forensic sciences research, 4*(1), 29-44.

Bartlett, M. S. (1937). Properties of sufficiency and statistical tests. *Proceedings of the Royal Society of London. Series A-Mathematical and Physical Sciences, 160*(901), 268-282.

Barton, K., & Barton, M. K. (2015). Package 'mumin'. Version, 1(18), 439.

Bataille, C. P., & Bowen, G. J. (2012). Mapping 87Sr/86Sr variations in bedrock and water for large scale provenance studies. *Chemical Geology, 304*, 39-52.

Bataille, C. P., Crowley, B. E., Wooller, M. J., & Bowen, G. J. (2020). Advances in global bioavailable strontium isoscapes. *Palaeogeography, palaeoclimatology, palaeoecology*, 109849.

Bataille, C. P., von Holstein, I. C., Laffoon, J. E., Willmes, M., Liu, X.-M., & Davies, G. R. (2018). A bioavailable strontium isoscape for Western Europe: A machine learning approach. *PloS One, 13*(5), e0197386.

Beard, B. L., & Johnson, C. M. (2000). Strontium isotope composition of skeletal material can determine the birth place and geographic mobility of humans and animals. *Journal of Forensic Science, 45*(5), 1049-1061.

Bentley, R. A. (2006). Strontium isotopes from the earth to the archaeological skeleton: a review. *Journal of archaeological method and theory, 13*(3), 135-187.

Bertin, B. Z. B. G., & Wittig, R. (2019). Long-term diet of the chimpanzees (Pan troglodytes verus) in Taï National Park: interannual variation in consumption. In C. Boesch, R. Wittig, C. Crockford, L. Vigilant, T. Deschner, & F. Leendertz (Eds.), *The Chimpanzees of Taï Forest: 40 Years of Research*.

Boesch, C. (1991). The Effects of Leopard Predation On Grouping Patterns in Forest Chimpanzees. *Behaviour, 117*(3-4), 220-241. doi:https://doi.org/10.1163/156853991X00544

Boesch, C. (1997). Evidence for dominant wild female chimpanzees investing more in sons. *Animal Behaviour, 54*(4), 811-815.

Boesch, C., & Boesch, H. (1984). Possible causes of sex differences in the use of natural hammers by wild chimpanzees. *Journal of human evolution, 13*(5), 415-440.

Boesch, C., & Boesch, H. (1989). Hunting behavior of wild chimpanzees in the Tai National Park. *American journal of physical anthropology, 78*(4), 547-573.

Boesch, C., & Boesch-Achermann, H. (2000). *The chimpanzees of the Taï Forest: Behavioural ecology and evolution*: Oxford University Press, USA.

Boesch, C., Kohou, G., Néné, H., & Vigilant, L. (2006). Male competition and paternity in wild chimpanzees of the Taï forest. *American Journal of Physical Anthropology: The Official Publication of the American Association of Physical Anthropologists, 130*(1), 103-115.

Boesch, C., & Wittig, R. (2019). Demography and life history of five chimpanzee communities in Taï National Park. In C. Boesch, R. Wittig, C. Crockford, L. Vigilant, T. Deschner, & F. Leendertz (Eds.), *The Chimpanzees of the Taï Forest: 40 Years of Research* (pp. 159-177). Cambridge: Cambridge University Press.

Boesch, C., Gotanegre, A., Hillers, A., Kouassi, J., Boesch, H., Kizila, P., & Normand, E. (2021). Lessons learned while protecting wild chimpanzees in West Africa. *American journal of primatology, 83*(4), e23209.

Bolker, B. M., Brooks, M. E., Clark, C. J., Geange, S. W., Poulsen, J. R., Stevens, M. H. H., & White, J.-S. S. (2009). Generalized linear mixed models: a practical guide for ecology and evolution. *Trends in ecology & evolution, 24*(3), 127-135. doi:https://doi.org/10.1016/j.tree.2008.10.008

Brennan, S. R., Zimmerman, C. E., Fernandez, D. P., Cerling, T. E., McPhee, M. V., & Wooller, M. J. (2015). Strontium isotopes delineate fine-scale natal origins and migration histories of Pacific salmon. *Science advances, 1*(4), e1400124.

Britton, K., Le Corre, M., Willmes, M., Moffat, I., Grün, R., Mannino, M. A., . . . Jaouen, K. (2020). Sampling Plants and Malacofauna in 87Sr/86Sr Bioavailability Studies: Implications for Isoscape Mapping and Reconstructing of Past Mobility Patterns. *Frontiers in Ecology and Evolution, 8*(446). doi:10.3389/fevo.2020.579473

Brooks, M., Bolker, B., Kristensen, K., & Maechler, M. (2022). Package 'glmmTMB'.

Burton, J. H., & Price, T. D. (2002). The use and abuse of trace elements for paleodietary research. In *Biogeochemical approaches to paleodietary analysis* (pp. 159-171): Springer.

Burton, J. H., & Wright, L. E. (1995). Nonlinearity in the relationship between bone Sr/Ca and diet: paleodietary implications. *American journal of physical anthropology, 96*(3), 273-282.

Campbell, G., Kuehl, H., Kouamé, P. N. G., & Boesch, C. (2008). Alarming decline of West African chimpanzees in Côte d'Ivoire. *Current Biology, 18*(19), R903-R904.

Capo, R. C., Stewart, B. W., & Chadwick, O. A. (1998). Strontium isotopes as tracers of ecosystem processes: theory and methods. *Geoderma, 82*(1-3), 197-225.

Chappell, B. W., & White, A. J. R. (2001). Two contrasting granite types: 25 years later. *Australian Journal of Earth Sciences, 48*(4), 489-499. doi:10.1046/j.1440-0952.2001.00882.x

Chazan, M. (2022). Early hominin group size: A perspective from Bestwood 1, Northern Cape Province, South Africa. *Quaternary international, 614*, 7-15. doi:https://doi.org/10.1016/j.quaint.2021.05.017

Clutton-Brock, T. H., & Lukas, D. (2012). The evolution of social philopatry and dispersal in female mammals. *Molecular Ecology, 21*(3), 472-492. doi:https://doi.org/10.1111/j.1365-294X.2011.05232.x

Collinet, J., Monteny, B., & Pouyaud, B. (1984). Le milieu physique. Pp in: Recherche et aménagement en milieu forestier tropical humide: le Projet Taï de Côte d'Ivoire,(éd.) Guillaumet, JL, Couturier, G. et Dosso, H. Notes du MAB, n 15. In: UNESCO, Paris, France.

Copeland, S. R., Sponheimer, M., de Ruiter, D. J., Lee-Thorp, J. A., Codron, D., le Roux, P. J., . . . Richards, M. P. (2011). Strontium isotope evidence for landscape use by early hominins. *Nature, 474*(7349), 76.

Copeland, S. R., Sponheimer, M., le Roux, P. J., Grimes, V., Lee-Thorp, J. A., de Ruiter, D. J., & Richards, M. P. (2008). Strontium isotope ratios (87Sr/86Sr) of tooth enamel: a comparison of solution and laser ablation multicollector inductively coupled plasma mass spectrometry methods. *Rapid Communications in Mass Spectrometry: An International Journal Devoted to the Rapid Dissemination of Up-to-the-Minute Research in Mass Spectrometry, 22*(20), 3187-3194.

Cressie, N. (1990). The origins of kriging. *Mathematical geology, 22*(3), 239-252.

Cressie, N. (2015). *Statistics for spatial data*: John Wiley & Sons.

Crowley, B. E., & Godfrey, L. R. (2019). Strontium Isotopes Support Small Home Ranges for Extinct Lemurs. *Frontiers in Ecology and Evolution, 7*(490). doi:10.3389/fevo.2019.00490

Crowley, B. E., Miller, J. H., & Bataille, C. P. (2017). Strontium isotopes (87Sr/86Sr) in terrestrial environmental and palaeoenvironmental research: empirical efforts and recent advances in continental-scale models. *Biological Reviews, 92*(1), 43-59.

Delignette-Muller, M. L., & Dutang, C. (2015). fitdistrplus: An R package for fitting distributions. *Journal of Statistical Software, 64*, 1-34.

Deniel, C., & Pin, C. (2001). Single-stage method for the simultaneous isolation of lead and strontium from silicate samples for isotopic measurements. Analytica Chimica Acta, 426(1), 95–103.

Dominy, N. J., Ikram, S., Moritz, G. L., Wheatley, P. V., Christensen, J. N., Chipman, J. W., & Koch, P. L. (2020). Mummified baboons reveal the far reach of early Egyptian mariners. *eLife, 9*. doi:10.7554/eLife.60860

Driessens, F. C., & Verbeeck, R. (1990). *Biominerals*: CRC press.

Fannin, L. D., Yeakel, J. D., Venkataraman, V. V., Seyoum, C., Geraads, D., Fashing, P. J., . . . Dominy, N. J. (2021). Carbon and strontium isotope ratios shed new light on the paleobiology and collapse of Theropithecus, a primate experiment in graminivory. *Palaeogeography, palaeoclimatology, palaeoecology, 572*, 110393.

Faure, G., & Powell, J. L. (2012). *Strontium isotope geology* (Vol. 5): Springer Science & Business Media.

Frumkin, A., & Stein, M. (2004). The Sahara–East Mediterranean dust and climate connection revealed by strontium and uranium isotopes in a Jerusalem speleothem. *Earth and Planetary Science Letters, 217*(3-4), 451-464.

Gagneux, P., Boesch, C., & Woodruff, D. S. (1999). Female reproductive strategies, paternity and community structure in wild West African chimpanzees. *Animal Behaviour, 57*(1), 19-32.

Goldstein, S. J., & Jacobsen, S. B. (1987). The Nd and Sr isotopic systematics of river-water dissolved material: Implications for the sources of Nd and Sr in seawater. *Chemical Geology: Isotope Geoscience section, 66*(3), 245-272. doi:https://doi.org/10.1016/0168-9622(87)90045-5

Goodall, J. (1986). The chimpanzees of Gombe: Patterns of behavior.

Gordon, A. D., Green, D. J., & Richmond, B. G. (2008). Strong postcranial size dimorphism in Australopithecus afarensis: results from two new resampling methods for multivariate data sets with missing data. *American Journal of Physical Anthropology: The Official Publication of the American Association of Physical Anthropologists, 135*(3), 311-328.

Gosz, J. R., Brookins, D. G., & Moore, D. I. (1983). Using strontium isotope ratios to estimate inputs to ecosystems. *Bioscience, 33*(1), 23-30.

Grimstead, D. N., Nugent, S., & Whipple, J. (2017). Why a Standardization of Strontium Isotope Baseline Environmental Data Is Needed and Recommendations for Methodology. *Advances in Archaeological Practice, 5*(2), 184-195. doi:10.1017/aap.2017.6

Gross, A., Palchan, D., Krom, M. D., & Angert, A. (2016). Elemental and isotopic composition of surface soils from key Saharan dust sources. *Chemical Geology, 442*, 54-61. doi:https://doi.org/10.1016/j.chemgeo.2016.09.001

Guillaumet, J.-L., & Adjanohoun, E. (1971). La végétation de la Côte d'Ivoire. *Le milieu naturel de la Côte d'Ivoire*(50), 166-262. https:// www.documentation.ird.fr/hor/fdi:16372

Hamilton, M. I., Fernandez, D. P., & Nelson, S. V. (2021). Using strontium isotopes to determine philopatry and dispersal in primates: a case study from Kibale National Park. *Royal Society open science, 8*(2), 200760.

Hamilton, M. I., Nelson, S. V., Fernandez, D. P., & Hunt, K. D. (2019). Detecting riparian habitat preferences in "savanna" chimpanzees and associated Fauna with strontium isotope ratios: Implications for reconstructing habitat use by the chimpanzee-human last common ancestor. *American journal of physical anthropology, 170*(4), 551-564.

Hammond, R. L., Lawson Handley, L. J., Winney, B. J., Bruford, M. W., & Perrin, N. (2006). Genetic evidence for female-biased dispersal and gene flow in a polygynous primate. *Proceedings of the Royal Society B: Biological Sciences, 273*(1585), 479-484.

Hartig, F., & Hartig, M. F. (2017). Package 'DHARMa'. *Vienna, Austria: R Development Core Team*.

Heydari-Guran, S., & Ghasidian, E. (2020). Late Pleistocene hominin settlement patterns and population dynamics in the Zagros Mountains: Kermanshah region. *Archaeological Research in Asia, 21*, 100161. doi:https://doi.org/10.1016/j.ara.2019.100161

Hill, K. R., Walker, R. S., Božičević, M., Eder, J., Headland, T., Hewlett, B., . . . Wood, B. (2011). Co-residence patterns in hunter-gatherer societies show unique human social structure. *Science, 331*(6022), 1286-1289.

Hoppe, K. A., Koch, P. L., & Furutani, T. (2003). Assessing the preservation of biogenic strontium in fossil bones and tooth enamel. *International Journal of Osteoarchaeology, 13*(1-2), 20-28.

Hurst, R. W., & Davis, T. E. (1981). Strontium isotopes as tracers of airborne fly ash from coal-fired power plants. *Environmental Geology, 3*(6), 363-367. doi:10.1007/bf02473525

Inoue, E., Inoue-Murayama, M., Vigilant, L., Takenaka, O., & Nishida, T. (2008). Relatedness in wild chimpanzees: influence of paternity, male philopatry, and demographic factors. *American Journal of Physical Anthropology: The Official Publication of the American Association of Physical Anthropologists, 137*(3), 256-262.

Johnson, M. L., & Gaines, M. S. (1990). Evolution of dispersal: theoretical models and empirical tests using birds and mammals. *Annual review of ecology and systematics, 21*(1), 449-480.

Journel, A. G., & Journel, A. G. (1989). *Fundamentals of geostatistics in five lessons* (Vol. 8): American Geophysical Union Washington.

Knight, A., Chapman, H. M., & Hale, M. (2016). Habitat fragmentation and its implications for Endangered chimpanzee Pan troglodytes conservation. *Oryx, 50*(3), 533-536. doi:10.1017/S0030605315000332

Knipper, C., Mittnik, A., Massy, K., Kociumaka, C., Kucukkalipci, I., Maus, M., . . . Stockhammer, P. W. (2017). Female exogamy and gene pool diversification at the transition from the Final Neolithic to the Early Bronze Age in central Europe. *Proceedings of the National Academy of Sciences, 114*(38), 10083-10088. doi:doi:10.1073/pnas.1706355114

Koch, P. L., Heisinger, J., Moss, C., Carlson, R. W., Fogel, M. L., & Behrensmeyer, A. K. (1995). Isotopic tracking of change in diet and habitat use in african elephants. *Science, 267*(5202), 1340-1343. doi:10.1126/science.267.5202.1340

Koenig, A., & Borries, C. (2012). Hominoid dispersal patterns and human evolution. *Evolutionary Anthropology: Issues, News, and Reviews, 21*(3), 108-112.

Koffi, K. K. S., Dosso, K., Barot, S., Wittig, R. M., Aristophanous, M., Moretto, P., . . . Seydou, T. (2022). Chimpanzees, dung beetles and seed dispersal: implications for habitat conservation of the West African chimpanzee Pan troglodytes verus in Taï National Park, Côte d'Ivoire. *Research Square*.

Kolongo, T. S. D., Decocq, G., Yao, C. Y. A., Blom, E. C., & Van Rompaey, R. S. (2006). Plant species diversity in the southern part of the Tai National Park (Côte d'Ivoire). *Biodiversity & Conservation, 15*(7), 2123-2142.

Kouakou, C. Y., Boesch, C., & Kuehl, H. S. (2011). Identifying hotspots of chimpanzee group activity from transect surveys in Taï National Park, Côte d'Ivoire. *Journal of Tropical Ecology, 27*(6), 621-630. doi:10.1017/S0266467411000423

Kühl, H. S., Sop, T., Williamson, E. A., Mundry, R., Brugière, D., Campbell, G., . . . Boesch, C. (2017). The Critically Endangered western chimpanzee declines by 80. *Am J Primatol, 79*(9). doi:10.1002/ajp.22681

Kumle, L., Võ, M. L.-H., & Draschkow, D. (2021). Estimating power in (generalized) linear mixed models: An open introduction and tutorial in R. Behavior research methods, 53(6), 2528-2543.

Langergraber, K. E., Rowney, C., Crockford, C., Wittig, R., Zuberbühler, K., & Vigilant, L. (2014). Genetic analyses suggest no immigration of adult females and their offspring into the Sonso community of chimpanzees in the Budongo Forest Reserve, Uganda. *American journal of primatology, 76*(7), 640-648.

Langergraber, K. E., Siedel, H., Mitani, J. C., Wrangham, R. W., Reynolds, V., Hunt, K., & Vigilant, L. (2007). The genetic signature of sex-biased migration in patrilocal chimpanzees and humans. *PloS One, 2*(10), e973.

Lawson Handley, L., & Perrin, N. (2007). Advances in our understanding of mammalian sex-biased dispersal. *Molecular Ecology, 16*(8), 1559-1578.

Lee, P. C., & Strier, K. B. (2015). Complexities of understanding female dispersal in primates. *Dispersing primate females: Life history and social strategies in male-philopatric species*, 215-230.

Lehmann, J., & Boesch, C. (2003). Social influences on ranging patterns among chimpanzees (Pan troglodytes verus) in the Tai National Park, Cote d'Ivoire. *Behavioral Ecology, 14*(5), 642-649.

Lehmann, J., & Boesch, C. (2005). Bisexually bonded ranging in chimpanzees (Pan troglodytes verus). *Behavioral Ecology and Sociobiology, 57*(6), 525-535. doi:10.1007/s00265-004-0891-5.

Lehmann, J., & Boesch, C. (2008). Sexual Differences in Chimpanzee Sociality. *International Journal of Primatology, 29*(1), 65-81. doi:10.1007/s10764-007-9230-9

Lehmann, J., & Boesch, C. (2009). Sociality of the dispersing sex: the nature of social bonds in West African female chimpanzees, Pan troglodytes. *Animal Behaviour, 77*(2), 377-387.

Lemoine, S., Boesch, C., Preis, A., Samuni, L., Crockford, C., & Wittig, R. M. (2020). Group dominance increases territory size and reduces neighbour pressure in wild chimpanzees. *Royal Society open science, 7*(5), 200577. doi:doi:10.1098/rsos.200577

Lemoine, S., Crockford, C., & Wittig, R. (2019). Spatial integration of unusually high numbers of immigrant females into the South Group: further support for the bisexually bonded model in Taï chimpanzees. In C. Boesch, R. Wittig, C. Crockford, L. Vigilant, T. Deschner, & F. Leendertz (Eds.), *The chimpanzees of the Taï Forest: 40 years of research*: Cambridge University Press.

Lenth, R., Singmann, H., Love, J., Buerkner, P., & Herve, M. (2021). Emmeans: Estimated marginal means, aka least-squares means. R Package Version 1 (2018). In.

Li, X. Y., & Kokko, H. (2019). Sex-biased dispersal: A review of the theory. *Biological Reviews, 94*(2), 721-736.

Lockwood, C. A., Menter, C. G., Moggi-Cecchi, J., & Keyser, A. W. (2007). Extended male growth in a fossil hominin species. *Science, 318*(5855), 1443-1446.

Lovejoy, C. O. (2009). Reexamining human origins in light of Ardipithecus ramidus. *Science, 326*(5949), 74-74e78.

Lowry, B., Wittig, R. M., Pittermann, J., & Oelze, V. (2021). Stratigraphy of stable isotope ratios and leaf structure within an African rainforest canopy with implications for primate isotope ecology. *Scientific Reports, 11*(1), 1-11.

Luncz, L. V., & Boesch, C. (2014). Tradition over trend: Neighboring chimpanzee communities maintain differences in cultural behavior despite frequent immigration of adult females. *American journal of primatology, 76*(7), 649-657. doi:https://doi.org/10.1002/ajp.22259

Luncz, L. V., Proffitt, T., Kulik, L., Haslam, M., & Wittig, R. M. (2016). Distance-decay effect in stone tool transport by wild chimpanzees. Proceedings of the Royal Society B: Biological Sciences, 283(1845), 20161607. https://doi.org/10.1098/rspb.2016.1607

Magnusson, A., Skaug, H., Nielsen, A., Berg, C., Kristensen, K., Maechler, M., . . . Brooks, M. M. (2017). Package 'glmmtmb'. *R Package Version 0.2. 0*.

Mangenot, G. (1950a). Essai sur les forêts denses de la Côte d'Ivoire. *Bulletin de la Société Botanique de France, 97*(7-9), 159-162.

Mangenot, G. (1950b). Les forêts de la Côte d'Ivoire. *Bulletin de la Société Botanique de France, 97*(7-9), 156-157.

Mangenot, G. (1955). Etude sur les forêts des plaines et plateaux de la Côte-d'Ivoire. *Etudes éburnéennes*(4), 6-61.

Marchesi, P., Marchesi, N., Fruth, B., & Boesch, C. (1995). Census and distribution of chimpanzees in Cote d'Ivoire. *Primates, 36*, 591-607.

McArthur, J. M., Howarth, R., & Bailey, T. (2001). Strontium isotope stratigraphy: LOWESS version 3: best fit to the marine Sr-isotope curve for 0–509 Ma and accompanying look-up table for deriving numerical age. *The Journal of Geology, 109*(2), 155-170.

Moore, D. L., Langergraber, K. E., & Vigilant, L. (2015). Genetic analyses suggest male philopatry and territoriality in savanna-woodland chimpanzees (Pan troglodytes schweinfurthii) of Ugalla, Tanzania. *International Journal of Primatology, 36*, 377-397.

Murdock, G. P. (1981). *Atlas of world cultures*: University of Pittsburgh Pre.

Nishida, T. (2011). *Chimpanzees of the lakeshore: natural history and culture at Mahale*: Cambridge University Press.

Oelze, V. M., Koch, J. K., Kupke, K., Nehlich, O., Zäuner, S., Wahl, J., . . . Richards, M. P. (2012). Multi-isotopic analysis reveals individual mobility and diet at the early Iron Age monumental tumulus of Magdalenenberg, Germany. *American journal of physical anthropology, 148*(3), 406-421.

Oelze, V. M., Fuller, B. T., Richards, M. P., Fruth, B., Surbeck, M., Hublin, J.-J., & Hohmann, G. (2011). Exploring the contribution and significance of animal protein in the diet of bonobos by stable isotope ratio analysis of hair. *Proceedings of the National Academy of Sciences, 108*(24), 9792-9797. doi:doi:10.1073/pnas.1018502108

Oelze, V. M. (2016). Reconstructing temporal variation in great ape and other primate diets: A methodological framework for isotope analyses in hair. *American journal of primatology, 78*(10), 1004-1016.

Oelze, V. M., Percher, A. M., Nsi Akoué, G., El Ksabi, N., Willaume, E., & Charpentier, M. J. E. (2020). Seasonality and interindividual variation in mandrill feeding ecology revealed by stable isotope analyses of hair and blood. *American journal of primatology, 82*(12), e23206. doi:https://doi.org/10.1002/ajp.23206

Parr, L. A., & de Waal, F. B. (1999). Visual kin recognition in chimpanzees. *Nature, 399*(6737), 647-648.

Petters, S. W. (1991). *Regional geology of Africa*: Springer.

PL, I. E., & Srivastava, R. (1989). An introduction to applied geostatistics. In: Oxford, Oxford University Press.

Poszwa, A., Dambrine, E., Ferry, B., Pollier, B., & Loubet, M. (2002). Do deep tree roots provide nutrients to the tropical rainforest? *Biogeochemistry, 60*(1), 97-118.

Poszwa, A., Ferry, B., Dambrine, E., Pollier, B., Wickman, T., Loubet, M., & Bishop, K. (2004). Variations of bioavailable Sr concentration and 87Sr/86Sr ratio in boreal forest ecosystems. *Biogeochemistry, 67*(1), 1-20.

Price, T. D., Burton, J. H., & Bentley, R. A. (2002). The characterization of biologically available strontium isotope ratios for the study of prehistoric migration. *Archaeometry, 44*(1), 117-135.

Pusey, A., & Packer, C. (1986). Dispersal and philopatry. Primate societies. *Smuts BB, Cheney DL, Seyfarth RM, Wrangham RW & Struhsaker TT*, 150-166.

R Core Development Team. (2024). R: A Language and Environment for Statistical Computing. *R Foundation for Statistical Computing, Vienna, Austria*.

Rouw, A. d., Vellema, H., & Blokhuis, W. A. (1990). *Land unit survey of the Tai region south-west Cote d'Ivoire*.

Runia, L. T. (1987). Strontium and calcium distribution in plants: effect on palaeodietary studies. *Journal of Archaeological Science, 14*(6), 599-608.

Schulz-Kornas, E., Stuhlträger, J., Clauss, M., Wittig, R. M., & Kupczik, K. (2019). Dust affects chewing efficiency and tooth wear in forest dwelling Western chimpanzees (Pan troglodytes verus). *American journal of physical anthropology, 169*(1), 66-77.

Schwartz, G. T., Reid, D. J., Dean, M., & Chandrasekera, M. S. (2000). *Aspects of tooth crown development in common chimpanzees (Pan troglodytes) with a note on the possible role of sexual dimorphism in canine growth.* Paper presented at the Proceedings of 11th International Symposium on Dental Morphology, Oulu.

Shagina, N. B., Tolstykh, E. I., Fell, T. P., Harrison, J. D., Phipps, A. W., & Degteva, M. O. (2007). In utero and postnatal haemopoietic tissue doses resulting from maternal ingestion of strontium isotopes from the Techa river. *Radiation Protection Dosimetry, 127*(1-4), 497-501. doi:10.1093/rpd/ncm357

Sillen, A., Hall, G., Richardson, S., & Armstrong, R. (1998). 87Sr/86Sr ratios in modern and fossil food-webs of the Sterkfontein Valley: implications for early hominid habitat preference. *Geochimica et Cosmochimica Acta, 62*(14), 2463-2473.

Smith, T. M., Austin, C., Ávila, J. N., Dirks, W., Green, D. R., Williams, I. S., & Arora, M. (2022). Permanent signatures of birth and nursing initiation are chemically recorded in teeth. *Journal of Archaeological Science, 140*, 105564.

Smith, T. M., Reid, D. J., Dean, M. C., Olejniczak, A. J., & Martin, L. B. (2007). Molar development in common chimpanzees (Pan troglodytes). *Journal of human evolution, 52*(2), 201-216.

Smith, T. M., Smith, B. H., Reid, D. J., Siedel, H., Vigilant, L., Hublin, J.-J., & Boesch, C. (2010). Dental development of the Taï Forest chimpanzees revisited. *Journal of human evolution, 58*(5), 363-373.

Stojanowski, C. M., & Knudson, K. J. (2011). Biogeochemical inferences of mobility of early Holocene fisher-foragers from the Southern Sahara Desert. *American journal of physical anthropology, 146*(1), 49-61. doi:https://doi.org/10.1002/ajpa.21542

Stoorvogel, J. J., Van Breemen, N., & Jassen, B. H. (1997). The nutrient input by Harmattan dust to a forest ecosystem in Côte d'Ivoire, Africa. *Biogeochemistry, 37*(2), 145-157. doi:10.1023/A:1005734225727

Stumpf, R. M., Thompson, E. M., Muller, M. N., & Wrangham, R. W. (2009). The context of female dispersal in Kanyawara chimpanzees. *Behaviour, 146*(4-5), 629-656.

Sugiyama, N., Sugiyama, S., Cagnato, C., France, C. A. M., Iriki, A., Hughes, K. S., . . . Hofman, C. A. (2022). Earliest evidence of primate captivity and translocation supports gift diplomacy between Teotihuacan and the Maya. *Proceedings of the National Academy of Sciences, 119*(47), e2212431119. doi:doi:10.1073/pnas.2212431119

Tagini, B. (1966). Esquisse géotechnique de la Côte d'Ivoire. *Rapport SO. DE. MI*(107).

Tagini, B. (1972). *Notice explicative à la carte géologique de la Côte d'Ivoire au 1/2 000 000*: SODEMI.

Thompson, M. E. (2013). Reproductive ecology of female chimpanzees. *American journal of primatology, 75*(3), 222-237.

Vautour, G., Poirier, A., & Widory, D. (2015). Tracking mobility using human hair: What can we learn from lead and strontium isotopes? *Science & Justice, 55*(1), 63-71.

Vigilant, L., Hofreiter, M., Siedel, H., & Boesch, C. (2001). Paternity and relatedness in wild chimpanzee communities. *Proceedings of the National Academy of Sciences, 98*(23), 12890-12895. doi:10.1073/pnas.231320498

Walker, K. K., & Pusey, A. E. (2020). Inbreeding risk and maternal support have opposite effects on female chimpanzee dispersal. *Current Biology, 30*(2), R62-R63.

Wang, X., Bocksberger, G., Agbor, A., Angedakin, S., Aubert, F., Ayuk Ayimisin, E, Bailey, E., Barubiyo, D., Bessone, M., Bobe, R., Bonnet, M., Boucher, R., Brazzola, G., Brewer, S., Lee, K., Carvalho, S., Chancellor, R., Cipoletta, C., Cohen, H., … Oelze, V. M. (in review). Strontium isoscape of sub-Saharan Africa allows tracing origins of victims of the transatlantic slave trade.

Whipkey, C., Capo, R. C., Chadwick, O., & Stewart, B. (2000). The importance of sea spray to the cation budget of a coastal Hawaiian soil: a strontium isotope approach. *Chemical Geology, 168*(1-2), 37-48.

White, T. D., Black, M. T., & Folkens, P. A. (2011). *Human osteology*: Academic press.

Wilkins, J. F., & Marlowe, F. W. (2006). Sex-biased migration in humans: what should we expect from genetic data? *BioEssays, 28*(3), 290-300.

Wittig, R. (2018). Tai Chimpanzees (advance online). *Encyclopedia of animal cognition and behavior., In J. Vonk, & T. K. Shackelford (Eds.)*(Cham: Springer International Publishing.).

Wittig, R., and, & Boesch, C. (2019). Observation protocol and long-term data collection in Taï. In C. Boesch, R. Wittig, C. Crockford, T. Deschner, L. Vigilant, & F. Leendertz (Eds.), *The Chimpanzees of Taï Forest: 40 years of Research*.

Wright, L. E. (2005). Identifying immigrants to Tikal, Guatemala: defining local variability in strontium isotope ratios of human tooth enamel. *Journal of Archaeological Science, 32*(4), 555-566.

2.9. Supplementary Information

Strontium isotope biogeochemistry

Similarities in ionic radius size and electron valence configuration allow minor amounts of Sr to replace Ca in the hydroxyapatite of skeletal tissues during biomineralization (Beard & Johnson, 2000; Bentley, 2006; Capo et al., 1998). Given its high atomic mass, fractionation of Sr isotopes in the biosphere is negligible. Hence, the $^{87}Sr/^{86}Sr$ ratio of bioapatite will largely reflect the isotopic fingerprint of the geological location an individual inhabited during tissue formation early in ontogeny (Beard & Johnson, 2000; Bentley, 2006; Capo et al., 1998; Faure & Powell, 2012; Gosz et al., 1983; Hurst & Davis, 1981). We can use this geological fingerprint to make estimates about the provenance and mobility of organisms in various contexts, such as archaeological human populations (Beard & Johnson, 2000; Bentley, 2006; Capo et al., 1998; Faure & Powell, 2012; Gosz et al., 1983; Hurst & Davis, 1981) and non-human primate species (Crowley & Godfrey, 2019; Dean et al., 2020; Dominy et al., 2020; Fannin et al., 2021; Hamilton et al., 2021; Hamilton et al., 2019; Humphrey et al., 2008; T. M. Smith et al., 2021; Sugiyama et al., 2022).

The sources of environmental baseline $^{87}Sr/^{86}Sr$ variations are well understood. Different types of bedrock underlying the soils and bodies of water on a landscape result in different $^{87}Sr/^{86}Sr$ ratios. For example, younger basalts tend to

have lower $^{87}Sr/^{86}Sr$ ratios (0.704-0.705), whereas younger granites tend to have higher ratios (0.712-0.720). As the volcanic sources that generate ash vary compositionally between granitic and basaltic endmembers, the tuff resulting from volcanic eruptions can have intermediate ratios (Davies & Halliday, 1998), and very old igneous or metamorphic rocks may have isotopic ratios greater than 0.8 (Bataille & Bowen, 2012; Chappell & White, 2001). Variations among rock types associated with chemical composition or age result from differences in the initial $^{87}Sr/^{86}Sr$ ratio of the rock and the production of stable ^{87}Sr from radioactive decay with age. Clastic sedimentary bedrock can be highly variable, depending on the rocks and minerals eroding to form the original sedimentary packet and the geologic age of the bedrock. Marine carbonate rocks have high Sr concentrations and they show well-characterized variations in the range of 0.707-0.709 through the Proterozoic and Cenozoic (DePaolo & Ingram, 1985; McArthur et al., 2001), which can affect environmental baseline $^{87}Sr/^{86}Sr$, however they do not occur in the region under study.

Supplementary Tables

Table 2.9.1. GLMM model outputs for environmental samples (n = 35).
Model outputs of beta fitted generalized linear model [($^{87}Sr/^{86}Sr$ ~ Territory + (1 | sample type)], testing for the differences in $^{87}Sr/^{86}Sr$ isotope ratios between environmental samples within the TCP study area (n = 35).

Response variable	n	Random effects	Predictor variable	Estimate ± SE	Z-value	p-value
Full	35	Sample type	(intercept)	0.93± 0.01	115.74	**<0.00001**
AICc = - 276.83			North 1	0.005 ± 0.01	0.46	0.64
df = 9			North 2	0.07 ± 0.01	5.38	**<0.00001**
			Northeast	0.03 ± 0.01	2.58	**0.01**
			Northwest	0.04 ± 0.01	4.19	**<0.00001**
			South	0.008 ± 0.01	0.71	0.48

			Middle	0.006 ± 0.01	0.6	0.57
Null AICc = - 263.36 df = 3	35	Sample type	-	-	-	-

Table 2.9.2. Summary of contrasts for environmental samples (n = 35).
Summary of contrasts estimated by the Bonferroni method for the GLMM testing for the differences in $^{87}Sr/^{86}Sr$ isotope ratios between environmental samples within the TCP study area (n = 35).

Contrast	Ratio ± SE	z-ratio	p-value	power
East-Middle	1 ± 0.01	-0.6	1	0.04
East-North 1	1 ± 0.01	-0.46	1	0.03
East-North 2	**0.94 ± 0.01**	**-5.38**	**< 0.0001**	0.02
East-Northeast	0.97 ± 0.01	-2.58	0.21	0.99
East-Northwest	**0.96 ± 0.01**	**-4.19**	**0.0006**	**0.80**
East-South	0.99 ± 0.01	-0.71	1	0.48
Middle-North 1	1 ± 0.01	0.08	1	0.01
Middle-North 2	**0.94 ± 0.01**	**-5.11**	**< 0.0001**	0.01
Middle-Northeast	0.98 ± 0.01	-2.13	0.69	0.97
Middle-Northwest	**0.97 ± 0.01**	**-3.83**	**0.003**	**0.63**
Middle-South	1 ± 0.01	-0.15	1	0.22
North 1-North 2	**0.94 ± 0.01**	**-4.96**	**< 0.0001**	0.01
North 1-Northeast	0.98 ± 0.01	-2.09	0.76	0.98
North 1-Northwest	**0.97 ± 0.01**	**-3.64**	**0.006**	**0.66**
North 1-South	1 ± 0.01	-0.22	1	0.27
North 2-Northeast	**1.04 ± 0.01**	**3.27**	**0.02**	**0.98**
North 2-Northwest	1.03 ± 0.01	2.41	0.34	0.68
North 2-South	**1.06 ± 0.01**	**4.98**	**< 0.0001**	0.29
Northeast-Northwest	0.99 ± 0.01	-1.4	1	0.37
Northeast-South	1.02 ± 0.01	1.98	1	0.76
Northwest-South	**1.03 ± 0.01**	**3.65**	**0.005**	0.08

Table 2.9.3. GLMM model outputs for chimpanzee samples (n = 27).
Model outputs of beta fitted generalized linear model [$^{87}Sr/^{86}Sr \sim$ Origin + (1 | Teeth_Sampled)], testing for the differences in $^{87}Sr/^{86}Sr_{enamel}$ isotope ratios between North community origin groups (natal: n = 16, Unknown Female (pre-1980): n = 4, Unknown Female (post-1980): n = 7) within the TCP study area (n = 27).

Response variable	n	Random effects	Predictor variable	Estimate ± SE	Z-value	p-value
Full	27	Tooth type	(intercept)	0.94 ± 0.003	308.74	**0.000001**
AICc = -242.83			Unknown Female (pre-1980)	-0.008 ± 0.006	-1.47	0.14
df = 5			Unknown Female (post-1980)	0.02 ± 0.005	4.08	**0.000001**
Null	27	Tooth type	-	-	-	-
AICc = -232.13						
df = 3						

Table 2.9.4. Summary of contrasts for chimpanzee samples (n = 27).
Summary of contrasts estimated by the Bonferroni method for the GLMM testing for the differences in $^{87}Sr/^{86}Sr_{enamel}$ isotope ratios between North community origin groups within the TCP study area (n = 27).

Contrast	Ratio ± SE	z-ratio	p-value	power
Natal (post-1980) - Unknown Female (pre-1980)	1.01 ± 0.006	1.47	0.42	0.31
Natal (post-1980) - Unknown Female (post-1980)	**0.98 ± 0.005**	**-4.08**	**0.0001**	**0.94**
Unknown Female (pre-1980) - (post-1980)	**1.03 ± 0.007**	**4.41**	**< 0.0001**	**1.00**

Supplementary Figures

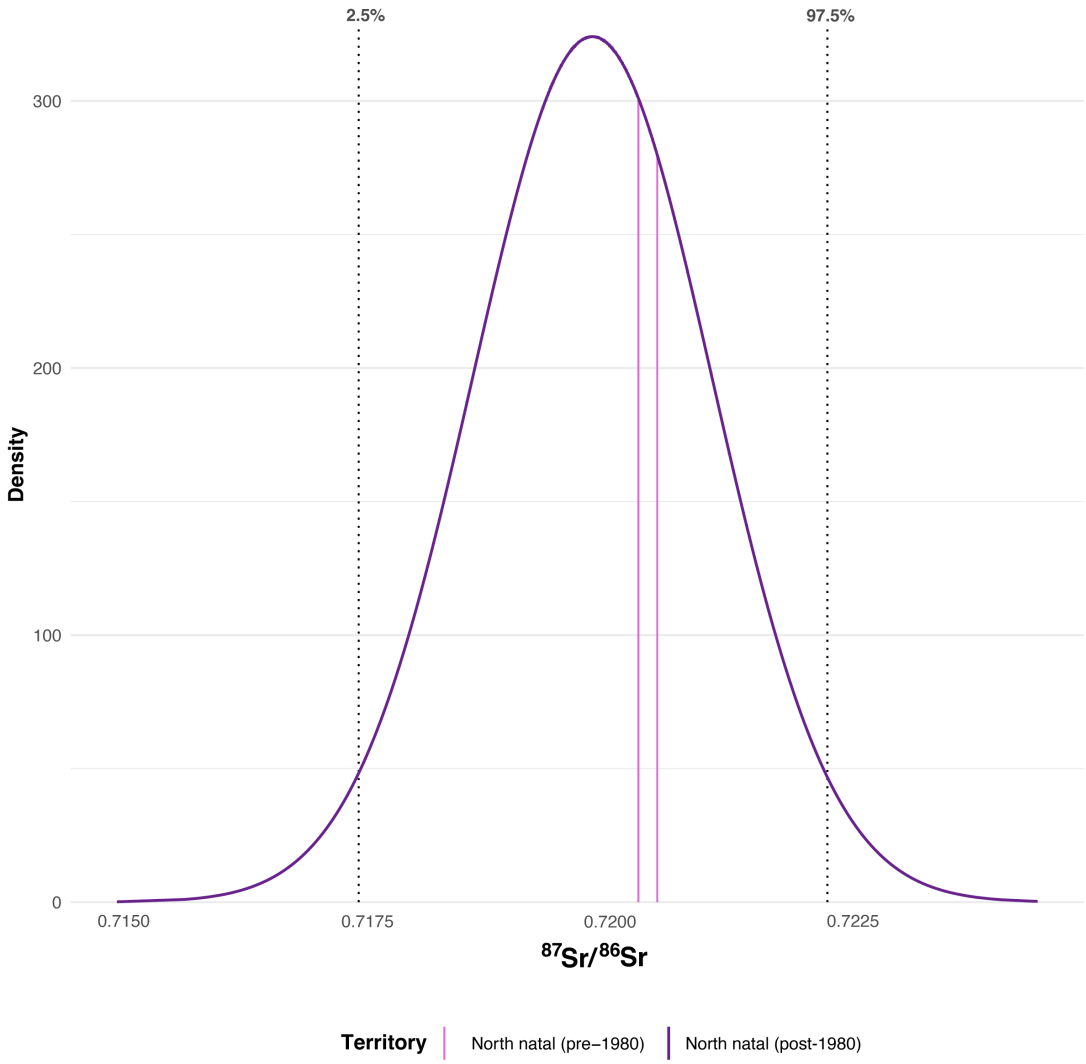

Figure 2.9.1. Theoretical density of $^{87}Sr/^{86}Sr_{enamel}$ isotope ratios for North community natal males (post-1980, n = 8).
Theoretical density (fit to a beta distribution) of the $^{87}Sr/^{86}Sr_{enamel}$ isotope ratios for North community natal males (post-1980, n = 8), where the 2.5% quantile is 0.718 and the 97.5%

quantile is 0.722. The light purple lines indicate the $^{87}Sr/^{86}Sr_{enamel}$ isotope ratios for the North community natal males (pre-1980, n = 2).

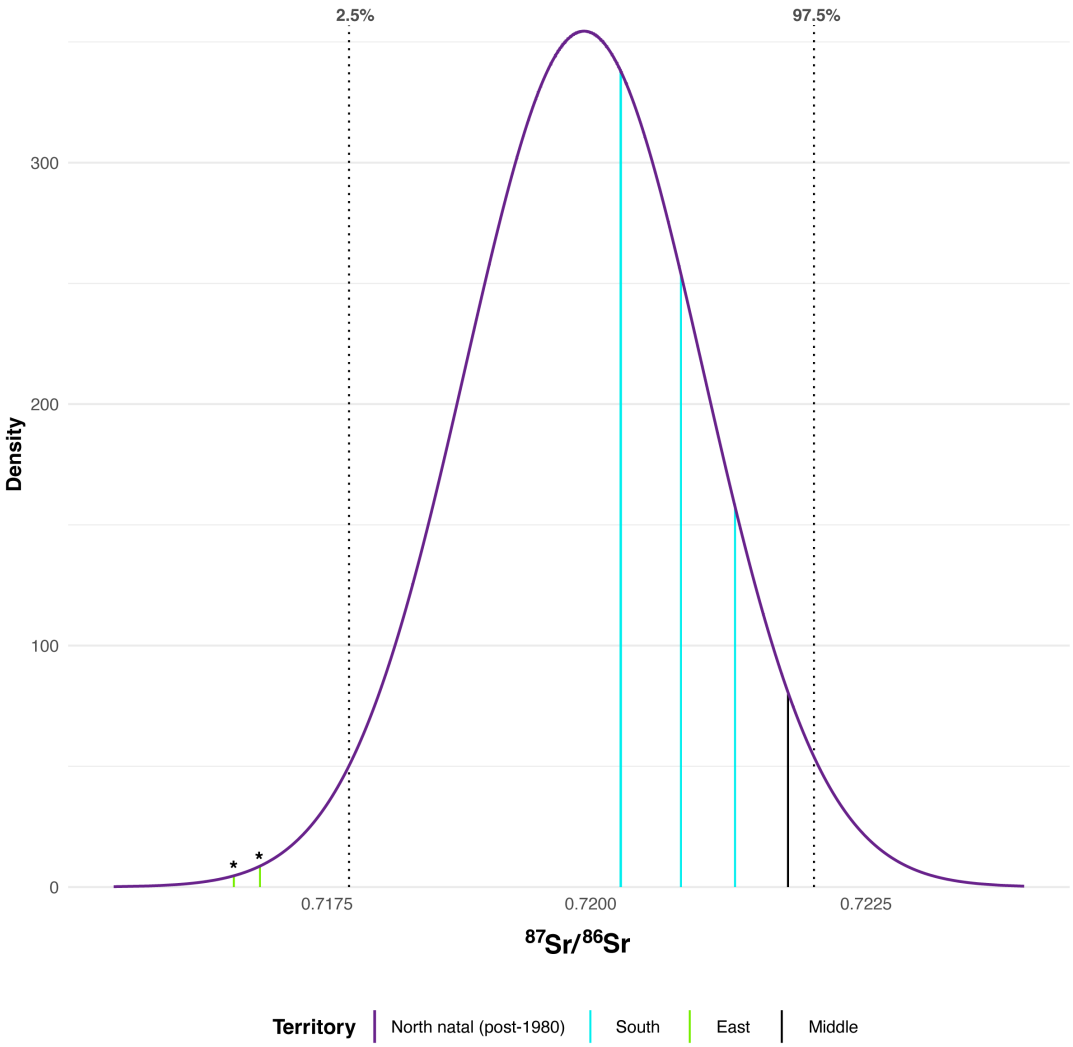

Figure 2.9.2. Theoretical density (fit to a beta distribution) of the $^{87}Sr/^{86}Sr_{enamel}$ isotope ratios for North community natal males (n = 10) with the mean $^{87}Sr/^{86}Sr_{enamel}$ isotope ratios for natal males from other chimpanzee communities overlayed (n = 7).
Theoretical density (fit to a beta distribution) of the $^{87}Sr/^{86}Sr_{enamel}$ isotope ratios for North community natal males (n = 10), where the 2.5% quantile is 0.717 and the 97.5% quantile is 0.722. The lines indicate the $^{87}Sr/^{86}Sr_{enamel}$ isotope ratios for the other chimpanzee communities: cyan is South community (n = 4), light green is East community (n = 2), and Middle is black (n = 1). Two males from South community overlap in $^{87}Sr/^{86}Sr_{enamel}$ isotope ratios (0.720). The asterisk (*) indicates chimpanzee communities that are outside of the 2.5% and 97.5% quantiles.

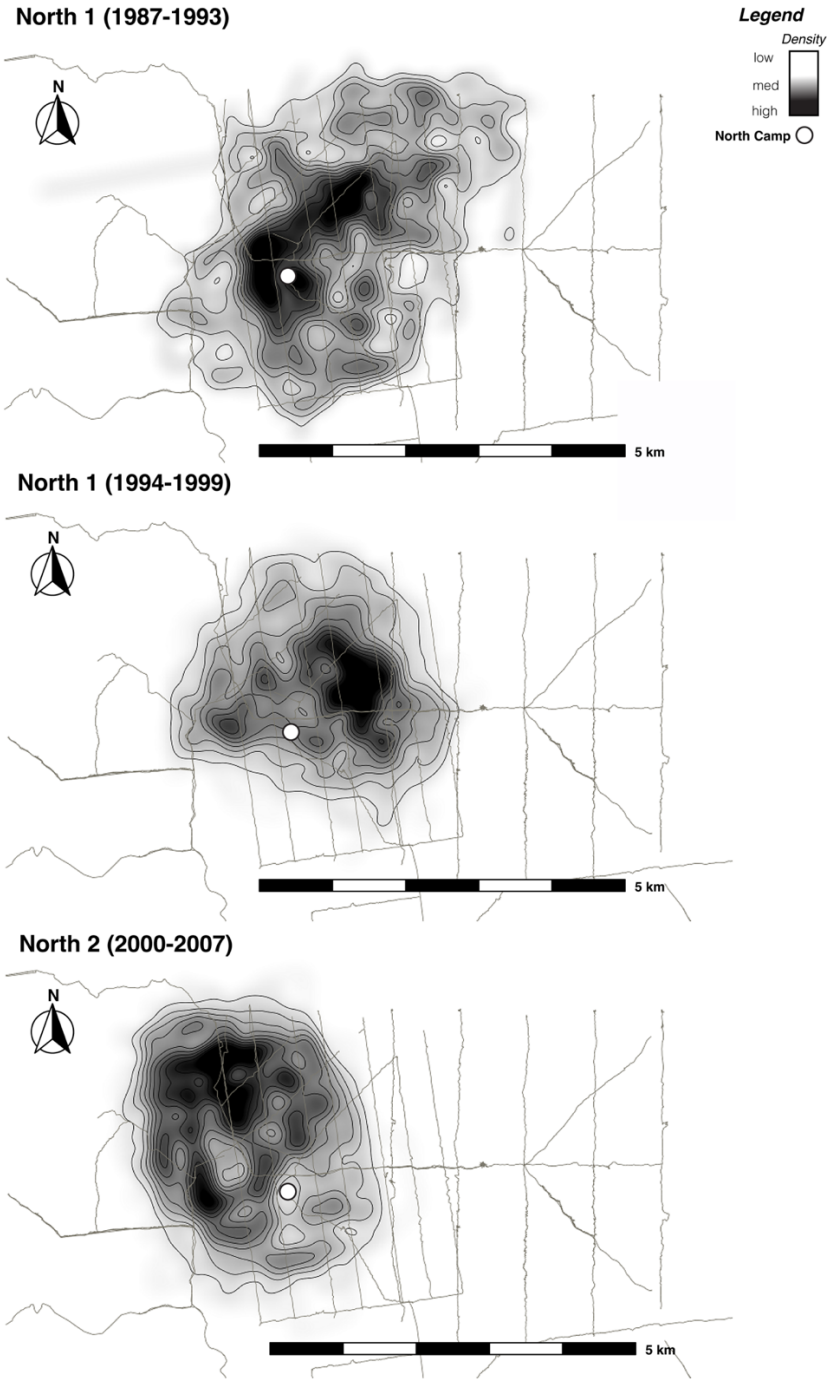

Figure 2.9.3. Density plots of chimpanzee tracking data indicating North Group territory shifts during the TCP skeletal collection sampling period (1980-2009).

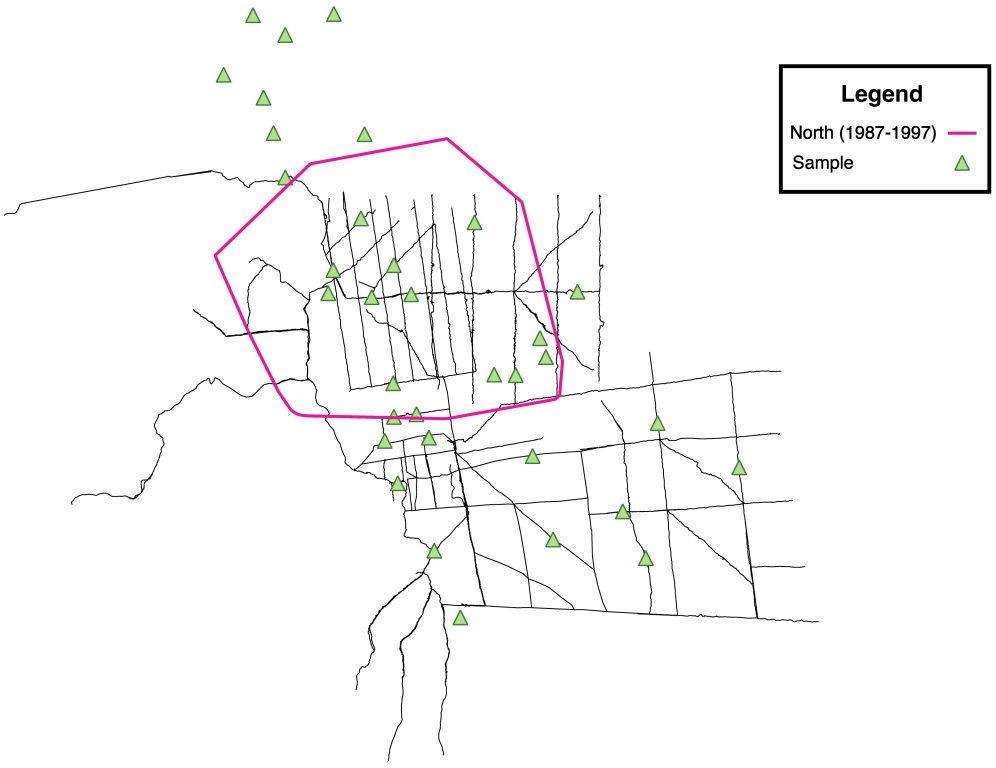

Figure 2.9.4. Minimum Convex polygons (100%) of the North community territory range based on all locations used during the respective time window (1987-1997).
Green triangles show environmental sample locations within the TCP study area, and black lines show the TCP study area trails.

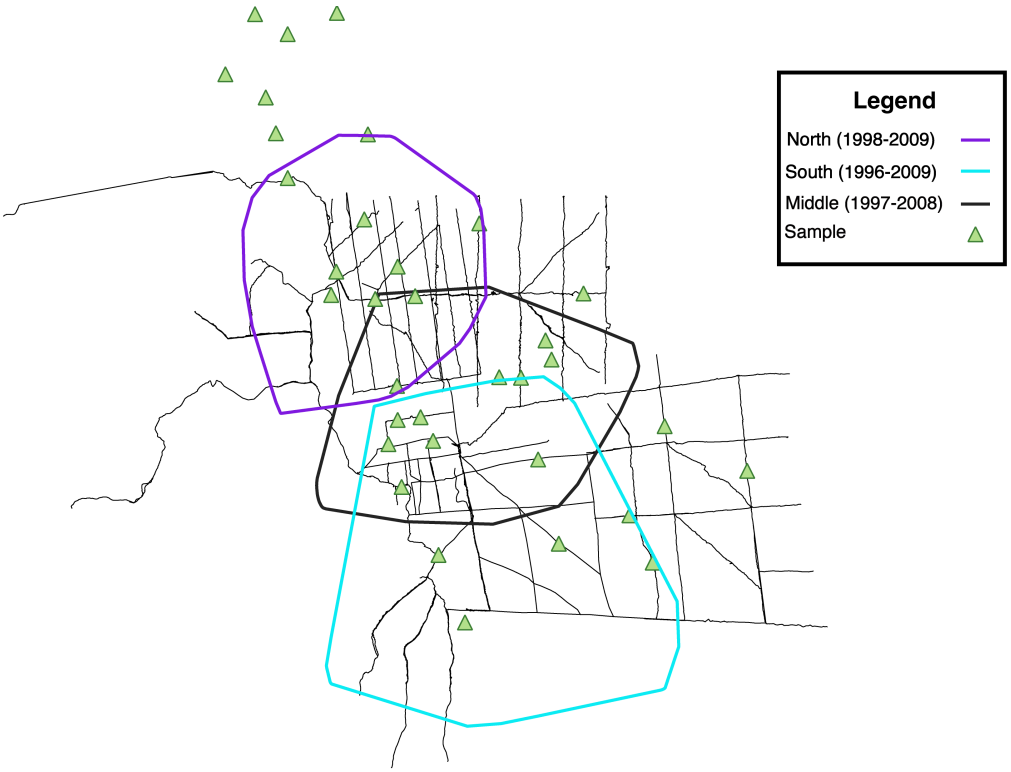

Figure 2.9.5. Minimum Convex polygons (100%) of TCP-established community (North, South, Middle) territory ranges based on all locations used during the respective time window (1997-2009).
Green triangles show environmental sample locations within the TCP study area, and black lines show the TCP study area trails.

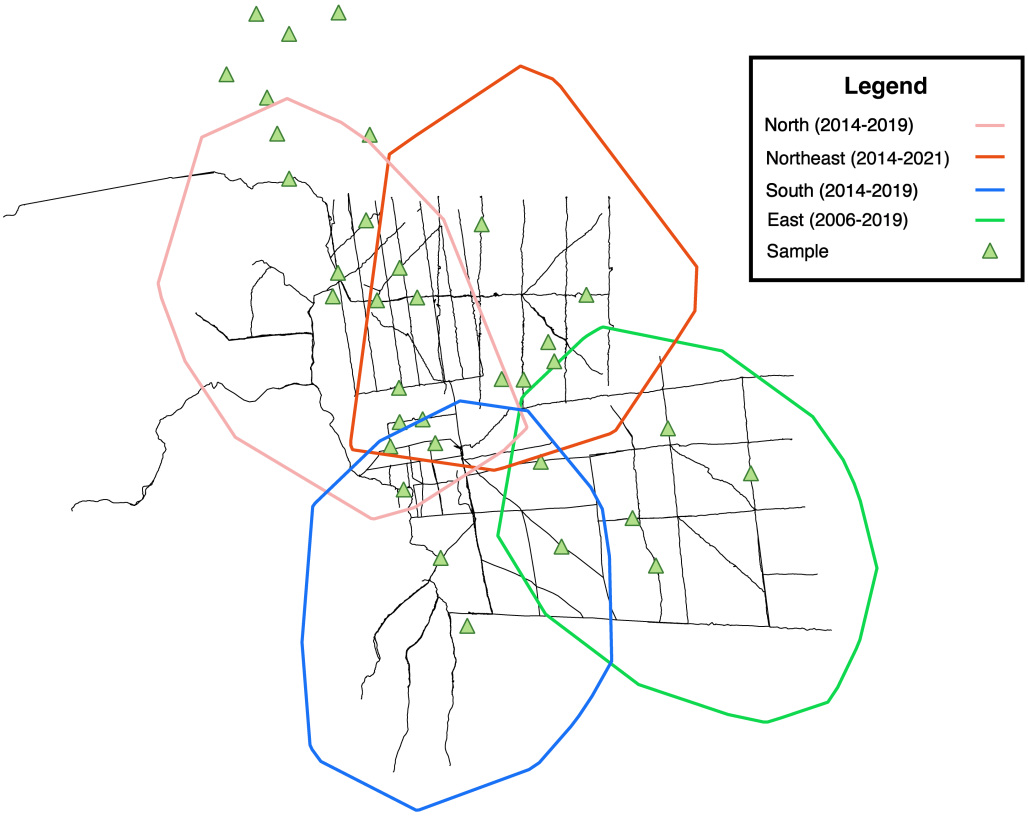

Figure 2.9.6. Minimum Convex polygons (100%) of TCP-established community (North, Northeast, South, East) territory ranges based on all locations used during the respective time window (2014-2019).
Green triangles show environmental sample locations within the TCP study area, and black lines show the TCP study area trails.

References Cited

Bataille, C. P., & Bowen, G. J. (2012). Mapping 87Sr/86Sr variations in bedrock and water for large scale provenance studies. *Chemical Geology, 304*, 39-52.

Beard, B. L., & Johnson, C. M. (2000). Strontium isotope composition of skeletal material can determine the birth place and geographic mobility of humans and animals. *Journal of Forensic Science, 45*(5), 1049-1061.

Bentley, R. A. (2006). Strontium isotopes from the earth to the archaeological skeleton: a review. *Journal of archaeological method and theory, 13*(3), 135-187.

Capo, R. C., Stewart, B. W., & Chadwick, O. A. (1998). Strontium isotopes as tracers of ecosystem processes: theory and methods. *Geoderma, 82*(1-3), 197-225.

Chappell, B. W., & White, A. J. R. (2001). Two contrasting granite types: 25 years later. *Australian Journal of Earth Sciences, 48*(4), 489-499. doi:10.1046/j.1440-0952.2001.00882.x

Crowley, B. E., & Godfrey, L. R. (2019). Strontium Isotopes Support Small Home Ranges for Extinct Lemurs. *Frontiers in Ecology and Evolution, 7*(490). doi:10.3389/fevo.2019.00490

Davies, G. R., & Halliday, A. N. (1998). Development of the Long Valley rhyolitic magma system: strontium and neodymium isotope evidence from glasses and individual phenocrysts. *Geochimica et Cosmochimica Acta, 62*(21-22), 3561-3574.

Dean, M. C., Le Cabec, A., Van Malderen, S. J. M., & Garrevoet, J. (2020). Synchrotron X-ray fluorescence imaging of strontium incorporated into the enamel and dentine of wild-shot orangutan canine teeth. *Archives of Oral Biology, 119*, 104879. doi:https://doi.org/10.1016/j.archoralbio.2020.104879

DePaolo, D. J., & Ingram, B. L. (1985). High-resolution stratigraphy with strontium isotopes. *Science, 227*(4689), 938-941.

Dominy, N. J., Ikram, S., Moritz, G. L., Wheatley, P. V., Christensen, J. N., Chipman, J. W., & Koch, P. L. (2020). Mummified baboons reveal the far reach of early Egyptian mariners. *eLife, 9*. doi:10.7554/eLife.60860

Fannin, L. D., Yeakel, J. D., Venkataraman, V. V., Seyoum, C., Geraads, D., Fashing, P. J., . . . Dominy, N. J. (2021). Carbon and strontium isotope ratios shed new light on the paleobiology and collapse of Theropithecus, a primate experiment

in graminivory. *Palaeogeography, palaeoclimatology, palaeoecology, 572*, 110393.

Faure, G., & Powell, J. L. (2012). *Strontium isotope geology* (Vol. 5): Springer Science & Business Media.

Gosz, J. R., Brookins, D. G., & Moore, D. I. (1983). Using strontium isotope ratios to estimate inputs to ecosystems. *Bioscience, 33*(1), 23-30.

Hamilton, M. I., Fernandez, D. P., & Nelson, S. V. (2021). Using strontium isotopes to determine philopatry and dispersal in primates: a case study from Kibale National Park. *Royal Society open science, 8*(2), 200760.

Hamilton, M. I., Nelson, S. V., Fernandez, D. P., & Hunt, K. D. (2019). Detecting riparian habitat preferences in "savanna" chimpanzees and associated Fauna with strontium isotope ratios: Implications for reconstructing habitat use by the chimpanzee-human last common ancestor. *American journal of physical anthropology, 170*(4), 551-564.

Humphrey, L. T., Dirks, W., Dean, M. C., & Jeffries, T. E. (2008). Tracking dietary transitions in weanling baboons (Papio hamadryas anubis) using strontium/calcium ratios in enamel. *Folia Primatologica, 79*(4), 197-212.

Hurst, R. W., & Davis, T. E. (1981). Strontium isotopes as tracers of airborne fly ash from coal-fired power plants. *Environmental Geology, 3*(6), 363-367. doi:10.1007/bf02473525

McArthur, J. M., Howarth, R., & Bailey, T. (2001). Strontium isotope stratigraphy: LOWESS version 3: best fit to the marine Sr-isotope curve for 0–509 Ma and accompanying look-up table for deriving numerical age. *The Journal of Geology, 109*(2), 155-170.

Smith, T. M., Cook, L., Dirks, W., Green, D. R., & Austin, C. (2021). Teeth reveal juvenile diet, health and neurotoxicant exposure retrospectively: What biological rhythms and chemical records tell us. *BioEssays, 43*(9), 2000298. doi:https://doi.org/10.1002/bies.202000298

Sugiyama, N., Sugiyama, S., Cagnato, C., France, C. A. M., Iriki, A., Hughes, K. S., . . . Hofman, C. A. (2022). Earliest evidence of primate captivity and translocation supports gift diplomacy between Teotihuacan and the Maya. *Proceedings of the National Academy of Sciences, 119*(47), e2212431119. doi:doi:10.1073/pnas.2212431119

CHAPTER 3: Zinc isotope ratios ($\delta^{66}Zn$) suggest a sex difference in diet among wild chimpanzees (*Pan troglodytes verus*)

Authors: Renee D. Boucher[1*], Klervia Jaouen[2], Roman M. Wittig[3,4], Paul L. Koch[5], Vicky M. Oelze[1*]

[2]Department of Anthropology, University of California, Santa Cruz, CA 95064, USA

[2]Géosciences Environnement Toulouse, UMR 5563, CNRS, Observatoire Midi Pyrénées, Toulouse, France

[3]Taï Chimpanzee Project, CSRS, Abidjan, Ivory Coast

[4]Institute of Cognitive Sciences, UMR5229 CNRS, 67 Boulevard Pinel, 69675 Bron cedex, France

[5]Department of Earth and Planetary Sciences, University of California, Santa Cruz, CA, 95064, USA

Note: *In Review* with American Journal for Biological Anthropology, 2024. Formatting has been modified from origin article to fit dissertation guidelines. Permission to include this article has been granted by all co-authors and signed permission letter submitted to ProQuest.

Reference: TBD

3.1. Abstract

A higher trophic position related to meat consumption is thought to have contributed to increased brain size in early hominins. Stable isotope analysis of nitrogen isotope is a key method for dietary reconstruction in archaeology, however its application in deep time is limited by protein preservation. Stable isotope ratios of zinc ($\delta^{66}Zn$) measured in tooth enamel have been shown to relate to trophic position in a variety of animal species and have also been associated with breastfeeding effects. In this study, we use $\delta^{66}Zn$ analysis in local plant and animal foods (n = 28) alongside tooth enamel

[2] Department of Anthropology, University of California, Santa Cruz, CA 95064, USA

of chimpanzees (*Pan troglodytes* verus, n = 34) from Taï National Park, Côte d'Ivoire, to assess the differences in $\delta^{66}Zn$ between individuals in relation to their sex and age class as a potential framework for future research on fossil hominins. We found that adolescent male chimpanzees have significantly lower $\delta^{66}Zn$ values than their female counterparts, indicating a higher trophic position. We suggest that $\delta^{66}Zn$ analysis can indicate trophic position in wild primates, with the potential to assess dietary niche and particularly carnivory in the enamel of fossil hominins.

3.2. Significance Statement

Dietary adaptations, including increased hunting and meat consumption are suggested to have spurred the transition from australopithecines to modern humans, but we have a limited isotope toolkit to assess meat consumption in fossil hominins. An isotopic study on the predominantly frugivorous Taï chimpanzees showed higher $\delta^{15}N$ values in males, and especially gifted male hunters, suggesting higher average amounts of meat in their diets. However, when accounting for observed meat consumption amounts and intergroup variation, a follow-up study did not find a relationship between meat amounts consumed and $\delta^{15}N$ values. Here, we measure Zn isotope ratios in the tooth enamel of the Taï chimpanzees and found significant sex differences in this isotope system, which are primarily linked to trophic position. Hence, our data indicates higher average meat consumption frequencies in males, which is confirmed by long-term trends in observational data. We conclude that Zn isotope analysis has the potential to be a useful dietary proxy for inferring trophic position in early hominins.

3.3. Introduction

During human evolution, hunting or scavenging and consuming vertebrate animal meat and fat may have contributed to the increase in brain size in the genus *Homo* (Tennie et al., 2009; Williams & Dunbar, 2014). Stable isotope analyses have been used to investigate the diet of past human and animal populations. Some initial evidence from australopiths suggests that they consumed low levels of animal resources (Lüdecke et al., 2018; Lüdecke et al., 2022). Rich archaeological evidence indicates a more omnivorous diet in *Homo habilis* that transitions to a diet even more reliant on meat in *Homo erectus* (Ben-Dor et al., 2021). Nitrogen isotope values ($\delta^{15}N$) are a valuable proxy when considering the incorporation of meat into the diet, as they reflect the isotopic composition of dietary protein, with a ^{15}N-enrichment of 3 to 5‰, and thus progressively higher $\delta^{15}N$ values with each trophic step (Ambrose, 1991; Bocherens & Drucker, 2003; Hedges & Reynard, 2007). Recent advances in $\delta^{15}N$ analysis demonstrate that the organic matter within tooth enamel can sometimes preserve endogenous nitrogen in ancient fossils (Leichliter et al., 2023). However, the results of enamel $\delta^{15}N$ analysis are difficult to interpret without the complementary use of bone collagen $\delta^{15}N$ and enamel $\delta^{13}C$ analysis, as samples are often from different localities and subject to variable abiotic and biotic factors (Leichliter et al., 2023).

Another novel proxy, the stable isotope ratios of zinc ($^{66}Zn/^{64}Zn$, expressed as $\delta^{66}Zn$) has been shown to reliably record trophic position in

extant vertebrates (Jaouen et al., 2016; Jaouen et al., 2013). The Zn in animal tissues is derived from the diet, where the average diet-bone fractionation ($\Delta^{66}Zn_{diet\text{-}bone}$) is + 0.3‰ , the average $\Delta^{66}Zn_{diet\text{-}enamel}$ is +0.1‰, and the average $\Delta^{66}Zn_{diet\text{-}muscle}$ is - 0.31‰ (Bourgon et al., 2024; Moynier et al., 2013; see SI, Supporting Information 3.9.3.6). There is also Zn variation between tissue types, where the average bone-enamel fractionation ($\Delta^{66}Zn_{bone\text{-}enamel}$) is - 0.2‰ (Jaouen et al., 2019), see SI, Supporting Information 3.9.3.6). The teeth sampled in this study reflect life stages ranging from *in utero* to age 8 years, at which chimpanzees can be considered adolescent (see Table 3.3.1 and Supporting Information 3.9.3). Zn is incorporated into enamel at two stages of tooth formation: the first is continuous during tooth calcification (Model 1), and the second is at the end of crown completion before eruption (Model 2). To be conservative in light of bulk enamel sampling, we compare both models and assess which is best supported by our data.

Table 3.3.1. The tooth crown formation age range (in years) for different tooth types in wild chimpanzees.
The tooth crown formation age range (in years) for different tooth types in wild chimpanzees, from initiation to completion (after (Schwartz et al., 2000)[a]; (Smith et al., 2007)[b]; (Smith et al., 2010)[c]; (Kelley et al., 2020)[d]; (Dean et al., 2023)[e], (Smith et al., in review)[f]) alongside the anticipated Zn incorporation age (in years), and the corresponding life stage (Samuni, Wegdell, et al., 2020)[g] for the types of teeth sampled in this study (n = 34, see SI, Supporting Information 3.9.2 and 3.9.3).

tooth type	n	crown initiation[a,f]	crown completion[b,c,d,f]	Zn deposition[e,f]	life stage[g,f]
deciduous premolars (dp3 and dp4)	5	-0.08 to 0.4	0.4	0.4	*in utero* to nursing
first molar (M1)	2	-0.1	2.8	2.8	nursing
second molar (M2)	15	1.8	4.5 to 5.2	4.5 to 5.2	end of nursing to weaned

third molar (M3)	12	3.6 to 4.7	6.6 to 8.0	6.6 to 8.0	fully weaned

Archaeological studies have demonstrated that $\delta^{66}Zn$ values retrieved from tooth enamel can reveal trophic position even in deep time (Bourgon et al., 2020; Bourgon et al., 2021; McCormack et al., 2022). Here, the trophic level effect on $\delta^{66}Zn$ is opposite from the effect on $\delta^{15}N$ values. Carnivores at the highest trophic position have the lowest $\delta^{66}Zn$ values whereas and herbivores at the lowest trophic position have the highest $\delta^{66}Zn$ values (see SI, Supporting Information 3.9.2, (Bourgon et al., 2020; Bourgon et al., 2021; McCormack et al., 2022)). In addition, $\delta^{66}Zn$ values are higher in individuals presumed to be breastfeeding relative to those associated with post-weaned individuals (Jaouen et al., 2020), and zinc concentrations ([Zn], in ppm) are higher at the surface of enamel in all teeth (see SI, Supporting Information 3.9.3). The breastfeeding effect is not intuitive, in that if this was a standard trophic position change, nursing offspring would be expected to have lower $\delta^{66}Zn$ values. This is probably due to an enrichment of milk in heavy zinc isotopes compared to other body tissues (Jaouen et al., 2020).

To date, $\delta^{66}Zn$ variation amongst non-human primates has only been studied in archaeological samples from Pleistocene sites in Southeast Asia, which validate that orangutans (n = 2) and macaques (n = 5) are omnivores relative to other sampled fauna (Bourgon et al., 2020; Bourgon et al., 2021). When exploring $\delta^{66}Zn$ variation in modern food webs, however, it is

important to consider the environmental baseline, as $\delta^{66}Zn$ values can vary substantial in plants (Bourgon et al., 2020; Jaouen et al., 2016). Additionally, the $\delta^{66}Zn$ values observed in different food webs may vary because of isotopic differences in bioavailable Zn associated with differences in bedrock geology or atmospheric deposition on soils (Cloquet et al., 2008).Therefore, we will explore how $\delta^{66}Zn$ values vary in the environment, including the typical animal and plant foods that chimpanzees consume. These data will bolster our current understanding of $\delta^{66}Zn$ variation in a modern ecosystem inhabited by chimpanzees, with the potential to improve our interpretation of $\delta^{66}Zn$ values in paleoanthropological contexts.

Chimpanzees (*Pan troglodytes*) are important models for reconstructing early hominin behavior and ecology (Andrews, 2020; Boesch-Achermann & Boesch, 1994; Riedel et al., 2020). In Taï National Park (Côte d'Ivoire), the Taï Chimpanzee Project (TCP) has habituated five neighboring chimpanzee groups and studied their behavior for more than 40 years (see Supporting Information 3.9.1 to 3.9.3, Figure 3.9.1, (Boesch & Wittig, 2019). In Taï chimpanzees, weaning is estimated to begin around 3 years and cease around 4 to 5 years of age , although, starting already at around 6 months, infant chimpanzees are typically supplemented with solid foods by their mothers (Bădescu et al., 2017; Fahy et al., 2014; Samuni, Tkaczynski, et al., 2020; Smith et al., 2013). Chimpanzees are primarily frugivorous, and long-term observations (percent feeding time) reveal that plant foods (fruits, leaves, nuts, seeds) comprise 97% of the Taï chimpanzee diet (Goné Bi & Wittig, 2019). The primarily plant-based diet of Taï chimpanzees is supplemented by insects (*Dorylus spp.* ants;

Thoracotermes spp., *Cubitermes spp*., and *Macrotermes spp.* termites; caterpillars), honey and mushrooms (Boesch & Boesch, 1990; Boesch & Boesch-Achermann, 2000a; Luncz & Boesch, 2015). The consumption of vertebrate animal meat (referred to as meat moving forward) makes up the remaining fraction of their diet, and the hunting of medium-sized prey occurs year-round (Boesch & Boesch, 1989; Boesch & Boesch-Achermann, 2000a; Fahy et al., 2013; Oelze et al., 2020; Riedel et al., 2020). For chimpanzees, while the consumption of insects and meat occur at low levels, they can provide supplemental protein, fats, and essential micronutrients, such as calcium, sodium, iron, zinc, B6 and B12, which are often completely absent from plant foods (Orkusz, 2021; Tennie et al., 2014). In addition, dietary proteins from animal products are associated with higher Zn uptake, whereas plant products contain natural antinutrients, such as phytate and tannins, which tend to inhibit Zn adsorption and reduce bioavailability (Bourgon et al., 2024). An isotopic study of Taï chimpanzee hair keratin and bone collagen found higher $\delta^{15}N$ values to correspond to the higher trophic position of successful male hunters, relative to females and other, less successful males (Fahy et al., 2013). However, when considering the actual observed quantities of meat eaten by a given individual, there was no association between meat eating amounts and hair $\delta^{15}N$ values, most likely due to environmental baseline differences in plant $\delta^{15}N$ values between the territories of the two Taï communities studied (Oelze et al., 2020). Taï chimpanzees are among the

most specialized hunters (Fahy et al., 2013; Goné Bi & Wittig, 2019; Oelze et al., 2020), but due to conflicting $\delta^{15}N$ evidence, it remains disputed if isotopic analysis can detect infrequent meat-eating in the body tissues of a mostly frugivorous species, which could serve as a valuable analog for some early hominins who are suspected of having consumed comparably low proportions of meat (Fahy et al., 2013; Oelze et al., 2020). Here, we investigate if meat consumption and nursing are recorded in the tooth enamel of Taï chimpanzees using a novel proxy, zinc (Zn) isotope analysis.

We present a comprehensive study employing $\delta^{66}Zn$ analysis in tooth enamel of a modern population of wild primates with known diets, specifically western chimpanzees (*P. t. verus*), alongside the $\delta^{66}Zn$ analysis of some of their food. First, we explore how $\delta^{66}Zn$ values as well as Zn concentrations vary in a selection of chimpanzee foods items, and we estimate the $\delta^{66}Zn$ values for the chimpanzees' preferred vertebrate prey, colobine monkeys. Second, as the overall $\delta^{66}Zn$ values of an ecosystem can be influenced by the underlying geology, we consider possible geological influences on enamel $\delta^{66}Zn$ values by referring to enamel $^{87}Sr/^{86}Sr$ data from the same Taï chimpanzees (Boucher et al., 2024). Third, we explore how $\delta^{66}Zn$ values vary among Taï chimpanzees if we consider age at tooth formation, especially in relationship to nursing (see Table 3.3.1), and we compare $\delta^{66}Zn$ values between male and female chimpanzees to assess average differences in meat consumption between the sexes. This study in extant chimpanzees will advance our understanding of $\delta^{66}Zn$ variation in a modern ecosystem and its potential application to hominin fossils.

3.4. Materials and Methods

Sample Collection

The material used in this study consists of common plant and animal foods that have been observed being consumed by Taï chimpanzees (n = 28, Table 3.9.1), and were collected under the scope of two other studies (Boucher et al., 2024; Lowry et al., 2021). Tooth enamel from the Taï chimpanzees (*Pan troglodytes verus*, n = 34) was sampled from the Taï chimpanzee skeletal collection at the Max Planck Institute for Evolutionary Anthropology (MPI-EVA, see Table 3.9.2 and the SI, Supporting Information 3.9.1 to 3.9.2 for more details).

Stable Isotope Analysis

The samples were processed for isotope analysis using a modified ion exchange method adapted from Moynier et al. (Moynier et al., 2009) and first described in Jaouen et al. (Jaouen et al., 2016). $\delta^{66}Zn$ values were determined on a ThermoScientific Neptune Plus MC-ICP-MS at the *Géosciences Environnement Toulouse - Observatoire Midi-Pyrénées* (Toulouse, France), following the protocols in SI, Supporting Information 3.9.3. The $\delta^{66}Zn$ measurement uncertainties were estimated from the repeated measurement of an internal standard (AA-GET) used for standard bracketing (0.30 ± 0.08‰), and the standard replicate analyses ranged from ± 0.003‰ to ± 0.12‰ (2σ, see SI, Supporting Information 3.9.3.4 to 3.9.3.5).

Data Analysis

All statistical analyses were performed using the R software program (version 4.3.2) (R Core Development Team, 2022). To test our hypotheses of predictor variables associated with variability in $\delta^{66}Zn_{enamel}$ values, we fitted two generalized linear mixed models (GLMM, (Bolker et al., 2009; Brooks et al., 2022) with a Gaussian distribution and Bonferroni error correction using the R package "glmmTMB" (version 1.1.8) (Brooks et al., 2017). In the full method, $\delta^{66}Zn$ values are predicted by tooth type and sex, as fixed effects, and chimpanzee community (North, South, East, Middle) was included as a random effect (for details see SI, Supporting Information 3.9.3.8). A complete description of the materials and methods used in this study is included in SI, Supporting Information 3.9.3.

3.5. Results

In Taï, the mean $\delta^{66}Zn$ value is 0.48 ± 0.50‰ for plant leaves (n = 7), 0.15‰ for honey, 0.14 ‰ for fungus, 0.22 ± 0.48‰ for termites (n = 10), and 0.00 ± 0.14‰ for ants (n = 9) (all error is reported to 2σ, Figure 3.6.1 and Table 3.9.1). Based on the mean $\delta^{66}Zn$ value for plant leaves, the estimated $\delta^{66}Zn$ value for colobus monkey meat is 0.17‰ (2σ cannot be reliably estimated, see Supporting Information 3.9.3.6, Table 3.9.7, Figure 3.9.3). In the modern Taï ecosystem, plants, ants, and termites significantly differ in $\delta^{66}Zn$ values ($\chi2 = 13.1$, df = 2, p = 0.001) and [Zn] ($\chi2 = 18.8$, df = 2, p = 0.0001). In $\delta^{66}Zn$ values, plants differ significantly from ants (p = 0.001),

but not from termites ($p = 0.07$), and ants and termites differ significantly from each other ($p = 0.04$). In [Zn], plants differ significantly from termites ($p = 0.04$), as well as ants ($p = 0.0004$), and similarly, ants and termites differ significantly from each other ($p < 0.0001$). Average [Zn] are 253 ± 99 ppm for ants, considerably higher than those for plant leaves (28 ± 25 ppm), termites (59 ± 66 ppm), honey (75 ppm) or fungus (95 ppm) (see Figure 3.9.4 and Table 3.9.1). Based on the average [Zn] in plants, and the drop in concentration between diet and muscle observed in feeding studies (~66.6%, see Supporting Information 3.9.3.6), the estimated [Zn] in colobus meat is 19 ppm. Within the TCP study area, enamel $^{87}Sr/^{86}Sr$ ratios range from 0.71639 to 0.73049 in all chimpanzees (Boucher et al., 2024), and Sr and Zn isotope ratios show no correlation ($R_\tau = 0.04$, $p = 0.72$), Figure 3.9.5).

The mean $\delta^{66}Zn$ value for all sampled Taï chimpanzees ($n = 34$) is 0.30 ± 0.24‰, ranging from 0.03 to 0.51 ‰ (Figure 3.9.2; Tables 3.9.2). When we account for the $\Delta^{66}Zn_{enamel\text{-}diet}$ offset of -0.1‰, the Taï chimpanzee diet is estimated to be around 0.14‰ for males and 0.19 ‰ for females (Figure 3.9.3 and Supporting Information 3.9.3.6). First, we compared the $\delta^{66}Zn$ values among tooth types with enamel forming at different life stages. We found no significant difference in $\delta^{66}Zn$ values among all tooth types sampled (glmm, p

> 0.05, Figure 3.6.2; Tables 3.9.3 and 3.9.4). However, when examining all tooth types, there was a significant difference in $\delta^{66}Zn$ values between sexes ($t_{26} = 2.61$, $p = 0.02$, power = 0.72; see Tables 3.9.3 and 3.9.4). To examine this difference further, we tested if $\delta^{66}Zn$ values differ between the sexes in pre-weaned (dp, M1, M2) and post-weaned (M3) individuals. There is not a significant difference in $\delta^{66}Zn$ values between sexes for deciduous premolars, first molars, nor second molars (see Figure 3.9.2, $t(7.26) = -1.63$, $p = 0.15$)).

However, when comparing second and third molars, the teeth bearing the cleanest temporal segregation of nursing (M2) versus solid food consumption post-weaning (M3), we found a significant difference in $\delta^{66}Zn$ values ($t(22.1) = 2.38$, $p = 0.03$), with lower $\delta^{66}Zn$ values in third molars. To explore the effect of sex further, we examined only M3s, which reflect individuals feeding themselves on solid foods (excluding teeth formed *in utero* or when individuals might be nursing, as well as too outliers among M3s) (Table 3.3.1). For third molars, females have significantly higher $\delta^{66}Zn$ values (0.34 ± 0.05‰, n = 4) than males (0.20 ± 0.06‰, n = 6; $t(5.13) = 3.04$, $p = 0.03$; effect size = 2.02, power = 0.99, see Figure 3.6.3). We estimated the proportion of animal versus plant foods for both male and female chimpanzees (see Supporting Information 3.9.3.7 and Table 3.9.8) and found that the female chimpanzee diet is comprised of 97.4% plant and 2.6% animal foods, whereas the male chimpanzee diet is composed of 95.1% plant and 4.9% animal foods.

3.6. Discussion

Zn isotope variation in the modern Taï ecosystem

Among chimpanzee foods, we found the expected trophic-level shifts, where *Dorylus* ants occupy the highest trophic position with the lowest $\delta^{66}Zn$ values, likely due to their strongly carnivorous and insectivorous diet (Schöning & Moffett, 2007). Termite $\delta^{66}Zn$ values are intermediate, and plant leaves have the highest $\delta^{66}Zn$ values (Figure 3.6.1). By contrast, [Zn] are the highest in ants, followed by termites, and then lastly, plant leaves (Figure 3.9.4). Termites and plant leaves are less likely to contribute to the Taï chimpanzee diet, since [Zn] are fairly low, averaging about 59.4 ± 67 ppm relative to ants (253 ± 99 ppm), plant leaves (28 ± 25 ppm), and monkey meat (19 ppm) (see Figure 3.9.4 and Table 3.9.1). We sampled more species for plant leaves (n = 6) and termites (n = 3) relative to ants (n = 2), which could be contributing to the higher variance in $\delta^{66}Zn$ values for these groups (see Figures 3.6.1 and 3.9.4, Table 3.9.1). Indeed, the $\delta^{66}Zn$ variation observed within termites could be related to differing diets in the species sampled. Specifically, *Cubitermes* and *Thoracotermes spp* feed primarily on detritus and soil ($\delta^{66}Zn$ = 0.32 ± 0.43‰, [Zn] = 49 ± 32 ppm), whereas *Macrotermes spp.* feed on fungus and leaf litter ($\delta^{66}Zn$ = 0.00 ± 0.27‰, [Zn] = 84 ± 109 ppm) (Sanz et al., 2014; Tayasu et al., 1998).

Although chimpanzees mainly consume ripe fruit, we analyzed only plant leaves as these were readily available within the scope of another study

(Boucher et al., 2024). In comparison to plant leaves, fruit has been shown to have around the same [Zn], with an average of 19 ppm for *Ficus spp.* and 6 ppm for *Parinari excelsia,* which are the most preferred fruits for Taï chimpanzees (Goné Bi & Wittig, 2019; Rode et al., 2003; Stadlmayr, 2012). There are currently no δ^{66}Zn values reported for the other fruit species consumed by Taï chimpanzees. When considering the influence of each food item to the Taï chimpanzee diet, we suggest that food sources with higher [Zn], such ants could contribute more strongly to the total δ^{66}Zn isotopic composition compared to plant foods. Since consuming animal foods has been associated with higher Zn uptake and adsorption (Bourgon et al., 2024), we suggest that the bioavailable Zn in the Taï chimpanzee's diet could mainly come from the average of animal foods consumed (insect and monkey meat).

Moreover, we found considerable δ^{66}Zn variation in the plant and animal foods from the TCP study area that, given the lack of covariation between Sr and Zn isotopes, appears to be unrelated to the underlying geology of this region (Figure 3.9.5). Since the plant samples reported in this study (0.18‰ to 0.74‰) fall within the range of other studies in Africa (-0.09 to 0.97‰), we suggest that there is relatively low δ^{66}Zn variation within sub-Saharan Africa relative to modern greenhouses (-0.6‰ to 1.3‰) (Jaouen et al., 2016; Weiss et al., 2005). Therefore, it may be possible to more directly compare Zn isotopic data from other studies within Africa to better inform interpretations of diet.

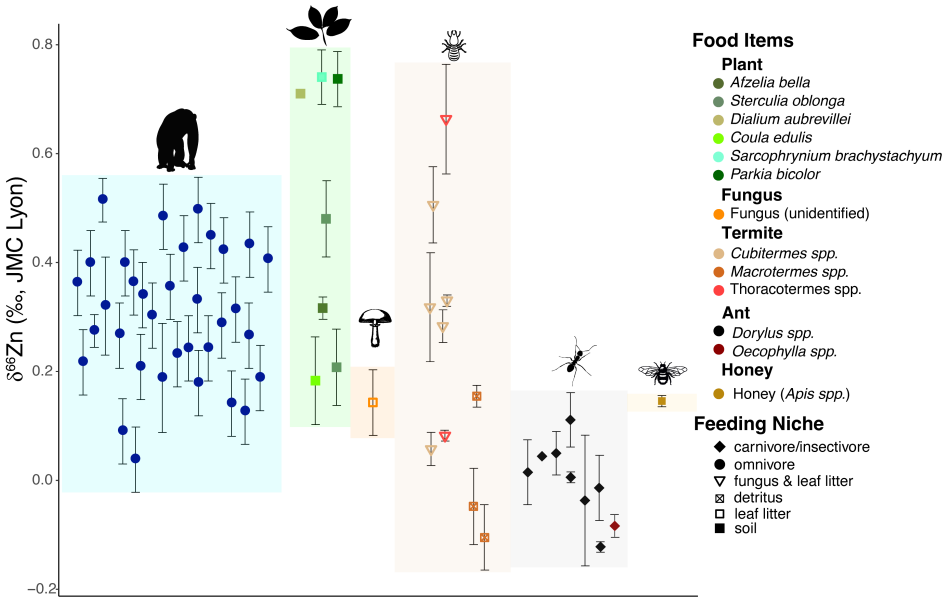

Figure 3.6.1. The δ^{66}Zn values (in ‰) in plant and animal samples from Taï forest. Measurement uncertainty is indicated at the 2σ level for each datapoint.

Zn uptake and the Taï chimpanzee diet

There is considerable δ^{66}Zn and [Zn] variation in the foods consumed as part of the Taï chimpanzee diet. The estimated Taï chimpanzee diet aligns more with the δ^{66}Zn values for animal foods rather than plant foods (Figure 3.9.3 and Supporting Information 3.9.3.6). Given that the majority of the chimpanzee diet is plant-based, we explore what could be contributing to the low δ^{66}Zn values observed for the chimpanzee enamel and their estimated diet. The isotopic composition of enamel is the average [Zn], δ^{66}Zn values, and the Zn absorption or uptake from the diet. Plant leaves and fruit have fairly low [Zn], and these concentrations can be further reduced by the prevalence of antinutrients. Antinutrients, such as phytate inhibit Zn

adsorption by binding bioavailable Zn to phosphate groups, thereby impairing Zn uptake in the intestines (Bourgon et al., 2024; Jaouen et al., 2019). Similarly, the presence of tannins, which are common in many fruits, plant leaves, seeds and nuts have also been shown to reduce the absorption of Zn (Behie & Pavelka, 2012). By contrast, consuming supplementary animal proteins actually negates the effects of phytates and in fact, increases the bioavailable Zn, thus increasing Zn adsorption (Bourgon et al., 2024). We suggest that the isotopic composition of the Taï chimpanzee's diet is a mix of bioavailable [Zn] from plant and animal foods (Bourgon et al., 2024), where the more bioavailable Zn in monkey and insect meat likely contributes a larger proportion of Zn to the diet than fruit, plant leaves, and nuts. Since ants have especially low δ^{66}Zn values (0.00), but high [Zn] (253 ppm), they are likely contributing more strongly to the reported diet δ^{66}Zn values. Therefore, the Taï chimpanzee's diet has lower δ^{66}Zn values, mainly resembling the isotopic signal of animal foods (0.00 to 0.22‰) rather than plant foods (0.48‰), however, it is difficult to assess if this is related to monkey or ant meat consumption.

The effect of sex on diet

We found a significant difference in δ^{66}Zn values in the Taï chimpanzees, most likely related to dietary differences between the sexes, with males having lower δ^{66}Zn values than their female counterparts overall (Figure 3.6.3; Tables 3.9.3 to 3.9.4). Reported enamel δ^{66}Zn values for male (0.24 ± 0.19‰) and female Taï chimpanzees (0.29 ± 0.27‰) are in line with those reported for other primate species, such as macaques (0.27 ± 0.16‰) and orangutans (0.36 ± 0.06‰) despite the large

distance between study areas (Bourgon et al., 2020). Taï chimpanzees dental enamel sit intermediate between plant leaves, monkey meat, and termites (see Figure 3.9.3), where *Dorylus spp.* ants are on average lower than monkey meat.

A similar dietary sex difference in adult Taï chimpanzees has been demonstrated with $\delta^{15}N$ values in bone collagen (Fahy et al., 2013). Observations of the hunting prowess of male chimpanzees support that Taï chimpanzee males are the primary hunters, and higher $\delta^{15}N$ values as well as lower $\delta^{66}Zn$ values for males likely relates to their higher interest in hunting and meat sharing events, where on average, males consume seven times more meat relative to females (Boesch, 2003a; Boesch & Boesch-Achermann, 2000a; Riedel et al., 2020). Therefore, we suggest that the occasional consumption of monkey meat could contribute to male chimpanzees occupying a higher trophic position than female chimpanzees (Figures 3.6.3 and 3.9.3). There are behavioral observations which demonstrate that adolescent chimpanzees (age 10 to 15 years) can successfully attain as much meat as adults, where in 7 months, cumulative meat consumption for adult males and females is on average 3.1 kg and 2.1 kg, whereas for adolescent males and females is on average 2.4 kg and 2.5 kg, respectively (Oelze et al., 2020). Similarly, between 1987 to 1991, when about 35% of Taï chimpanzees were forming tooth enamel sampled in this study, daily meat intake was higher, around 186 g for males and 25 g for females (Boesch & Boesch-

Achermann, 2000b). Therefore, it is possible that the sex difference in $\delta^{66}Zn$ values for adolescent chimpanzees is related to higher frequencies of hunting participation and meat consumption in adolescent males, which could lead to continued investment into hunting as adults (Boesch, 2003a). In the cases of chimpanzees SM03 (0.13‰) and SM04 (0.19‰), there is sufficient behavioral data that suggests these males had high hunting success in their adult life, participating in over 100 meat eating events out of 376 (Riedel et al., 2020). Also, some high-ranking females are known to maximize their access to meat compared to subordinates, often showing more interest in meat eating events when in estrus or lactating (Oelze et al., 2020; Riedel et al., 2020). In the case of chimpanzee NF06 (0.09‰), lower $\delta^{66}Zn$ values (< 0.15‰) relative to the average female (0.29‰) during adolescence are consistent with a higher trophic position, and there is behavioral data that supports that she was participating in over 100 out of 496 meat eating events when she as an adult (Riedel et al., 2020). Therefore, we suggest that $\delta^{66}Zn$ values support an isotopic signal of higher meat consumption in some high-ranking females as well as males, although most females have higher $\delta^{66}Zn$ values, most likely related to their lower frequency to engage in meat-sharing events (Boesch, 2003a).

Overall, in habituated populations, estimating dietary intake via direct observations alone, e.g., by considering time spent feeding, is not directly quantifiable to food mass (Fahy et al., 2013; Lemoine et al., 2019; Möbius et al., 2008). We cannot discount that the sex difference in $\delta^{66}Zn$ values could be related to the consumption of other insect foods that make up roughly 3% of the Taï chimpanzee diet. In some

females (NF12-0.22‰, NF03-0.27‰), where behavioral data does not suggest that they engage in hunting behavior nor meat consumption, we suggest that ants are contributing more to the lower δ^{66}Zn values observed. There is no sex difference observed in termite foraging behavior, so this is unlikely contributing to the pattern we observe in Taï chimpanzees (see Supporting Information 3.9.1.3). In Taï, the consumption of monkey and insect meat is a small proportion of the overall diet, but it appears to be influencing the δ^{66}Zn values in adolescent Taï male and female chimpanzees more substantially due to low δ^{66}Zn values in insect and monkey meat. However, we cannot discount that the small contributions of *Dorylus spp.* ants and possibly termites could be influencing male Taï chimpanzees' enamel δ^{66}Zn values more strongly than monkey meat. Therefore, we suggest that the occasional consumption of monkey meat and insects could both contribute to the sex differences in diet observed for enamel δ^{66}Zn values in the Taï chimpanzees.

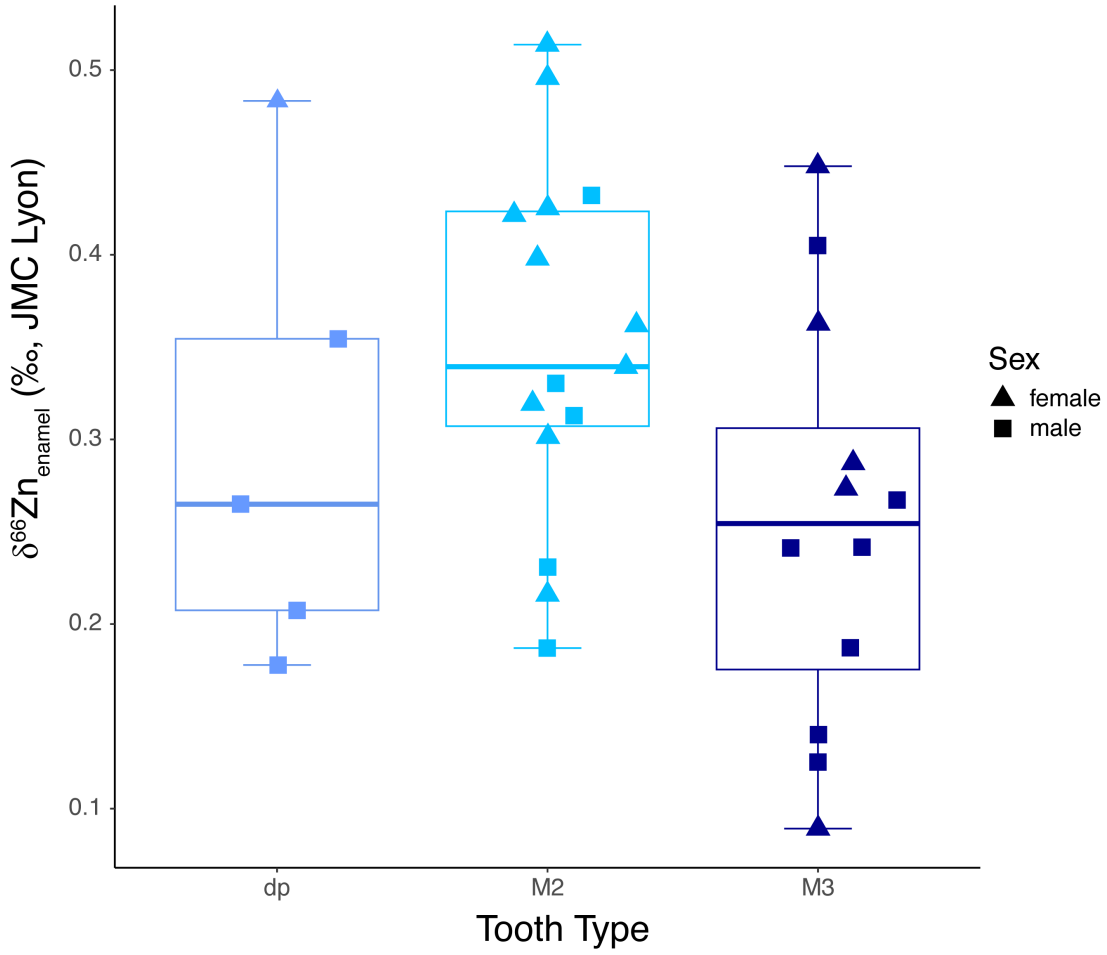

Figure 3.6.2. Boxplots showing the medians, upper (75%) and lower (25%) quartiles of the $\delta^{66}Zn$ values by tooth type (dps, M2s, M3s) in Taï chimpanzees (n = 32).

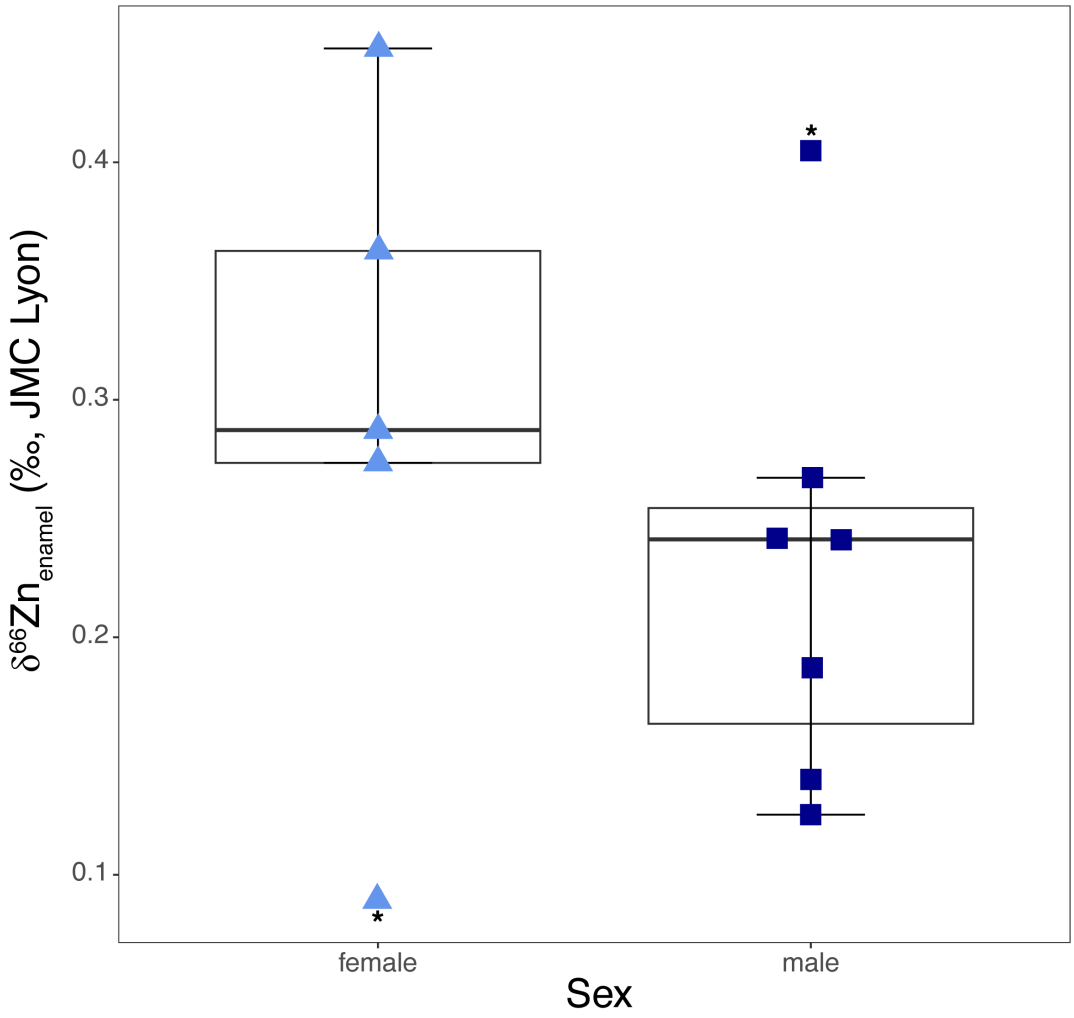

Figure 3.6.3. Boxplots depicting the differences in $\delta^{66}Zn$ values between fully weaned male and female chimpanzees from Taï National Park in Côte d'Ivoire (n = 12).
The teeth sampled (M3) reflect the diet of these individuals during tooth formation (6-9 years). Measurement uncertainty is indicated at the 2σ level. The * indicate outliers, which were excluded from statistical analyses, as they were 1.5 times greater than the interquartile range.

The timing of Zn deposition and its effect on breastfeeding signals

We found a significant difference between second and third molars, where second molars have higher δ^{66}Zn values relative to third molars. We suggest that this confirms that there is an isotopic signal of breastfeeding in second molars, which is more in line with a continuous Zn deposition (Model 1) within enamel (see Table 3.3.1 and Supporting Information 3.9.3.3). This means that bulk enamel sampling likely encompasses the entire time of crown formation, resulting in a mixed dietary signal between ontogenetic stages (Dean et al., 2023). While the assessment of a breastfeeding effect is complicated by mixed dietary signals from *in-utero* to nursing, we found some evidence of a breastfeeding effect in a subsample of mother-offspring dyads (n = 5), suggesting that enamel that overlaps with nursing has higher δ^{66}Zn values (see Supporting Information 3.9.4.1-3.9.4.2 and Figure 3.9.9).

Previous work on archaeological human teeth samples suggested a possible breastfeeding effect in δ^{66}Zn values, with early forming teeth having 0.3‰ higher δ^{66}Zn values on average relative to late-forming teeth (Jaouen et al., 2020). This ^{66}Zn-enrichment is only present in deciduous premolars and first molars for humans (Jaouen et al., 2020), which in chimpanzees form *in-utero* and during early infancy through nursing (Table 3.3.1). In chimpanzees, it appears that the ^{66}Zn-enrichment is present in second molars (see Table 3.3.1 and Figure 3.6.2 and 3.9.2). We suggest that this could be related to higher Zn absorption from breast milk (~ 41%) during nursing (Jaouen et al., 2020). Therefore, when assessing if there is a breastfeeding signal in enamel, it is important to consider the timing of Zn deposition and how this relates to

species-specific crown formation times. This study only provides limited insights into the potential breastfeeding effect in $\delta^{66}Zn$ values, supporting some of what we see in Neanderthals and humans (Bourgon et al., 2021; Jaouen et al., 2022).

3.7. Acknowledgments

We thank the late Christophe Boesch (1951- 2024), founder of the Taï Chimpanzee Project, for his lifelong devotion to the study and conservation of chimpanzees. Without his wise foresight the Taï chimpanzee skeletal collection would not have been available for comparative research. We are grateful to the Ministry of Research in Côte d'Ivoire, the Ministry of Environment and Forests in Côte d'Ivoire and the *Office Ivoirien des Parcs et Réserves* for their permission to conduct the research. We thank the *Centre Suisse de Recherches Scientifiques en Côte d'Ivoire* and the staff of the Taï Chimpanzee Project for their continuous support. We thank Heiko Temming and Zewdi Tsegai for assisting with CT-scanning all teeth prior to sampling, as well as Manuel Trost for help in the clean lab. We thank Pauline Méjean, Manuel Henry, Jérôme Chmeleff, Camille Duquenoy, Danaé Guiserix, and Jessica Mendes Cardoso at the *Géosciences Environnment Toulouse* lab.and Shauhin Alavi, for support with data analysis. This research was funded by the U.S. National Science Foundation (grant No. 2216033), the ERC (grant number 803676), the L.S.B. Leakey Foundation, and the Lambda Alpha National Anthropology Honor Society, and the Max Planck Society.

3.8. References Cited

Fahy GE, Richards M, Riedel J, Hublin J-J, Boesch C. Stable isotope evidence of meat eating and hunting specialization in adult male chimpanzees. Proceedings of the National Academy of Sciences. 2013;110(15):5829-33.

Tennie C, Gilby IC, Mundry R. The meat-scrap hypothesis: small quantities of meat may promote cooperative hunting in wild chimpanzees (Pan troglodytes). Behavioral Ecology and Sociobiology. 2009;63(3):421-31.

Williams AC, Dunbar RI. Big brains, meat, tuberculosis and the nicotinamide switches: co-evolutionary relationships with modern repercussions on longevity and disease? Medical hypotheses. 2014;83(1):79-87.

Lüdecke T, Kullmer O, Wacker U, Sandrock O, Fiebig J, Schrenk F, et al. Dietary versatility of Early Pleistocene hominins. Proceedings of the National Academy of Sciences. 2018;115(52):13330-5.

Lüdecke T, Leichliter JN, Duprey NN, Stratford D, Vonhof HB, Bamford MK, et al., editors. First enamel nitrogen isotope data of early hominins: Early Pleistocene Australopithecus (Sterkfontein Member 4, South Africa) did not consume significant amounts of animal resources. American Journal of Biological Anthropology; 2022.

Ben-Dor M, Sirtoli R, Barkai R. The evolution of the human trophic level during the Pleistocene. American journal of physical anthropology. 2021;175:27-56.

Ambrose SH. Effects of diet, climate and physiology on nitrogen isotope abundances in terrestrial foodwebs. Journal of archaeological science. 1991;18(3):293-317.

Bocherens H, Drucker D. Trophic level isotopic enrichment of carbon and nitrogen in bone collagen: case studies from recent and ancient terrestrial ecosystems. Int J Osteoarchaeol. 2003;13(1-2):46-53.

Hedges R, Reynard LM. Nitrogen isotopes and the trophic level of humans in archaeology. Journal of archaeological science. 2007;34(8):1240-51.

Leichliter JN, Lüdecke T, Foreman AD, Bourgon N, Duprey NN, Vonhof H, et al. Tooth enamel nitrogen isotope composition records trophic position: a tool for reconstructing food webs. Commun Biol. 2023;6(1):373.

Jaouen K, Pons M-L, Balter V. Iron, copper and zinc isotopic fractionation up mammal trophic chains. Earth and Planetary Science Letters. 2013;374:164-72.

Jaouen K, Beasley M, Schoeninger M, Hublin JJ, Richards MP. Zinc isotope ratios of bones and teeth as new dietary indicators: results from a modern food web (Koobi Fora, Kenya). Sci Rep. 2016;6:26281.

Moynier F, Fujii T, Shaw AS, Le Borgne M. Heterogeneous distribution of natural zinc isotopes in mice. Metallomics. 2013;5(6):693-9.

Bourgon N, Tacail T, Jaouen K, Leichliter JN, McCormack J, Winkler DE, et al. Dietary and homeostatic controls of Zn isotopes in rats: A controlled-feeding experiment and modelling approach. Metallomics. 2024.

Jaouen K, Pouilloux L, Balter V, Pons M-L, Hublin J-J, Albarède F. Dynamic homeostasis modeling of Zn isotope ratios in the human body. Metallomics. 2019;11(6):1049-59.

Bourgon N, Jaouen K, Bacon A-M, Jochum KP, Dufour E, Duringer P, et al. Zinc isotopes in Late Pleistocene fossil teeth from a Southeast Asian cave setting preserve paleodietary information. Proceedings of the National Academy of Sciences. 2020;117(9):4675-81.

Bourgon N, Jaouen K, Bacon AM, Dufour E, McCormack J, Tran NH, et al. Trophic ecology of a Late Pleistocene early modern human from tropical Southeast Asia inferred from zinc isotopes. J Hum Evol. 2021;161:103075.

McCormack J, Griffiths ML, Kim SL, Shimada K, Karnes M, Maisch H, et al. Trophic position of Otodus megalodon and great white sharks through time revealed by zinc isotopes. Nature Communications. 2022;13(1):1-10.

Jaouen K, Trost M, Bourgon N, Colleter R, Le Cabec A, Tütken T, et al. Zinc isotope variations in archeological human teeth (Lapa do Santo, Brazil) reveal dietary transitions in childhood and no contamination from gloves. PloS one. 2020;15(5):e0232379.

Jaouen K, Szpak P, Richards MP. Zinc isotope ratios as indicators of diet and trophic level in arctic marine mammals. PloS One. 2016;11(3):e0152299.

Cloquet C, Carignan J, Lehmann MF, Vanhaecke F. Variation in the isotopic composition of zinc in the natural environment and the use of zinc isotopes in biogeosciences: a review. Analytical and bioanalytical chemistry. 2008;390(2):451-63.

Boesch-Achermann H, Boesch C. Hominization in the rainforest: The chimpanzee's piece of the puzzle. Evolutionary Anthropology: Issues, News, and Reviews. 1994;3(1):9-16.

Riedel J, Polansky L, Wittig RM, Boesch C. Social rank overrides environmental and community fluctuations in determining meat access by female chimpanzees in the Taï National Park, Côte d'Ivoire. PeerJ. 2020;8:e8283.

Andrews P. Last common ancestor of apes and humans: Morphology and environment. Folia Primatologica. 2020;91(2):122-48.

Boesch C, Wittig R. Demography and life history of five chimpanzee communities in Taï National Park. In: Boesch C, Wittig R, Crockford C, Vigilant L, Deschner T, Leendertz F, editors. The Chimpanzees of the Taï Forest: 40 Years of Research. Cambridge: Cambridge University Press; 2019. p. 159-77.

Smith TM, Machanda Z, Bernard AB, Donovan RM, Papakyrikos AM, Muller MN, et al. First molar eruption, weaning, and life history in living wild chimpanzees. Proceedings of the National Academy of Sciences. 2013;110(8):2787-91

Fahy GE, Richards MP, Fuller BT, Deschner T, Hublin JJ, Boesch C. Stable nitrogen isotope analysis of dentine serial sections elucidate sex differences in weaning patterns of wild chimpanzees (Pan troglodytes). American Journal of Physical Anthropology. 2014;153(4):635-42.

Bădescu I, Katzenberg MA, Watts DP, Sellen DW. A novel fecal stable isotope approach to determine the timing of age-related feeding transitions in wild infant chimpanzees. American journal of physical anthropology. 2017;162(2):285-99.

Samuni L, Tkaczynski P, Deschner T, Löhrrich T, Wittig RM, Crockford C. Maternal effects on offspring growth indicate post-weaning juvenile dependence in chimpanzees (Pan troglodytes verus). Frontiers in Zoology. 2020;17(1):1.

Goné Bi ZB, Wittig R. Long-term diet of the chimpanzees (Pan troglodytes verus) in Taï National Park: interannual variations in consumption. In: The Chimpanzees of the Taï Forest: Cambridge University Press; 2019.

Boesch C, Boesch H. Tool use and tool making in wild chimpanzees. Folia Primatol (Basel). 1990;54(1-2):86-99.

Boesch C, Boesch-Achermann H. The chimpanzees of the Taï Forest: Behavioural ecology and evolution: Oxford University Press, USA; 2000.

Luncz LV, Boesch C. The extent of cultural variation between adjacent chimpanzee (Pan troglodytes verus) communities; A microecological approach. American Journal of Physical Anthropology. 2015;156(1):67-75.

Boesch C, Boesch H. Hunting behavior of wild chimpanzees in the Tai National Park. American journal of physical anthropology. 1989;78(4):547-73.

Oelze VM, Wittig RM, Lemoine S, Kühl HS, Boesch C. How isotopic signatures relate to meat consumption in wild chimpanzees: A critical reference study from Taï National Park, Côte d'Ivoire. Journal of Human Evolution. 2020.

Tennie C, O'Malley RC, Gilby IC. Why do chimpanzees hunt? Considering the benefits and costs of acquiring and consuming vertebrate versus invertebrate prey. Journal of Human Evolution. 2014;71:38-45.

Orkusz A. Edible Insects versus Meat—Nutritional Comparison: Knowledge of Their Composition Is the Key to Good Health. Nutrients. 2021;13(4):1207.

Boucher RD, Wittig RM, Lemoine S, Maro A, Wang X, Koch PL, Oelze, VM. Strontium isotopes track female dispersal in Taï chimpanzees. American Journal of Biological Anthropology. 2024.

Moynier F, Pichat S, Pons M-L, Fike D, Balter V, Albarède F. Isotopic fractionation and transport mechanisms of Zn in plants. Chemical Geology. 2009;267(3-4):125-30.

R Core Development Team. R: A language and environment for statistical computing. R Foundation for Statistical Computing, Vienna, Austria. 2024.

Brooks M, Bolker B, Kristensen K, Maechler M. Package 'glmmTMB'. 2022.

Schöning C, Moffett MW. Driver ants invading a termite nest: why do the most catholic predators of all seldom take this abundant prey? Biotropica. 2007;39(5):663-7.

Tayasu I, Inoue T, Miller LR, Sugimoto A, Takeichi S, Abe T. Confirmation of soil-feeding termites (Isoptera; Termitidae; Termitinae) in Australia using stable isotope ratios. Functional Ecology. 1998;12(4):536-42.

Sanz CM, Deblauwe I, Tagg N, Morgan DB. Insect prey characteristics affecting regional variation in chimpanzee tool use. Journal of Human Evolution. 2014;71:28-37.

Rode KD, Chapman CA, Chapman LJ, McDowell LR. Mineral resource availability and consumption by colobus in Kibale National Park, Uganda. International Journal of Primatology. 2003;24(3):541-73.

Stadlmayr B. West African food composition table/table de composition des aliments d'Afrique de l'Ouest. 2012.

Weiss DJ, Mason TFD, Zhao FJ, Kirk GJD, Coles BJ, Horstwood MSA. Isotopic discrimination of zinc in higher plants. New Phytologist. 2005;165(3):703-10.

Behie AM, Pavelka MSM. The Role of Minerals in Food Selection in a Black Howler Monkey (Alouatta Pigra) Population in Belize Following a Major Hurricane. American Journal of Primatology. 2012;74(11):1054-63.

Boesch C. 4. Complex Cooperation among Taï Chimpanzees. In: Frans BMdW, Peter LT, editors. Animal Social Complexity. Cambridge, MA and London, England: Harvard University Press; 2003. p. 93-110.

Boesch C, Boesch-Achermann H. The chimpanzees of the Taï Forest: Behavioural ecology and evolution. Oxford University Press, USA; 2000.

Möbius Y, Boesch C, Koops K, Matsuzawa T, Humle T. Cultural differences in army ant predation by West African chimpanzees? A comparative study of microecological variables. Animal Behaviour. 2008;76(1):37-45.

Lemoine S, Crockford C, Wittig R. Spatial integration of unusually high numbers of immigrant females into the South Group: further support for the bisexually bonded model in Taï chimpanzees. In: Boesch C, Wittig R, Crockford C, Vigilant L, Deschner T, Leendertz F, editors. The chimpanzees of the Taï Forest: 40 years of research: Cambridge University Press; 2019.

Dean MC, Garrevoet J, Van Malderen SJM, Santos F, Mirazón Lahr M, Foley R, et al. The Distribution and Biogenic Origins of Zinc in the Mineralised Tooth Tissues of Modern and Fossil Hominoids: Implications for Life History, Diet and Taphonomy. Biology. 2023;12(12):1455.

Jaouen K, Villalba-Mouco V, Smith GM, Trost M, Leichliter J, Lüdecke T, et al. A Neandertal dietary conundrum: Insights provided by tooth enamel Zn isotopes from Gabasa, Spain. Proceedings of the National Academy of Sciences. 2022;119(43):e2109315119.

3.9. Supplementary Information

Supporting Information 3.1: Context

3.9.1.1. History, location, and geological context

In 1978, the evergreen tropical rainforest of Taï National Park (TNP, Figure 3.9.1; 5°45'N, 7°7'W), Côte d'Ivoire was registered as a Biosphere Reserve (Boesch & Boesch-Achermann, 2000a; Guillaumet & Adjanohoun, 1971; Kolongo et al., 2006; Mangenot, 1950a, 1950b, 1955). At 5,082 km^2, the park is one of the largest remaining areas of tropical rainforest in West Africa[3]. The TNP consists of an ancient sloping peneplain broken by several rocky outcrops of Paleoproterozoic and Archean rock, which stand out from encircling plains as isolated inselbergs, including Mount Niénokoué (396 m) (Kolongo et al., 2006). The TCP study area is largely composed of Paleoproterozoic volcanic-sedimentary bedrock, with small outcrops of Archean rock. The Cavally river forms a natural border between Côte d'Ivoire and Liberia, with Archean bedrock on the Liberian side (Petters, 1991). During the dry Winter months (December-January), the Harmattan Season northeasternly winds deposit Saharan dust across TNP (Stoorvogel et al., 1997). Reported $\delta^{66}Zn$ values of Harmattan dust are around 0.17‰, yet it remains unclear how much the $\delta^{66}Zn$ values for plants analyzed in this study ($\overline{x}$ = 0.48 ± 0.04‰, 2σ) are influenced by this dust (Maréchal, 1998; Stoorvogel et al., 1997).

[3] According to the *Office Ivorien des Parcs et Réserves* TNP was enlarged in 2018 (http://www.oipr.ci/index.php/parcs-reserves/parcs-nationaux/parcnational-de-tai)

3.9.1.2. Demography of Taï Chimpanzee Project (TCP)

Since 1979, the Taï Chimpanzee Project (TCP) has operated in an area on the western side of the park (400 km^2), successfully habituating five neighboring chimpanzee communities to human observations and research (Boesch & Wittig, 2019; Wittig & Boesch, 2019). The communities have been named per their territory's location within the TCP study area: North, Northeast, South, East, and Middle (Arandjelovic et al., 2020; Boesch & Boesch-Achermann, 2000b). Within the TCP study area as of 2019, 467 chimpanzees have been identified, including: 257 females, 192 males, and 18 individuals of indeterminate sex (Boesch & Wittig, 2019). As part of the 40-years of research, individual life histories and genealogies have been well documented.

Since the early 1980s, the TCP has been collecting behavioral data, which is hosted by the TCP long-term database. From these observations, data relevant to the level of meat-eating, hunting success, dominance rank, age, cooperation, and alliances were extrapolation (Boesch & Boesch-Achermann, 2000a; Riedel et al., 2020). For observation time, long-term data has been collected using a focal, or target chimpanzee of which was followed from nest-to-nest for one full day or for as long as possible with no significant inter-observer bias, where mean daily observation time for both North and South is 9.8 ± SD 2.4 h (Riedel et al., 2011). Data for observation time begins in 1992 for North, 1999 for South and Middle, and in 2007 for East. For hunting behavior, this dataset includes 496 hunting events from March 1984 - December 2014 for North, 376 hunting events from June 1999 - December 2014 for

South, and 24 hunting events from March 2000 - September 2003 for Middle (Riedel et al., 2020). There were very limited data from East, only recording 2 hunting events in March 2008. Long-term hunting and observation data was excluded from this study, as the range of crown formation times for teeth relevant to the transition to solid food (M3) of most sampled individuals pre-date data acquisition (n = 23, see ***"Supporting Information 3.9.3: Methods - 3.9.3.2 Tooth formation in chimpanzees and 3.9.3.3. Zn incorporation and deposition in tooth enamel"***)

3.9.1.3. Taï Chimpanzee Diet

Taï chimpanzees are predominantly frugivorous, consuming a variety of plant species, including fruit, nuts, leaves, and pith (Goné Bi & Wittig, 2019). The major plant part consumed is the fruit, followed by leaves, pith, nuts and other parts (Goné Bi & Wittig, 2019). The dominant plant species consumed are *Parinari excelsa*, *Sacoglottis gabonensis*, *Coula edulis*, *Ficus spp*., *Klainedoxa gabonensis*, *Scottellia klaineana*, *Chrysophyllum taiense*, from which chimpanzees spend the majority of their time feeding on *Parinari excelsa*. Taï chimpanzees also have a distinct nut-cracking behavior, where they use wood or stones as hammers to access the nutritious kernels inside the nuts of *Parinari excelsa*, *Coula edulis* and *Sacoglottis gabonensis* (Boesch-Achermann & Boesch, 1993).

Despite their largely herbivorous diet, Taï chimpanzees are colloquially considered omnivores as they infrequently consume the raw meat of arboreal primates, such as the red colobus (*Pilocolobus badius*) (which is their preferred prey),

as well as the western black-and-white colobus (*Colobus polykomos*), diana (*Cercopithecus diana*), mona (*Cercopithecus mona*), and lesser spot-nosed (*Cercopithecus petaurista*) monkeys, and soothy mangabeys (*Cercocebus atys*) (Fahy et al., 2013; Oelze et al., 2020). Based on long-term research, hunting rates are known to differ substantially between chimpanzee communities, where successful male hunters and higher-ranking males usually consume more meat than other individuals within communities (Boesch & Boesch, 1989; Fahy et al., 2013; Oelze et al., 2020). Chimpanzee hunting is relatively infrequent, where out of a 7-year study (1979-1986) in Taï National Park, only 135 episodes were observed, one-third of which were considered opportunistic (Boesch & Boesch, 1989). In each hunting event, dominant males are proposed to eat ~300g of meat, with the remainder distributed to subordinate male, female, and juvenile beneficiaries (Boesch & Boesch, 1989). However, more recent studies have shown that meat consumption in Taï National Park has decreased substantially. In 2016-2017, a 7-month study found that there is significant intergroup variation in meat consumption estimates, where East community ate much more meat at ~7.8kg/individual relative to North community at ~ 2.6kg/individual with an average daily intake of 50g/adult male (Oelze et al., 2020). While some estimates are possible, the meat-sharing practice makes it difficult to quantify the exact proportion of meat consumed by individuals. Some isotopic data support a portion of observational data, where males and lactating females have higher $\delta^{15}N$ and $\delta^{13}C$ values than other community members (Fahy et al., 2013; Oelze et al., 2020). However, these data can be significantly influenced by environmental

baseline differences in the $\delta^{15}N$ values of plants, which makes it difficult to interpret $\delta^{15}N$ and $\delta^{13}C$ values (Oelze et al., 2020).

Ant and termites are also important dietary resources, contributing significantly to the roughly 3% of animal foods that make up the Taï chimpanzees' otherwise frugivorous and herbivorous diet (Goné Bi & Wittig, 2019). Ant dipping is a common practice for Taï chimpanzees, where manual extraction can result in up to 60 g of ants and brood per handful, with chimpanzees mainly seeking the nutritious ant brood (Fahy et al., 2013; Lemoine et al., 2019; Möbius et al., 2008). Taï chimpanzee females typically participate in ant dipping behavior more than males, although it is unclear if they consume more ants (Boesch & Boesch, 1990). Since the average female typically consumes less meat than males, consuming more ants could be a valuable supplement to their herbivorous diet that contributes to lower $\delta^{66}Zn$ values (Möbius et al., 2008). However, since we only sampled ants and not their brood, it is unclear if the ants sampled in this study are equally representative of their brood (Fahy et al., 2013; Möbius et al., 2008). Similarly, both male and female chimpanzees engage in termite mound pounding, where the mounds are pounded open to access the *Thoracotermes spp.* termites and termite fishing, where long grass stems are inserted into mounds to retrieve *Cubitermes* and *Macrotermes spp.* termites (Boesch, 2003b; Boesch & Boesch-Achermann, 2000a; Luncz & Boesch, 2015). Therefore, in addition to ants, termites could also be contributing to the lower

$\delta^{66}Zn$ values, but as males and females engage in termite foraging behavior equally, a sex difference related to termite eating alone is unlikely (see Supporting Information 3.1, and Table 3.9.1).

Supporting Information 3.2: Stable isotope analysis

3.9.1.4. Zinc isotope fractionation

Zinc (Zn) has five naturally occurring stable isotopes, ^{64}Zn (48.63%), ^{66}Zn (27.90%), ^{67}Zn (4.10%), and ^{68}Zn (18.75%), with an average relative atomic mass of 65.378 (Ponzevera et al., 2006; Rosman & Taylor, 1998). Zn is an important trace element, and is often included with transition metals, such as iron (Fe) and copper (Cu). Zn plays an essential role in mammalian cells, enabling the proliferation, differentiation, and metabolic function of cells (Prashanth et al., 2015). Metalloproteinases, which are enzymes that break down proteins, such as collagen, which fills the spaces between cells in tissues are Zn-dependent (Cabral-Pacheco et al., 2020). Metalloproteinases are also associated with the optimal function of reproductive, neurological, immune, dermatological, and gastrointestinal tract systems (Prashanth et al., 2015). Zn also is critical to normal growth and development during pregnancy, childhood and adolescence, where a marked decrease in plasma Zn levels occurs during pregnancy, fluid loss, oral contraceptive usage, blood loss, acute myocardial infarction, infections, and malignancies (Das & Das, 2012; Favier et al., 1993). As a result, the stable isotope ratios of Zn ($^{66}Zn/^{64}Zn$, expressed as $\delta^{66}Zn$) have emerged as a novel

diagnostic tool for a variety of diseases in biomedicine (Costas-Rodríguez et al., 2016).

Additionally, the analysis of $\delta^{66}Zn$ values have been applied in biological anthropology, specifically in archaeological contexts, as it has also been shown to indicate trophic relationships in various food webs and ecosystems (Bourgon et al., 2020; Bourgon et al., 2021; Costas-Rodríguez et al., 2014; Jaouen, 2018; K. Jaouen et al., 2016; Klervia. Jaouen et al., 2013; Van Heghe et al., 2014). Being a heavy element, zinc isotopes fractionate along food chains by about 1‰, with higher values in herbivores, lower values in carnivores, and intermediate values in omnivores (Bourgon et al., 2020; Bourgon et al., 2021; Jaouen, 2018; K. Jaouen et al., 2016; Klervia. Jaouen et al., 2013). There are three main factors contributing to the isotopic distinction between trophic positions: **(1)** the preferential absorption of ^{66}Zn in plants (Bourgon et al., 2020; Bourgon et al., 2021; Moynier et al., 2009; Viers et al., 2007; D. Weiss et al., 2005), **(2)** muscle tissue is ^{66}Zn-depleted relative to bone (Balter et al., 2013; Bourgon et al., 2020; Bourgon et al., 2021; Costas-Rodríguez et al., 2014; Jaouen, 2018; K. Jaouen et al., 2016; Klervia. Jaouen et al., 2013), and **(3)** body tissues' $\delta^{66}Zn$ values are dependent on the total Zn isotopic composition of the foods consumed (Klervia. Jaouen et al., 2013). For each of the main factors, depending on dietary source (plant vs. animal), there are biochemical processes that occur within the body to cause lower or higher $\delta^{66}Zn$ values depending on trophic position. First, plant-based foods contain phytic acid and during digestion, heavy Zn is preferentially

bound to the phosphate groups of phytates and is absorbed by the body, leaving light Zn isotopes to be preferentially precipitated (Jaouen et al., 2019). Additionally, in plants, the active uptake of heavy Zn isotopes leads to a gradient effect, where δ^{66}Zn values become progressively lower from root to leaves with further variation dependent on plant species (Bourgon et al., 2020; Jaouen, 2018; Klervia. Jaouen et al., 2013; Klervia. Jaouen et al., 2016). Thus, a grazer is proposed to have lower δ^{66}Zn values relative to a browser (Bourgon et al., 2020; Bourgon et al., 2021; Jaouen, 2018; K. Jaouen et al., 2016; Klervia. Jaouen et al., 2013). Second, the isotopic composition of muscle exhibits low δ^{66}Zn values relative to the average isotopic composition of the body, therefore the consumption of muscle by carnivores will lower δ^{66}Zn values, while the consumption of bone will do the opposite (Bourgon et al., 2020; Bourgon et al., 2021; Jaouen, 2018; K. Jaouen et al., 2016; Klervia. Jaouen et al., 2013; Jaouen et al., 2019). Therefore, the proportion of plants and muscle tissue in a diet will directly inform the total Zn isotopic composition of the body. Since δ^{66}Zn values preserve in enamel bioapatite and are sensitive to subtle changes in the diet (Bourgon et al., 2020; Bourgon et al., 2021; Jaouen, 2018; K. Jaouen et al., 2016; Klervia. Jaouen et al., 2013), they are useful in studying the influence of meat-eating in a relatively frugivorous primate.

Supporting Information 3.3: Methods

3.9.1.5. Sample collection

In 2015-2021, ecological samples were obtained from 28 plant and animal food items from chimpanzee territories within the TCP study area, Taï National Park (Côte d'Ivoire, Table 3.9.1 and 3.9.2). We also sampled some common plant and animal chimpanzee food items, including *Dorylus* ants (n = 8), *Oecophylla* ant (n = 1), *Thoracotermes* (n = 2), *Cubitermes* (n = 5), *Macrotermes* (n = 3), *Apis* honey (n = 1), unidentified fungus from a termite mound (n = 1), and several plant species (n = 7).

In 2019, chimpanzee samples were obtained from the Taï Chimpanzee Collection (TCC), which is housed at the Max Planck Institute for Evolutionary Anthropology (MPI-EVA) in Leipzig, Germany. Individual identification of skeletal elements used in this study were based on field researchers' daily observations of the demography and disappearances of Taï chimpanzee communities. In samples where there was advanced decay, individuals were identified as part of an ongoing genetic investigation on familial relationships at MPI-EVA (Boesch et al., 2006; Vigilant et al., 2001). Individual chimpanzee remains were selected based on the presence of molars, which were CT-scanned prior to destructive analysis. These established which cusps were suitable for sampling and ensured the preservation of dental morphometric information for future research. The sample included males, females and subadults from North community (n = 27) and a small number of adult residential males from three other habituated communities under long-term study (Middle: n = 1,

South n = 4, East n = 2). In total we collected samples from 10 adult males, 9 adult females, 7 subadult males, and 8 subadult females, including 7 mother-offspring dyads from 1984-2009.

Dental enamel was sampled from 34 chimpanzees (*Pan troglodytes verus*), including deciduous (dm1s, dm2s, M1s; n = 6) and late-forming teeth (M2s or M3s; n = 28, see Table 3.9.2). The dental calculus and staining on enamel were cleaned mechanically with a diamond-tipped burr, and a superficial layer of enamel was removed. Then, a diamond-tipped wheel was used to cut 50 mg from the full height of the crown, where only 5 mg is required for Zn stable isotope analysis, and the remainder was reserved for other analyses, as part of separate study. The isotopic integrity in enamel is assumed without pretreatment (Bourgon et al., 2020; Jaouen, 2018; Jaouen & Pons, 2016; Reynard & Balter, 2014).

3.9.1.6. Tooth formation in chimpanzees

In chimpanzees, tooth enamel forms during a specific developmental time range on each tooth and does not subsequently remodel (Driessens & Verbeeck, 1990; White et al., 2011). The enamel on tooth crowns used in this study corresponds to the following age ranges in years +/- 1 year: dm1 and dm2 (*in utero*), M1 (*in utero* to 2.8), M2 (1.8-5.6), and M3 (3.6-8) (Kelley et al., 2020; Schwartz et al., 2000; Smith et al., 2007; Smith et al., 2010). Since high concentrations of Zn are deposited on tooth crowns at the end of enamel maturation (see ***"Supporting Information 3.9.3: Methods – 3.9.3.3. Zn incorporation and deposition in tooth enamel"***), we assume

Zn is incorporated in the last year of crown formation to estimate the following ontogenetic ages for the Zn sample from these tooth types: dm1 and dm2 (*in utero*), M1 (2-3 years), M2 (5-6 years), and M3 (8-9 years) [see main text, Table 3.3.1, (Dean et al., 2023; Smith et al., 2022)]. We assume that deciduous teeth, which formed prior to birth, reflect the diet of the mother without a physiological isotope fractionation, though we will explore this assumption for the five dms in our sample collection (Jaouen et al., 2020; Smith et al., 2022). For δ^{66}Zn values from the remaining teeth, based on the time of Zn incorporation, we assume they reflect the following ontogenetic events: nursing initiation for M1s, nursing to just weaned for M2s, and transition to solid food for M3s (Samuni, Tkaczynski, et al., 2020).

3.9.1.7. Zn incorporation and deposition in tooth enamel

Since Zn has a similar molecular structure to Ca, it is incorporated into the enamel bioapatite crystal lattice as a trace element during tooth growth (Bentley, 2006; Bourgon et al., 2020; Dean et al., 2018; Dean et al., 2023; Price et al., 2002). Zn has been shown to stimulate osteoblast proliferation and its presence on the crystal lattice within enamel blocks further demineralization and resorption by osteoclasts (Dean et al., 2018). By stimulating osteoblast proliferation, Zn has been shown to be closely related to enamel and cementum mineralization (Dean et al., 2018). These characteristics enable the retention of endogenous Zn in enamel bioapatite, despite the diagenetic changes that occur during fossilization (Dean et al., 2018). Zn concentrations are elevated at the enamel surface, at the neonatal line, and at the enamel-dentin junction in deciduous, permanent, and fossil teeth (Dean et al., 2023;

Dean et al., 2019; Jaouen et al., 2020; Smith et al., 2022). This trend has been shown to persist in unerupted teeth, which were known to never have been exposed to the oral environment and anthropogenic contamination (Dean et al., 2023). The highest concentrations of Zn, ranging from 197 to 1743 ppm are found at the cuspal, mid-lateral and cervical surface enamel (Dean et al., 2023). The next highest concentrations of Zn, ranging from 200 to 500 ppm are found at the neonatal line, which has been proposed to relate to the release of stored Zn from the liver at birth, and in nursing infants, he high levels of Zn in colostrum (Dean et al., 2023; Dean et al., 2019). Similar concentrations observed at the neonatal line were also found at the enamel-dentin junction (200 to 500 ppm), which may result from metalloprotease activity in this region during mineralization (Dean et al., 2023). Overall, deciduous teeth have consistently higher Zn concentrations relative to permanent teeth, although the Zn concentrations at the cuspal, mid-lateral and cervical regions are consistent between deciduous and permanent teeth (Dean et al., 2023). The elevated concentrations of Zn on the outermost layers of enamel have been proposed to be a biochemical signal of the termination of enamel maturation (Bourgon et al., 2020; Dean et al., 2019; Tacail et al., 2017) or a signal of nursing initiation (Smith et al., 2022). In enamel, endogenous Zn concentrations, and their respective isotopic composition is highly stable and resilient, where Zn distribution is only altered after demineralization (Dean et al., 2023). Despite the high concentrations in the enamel surface, the diffuse nature of Zn distribution constrains the sequential temporal resolution based on tooth type to the crown formation period (Dean et al., 2023). In

order to discern which layer of Zn was sampled, histological analyses coupled with laser ablation-inductively coupled plasma-mass spectrometry (LA-ICPMS) can be used (Dean et al., 2023; Smith et al., in review; T. M. Smith et al., 2021), however in order to reliably measure the Zn isotopic composition of enamel, bulk samples of ~ 5 mg are needed for column chromatography. As bulk enamel samples were used in this study to be conservative in the estimated age ranges (in years) based on tooth type, we compare two models of Zn incorporation and assess which best matches our data. In Model 1, Zn is incorporated continuously throughout enamel formation and subsequent calcification, therefore Zn incorporation spans the entire range of crown formation (see main text, Table 3.3.1). In Model 2, Zn is incorporated at the end of crown completion before tooth eruption. For both models, the age range of crown formation +/- 1 year was used to estimate the ontogenetic stages that corresponded to each tooth's crown formation range (see main text, Table 3.3.1).

3.9.1.8. Zn analytical technique

The plant samples were cleaned with MQ H2O, then dried at 50°C in an oven for 24 hours. The remaining sample was reduced to ash in a muffle furnace at 500°C for 8 hours, and then ~100 mg of sample was reserved for Zn stable isotope analysis. The animal food samples were grinded to a powder in an agate mortar, and then dried at 50°C for 4 hours. Then, about 50 mg of each dried sample was dissolved in 10 ml of bidistilled 15.9M HNO_3 by microwave digestion (iPrep Mars 6). After microwave digestion, samples were transferred to acid-cleaned Teflon beakers and evaporated to dryness at 100°C. To remove the nitrates, samples were resolved in 1mL of 8M HCl

with ultrasonication for 30 minutes. Then, samples were evaporated to dryness at 90°C, and resolved in 1M HCl with ultrasonication for 30 minutes. The remaining solution was evaporated to dryness at 90°C and redissolved in 1ml 1.5M HBr with ultrasonication for 30 minutes. Since the samples were digested in HNO_3, they were resolved in 0.5ml of 8M HCl in an ultrasonic bath for 30 minutes. The remaining solution was evaporated to dryness and redissolved in 1ml 1.5M HBr in an ultrasonic bath for 30 minutes. The enamel samples were digested in 2ml of 65% HNO_3 at 120°C for 2 hours. After, the digested sample was transferred into cleaned glass vials for transport and evaporated to dryness over a 24-hour period at 120°C. Aliquots were divided accordingly for each isotope analytical technique, then samples for Zn stable isotope analysis were resolved in 0.5ml of 8M HCl with ultrasonication for 30 minutes. The remaining solution was evaporated to dryness at 90°C and redissolved in 1ml 1.5M HBr with ultrasonication for 30 minutes.

Then, the samples were processed for isotope analysis using a modified ion exchange method adapted from Moynier et al. (Moynier et al., 2009) and first described in Jaouen et al. (K. Jaouen et al., 2016). Zn was purified on 1ml of AG1-X8 (200-400 dry mesh size, 106-180 µm wet bead size), using 2ml 1.5 HBr for matrix elution, followed by 5ml 0.5 M HNO_3 for Zn elution. Three reference materials (BCR-482, lichen; ERM CD-281, rye grass and SRM-1577c, bovine liver) and a blank were included and analyzed alongside all plant samples. One reference material (NIST SRM 1400, bone ash) and a blank were included and analyzed alongside all enamel samples.

Zn isotope ratio measurements were determined on a ThermoScientific Neptune Plus MC-ICP-MS at the Géosciences Environnement Toulouse - Observatoire Midi-Pyrénées (Toulouse, France), using the Cu-doping protocol of Toutain et al. (Toutain et al., 2008). Zn concentrations were estimated following a protocol adapted from one used for Sr by Copeland et al. (Copeland et al., 2008), applying a regression equation based on the ^{64}Zn signal intensity (V) of three solutions with known Zn concentrations (150, 300 and 600 ppb), diluted from a solution of 1,000 ppm (Alfa Aesar). The in-house reference material, Zn AA-MPI was used for standard bracketing. Zn isotope ratios are expressed relative to the JMC-Lyon reference material and isotope abundances are expressed in delta (δ) notation, expressed in per mil (‰) as follows: $\delta^{66}Zn = (^{66}Zn/^{64}Zn_{sample}/^{66}Zn/^{64}Zn_{standard} - 1) * 1000$. The $\delta^{66}Zn$ measurement uncertainties were estimated from the repeated measurement of an internal standard (AA-GET) used for standard bracketing (0.30 ± 0.08‰), and the standard replicate analyses ranged from ± 0.003‰ to ± 0.12‰ (2SD). Samples were typically measured at least twice with mean analytical repeatability of < 0.05‰ (2 SD, n = 71). Additional reference materials ERM CD-281 (n = 1), SRM BCR-482 (n = 2), SRM 1577c (n = 2) and SRM 1400 (n = 2) were analyzed alongside the samples and had the following $\delta^{66}Zn$ values 0.55 ± 0.08‰ (CD-281), 0.14 ± 0.05‰ (BCR-482), -0.09 ± 0.05‰ (SRM-1577c), and 0.91 ± 0.05‰ (SRM-1400), which align with published values (Cloquet et al., 2008; Jaouen et al., 2020). All samples showed Zn mass dependent isotopic fractionation which

implied the absence of isobaric interferences, as the $\delta^{66}Zn$ vs $\delta^{67}Zn$ values fall onto lines with slopes close to the theoretical value (Figure 3.9.7 and 3.9.8).

3.9.1.9. Strontium (Sr) analytical technique

A detailed description of the Sr analytical technique can be found in Chapter 2: Strontium isotopes track female dispersal in Taï chimpanzees, section 2.3. Methods.

3.9.1.10. Zn isotope fractionation between tissue types

As part of this study, we estimate the isotope fractionation between different tissue types (bone, muscle) for the Taï chimpanzee's preferred prey item, colobine monkeys (e.g., the red colobus monkey, see ***"Supporting Information 3.1: Context – 3.9.1.3. Taï Chimpanzee Diet"***). In order to estimate the Zn for monkey muscle tissue (referred to as meat), we took the average isotope fractionation from the diet to the muscle ($\Delta^{66}Zn_{\text{diet-muscle}}$) measured in captive feeding studies (Table 3.9.7). Then, we calculated the mean $\delta^{66}Zn$ values from various food items in Taï forest (Table 3.9.1).

When estimating the $\delta^{66}Zn$ values and relative trophic position of colobine monkeys, we assume that they are most like herbivores and ruminants in their digestive physiology. Colobine monkeys are similar to ruminants (cattle, sheep, deer, and related species) in that they have a sacculated foregut that aids in fermentation of cellulose-rich foods, and a relatively small hindgut (Liu et al.,

2022). First, we compiled $\delta^{66}Zn$ values from captive populations, where feeding experiments had controlled diet, and there were published values for the diet ($\delta^{66}Zn_{diet}$), bone ($\delta^{66}Zn_{bone}$), and muscle ($\delta^{66}Zn_{muscle}$) (Balter et al., 2013; Vincent Balter et al., 2010; Mahan et al., 2018; Moynier et al., 2013). With these data, we were able to estimate the relative isotope fractionation between diet and the two relevant tissue types: muscle and bone (Table 3.9.7). This ultimately allows us to estimate monkey meat, in comparison to the measured food items from Taï forest.

In a recent model of Zn isotope fractionation, tissues such as muscle and bone were shown to have extremely slow flux, however, depending on the species, muscle and bone may be equal in $\delta^{66}Zn$ values, or bone may be ^{66}Zn-enriched and muscle ^{66}Zn-depleted (Balter et al., 2013). The reported $\delta^{66}Zn$ values of sheep bone is 0.45 ± 0 .03‰ and lamb meat are -0.32 ± 0.04‰, therefore we suggest it is the latter (V. Balter et al., 2010; Costas-Rodríguez et al., 2014). Since $\delta^{66}Zn$ values will vary based on isotopic differences in bioavailable Zn in the underlying bedrock and soils, the more conservative estimate uses reported values from controlled feeding studies (Cloquet et al., 2008). In order to estimate the isotope fractionation diet to muscle ($\Delta^{66}Zn_{\text{diet-muscle}}$), we used published captive feeding studies on mice (n = 19), sheep (n = 4), and minipigs (n = 7) (Balter et al., 2013; V. Balter et al., 2010; Mahan et al., 2018; Moynier et al., 2013). The average $\Delta^{66}Zn_{\text{diet-muscle}}$ from the reported studies is about -0.31‰.

In modern wild populations, $\delta^{66}Zn_{diet}$ values of herbivores were obtained by measuring plants in the local environment (K. Jaouen et al., 2016; Klervia.

Jaouen et al., 2013). In wild populations, the herbivore $\Delta^{66}Zn_{diet\text{-}bone}$ is +0.8‰, which is substantially higher than what is reported from captive populations, where the $\Delta^{66}Zn_{diet\text{-}bone}$ is +0.30‰ (Balter et al., 2013; V. Balter et al., 2010; K. Jaouen et al., 2016; Moynier et al., 2013). Further, there is a 0.2‰ depletion from bone to enamel ($\Delta^{66}Zn_{\ bone\text{-}enamel}$), whereas from $\delta^{66}Zn_{enamel}$ to $\delta^{66}Zn_{bone}$ values, there is a 0.2‰ enrichment for a given individual (Jaouen et al., 2019). When considering the reported $\delta^{66}Zn$ values for wild herbivores, the $\Delta^{66}Zn_{diet\text{-}enamel}$ is on average +0.56‰ (K. Jaouen et al., 2016). However, it is unclear if the plant material measured encompasses the entire diet of the individual. In the same ecosystem, to estimate the $\delta^{66}Zn_{diet}$ values for carnivores, the mean $\delta^{66}Zn$ value for herbivore bone is used, which means there is no precise estimate of herbivore meat, nor a consideration of the variable fractionation between these tissues (Klervia. Jaouen et al., 2013). Since enamel was not measured in the captive populations, this value is uncertain, therefore we try to estimate the diet to enamel isotope fractionation from reported values in the literature. The $\Delta^{66}Zn_{diet\text{-}bone}$ (+ 0.30‰) and the $\Delta^{66}Zn_{\ bone\text{-}enamel}$ (-0.2‰), therefore the $\Delta^{66}Zn_{diet\text{-}enamel}$ is estimated to be ~ +0.1‰.

Therefore, when considering only the average $\Delta^{66}Zn_{\ diet\text{-}muscle}$ value (-0.31‰) and the average $\delta^{66}Zn$ value for plant leaves (0.48‰), monkey meat would be about 0.17‰ ($\delta^{66}Zn_{muscle}$, Figure 3.9.3). Based on the reported range of $\delta^{66}Zn_{enamel}$ values in African ruminants (0.35 to 1.51‰), and the reported values for captive population (-1.05 to 0.59‰) and store-bought meat (-0.32 to -0.74‰),

this estimated $\delta^{66}Zn_{muscle}$ value aligns well (Balter et al., 2013; V. Balter et al., 2010; Costas-Rodríguez et al., 2014; K. Jaouen et al., 2016; Mahan et al., 2018; Moubtahij et al., 2023; Moynier et al., 2013). Additionally, we observe a 67% reduction in Zn concentrations from the average $\Delta^{66}Zn_{diet\text{-}muscle}$ value, which allows the estimation of the Zn concentrations for monkey meat from the observed average Zn concentrations of plant leaves (248 ppm, Table 3.9.1). Thus, the Zn concentrations for monkey meat would be around 19 ppm.

3.9.1.11. Two-source mixing model

We included a two-source mixing model, as outlined by Faure and Mensing (Faure & Mensing, 2005). Within this model, we include the $\delta^{66}Zn$ value, Zn concentrations, and Zn absorption for animal foods (termite, ant, monkey meat) and plant foods (leaves). The $\delta^{66}Zn$ value for each source is corrected based on the $\Delta^{66}Zn_{diet\text{-}enamel}$ fractionation for chimpanzees (see Supporting Information 3.6). Zn absorption in animal foods is estimated to be 100% and Zn absorption in plant foods is estimated to be 30%, due to inhibition of absorption by phytates and tannins (Hortin et al., 1991; Hunt, 2003). For the model presented in the paper, we used the average $\delta^{66}Zn$ value and Zn concentrations for all animal foods (ant, termite, monkey meat). We also conducted additional models that look at each individual animal food source (termite, ant, or monkey meat), which we detail the findings of in Table 3.9.8.

3.9.1.12. Statistical analyses

We performed the following statistical analyses with R software version 4.3.2 with a significance set at $\alpha = 0.05$ (R Core Development Team, 2022). The R '*stats*'

package was used to compare the means in isotopic data, and to determine if parametric or non-parametric analyses were needed for each dataset (R Core Development Team, 2022). Since we have a small sample size, we used the 'rstatix' to estimate the effect size (cohens d) and statistical power for ANOVAs (Cohen, 2013; Navarro, 2015).

In order to explore the association of $\delta^{66}Zn$ values to individual factors (tooth type, sex, territory), we fitted two generalized linear mixed models (GLMM, (Bolker et al., 2009; Brooks et al., 2022) with a Gaussian distribution and Bonferroni error correction using the "glmmTMB" package (Brooks et al., 2017). To test if there were differences in $\delta^{66}Zn_{enamel}$ values between tooth types (dps, M2s, M3s), we fitted two generalized linear mixed models with a gaussian distribution (GLMMs; (Bolker et al., 2009; Brooks et al., 2022) using the 'glmmTMB' package in R 4.2.1 (Brooks et al., 2022; Magnusson et al., 2017; R Core Development Team, 2024). We assessed all of the model fits using the diagnostic plots generated by the 'DHARMa' package (Hartig & Hartig, 2017). In the hypothesis (full) model, $\delta^{66}Zn$ values are predicted by tooth type and sex, as fixed effects, and chimpanzee community (North, South, East, Middle) was included as a random effect. In the null model, enamel $\delta^{66}Zn$ values are only predicted by chimpanzee community, as the random effect. Akaike Information Criterion (AICc), as part of the R package '*MuMIn*' package was used to perform a full-null model comparison and select the model with the best fit, i.e., the model with the lowest AICc scores, which corrects for small sample size (Barton & Barton, 2015; Burnham & Anderson). We estimated marginal means using the R package

"emmeans", and tested the significance of pairwise comparisons in $\delta^{66}Zn$ values between factors (tooth type, sex) by the Bonferroni method (Lenth et al., 2021). Since we have a small sample size, we also performed a power analysis for each pairwise difference generated by the 'emmeans' package (Kumle et al., 2021).

Supporting Information 3.4: Results

3.9.1.13. Mother-offspring dyads

We compare enamel $\delta^{66}Zn$ values in two mother-offspring dyads to assess if the breastfeeding effect shown in historical human enamel is replicable (Jaouen et al., 2020). We found a significant difference in $\delta^{66}Zn$ values between second and third molars ($t(22.1) = 2.38$, $p = 0.03$), with lower $\delta^{66}Zn$ values in third molars. In mother-offspring dyads A and B, second molars from mothers (formed when they were nursing) have higher $\delta^{66}Zn$ values than deciduous premolars from their respective offspring (which formed *in utero* through early nursing, and therefore mostly reflect the mothers' body chemistry and diet), as shown in Figure 3.9.9A. In mother-offspring dyads C, D and E, deciduous premolars (which reflect *in utero* to nursing) and second molars (which reflect end of nursing to weaned) from offspring have higher $\delta^{66}Zn$ values than third molars (which reflect adolescent diet) from their respective mothers, as shown in Figure 3.9.9B. This could suggest that deciduous premolars are influence by the mother's diet, whereas second molars reflect a mixed-

nursing signal and third molars reflect the transition to solid foods, however due to our small sample size, we are unable to test this.

3.9.1.14. Breastfeeding effect in mother-offspring dyads

In our small sample of mother-offspring dyads, we found that chimpanzee offspring (dps) in comparison to the permanent teeth (M2s) of their mothers have lower δ^{66}Zn values (Figure 3.9.9A). Further, we see yet a different pattern in three other mother-offspring dyads, where higher δ^{66}Zn values were observed in the second molars and deciduous premolars of offspring relative to the third molars of their mothers (Figure 3.9.9B).

Supporting Tables

Table 3.9.1. Summary of all Taï chimpanzee plant and animal food items (n = 28).
Summary of all Taï chimpanzee plant and animal food items (n = 28) sampled and analyzed in this study for their $\delta^{66}Zn$ values and Zn concentrations in parts per million, alongside their dietary specialization.

Sample ID	$\delta^{66}Zn$ (‰)	2σ	Zn (ppm)	species	diet	Sampling year
2056	0.32	0.10	49.68	*Cubitermes spp.*	detritus	2015
2057	0.51	0.07	44.45	*Cubitermes spp.*	detritus	2015
2058	0.06	0.03	18.48	*Cubitermes spp.*	detritus	2015
2059	0.33	0.01	68.00	*Cubitermes spp.*	detritus	2015
2060	0.28	0.03	53.42	*Cubitermes spp.*	detritus	2015
2065	0.08	0.01	43.77	*Thoracotermes spp.*	detritus	2015
2064	0.66	0.10	63.79	*Thoracotermes spp.*	detritus	2015
2061	0.15	0.02	119.80	*Macrotermes spp.*	fungus & leaf litter	2015
2062	-0.05	0.07	21.70	*Macrotermes spp.*	fungus & leaf litter	2015
2063	-0.10	0.06	111.30	*Macrotermes spp.*	fungus & leaf litter	2015
2067	0.14	0.06	94.80	*Fungus*	leaf litter	2015
2070	0.01	0.06	233.80	*Dorylus spp.*	carnivore/insectivore	2015
2069	0.04	0.00	264.54	*Dorylus spp.*	carnivore/insectivore	2015
2071	0.05	0.04	235.15	*Dorylus spp.*	carnivore/insectivore	2015
2072	0.11	0.05	298.15	*Dorylus spp.*	carnivore/insectivore	2015
2073	0.01	0.01	288.94	*Dorylus spp.*	carnivore/insectivore	2015
2074	-0.04	0.12	279.05	*Dorylus spp.*	carnivore/insectivore	2015
2075	-0.01	0.06	288.46	*Dorylus spp.*	carnivore/insectivore	2015
2076	-0.12	0.01	256.34	*Dorylus spp.*	carnivore/insectivore	2015
2077	-0.08	0.02	135.69	*Oecophylla spp.*	carnivore/insectivore	2015
2068	0.15	0.01	74.92	*Honey*	flower nectar	2015
257	0.32	0.02	193.63	*Afzelia bella*	NA	2017
507	0.48	0.07	273.16	*Sterculia oblonga*	NA	2017
1654	0.71	0.00	21.90	*Dialium aubrevillei*	NA	2021
1657	0.18	0.08	427.12	*Coula edulis*	NA	2021
1663	0.74	0.05	154.83	*Sarcophrynium brachystachyum*	NA	2021
1675	0.21	0.04	196.82	*Sterculia oblonga*	NA	2021
1682	0.74	0.05	468.79	*Parkia bicolor*	NA	2021

Table 3.9.2. Summary of all Taï chimpanzees sampled (n = 34).
Summary of all Taï chimpanzees sampled (n = 34), with their corrected $\delta^{66}Zn$ values and Zn concentrations in parts per million (Unknown birth years = NA); for tooth formation estimates see Table 3.3.1.

ID	community	age	sex	tooth	$\delta^{66}Zn$ (‰)	2σ	[Zn] ppm	birth year	crown formation year
†NF01	North	39	f	M2	0.4	0.06	161.86	1954	§1960
†NF02	North	23	f	M2	0.36	0.06	365.59	1969	§1975
†NF03	North	25	f	M3	0.27	0.03	84.01	1969	§1978
†NF04	North	27	f	M3	0.29	0.06	159.73	1972	§1981
†NF05	North	19	f	M2	0.5	0.06	216.36	1975	§1981
†NF06	North	28	f	M3	0.09	0.06	221.21	1973	§1982
NF07	North	22	f	M2	0.43	0.06	146.47	1976	§1998
NF08	North	16	f	M2	0.51	0.04	167.28	1977	§1983
‡NF09	North	5	f	*dm1	0.48	0.06	190.25	1987	§1987
NF10	North	12	f	M2	0.3	0.06	185.40	1982	§1988
NF11	North	27	f	M3	0.45	0.06	202.01	1978	1987
NF12	North	11	f	M2	0.22	0.06	240.38	1982	§1988
NF13	North	9	f	M3	0.36	0.06	221.40	1979	1988
NF14	North	6	f	M2	0.34	0.06	286.86	1984	1990
NF15	North	3	f	M1	0.4	0.06	140.56	1991	§1995
‡NF16	North	11	f	M2	0.42	0.06	233.05	1987	1993
NF17	North	10	f	M2	0.32	0.09	220.79	1991	1997
NM01	North	13	m	M2	0.31	0.06	153.53	1971	§1977
NM02	North	25	m	M3	0.41	0.06	153.56	1969	§1978
NM03	North	20	m	M3	0.27	0.06	200.91	1975	1984
‡NM04	North	2	m	*dm1	0.35	0.06	100.33	1989	§1989
NM05	North	5	m	*dm1	0.26	0.06	106.00	1990	§1990
NM06	North	14	m	M3	0.24	0.06	259.36	1980	1989
‡NM07	North	0.3	m	*dm1	0.21	0.06	252.30	1992	§1992
‡NM08	North	10	m	M2	0.33	0.06	242.63	1991	1997
‡NM09	North	2	m	*dm2	0.18	0.06	88.35	1997	§1997
‡NM10	North	8	m	M2	0.43	0.06	164.02	1991	1997
SM01	South	40	m	M3	0.24	0.06	243.67	1959	§1968
SM02	South	19	m	M1	0.04	0.06	126.13	1979	§1983

SM03	South	25	m	M3	0.13	0.06	167.59	1989	1998
SM04	South	NA	m	M3	0.19	0.06	265.26	1991	2000
EM01	East	NA	m	M2	0.23	0.06	153.75	NA	§NA
EM02	East	14	m	M3	0.14	0.06	253.07	1993	§2002
MM01	Middle	19	m	M2	0.19	0.10	149.84	1983	§1989

* Deciduous molars, lowercase letters correspond to deciduous dentition, and uppercase letters correspond to permanent dentition,† mother, in mother offspring-group, ‡ offspring, in mother-offspring group, § individuals where crown formation range does not overlap with behavioral data in the TCP long-term database

Table 3.9.3. GLMM model outputs for δ^{66}Zn values, tooth type and sex (n = 32).
Model outputs of Gaussian fitted generalized linear model [δ^{66}Zn ~ tooth type + sex + (1|community)], testing for the differences in δ^{66}Zn values between tooth type and sex in adolescent Taï chimpanzees (n = 32).

Response variable	n	Random effects	Predictor variable	Estimate	SE	Z-value	p-value
Full δ^{66}Zn (‰)	32	territory	(intercept)	0.37	0.05	7.451	< 0.00001
AIC = -49.9			M2	0.01	0.05	0.252	0.80
AICc = - 46.5			M3	-0.06	0.05	-1.24	0.21
df = 26			**Sex: Male**	**-0.09**	**0.04**	**-2.605**	**0.01***
Null δ^{66}Zn (‰)	32	NA	community	-	-	-	-
AIC = -47.3							
AICc = - 46.4							
df = 3							

Table 3.9.4. Summary of contrasts for ^{66}Zn values, tooth type and sex (n = 32).
Summary of contrasts estimated by the Bonferroni method for the GLMM testing for the differences in $\delta^{66}Zn_{enamel}$ values between tooth type and sex in adolescent Taï chimpanzees (n = 32).

Contrast	Ratio ± SE	t-ratio	p-value
female-male	**0.09 ± 0.03**	**2.61**	**0.02***
dm-M2	-0.01 ± 0.05	-0.25	1.00
dm-M3	0.06 ± 0.05	1.24	0.68
M2-M3	0.07 ± 0.04	0.21	0.32

Table 3.9.5. ANOVA testing for differences in $\delta^{66}Zn$ values for third molars of weaned chimpanzees (n = 13) compared to deciduous molars (n = 5), which are expected to represent the maternal signal.

Groups	Sum of Squares	df	Mean Square	F-value	p-value
Between Groups (Tooth Type)	0.02	2	0.009	0.66	0.53
Within Groups (Residuals)	0.19	14	0.013		
Total	0.20	16			

Table 3.9.6. Tukey-HSD post-hoc testing where $\delta^{66}Zn$ values for third molars of weaned chimpanzees (n = 13) differ relative to deciduous molars (n = 5), which are expected to represent the maternal signal.

		95% Confidence Interval		
Tooth Type	**Mean difference**	**Lower bound**	**Upper Bound**	**p-value**
female M3-dm	-0.005	-0.20	0.18	1.00
male M3-dm	-0.07	-0.24	0.11	0.58
male M3-female M3	-0.06	-0.24	0.11	0.63

Table 3.9.7. Diet to tissue (muscle, bone) isotope fractionation ($\Delta^{66}Zn$) reported in captive feeding studies.
The $\delta^{66}Zn$ values from the animals included in this table are after the following studies: (Mahan et al., 2018)[a], (Moynier et al., 2013)[b], (Balter et al., 2013)[c], (V. Balter et al., 2010)[d].

animal	$\delta^{66}Zn_{diet}$ (‰)	$\delta^{66}Zn_{muscle}$ (‰)	$\delta^{66}Zn_{bone}$ (‰)	$\Delta^{66}Zn_{diet-muscle}$ (‰)	$\Delta^{66}Zn_{diet-bone}$ (‰)	$[Zn_{diet}]$ ppm	$[Zn_{muscle}]$ ppm	$[Zn_{bone}]$ ppm
minipig[a]	0.15	-0.88		-1.03		54	17.27	
minipig[a]	0.15	-0.81		-0.96			17.53	
minipig[a]	0.15	-0.65		-0.80			17.85	
minipig[a]	0.15	-1.05		-1.20			17.69	
minipig[a]	0.15	-0.68		-0.83			21.71	
minipig[a]	0.15	-0.99		-1.14			18.06	
minipig[a]	0.15	-1.02		-1.17			15.96	
average	**0.15**	**-0.87**		**-1.02**				
mouse[b]	0.35		0.92		0.58			
mouse[b]	0.35	-0.34	0.64	-0.69	0.30			
mouse[b]	0.35		0.88		0.54			

mouse[b]	0.35	0.23	0.80	-0.12	0.46			
mouse[b]	0.35	0.14	0.94	-0.21	0.60			
mouse[b]	0.35	0.49	0.60	0.15	0.26			
mouse[b]	0.35		0.90		0.56			
mouse[b]	0.35		0.82		0.48			
mouse[b]	0.35		0.79		0.45			
mouse[b]	0.35		0.84		0.50			
mouse[b]	0.35		0.87		0.53			
mouse[b]	0.35		0.78		0.44			
mouse[b]	0.35		0.73		0.39			
mouse[b]	0.35		0.64		0.30			
mouse[b]	0.35		1.13		0.79			
mouse[b]	0.35		0.78		0.44			
mouse[b]	0.35	-0.34	0.64	-0.69	0.29			
mouse[b]	0.35	0.23	0.80	-0.12	0.45			
mouse[b]	0.35	0.14	0.94	-0.21	0.59			
average	**0.35**	**0.01**	**0.79**	**-0.27**	**0.46**			
mouse[c]	0.35	-	0.51	-	0.16			
mouse[c]	0.35	0.17	0.61	-0.18	0.26			
mouse[c]	0.35	0.18	0.65	-0.17	0.30			
mouse[c]	0.35	0.28	0.61	-0.07	0.26			
average	**0.35**	**0.21**	**0.62**	**-0.14**	**0.25**			
sheep[d]	0.27	0.46	0.43	0.19	0.16	144	50	78
sheep[d]	0.27	0.52	0.48	0.25	0.21		45	62
sheep[d]	0.27	0.26	0.36	-0.01	0.09		38	77
sheep[d]	0.27	0.59	0.53	0.32	0.26		56	78
average	**0.27**	**0.46**	**0.45**	**0.19**	**0.18**			
average of all studies				**-0.31**	**0.30**			

Table 3.9.8. The estimated proportion of animal versus plant foods in the Taï chimpanzee diet, according to the Faure and Mensing two-source mixing model (see Supporting Information 3.7).

Diet Type	Model Parameters					proportion (%)	
	$\delta^{66}Zn$ (‰)	$\delta^{66}Zn$ (‰) fractionation corrected	[Zn] ppm	[Zn] absorbed	Zn absorption factor	female chimpanzee	male chimpanzee
all animal food & plant foods							
plant (leaves)	0.48	0.38	28.46	8.54	0.3	97.4%	95.1%
animal foods (termite, monkey meat, ant)	0.13	0.03	110.47	110.47	1.0	2.6%	4.9%
animal food: termite only & plant foods							
plant (leaves)	0.48	0.38	28.46	8.54	0.3	92.9%	85.7%
animal foods (termite only)	0.22	0.12	59.4	59.4	1.0	7.1%	14.3%
animal food: ant only & plant foods							
plant (leaves)	0.48	0.38	28.46	8.54	0.3	99.3%	98.6%
animal foods (ant only)	0	-0.1	253	253	1.0	0.7%	1.4%
animal food: monkey meat only & plant foods							
plant (leaves)	0.48	0.38	28.46	8.54	0.3	86.3%	73%
animal foods (monkey meat only)		0.07	19	19	1.0	13.7%	27%

Supporting Figures

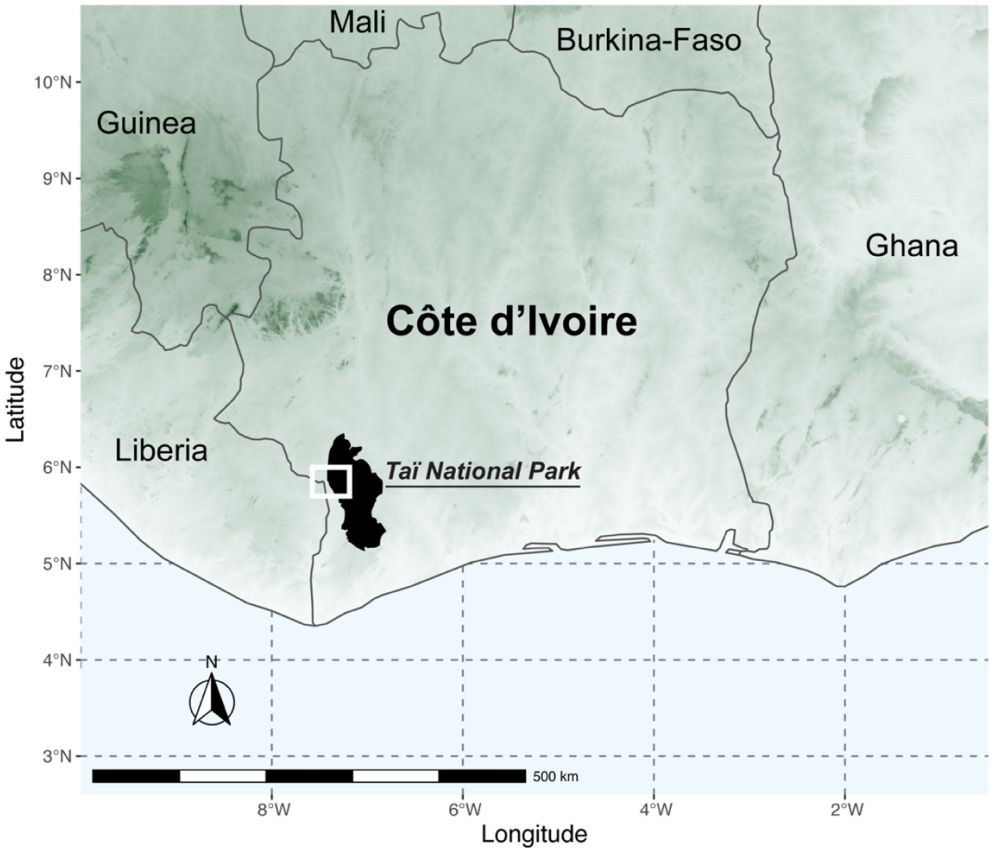

Figure 3.9.1. Topographic map of Côte d'Ivoire.
The study site demarcated by a white rectangle, within Taï National Park. Dark green corresponds to a higher elevation, whereas light green corresponds to a lower elevation (Boucher et al., 2024).

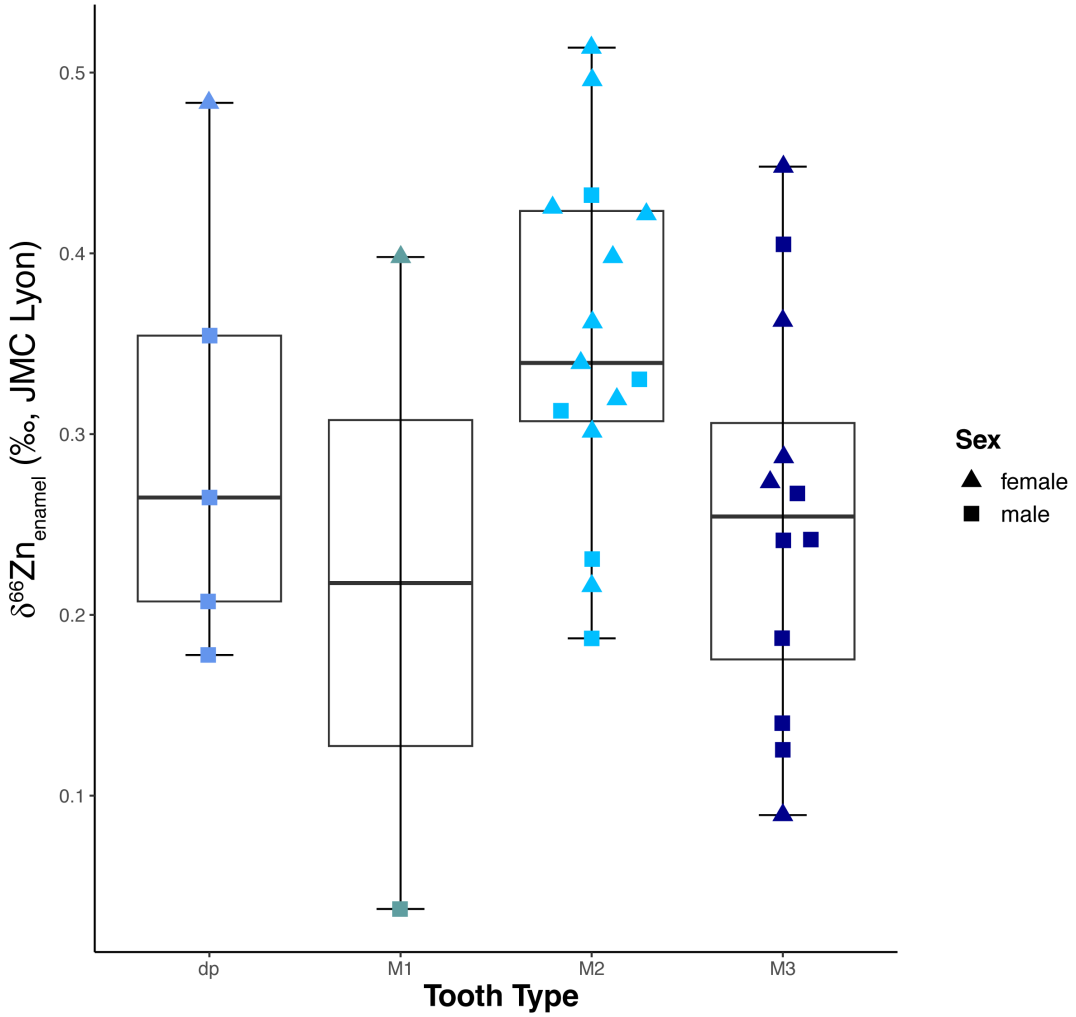

Figure 3.9.2. Boxplots showing the medians, upper (75%) and lower (25%) quartiles of the $\delta^{66}Zn$ values by tooth type (dps, M1s, M2s, M3s) in Taï chimpanzees (n = 34).

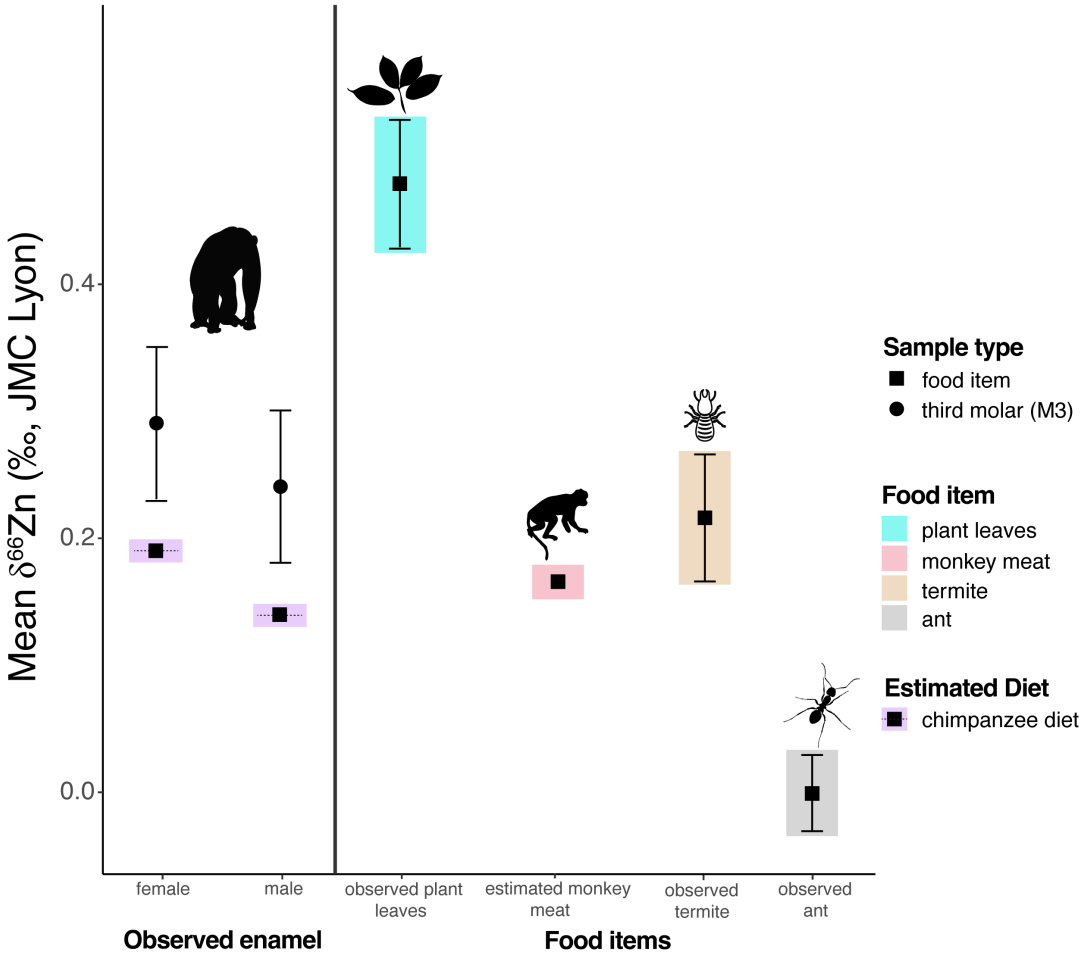

Figure 3.9.3. The mean δ^{66}Zn values and standard error (2σ) for chimpanzee third molars and food items in the Taï forest.
We estimated the δ^{66}Zn value for an herbivorous monkey (muscle tissue) based on the observed δ^{66}Zn values for plant leaves and known isotope fractionation values. The estimated diet for Taï chimpanzees is provided beneath the observed enamel δ^{66}Zn values (see Supporting Information 3.9.3.6 for details).

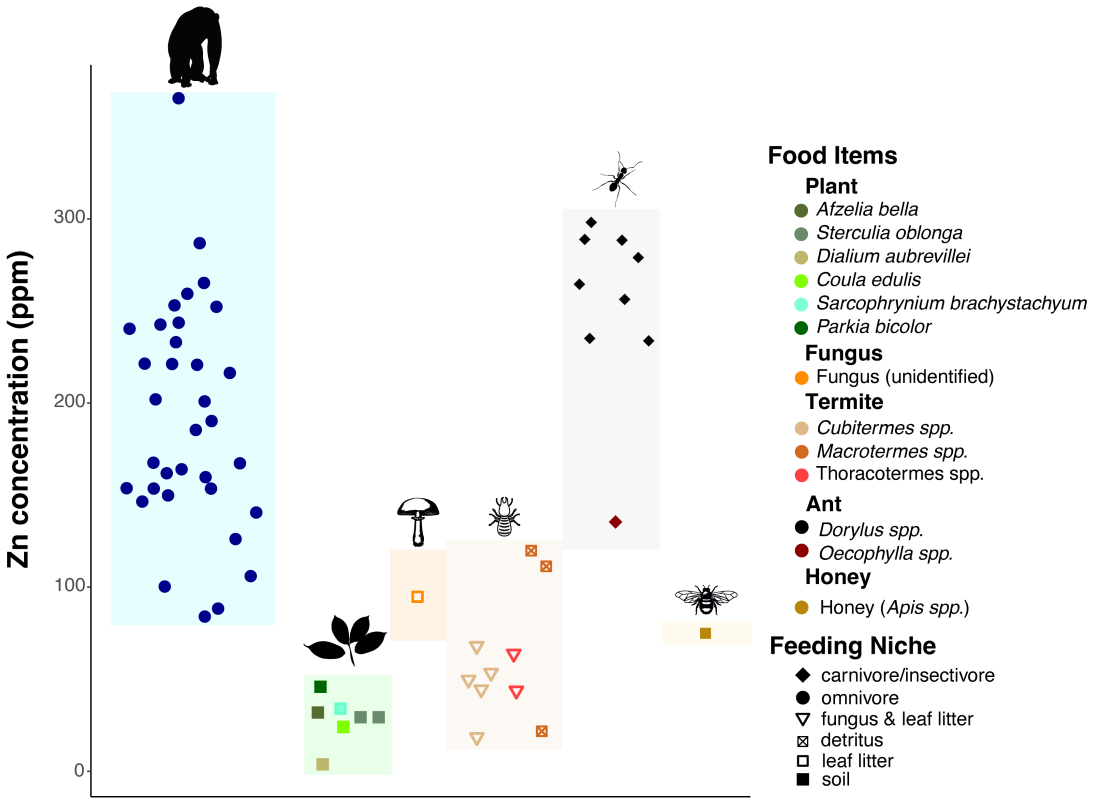

Figure 3.9.4. The Zn concentrations (in ppm) for plant and animal samples from Taï forest.

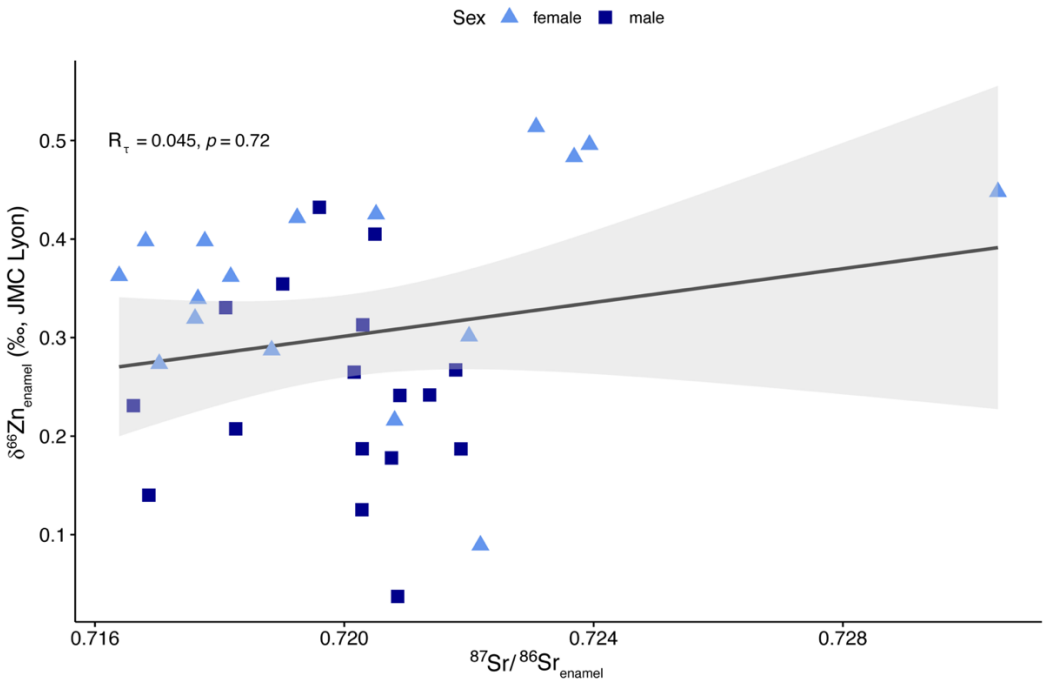

Figure 3.9.5. Scatterplot depicting the correlation (kendall, $R_\tau = 0.04$, $p = 0.72$) between enamel $\delta^{66}Zn$ values and $^{87}Sr/^{86}Sr$ ratios.

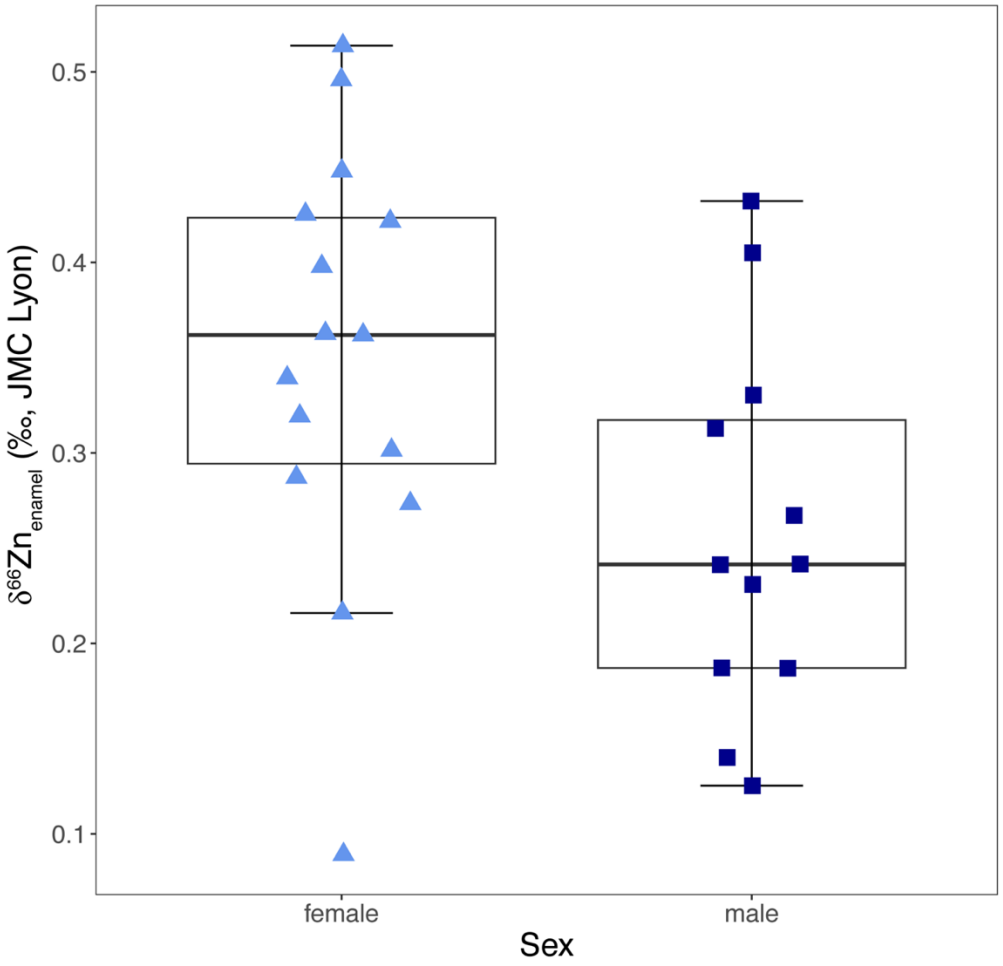

Figure 3.9.6. Boxplots depicting the differences in $\delta^{66}Zn$ values between female and male chimpanzees (n = 27) from Taï National Park in Côte d'Ivoire.
The teeth sampled (M2, M3) reflect the diet of these individuals during tooth formation (4-9 years of age).

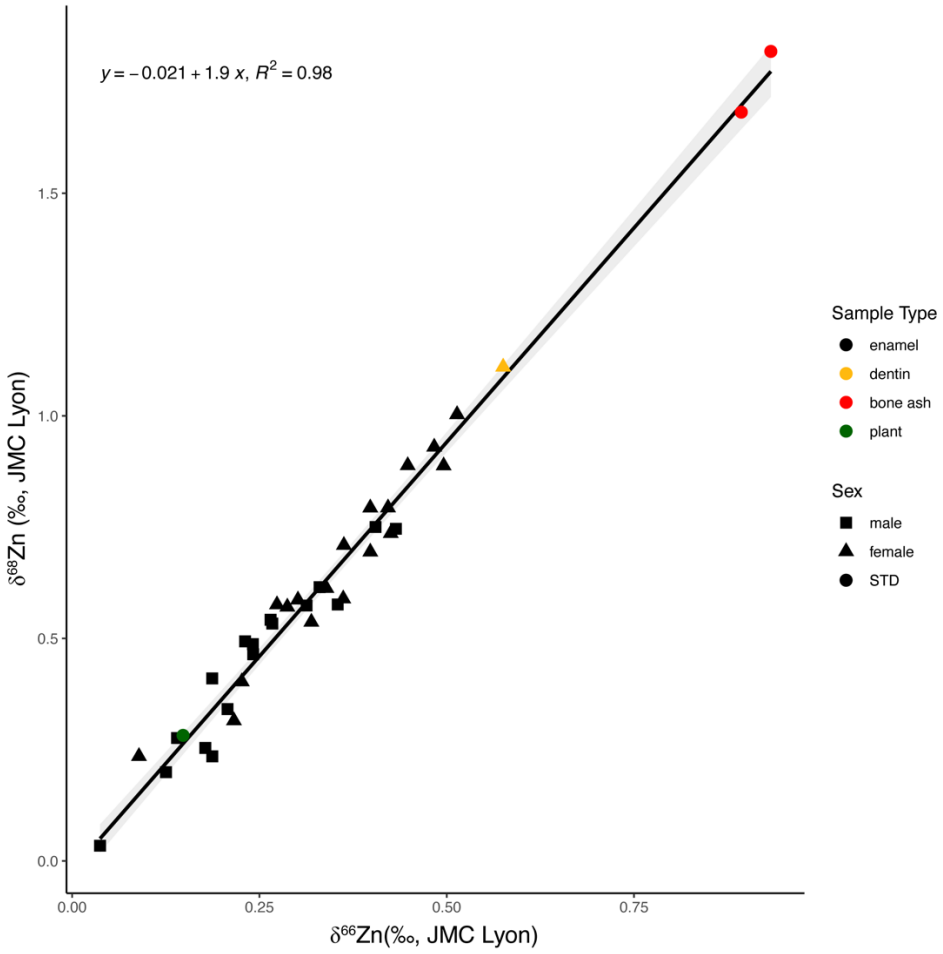

Figure 3.9.7. Mass-dependent fractionation line for Zn isotopes on the MC-ICPMS used in the present study including samples and standards.

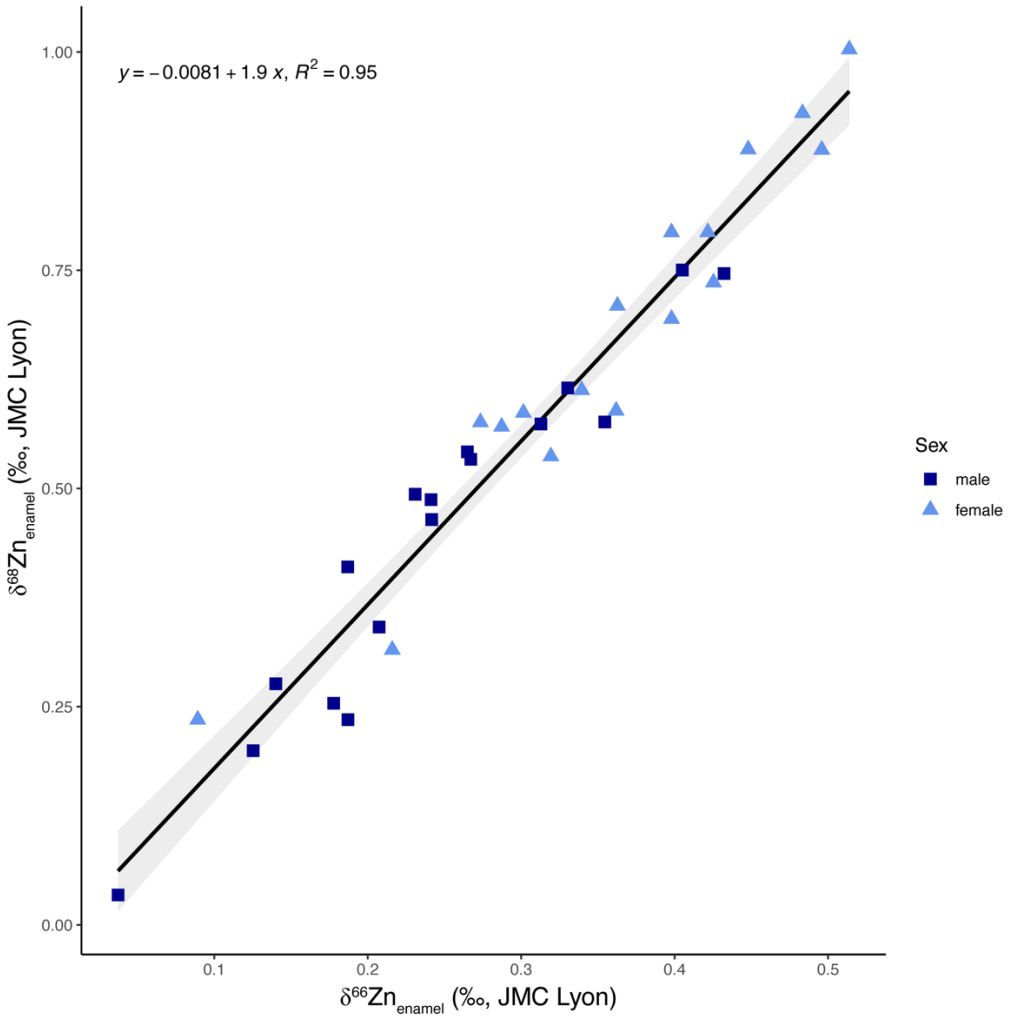

Figure 3.9.8. Mass-dependent fractionation line for Zn isotopes on the MC-ICPMS used in the present study including samples only.

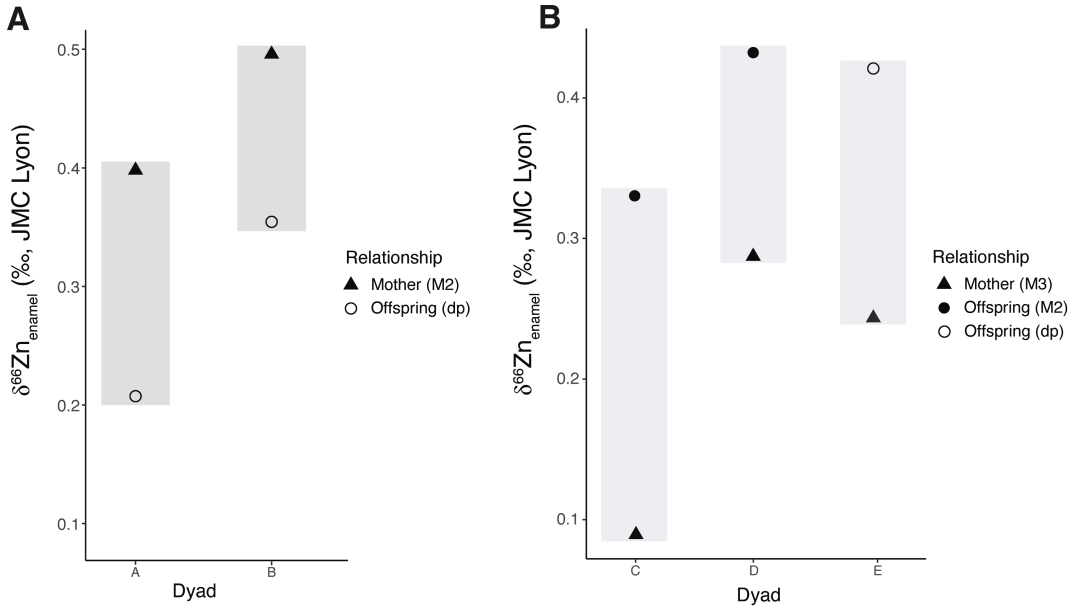

Figure 3.9.9. Scatterplots depicting the $\delta^{66}Zn$ values by chimpanzee mother-offspring dyads separated by tooth types analyzed
(A) the mothers represented by M2s (end of nursing to weaned), and (B) shows the mothers represented by M3s (fully weaned) and the offspring represented by dps (in utero to nursing) and M2s.

References Cited

Arandjelovic, M., Boesch, C., Campbell, G., Hohmann, G., Junker, J., Kouakou, Y., . . . Möbius, Y. (2020). Pan African Programme: the cultured chimpanzee. *Guidelines for Research and Data Collection*.

Balter, V., Lamboux, A., Zazzo, A., Telouk, P., Leverrier, Y., Marvel, J., . . . Albarede, F. (2013). Contrasting Cu, Fe, and Zn isotopic patterns in organs and body fluids of mice and sheep, with emphasis on cellular fractionation. *Metallomics, 5*(11), 1470-1482. doi:10.1039/c3mt00151b

Balter, V., Zazzo, A., Moloney, A. P., Moynier, F., Schmidt, O., Monahan, F. J., & Albarede, F. (2010). Bodily variability of zinc natural isotope abundances in sheep. *Rapid Communications in Mass Spectrometry, 24*(5), 605-612. doi:10.1002/rcm.4425

Balter, V., Zazzo, A., Moloney, A. P., Moynier, F., Schmidt, O., Monahan, F. J., & Albarede, F. (2010). Bodily variability of zinc natural isotope abundances in sheep. *Rapid Communications in Mass Spectrometry: An International Journal Devoted to the Rapid Dissemination of Up-to-the-Minute Research in Mass Spectrometry, 24*(5), 605-612.

Barton, K., & Barton, M. K. (2015). Package 'mumin'. *Version, 1*(18), 439.

Bentley, R. A. (2006). Strontium isotopes from the earth to the archaeological skeleton: a review. *Journal of archaeological method and theory, 13*(3), 135-187.

Boesch, C. (2003). Is culture a golden barrier between human and chimpanzee? *Evolutionary Anthropology: Issues, News, and Reviews: Issues, News, and Reviews, 12*(2), 82-91.

Boesch, C., & Boesch, H. (1989). Hunting behavior of wild chimpanzees in the Tai National Park. *American journal of physical anthropology, 78*(4), 547-573.

Boesch, C., & Boesch, H. (1990). Tool use and tool making in wild chimpanzees. *Folia Primatol (Basel), 54*(1-2), 86-99. doi:10.1159/000156428

Boesch, C., & Boesch-Achermann, H. (2000a). *The chimpanzees of the Taï Forest: Behavioural ecology and evolution*: Oxford University Press, USA.

Boesch, C., & Boesch-Achermann, H. (2000b). The chimpanzees of the Taï Forest: Behavioural ecology and evolution. In: Oxford University Press, USA.

Boesch, C., Kohou, G., Néné, H., & Vigilant, L. (2006). Male competition and paternity in wild chimpanzees of the Taï forest. *American Journal of Physical Anthropology: The Official Publication of the American Association of Physical Anthropologists, 130*(1), 103-115.

Boesch, C., & Wittig, R. (2019). Demography and life history of five chimpanzee communities in Taï National Park. In C. Boesch, R. Wittig, C. Crockford, L. Vigilant, T. Deschner, & F. Leendertz (Eds.), *The Chimpanzees of the Taï Forest: 40 Years of Research* (pp. 159-177). Cambridge: Cambridge University Press.

Boesch-Achermann, H., & Boesch, C. (1993). Tool use in wild chimpanzees: New light from dark forests. *Current Directions in Psychological Science, 2*(1), 18-21.

Bolker, B. M., Brooks, M. E., Clark, C. J., Geange, S. W., Poulsen, J. R., Stevens, M. H. H., & White, J.-S. S. (2009). Generalized linear mixed models: a practical guide for ecology and evolution. *Trends in ecology & evolution, 24*(3), 127-135. doi:https://doi.org/10.1016/j.tree.2008.10.008

Bourgon, N., Jaouen, K., Bacon, A.-M., Jochum, K. P., Dufour, E., Duringer, P., . . . Antoine, P.-O. (2020). Zinc isotopes in Late Pleistocene fossil teeth from a Southeast Asian cave setting preserve paleodietary information. *Proceedings of the National Academy of Sciences, 117*(9), 4675-4681.

Bourgon, N., Jaouen, K., Bacon, A. M., Dufour, E., McCormack, J., Tran, N. H., . . . Tütken, T. (2021). Trophic ecology of a Late Pleistocene early modern human from tropical Southeast Asia inferred from zinc isotopes. *J Hum Evol, 161*, 103075. doi:10.1016/j.jhevol.2021.103075

Brooks, M., Bolker, B., Kristensen, K., & Maechler, M. (2022). Package 'glmmTMB'.

Brooks, M. E., Kristensen, K., Van Benthem, K. J., Magnusson, A., Berg, C. W., Nielsen, A., . . . Bolker, B. M. (2017). glmmTMB balances speed and flexibility among packages for zero-inflated generalized linear mixed modeling. *The R journal, 9*(2), 378-400.

Burnham, K., & Anderson, D. R (2002) Model Selection and Multimodel Inference: A Practical Information-Theoretic Approach, Vol. In: Springer, New York.

Cabral-Pacheco, G. A., Garza-Veloz, I., Castruita-De la Rosa, C., Ramirez-Acuña, J. M., Perez-Romero, B. A., Guerrero-Rodriguez, J. F., . . . Martinez-Fierro, M.

L. (2020). The Roles of Matrix Metalloproteinases and Their Inhibitors in Human Diseases. *Int J Mol Sci, 21*(24). doi:10.3390/ijms21249739

Cloquet, C., Carignan, J., Lehmann, M. F., & Vanhaecke, F. (2008). Variation in the isotopic composition of zinc in the natural environment and the use of zinc isotopes in biogeosciences: a review. *Analytical and Bioanalytical chemistry, 390*(2), 451-463.

Cohen, J. (2013). *Statistical power analysis for the behavioral sciences*: Routledge.

Copeland, S. R., Sponheimer, M., le Roux, P. J., Grimes, V., Lee-Thorp, J. A., de Ruiter, D. J., & Richards, M. P. (2008). Strontium isotope ratios (87Sr/86Sr) of tooth enamel: a comparison of solution and laser ablation multicollector inductively coupled plasma mass spectrometry methods. *Rapid Communications in Mass Spectrometry: An International Journal Devoted to the Rapid Dissemination of Up-to-the-Minute Research in Mass Spectrometry, 22*(20), 3187-3194.

Costas-Rodríguez, M., Delanghe, J., & Vanhaecke, F. (2016). High-precision isotopic analysis of essential mineral elements in biomedicine: natural isotope ratio variations as potential diagnostic and/or prognostic markers. *TrAC Trends in Analytical Chemistry, 76*, 182-193. doi:10.1016/j.trac.2015.10.008

Costas-Rodríguez, M., Van Heghe, L., & Vanhaecke, F. (2014). Evidence for a possible dietary effect on the isotopic composition of Zn in blood via isotopic analysis of food products by multi-collector ICP-mass spectrometry. *Metallomics, 6*(1), 139-146.

Das, M., & Das, R. (2012). Need of education and awareness towards zinc supplementation: a review. *International journal of Nutrition and Metabolism, 4*(3), 45-50.

Dean, C., Le Cabec, A., Spiers, K., Zhang, Y., & Garrevoet, J. (2018). Incremental distribution of strontium and zinc in great ape and fossil hominin cementum using synchrotron X-ray fluorescence mapping. *Journal of the Royal Society Interface, 15*(138), 20170626.

Dean, M. C., Garrevoet, J., Van Malderen, S. J. M., Santos, F., Mirazón Lahr, M., Foley, R., & Le Cabec, A. (2023). The Distribution and Biogenic Origins of Zinc in the Mineralised Tooth Tissues of Modern and Fossil Hominoids: Implications for Life History, Diet and Taphonomy. *Biology, 12*(12), 1455.

Dean, M. C., Spiers, K. M., Garrevoet, J., & Le Cabec, A. (2019). Synchrotron X-ray fluorescence mapping of Ca, Sr and Zn at the neonatal line in human

deciduous teeth reflects changing perinatal physiology. *Archives of Oral Biology, 104*, 90-102.

Driessens, F. C., & Verbeeck, R. (1990). *Biominerals*: CRC press.

Fahy, G. E., Richards, M., Riedel, J., Hublin, J.-J., & Boesch, C. (2013). Stable isotope evidence of meat eating and hunting specialization in adult male chimpanzees. *Proceedings of the National Academy of Sciences, 110*(15), 5829-5833.

Faure, G., & Mensing, T. M. (2005). *Isotope Principle and Applications* (3rd ed.). Hoboken: John Wiley & Sons, Inc.

Favier, M., Faure, P., Roussel, A., Coudray, C., Blache, D., & Favier, A. (1993). Zinc deficiency and dietary folate metabolism in pregnant rats. *Journal of trace elements and electrolytes in health and disease, 7*(1), 19-24.

Goné Bi, Z. B., & Wittig, R. (2019). Long-term diet of the chimpanzees (Pan troglodytes verus) in Taï National Park: interannual variations in consumption. In *In: The Chimpanzees of the Taï Forest*: Cambridge University Press.

Guillaumet, J.-L., & Adjanohoun, E. (1971). La végétation de la Côte d'Ivoire. *Le milieu naturel de la Côte d'Ivoire*(50), 166-262.

Hartig, F., & Hartig, M. F. (2017). Package 'DHARMa'. *Vienna, Austria: R Development Core Team*.

Hortin, A. E., Bechtel, P. J., & Baker, D. H. (1991). Efficacy of Pork Loin as a Source of Zinc and Effect of Added Cysteine on Zinc Bioavailability. *Journal of Food Science, 56*(6), 1505-1507. doi:https://doi.org/10.1111/j.1365-2621.1991.tb08626.x

Hunt, J. R. (2003). Bioavailability of iron, zinc, and other trace minerals from vegetarian diets. *The American journal of clinical nutrition, 78*(3), 633S-639S.

Jaouen, K. (2018). What is our toolbox of analytical chemistry for exploring ancient hominin diets in the absence of organic preservation? *Quaternary Science Reviews, 197*, 307-318.

Jaouen, K., Beasley, M., Schoeninger, M., Hublin, J. J., & Richards, M. P. (2016). Zinc isotope ratios of bones and teeth as new dietary indicators: results from a

modern food web (Koobi Fora, Kenya). *Sci Rep, 6*, 26281. doi:10.1038/srep26281

Jaouen, K., & Pons, M.-L. (2016). Potential of non-traditional isotope studies for bioarchaeology. *Archaeological and Anthropological Sciences, 9*(7), 1389-1404. doi:10.1007/s12520-016-0426-9

Jaouen, K., Pons, M.-L., & Balter, V. (2013). Iron, copper and zinc isotopic fractionation up mammal trophic chains. *Earth and Planetary Science Letters, 374*, 164-172. doi:10.1016/j.epsl.2013.05.037

Jaouen, K., Pouilloux, L., Balter, V., Pons, M.-L., Hublin, J.-J., & Albarède, F. (2019). Dynamic homeostasis modeling of Zn isotope ratios in the human body. *Metallomics, 11*(6), 1049-1059.

Jaouen, K., Szpak, P., & Richards, M. P. (2016). Zinc isotope ratios as indicators of diet and trophic level in arctic marine mammals. *PloS One, 11*(3), e0152299.

Jaouen, K., Trost, M., Bourgon, N., Colleter, R., Le Cabec, A., Tütken, T., . . . Steinbrenner, S. (2020). Zinc isotope variations in archeological human teeth (Lapa do Santo, Brazil) reveal dietary transitions in childhood and no contamination from gloves. *PloS One, 15*(5), e0232379.

Kelley, J., Schwartz, G. T., & Smith, T. M. (2020). Age at first molar emergence in Pan troglodytes verus and variation in the timing of molar emergence among free-living chimpanzees. *Journal of human evolution, 145*, 102823.

Kolongo, T. S. D., Decocq, G., Yao, C. Y. A., Blom, E. C., & Van Rompaey, R. S. (2006). Plant species diversity in the southern part of the Tai National Park (Côte d'Ivoire). *Biodiversity & Conservation, 15*(7), 2123-2142.

Kumle, L., Võ, M. L.-H., & Draschkow, D. (2021). Estimating power in (generalized) linear mixed models: An open introduction and tutorial in R. *Behavior research methods, 53*(6), 2528-2543.

Lemoine, S., Crockford, C., & Wittig, R. (2019). Spatial integration of unusually high numbers of immigrant females into the South Group: further support for the bisexually bonded model in Taï chimpanzees. In C. Boesch, R. Wittig, C. Crockford, L. Vigilant, T. Deschner, & F. Leendertz (Eds.), *The chimpanzees of the Taï Forest: 40 years of research*: Cambridge University Press.

Lenth, R., Singmann, H., Love, J., Buerkner, P., & Herve, M. (2021). Emmeans: Estimated marginal means, aka least-squares means. R Package Version 1 (2018). In.

Liu, R., Amato, K., Hou, R., Gomez, A., Dunn, D. W., Zhang, J., . . . He, G. (2022). Specialized digestive adaptations within the hindgut of a colobine monkey. *The Innovation, 3*(2).

Luncz, L. V., & Boesch, C. (2015). The extent of cultural variation between adjacent chimpanzee (Pan troglodytes verus) communities; A microecological approach. *American journal of physical anthropology, 156*(1), 67-75.

Magnusson, A., Skaug, H., Nielsen, A., Berg, C., Kristensen, K., Maechler, M., . . . Brooks, M. M. (2017). Package 'glmmtmb'. *R Package Version 0.2. 0*.

Mahan, B., Moynier, F., Jørgensen, A. L., Habekost, M., & Siebert, J. (2018). Examining the homeostatic distribution of metals and Zn isotopes in Göttingen minipigs. *Metallomics, 10*(9), 1264-1281.

Mangenot, G. (1950a). Essai sur les forêts denses de la Côte d'Ivoire. *Bulletin de la Société Botanique de France, 97*(7-9), 159-162.

Mangenot, G. (1950b). Les forêts de la Côte d'Ivoire. *Bulletin de la Société Botanique de France, 97*(7-9), 156-157.

Mangenot, G. (1955). Etude sur les forêts des plaines et plateaux de la Côte-d'Ivoire. *Etudes éburnéennes*(4), 6-61.

Maréchal, C. (1998). *Géochimie des isotopes du cuivre et du zinc: méthode, variabilité naturelle et application océanographique.* Grenoble 1,

Möbius, Y., Boesch, C., Koops, K., Matsuzawa, T., & Humle, T. (2008). Cultural differences in army ant predation by West African chimpanzees? A comparative study of microecological variables. *Animal Behaviour, 76*(1), 37-45. doi:https://doi.org/10.1016/j.anbehav.2008.01.008

Moubtahij, Z., McCormack, J., Bourgon, N., Trost, M., Fuller, B., Smith, G., . . . Hublin, J.-J. (2023). Earliest isotopic evidence of high reliance on plant food in the Late Pleistocene hunter-gatherer population (Taforalt, Morocco).

Moynier, F., Fujii, T., Shaw, A. S., & Le Borgne, M. (2013). Heterogeneous distribution of natural zinc isotopes in mice. *Metallomics, 5*(6), 693-699. doi:10.1039/c3mt00008g

Moynier, F., Pichat, S., Pons, M.-L., Fike, D., Balter, V., & Albarède, F. (2009). Isotopic fractionation and transport mechanisms of Zn in plants. *Chemical Geology, 267*(3-4), 125-130.

Navarro, D. (2015). Learning statistics with R: A tutorial for psychology students and other beginners (version 0.6). *University of New South Wales*.

Oelze, V. M., Wittig, R. M., Lemoine, S., Kühl, H. S., & Boesch, C. (2020). How isotopic signatures relate to meat consumption in wild chimpanzees: A critical reference study from Taï National Park, Côte d'Ivoire. *Journal of human evolution*.

Petters, S. W. (1991). *Regional geology of Africa*: Springer.

Ponzevera, E., Quétel, C. R., Berglund, M., Taylor, P. D., Evans, P., Loss, R. D., & Fortunato, G. (2006). Mass discrimination during MC-ICPMS isotopic ratio measurements: investigation by means of synthetic isotopic mixtures (IRMM-007 series) and application to the calibration of natural-like zinc materials (including IRMM-3702 and IRMM-651). *Journal of the American Society for Mass Spectrometry, 17*(10), 1413-1427.

Prashanth, L., Kattapagari, K. K., Chitturi, R. T., Baddam, V. R. R., & Prasad, L. K. (2015). A review on role of essential trace elements in health and disease. *Journal of Dr. YSR University of Health Sciences, 4*(2), 75-85. doi:10.4103/2277-8632.158577

Price, T. D., Burton, J. H., & Bentley, R. A. (2002). The characterization of biologically available strontium isotope ratios for the study of prehistoric migration. *Archaeometry, 44*(1), 117-135.

R Core Development Team. (2022). R: A Language and Environment for Statistical Computing. *R Foundation for Statistical Computing, Vienna, Austria*.

R Core Development Team. (2024). R: A language and environment for statistical computing. *R Foundation for Statistical Computing, Vienna, Austria*.

Reynard, B., & Balter, V. (2014). Trace elements and their isotopes in bones and teeth: Diet, environments, diagenesis, and dating of archeological and paleontological samples. *Palaeogeography, palaeoclimatology, palaeoecology, 416*, 4-16. doi:10.1016/j.palaeo.2014.07.038

Riedel, J., Franz, M., & Boesch, C. (2011). How feeding competition determines female chimpanzee gregariousness and ranging in the Taï National Park, Côte d'Ivoire. *American journal of primatology, 73*(4), 305-313.

Riedel, J., Polansky, L., Wittig, R. M., & Boesch, C. (2020). Social rank overrides environmental and community fluctuations in determining meat access by female chimpanzees in the Taï National Park, Côte d'Ivoire. *PeerJ, 8*, e8283.

Rosman, K., & Taylor, P. (1998). Isotopic compositions of the elements 1997 (Technical Report). *Pure and Applied Chemistry, 70*(1), 217-235.

Samuni, L., Tkaczynski, P., Deschner, T., Löhrrich, T., Wittig, R. M., & Crockford, C. (2020). Maternal effects on offspring growth indicate post-weaning juvenile dependence in chimpanzees (Pan troglodytes verus). *Frontiers in Zoology, 17*(1), 1. doi:10.1186/s12983-019-0343-8

Schwartz, G. T., Reid, D. J., Dean, M., & Chandrasekera, M. S. (2000). *Aspects of tooth crown development in common chimpanzees (Pan troglodytes) with a note on the possible role of sexual dimorphism in canine growth.* Paper presented at the Proceedings of 11th International Symposium on Dental Morphology, Oulu.

Smith, T. M., Arora, M., Bharatiya, M., Leonard, N., Zhao, J.-x., & Austin, C. (in review). Brief Communication: Trace Element Patterns in Juvenile Wild Chimpanzees. *American Journal of Biological Anthropology*.

Smith, T. M., Austin, C., Ávila, J. N., Dirks, W., Green, D. R., Williams, I. S., & Arora, M. (2022). Permanent signatures of birth and nursing initiation are chemically recorded in teeth. *Journal of Archaeological Science, 140*, 105564.

Smith, T. M., Cook, L., Dirks, W., Green, D. R., & Austin, C. (2021). Teeth reveal juvenile diet, health and neurotoxicant exposure retrospectively: What biological rhythms and chemical records tell us. *BioEssays, 43*(9), 2000298. doi:https://doi.org/10.1002/bies.202000298

Smith, T. M., Reid, D. J., Dean, M. C., Olejniczak, A. J., & Martin, L. B. (2007). Molar development in common chimpanzees (Pan troglodytes). *Journal of human evolution, 52*(2), 201-216.

Smith, T. M., Smith, B. H., Reid, D. J., Siedel, H., Vigilant, L., Hublin, J.-J., & Boesch, C. (2010). Dental development of the Taï Forest chimpanzees revisited. *Journal of human evolution, 58*(5), 363-373.

Stoorvogel, J. J., Van Breemen, N., & Jassen, B. H. (1997). The nutrient input by Harmattan dust to a forest ecosystem in Côte d'Ivoire, Africa. *Biogeochemistry, 37*(2), 145-157. doi:10.1023/A:1005734225727

Tacail, T., Kovačiková, L., Brůžek, J., & Balter, V. (2017). Spatial distribution of trace element Ca-normalized ratios in primary and permanent human tooth enamel. *Science of the Total Environment, 603*, 308-318.

Toutain, J.-P., Sonke, J., Munoz, M., Nonell, A., Polvé, M., Viers, J., . . . Sumarti, S. (2008). Evidence for Zn isotopic fractionation at Merapi volcano. *Chemical Geology, 253*(1), 74-82. doi:https://doi.org/10.1016/j.chemgeo.2008.04.007

Van Heghe, L., Deltombe, O., Delanghe, J., Depypere, H., & Vanhaecke, F. (2014). The influence of menstrual blood loss and age on the isotopic composition of Cu, Fe and Zn in human whole blood. *Journal of Analytical Atomic Spectrometry, 29*(3), 478-482.

Viers, J., Oliva, P., Nonell, A., Gélabert, A., Sonke, J. E., Freydier, R., . . . Dupré, B. (2007). Evidence of Zn isotopic fractionation in a soil–plant system of a pristine tropical watershed (Nsimi, Cameroon). *Chemical Geology, 239*(1-2), 124-137.

Vigilant, L., Hofreiter, M., Siedel, H., & Boesch, C. (2001). Paternity and relatedness in wild chimpanzee communities. *Proceedings of the National Academy of Sciences, 98*(23), 12890-12895. doi:10.1073/pnas.231320498

Weiss, D., Mason, T. F., Zhao, F., Kirk, G., Coles, B., & Horstwood, M. (2005). Isotopic discrimination of zinc in higher plants. *New Phytologist, 165*(3), 703-710.

White, T. D., Black, M. T., & Folkens, P. A. (2011). *Human osteology*: Academic press.

Wittig, R., and, & Boesch, C. (2019). Observation protocol and long-term data collection in Taï. In C. Boesch, R. Wittig, C. Crockford, T. Deschner, L. Vigilant, & F. Leendertz (Eds.), *The Chimpanzees of Taï Forest: 40 years of Research*: Cambridge University Press.

CHAPTER 4: A refined protocol for the analysis of iron (Fe) and copper (Cu) isotopes in bones and their correlation with sex in great apes

Authors: Renee D. Boucher[1*], Linda V. Godfrey[2], Lars Fehren-Schmitz[3,4], Paul L. Koch[5]

[1]Department of Anthropology, University of California, Santa Cruz, CA 95064, USA
[2]Department of Earth and Planetary Sciences, Rutgers University, Piscataway, New Jersey 08854, USA
[3]UCSC Paleogenomics, Department of Anthropology, University of California, California, USA
[4]UCSC Genomics Institute, University of California, California, USA
[5]Department of Earth and Planetary Sciences, University of California, Santa Cruz, CA 95064, USA

Note: *In Preparation* for a peer-reviewed journal, 2024. Formatting has been modified from origin article to fit dissertation guidelines. Permission to include this article has been granted by all co-authors and signed permission letter submitted to ProQuest.

Reference: TBD

4.1. Abstract

Iron (Fe) and copper (Cu) stable isotopes may prove important to understanding sex-related differences in primates and humans. In humans, Fe and Cu isotope differences between the sexes have been attributed to the metabolic responses that result from conspicuous blood and tissue loss during menstruation. Our near relatives, chimpanzees (*Pan troglodytes*) and bonobos (*Pan paniscus*) reproduce for most of their adult lives, and unlike humans, they do not lose substantial blood and tissue during menstruation. To assess if chimpanzee menstruation or other factors related to reproduction influence the variation of Fe and Cu isotopes in females

relative to males, we measured $\delta^{56}Fe$ and $\delta^{65}Cu$ values in the bones of morphologically and/or genetically sexed chimpanzees and bonobos (n = 27). To do this, we refined chromatographic methods for isolating and collecting Fe and Cu (as well as Zn) to better suit phosphate-rich skeletal materials. Regarding all sampled individuals, we found a trend for sex differences in $\delta^{56}Fe$ values ($p = 0.07$), but not $\delta^{65}Cu$ values ($p = 0.30$). When excluding sexually immature individuals (aged 5 to 10), we no longer observe these differences in $\delta^{56}Fe$ values ($p = 0.19$), possibly due to small sample size. We propose that sex-related differences of $\delta^{56}Fe$ values in apes likely exist and could be related to (1) iron status and upregulation and (2) iron loss via estrous cycling and reproductive investment. Our new sample processing protocol could encourage future studies using these isotope systems in apes to explain these patterns further.

4.2. Introduction

Much of what is known regarding early human reproductive biology is derived from the study of skeletal remains, including the protein and DNA within them. Successful genome sequencing of human ancestors, or hominins, such as Neanderthals (*Homo sapiens neanderthalensis*), Denisovans (*Homo sapiens denisova*), as well as modern humans (*Homo sapiens*) has provided insights into fertility and reproduction in these species, but it is unclear if menstruation (loss of the endometrium during estrous cycling with significant vaginal discharge of blood and tissue) or menopause (the end of estrous cycling) occurred prior to the evolution of modern humans (Sengupta et al., 2023). In most other placental mammal species,

including some primates, the endometrium is fully resorbed at the end of each estrous cycle (Catalini & Fedder, 2020). In several primates, including great apes, the endometrium is shed, but discharge is absent or minimal (Emera et al., 2012). FOXO1 and WNT7A, the genes associated with endometrium remodeling and homeostasis (Adiguzel & Celik-Ozenci, 2021; Wang et al., 2020), have been identified in humans and rhesus macaques, but further investigation is needed to determine if these genes are expressed similarly in non-human primates.

There are substantial physiological and genetic similarities between humans and non-human primates, making non-human primates' important models for biomedical research (Vallender et al., 2023). As sister taxa, chimpanzees (*Pan troglodytes*) and bonobos (*Pan paniscus*) humans share a recent common ancestor with extant humans, so they provide important insights that can improve our understanding of reproduction in the extinct hominins that arose after the *Pan-Homo* split (Almécija et al., 2021). The arid and wet tropical environments in which early hominins evolved are subject to limited organic preservation due to the breakdown of protein and DNA after 50,000 years (Collins et al., 1995; Timmermann et al., 2022). Additionally, the fossil record is biased towards landscapes with optimal preservation conditions, meaning study areas with poorer preservation typically have less reference data for building DNA libraries (Sykes et al., 2019). Yet, understanding the evolution of menstruation and menopause in our ancestors is critical for addressing the adverse health effects that occur post-menopausal women (Gupta et al., 2009; Ishikawa et al., 2023; Kander et al., 2017; Vahter et al., 2004). While DNA analysis

and proteomics are promising, the application of these methods in deep-time paleoanthropology is limited, therefore, it is essential to develop additional methods to explore the evolution of human reproductive biology, such as the natural variations of iron and copper isotope composition of skeletal material. Chimpanzees and bonobos provide ideal animal models for developing and testing these new methods (Johnstone & Cant, 2019; Liu et al., 2021).

Iron (Fe) and copper (Cu) stable isotopes ($^{56}Fe/^{54}Fe$ and $^{65}Cu/^{63}Cu$, respectively) are reported relative to a standard using delta notation ($\delta^{56}Fe$ and $\delta^{65}Cu$, respectively) in per mil units (‰). Fe and Cu isotope analyses have revealed sex-related differences in some mammals that reflect metabolic and physiological differences between females and males that lead to differences in isotopic fractionation (Albarede et al., 2011; Boucher et al., 2021; Chamel et al., 2017; Jaouen et al., 2012; Jaouen et al., 2017; Jaouen & Pons, 2016). Table 4.7.2 compiles data on $\delta^{56}Fe$ and $\delta^{65}Cu$ values from a variety of studies on human and other mammals (rhesus macaques, mice, and sheep). Unsurprisingly, most of these studies focus on soft tissues, with just a few examining hard tissues, i.e., bones and teeth. In general, hard tissues show roughly the same values, so they are used together to explore patterns in the difference in isotope values between females and males ($\Delta^{56}Fe_{f\text{-}m} = \delta^{56}Fe_{female} - \delta^{56}Fe_{male}$ and similarly for $\Delta^{65}Cu_{f\text{-}m}$) in Figure 4.2.1. For blood and hard tissue data in the studies of reproductive-aged humans, the average $\Delta^{56}Fe_{f\text{-}m} \pm 2$ SD is +0.25 ± 0.27‰ (n = 17) and the $\Delta^{65}Cu_{f\text{-}m}$ is -0.15 ± 0.41‰ (n = 19). We conducted a one-sample Wilcoxon test ($\Delta^{56}Fe_{f\text{-}m}$)

and a one sample t-test ($\Delta^{65}Cu_{f\text{-}m}$) to explore whether these values are significantly different from 0‰ (i.e., the value expected for no difference between the sexes). The tests revealed significant differences for Fe ($V = 133$, $p < 0.001$) and Cu ($t(21) = -3.31$, $p = 0.003$). In the few studies reporting data on post-reproductive humans, the differences are diminished, $+0.03 \pm 0.05$‰ for $\Delta^{56}Fe_{f\text{-}m}$ and $+0.01 \pm 0.18$‰ for $\Delta^{65}Cu_{f\text{-}m}$ (see Figure 4.2.1 and Table 4.7.2). For iron isotopes, this difference has been attributed to the loss of Fe during menstruation (Hotz et al., 2012; Jaouen & Balter, 2014; Krayenbuehl et al., 2005). On average, human females (weighing ~ 63 kg) lose about 40 ml of blood (~1.01% total blood volume) and 15 mg of Fe (~40% of their monthly dietary uptake of 35 mg Fe) during menstruation each month (Jaouen & Balter, 2014; Tapiero et al., 2003). Studies have shown that blood Fe becomes ^{56}Fe-enriched after blood loss, because either heavy Fe stored in the liver is released to make up for the deficit and/or Fe uptake from the diet is upregulated, reducing the discrimination against ^{56}Fe across the gut lining (Albarède, 2015; Hotz et al., 2012; Jaouen & Pons, 2016; Krayenbuehl et al., 2005).

While the literature data are less consistent on the presence of a sex-related difference in Cu isotopes in humans, a potential link to Cu isotope variation comes via Fe transport. In the liver, the release of Fe from hepatocytes requires the Cu-hosting enzyme, ceruloplasmin (CP) to catalyze the oxidation of Fe (II, ferrous iron) to the less toxic Fe (III, ferric iron). Elevated CP activity and higher Cu turnover in menstruating women has been thought to produce lower

^{65}Cu values relative to men (Hunt et al., 2009; Jaouen & Balter, 2014), though the precise mechanism for this potential fractionation remains obscure.

Overall, in human females, menstrual blood loss has been viewed as the most significant factor affecting δ^{56}Fe values (Harvey et al., 2005), and due to the role of Cu-rich CP in Fe metabolism (Arredondo & Núñez, 2005), a potential factor affecting δ^{65}Cu values as well. Thus, any major blood loss occurring from menstruation or from injury, phlebotomy, and gestation/parturition is expected to result in the same pattern in δ^{56}Fe and potentially δ^{65}Cu values (Van Heghe et al., 2013). After menopause in humans, these patterns dissipate, as δ^{56}Fe and δ^{65}Cu values for females shift toward those for males, albeit at different rates given the contrast in turnover time for these elements (slower for Fe and faster for Cu) (Albarède et al., 2017; Jaouen & Balter, 2014; Van Heghe et al., 2014).

While in human females, menstruation is an important manifestation of the monthly estrous cycle, it is scarcely observed in other mammals, even most primate species (Emera et al., 2012). And in the few other species that have been examined, the linkage of Fe and Cu isotope fractionation to menstruation is less clear. In rhesus macaques (*Macaca mulatta*), which have a comparable estrous cycle to humans, with on average 7 ml of blood loss in their 25-to-35-day cycle (~2.01% total blood volume for average female weighing 5.3 kg), females δ^{56}Fe values are 0.39‰ higher and δ^{65}Cu values are 1.40‰ lower compared to males, though only the Cu difference is significant (Boucher et al., 2021). In mice, which do not menstruate, but rather reabsorb their endometrium, sex differences are present, but female bone δ^{56}Fe values

are 0.24‰ lower and bone $\delta^{65}Cu$ values are 0.4‰ higher relative to males, i.e., opposite of the pattern seen in humans and rhesus macaques (see Table 4.7.2) (Boucher et al., 2021; Moynier et al., 2019). These observations hint that sex-related Fe and Cu isotope differences in mammals may originate from mechanisms other than menstrual blood and tissue loss, though the nature of these effects in mice and other mammals remains unclear (Moynier et al., 2022).

Since Fe and Cu isotopes can be readily analyzed in bone, but are at trace levels in tooth enamel, applying $\delta^{56}Fe$ and $\delta^{65}Cu$ analysis to a large-bodied, wild primate such as the chimpanzee or bonobo enables the exploration of sex-related differences in a biologically meaningful model to early hominin and human ancestors (Boucher et al., 2021; Jaouen et al., 2017; Sayers et al., 2008). Chimpanzees and bonobos begin monthly estrous cycling at 8-10 years old and then have monthly cycles that average ~35-36 days (Deschner & Boesch, 2007; Deschner et al., 2004; Paoli et al., 2006; Piña-Aguilar et al., 2016; Thompson et al., 2012). There are few observations regarding the nature of menstruation (or menses) during these estrous cycles. Unlike humans, chimpanzees and bonobos experience hormonally stimulated sexual swellings of the anogenital region that signal fertility or ovulation (Deschner et al., 2004; Douglas et al., 2016). Detumescence is typically associated with the end of the estrous cycle, and is followed by menses (Wallis, 1992). In captive populations, when menses is observed, it is typically minimal, with on average 1 to 15 ml of blood loss (ranging from 0.14 to 0.42% of total blood volume for average female weighing 47 kg) (Lacreuse et al., 2008; Piña-Aguilar et al., 2016), and before menses, blood

within anogenital swellings is absorbed via detumescence. In wild chimpanzee populations, quantifying menses is more complex, as there are such small amounts of fluid loss, and the high incidence of injury to the swollen anogenital region of females often makes it hard to distinguish menstrual bleeding from injury bleeding (Melissa Emery Thompson and Zarin Machanda, personal communication). The dearth of data on menstruation in bonobos I even greater, making it unclear if menstruation could be a likely mechanism for any observable sex difference in Fe and Cu isotopes in either species (Hotz et al., 2012). Further, in some wild chimpanzee populations under long-term observation and low human impact, there is evidence of hormonal menopause (Wood et al., 2023), which suggests there could be similar post-menopausal changes in Fe and Cu isotope variation, as observed in humans.

Here, we measure Fe and Cu isotopes in chimpanzees and bonobos to explore a model of minimally menstruating hominins. We address the following questions with a museum-curated collection of wild and lab-reared chimpanzees and bonobos: (1) Are there sex-related differences in $\delta^{56}Fe$ and $\delta^{65}Cu$ values in great apes? (2) If yes, then what might be driving sex-related differences in Fe and Cu isotope fractionation?

In order to address these questions, we first refine the method for isolating Fe and Cu from bone samples, more specifically, the inorganic bioapatite matrix. There are several column chromatography protocols for isolating Fe and Cu (as well as Zn), however, the current matrix-matched protocol does not support the higher sample quantity needed to analyze trace metals in bioapatite, uses a high volume of

concentrated acid, requires expensive and easily broken custom quartz columns, and can be time intensive (Boucher et al., 2021; Jaouen, 2012; Maréchal et al., 1999; Sauzéat et al., 2021). In this study, we adjust existing protocols to be suitable for a higher quantity of sample (~100-150 mg), to minimize on-column Cu fractionation, to be more cost-effective (using a lower volume of concentrated acid), and to be less time intensive (see Supporting Information 4.7.1 for details).

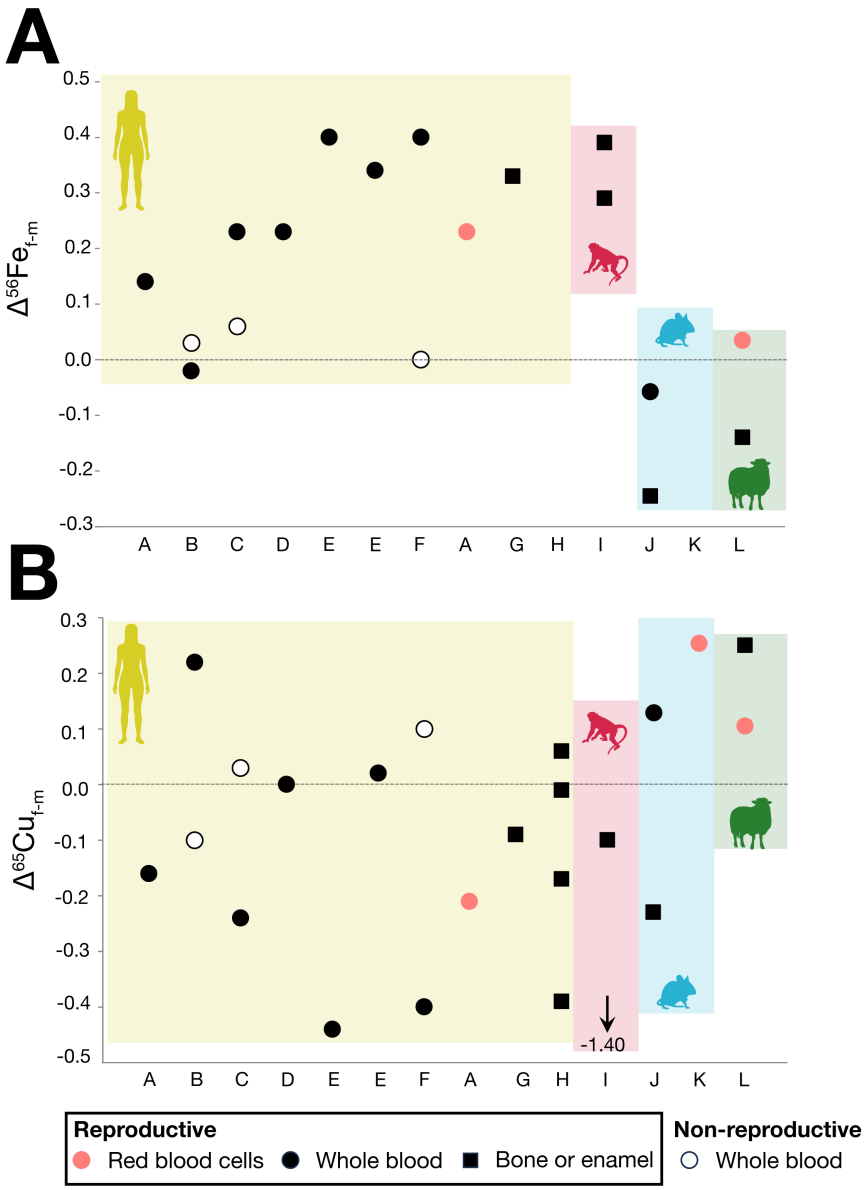

Figure 4.2.1. Scatterplots showing the difference in isotope values (Δ) between females and males, where (A) δ^{56}Fe values and (B) δ^{65}Cu values are given in per mil units (‰) for humans, rhesus macaques, mice, and sheep.
Letters on the x-axis correspond to the references in Table 4.7.2. The number of pregnancies and children (reproductive investment) is unknown for the samples included from the literature here. Hormonal contraceptive use is only known for one of the studies (study D). Multiple data points per study either indicate multiple tissue types or different cohorts of individuals within the study (e.g., those on different diets in study H). The outlier for rhesus macaque bone is indicated by the downward oriented arrow.

4.3. Materials & Methods

Individuals sampled

We sampled bone from 26 chimpanzees and 3 bonobos curated at the Museum of Comparative Zoology (MCZ, Cambridge, MA). The individuals sampled were either wild (n = 25) or lab-reared (n = 4) and included 18 sexually mature (greater than ~15 years old), 3 sexually mature but may not yet be reproducing (~10-15 years old), and 8 sexually immature (weaned to ~10 years old). Estrous cycles in females begin at ~10 years old and the first birth occurs at ~15 years old. In males, sexual maturity and first successful breeding can occur as early as 9 to 10 years old, with the majority of offspring sired after 15 years old (Boesch et al., 2006; Marson et al., 1991). Finally, especially in females, these ages can be highly variable and affected by environmental and maternal factors (Walker et al., 2018). Among the chimpanzees, we sampled 13 males, 11 females, and 2 individuals of indeterminate sex. For the bonobos, we sampled 2 males and 1 female (all adults). The wild individuals are from different localities, including various locations within Cameroon (n = 17), Democratic Republic of Congo (n = 3), and unspecified (n = 5). For a more detailed sample list see Table 4.7.1. Sex was initially estimated by the MCZ and

confirmed by visual inspection of the sexual dimorphism in the skull and post-cranial skeleton for 19 individuals by RB. For 10 individuals, sex could not be determined morphologically, and therefore, we performed DNA analysis (see below). Age class was estimated at the MCZ by combining evidence from permanent tooth eruption (M3, ~ 10 to 14 years), basicranial suture and epiphyseal fusion (Balolia, 2015; Bolter & Zihlman, 2012; Brimacombe et al., 2015, 2018; Smith & Boesch, 2011; Smith et al., 2021). Table 4.7.1 includes isotopic data for the two individuals of indeterminate sex as well as an infant in the MCZ collection. These data are not included in any of the statistical analyses or figures.

Sample preparation

We mechanically cleaned the sampling area with a diamond-tipped dental drill and then recovered about 150 mg of cortical bone, of which ~100 mg was used for Fe and Cu isotope analysis, and 50 mg was used for DNA analysis. Abraded bone was placed in cleaned glass beakers and sonicated for 5 minutes in 2 ml ultrapure water (MQ H_2O, resistivity ≥18.2 MΩ cm) obtained from a Milli-Q Element water purification to remove dust and exogenous contamination. Cleaned samples were then removed from the solution, transferred into clean Eppendorf tubes, and dried at 30°C to prevent DNA degradation.

Sample digestion and column chromatography

Sample preparation was performed in a class 1,000 suite (ISO 6) clean lab and consisted of digestion and target element isolation. The acids used for digestion and elution, HNO_3 (15.9 M) and HCl (12 M) were purified in-house via sub-boiling

distillation three times before use. The refined sample digestion and column chromatography procedure we used is presented in Figure 4.4.1. Rather than ashing dried samples to remove organic matter, 100 mg were weighed into acid washed Savillex® Teflon beakers, then 1 ml of ultrapure hydrogen peroxide (H2O2, J.T. Baker Ultrex® II) was added and left to react in the capped Teflon beaker for 2 hours at room temperature. After 2 hours, 1 ml of triple distilled 15.9M HNO_3 was added, the Teflon beaker was recapped, and the samples were allowed to digest at 110°C for 1 hour to fully dissolve the bioapatite. Once the samples were fully digested, they were evaporated to dryness at 90°C for at least 4 hours. The evaporated samples were dissolved in 1 ml 7N HCl + 0.001% H_2O_2 for 1 hour at 110°C along with one procedural blank and two standards (USGS SGR-1 and NIST SRM-1400). Once the samples were dissolved, we took a 20 µl aliquot for elemental concentration measurements.

The method for the isolation of Cu, Fe and Zn described by Maréchal et al. (1999) and modified by Van Heghe et al. (2012) was further adapted to only isolate Cu and Fe by reducing the sample loading volume (~80%) and increasing the elution acid volume (~ 60% for Cu and ~ 32% for Fe) to make it applicable to phosphate-rich bone samples. For chromatographic separation of Fe and Cu from other elements, we used analytical grade AG® MP-1 strong anion exchange resin (100–200 µm dry mesh size, chloride anionic form, Bio-Rad). To remove the finest particles, the resin was allowed to settle in MQ H_2O, and then the supernatant was discarded 10 times. This was repeated twice more with 0.5M HNO_3, and then MQ H_2O was added to the resin

before 2 ml were loaded in acid-washed polypropylene chromatography columns (Bio-Rad). Then, the resin was pre-cleaned with 10 ml of MQ H_2O, 10 ml of 7M HNO_3, and an additional 10 ml of MQ H_2O, 7 ml of 0.5M HNO_3, and 3 ml of MQ H_2O, before being conditioned with 7 ml of 7N HCl + 0.001 % H_2O_2. The remaining sample (~ 1 ml) was loaded onto the resin bed (2 ml), and the matrix was eluted using 9 ml of 7N HCl + 0.001% H_2O_2. Afterwards, Cu and Fe were eluted successively using 20 ml of 4N HCl + 0.001% H_2O_2 and 22 ml of 0.7N HCl and collected in acid washed Savillex® Teflon beakers. The purified fractions of Cu and Fe were evaporated to dryness at 90°C. The Fe and Cu fractions were taken up in 1 ml of 7N HCl + 0.001% H_2O_2 and subjected to the same chromatographic isolation a second time to remove any residual phosphate and calcium (Boucher et al., 2021). After the second chromatographic procedure, a 25 µl aliquot was taken for post-chemistry elemental concentration measurements. The samples were then evaporated to dryness at 90°C for subsequent isotope analysis.

DNA Analysis

DNA extractions for 10 samples (identified in Table 4.7.1) were carried out in the dedicated cleanroom facilities at the UCSC Paleogenomics Lab (UCSC-PGL) following strict precautions for contamination prevention (Llamas et al., 2017). Since these were museum collection samples with unknown treatment, extractions from cortical bone were performed following a silica-column based protocol optimized for the recovery of small ancient DNA molecules (Dabney et al., 2013) using ~50 mg of

pulverized sample. Before lysis, we added a bleach treatment pre-digestion as described by Boessenkool et al (Boessenkool et al., 2017). We quantified the DNA extracts using a Qubit v4 Fluorometer (Invitrogen, USA). Subsequently, 2 ng of DNA were used to build double-indexed single stranded DNA (ssDNA) sequencing libraries as described by Kapp et al. (Kapp et al., 2021) for each individual. The sequencing libraries were sequenced for 1 Mio reads each on an Illumina NextSeq2000 instrument (Illumina, Inc., San Diego, CA, USA) at UCSC-PGL, with 150 paired-end-run cycles using the manufacturer's protocol. The output was then de-multiplexed using bcl2fastq version 2.17.1.14 (Illumina conversion Software).

After demultiplexing, resulting sequencing reads were processed using the UCSC-PGL in-house computational pipeline developed for aDNA described in Fehren-Schmitz et al. (Fehren-Schmitz et al., 2017) and available at (https://github.com/mjobin/batpipe, v1, 05/10/2021). This pipeline, clips adapters, merges paired-end reads (default parameters), maps sequencing reads against a user specified reference genome, removes duplicate reads, and estimates quality traits. Sequencing reads were mapped using the Burrows–Wheeler Aligner (BWA) version 0.7.12 (Li & Durbin, 2009), disabling seeding (-l 16500, –n 0.01) against the PanTro-v1.1 Chimpanzee reference genome (NCBI RefSeq Assembly: GCF_028858775.1) Duplicates were removed with DeDup version 0.12.2 (Peltzer et al., 2016). A mapping quality filter of 30 was further applied using SAMtools version 1.3. We estimated patterns of DNA damage using MapDamage 2 (Jónsson et al., 2013) and

observed damage rates at the read termini >3% for all individuals, which is expected for authentic degraded DNA.

To determine the genetic sex of the individuals we calculated the Rx ratio, introduced by Mittnik et al. (Mittnik et al., 2016) for humans, and adapted for other animals by de Flamingh et al. (de Flamingh et al., 2020), which compares the proportion of sequencing reads mapping to the X chromosome and autosomal chromosomes. This ratio differs depending on the number of X-chromosomes in an individual's karyotype, thus allowing the differentiation between females and males. To compute the Rx ratio, we used the script by de Flamingh et al. (de Flamingh et al., 2020), adapting it to the Chimpanzee karyotype.

Isotopic and Elemental Analysis

During our development of the refined chromatographic procedure for isolating Fe and Cu, we made concentration measurements (in ppm) via High Resolution ICP-MS (inductively coupled plasma mass spectrometry, Element XR, ThermoFisher) in the Department of Earth and Planetary Sciences at the Plasma Analytical Lab, University of California, Santa Cruz. The pre- and post-chemistry aliquots were diluted in 2 ml of 5% HNO_3, and then measured alongside acid blanks and an in-house standard. The in-house standard was composed of 5% HNO_3 with 1 ppb of each of the elements of interest (Fe, Cu, Zn) as well as the elements that may introduce polyatomic or isobaric interferences (measured at ^{24}Mg, ^{27}Al, ^{31}P, ^{33}S, ^{43}Ca, ^{44}Ca, ^{47}Ti, ^{52}Cr, ^{55}Mn, ^{60}Ni, ^{88}Sr).

The $\delta^{56}Fe$ and $\delta^{65}Cu$ values were determined via MC-ICP-MS (multiple-collector, Neptune Plus, ThermoScientific) in the Department of Earth and Planetary Sciences, Rutgers University. The samples were introduced by free aspiration in 2% HNO_3, with a Cetac Aridus II desolvating nebulizer. For Fe and Cu, instrumental mass fractionation was corrected using standard-sample bracketing following the technique of Albarède et al (Albarede et al., 2004). The isotope reference standards used were NIST-976 (Cu) and IRMM-524A (Fe), which is identical to IRMM-014. The Fe and Cu isotope values are reported on a relative scale to the international standards (NIST-976 and IRMM-014) in per mil (‰) units. External reproducibility was determined by measuring NIST-976 (Cu) and IRMM-014 (Fe) as unknowns with the reference standards and samples. Further checks for $\delta^{65}Cu$ were made by analysis of an internal standard (1838 US penny), which overlapped with reported values of 0.06 ± 0.12‰ (2σ, n = 2) (Mathur et al., 2009; Zegkinoglou et al., 2023). For $\delta^{56}Fe$, IRMM-014 was used, which aligned with reported values of -0.11‰ (2σ, n = 4) (Phillips et al., 2017; Wu et al., 2012). The precision (external reproducibility, 2σ) on the isotopic ratios is ± 0.04‰ for Cu and ± 0.07‰ for Fe. Samples were typically measured at least twice and the standard replicate analyses (2σ) ranged from 0.01‰ to 0.53‰ with a mean of 0.18‰ for Fe and from 0.00‰ to 0.45‰ with a mean of 0.13‰ for Cu.

Statistical Analysis

The following statistical tests were performed with the R software version 4.3.2, using a significance value set at $\alpha = 0.05$ (R Core Development Team, 2022). First, the R '*stats*' package was used to determine if parametric or non-parametric analyses were needed for each dataset (R Core Development Team, 2022). For data that were found to be normally distributed (Shapiro-Wilk, $p > 0.05$), we proceeded with parametric tests, including Welch Two Sample t-tests and analysis of variance (ANOVA), then determined effect size using the Cohen's d function within the R '*rstatix*' package (Cohen, 2013). For data that were found to be non-normally distributed (Shapiro-Walk, $p < 0.05$), we proceeded with non-parametric tests, including Kruskal-Wallis and Wilcoxon tests in R (Hollander et al., 2013; R Core Development Team, 2024). In tests that had significant results, pairwise comparisons were performed using pairwise Wilcoxon rank sum tests in the R '*stats*'package. To determine the effect size of Wilcoxon tests, we used the shieh power function within the R '*wmwpow*' package (Shieh et al., 2006).

4.4. Results

Sex assessment

Of the unknown individuals (n = 10), we found that 4 were consistent with XY and were assigned as male, 4 were consistent with XX and were assigned as female, but 2 chimpanzees could not be assigned. As noted above, isotope values for these indeterminate samples will not be considered further.

Validation of the chromatographic separation procedure

The chromatographic procedure's effectiveness for separating the two target elements (Fe, Cu) was evaluated by elemental analysis of the separately collected 2 ml fractions. The chromatographic separation procedure is described in Figure 4.4.1 and the results of the method validation tests are provided in Figure 4.7.1, which shows the elution profile for a sample of NIST SRM-1400 and includes the concentrations of the target elements (in ng/g). The mean recovery for Fe and Cu is 102% and 98%, where all procedural blanks were < 1 ppb and < 0.1 ppb, which is negligible compared to the mean concentrations of the various samples (1,952 ppb for Fe and 217 ppb for Cu).

To assess the ability of our revised protocol to yield accurate isotope values, two standards were analyzed with each batch of samples (n = 2 batches), NIST SRM-1400 (bone ash) and USGS SGR-1 (green river shale). The NIST SRM-1400 apatite standard is matrix-matched with our samples. This is the first time it has been analyzed for Fe and Cu stable isotope compositions. Therefore, to assess the reproducibility, we only use the USGS SGR-1 shale standard. We include the measured standard values for each batch of samples, batch 1 (2401 to 2417) and batch 2 (2418 to 2430), respectively. For each batch of samples, the NIST SRM-1400, the δ^{56}Fe values were 0.09 ± 0.05‰ and 0.07 ± 0.02‰, δ^{65}Cu values were 1.40 ± 0.40‰ and 0.52 ± 0.16‰, respectively. For the USGS SGR-1 standard, the δ^{56}Fe values were -0.10 ± 0.06‰ and -0.05 ± 0.03‰, and the δ^{65}Cu values were 0.30‰ and 0.38‰, respectively, which align with published values (δ^{56}Fe: -0.04 to 0.15 ± 0.02‰ and δ^{65}Cu: 0.37 ± 0.07‰) and validates the isolation protocol (Sun et al., 2021).

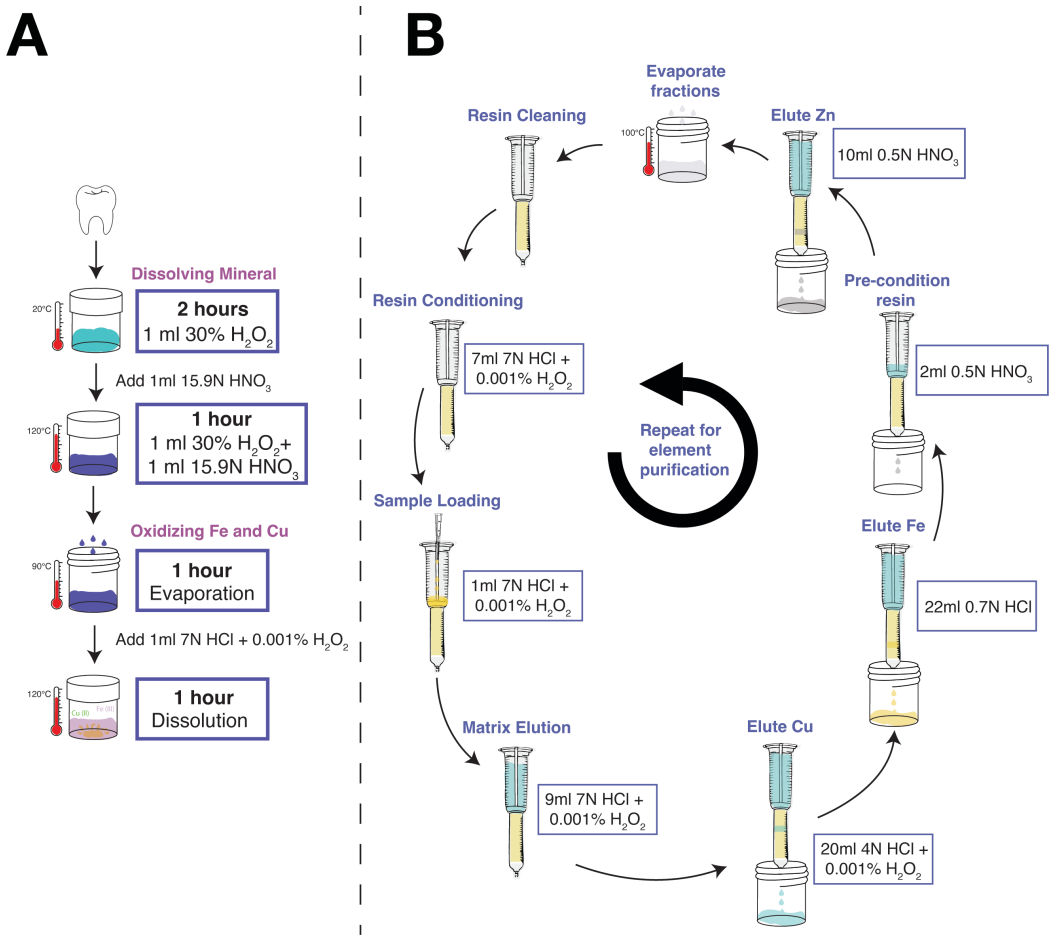

Figure 4.4.1. Flow chart of the (A) digestion protocol, and (B) the refined Fe and Cu isolation protocol.
The protocol begins on the left with resin cleaning (see Materials and Methods above for details) and ends with the evaporation of each fraction for Fe and Cu. This protocol was conducted twice for each samples' fraction of Fe and Cu to purify the sample.

Mass-dependent isotope fractionation

We checked that isotopic fractionation was mass-dependent for all the samples (see Supporting Information, Figures 4.7.2 and 4.7.3), where different slopes would indicate instrumental mass-independent fractionation. All the samples were found to

fall on the theoretical mass-dependent fractionation lines (see Figures 4.7.2 and 4.7.3, $y = 1.4x - 0.03$, $R^2 = 0.98$).

Origin of the samples

The sexed chimpanzees (n = 24) have variable origins, so we tested that there was no influence of geological location on $\delta^{56}Fe$ and $\delta^{65}Cu$ values. The $\delta^{56}Fe$ and $\delta^{65}Cu$ values were separated by sex. When considering $\delta^{56}Fe$ values, we found no significant difference by origin for either male ($\chi^2 = 6$, df = 5, p = 0.31) or female chimpanzees ($\chi^2 = 7.23$, df = 6, p = 0.30). Similarly, for $\delta^{65}Cu$ values, we found no significant difference in $\delta^{65}Cu$ values by origin for male ($\chi^2 = 2.8$, df = 5, p = 0.73) or female chimpanzees ($\chi^2 = 4.43$, df = 6, p = 0.62). The sampled bonobos were all from the same region, so the influence of location was not tested.

Sex differences in $\delta^{56}Fe$ and $\delta^{65}Cu$ values

First, we explored species-specific differences in $\delta^{56}Fe$ and δ65Cu values between the sexes in the entire set of samples within this study. When considering chimpanzees (n = 24, see Figure 4.4.2), males had mean $\delta^{56}Fe$ and $\delta^{65}Cu$ values of -1.02 ± 1.52‰ and 0.39 ± 0.70‰ (all error is reported to 2σ). By contrast, females had mean $\delta^{56}Fe$ and $\delta^{65}Cu$ values of -0.48 ± 0.39‰ and 0.68 ± 1.19‰.

To explore if the differences between the sexes in $\delta^{56}Fe$ and $\delta^{65}Cu$ values could be related to estrous cycling, we next compared sex-related differences in isotope values for sexually mature adults and adolescents (e.g., animals with an

estimated age greater than 10 years, n = 16). Among these individuals, the difference between sexes in δ^{56}Fe values ($t(10.93) = 1.39$, $p = 0.19$) or δ^{65}Cu values ($t(7.96) = 1.67$, $p = 0.13$) did not meet the threshold for statistical significance. However, the effect size, as measured by Cohen's d, was $d = 0.67$ for δ^{56}Fe values and $d = 0.88$ for δ^{65}Cu values, indicating a medium and large effect, respectively. Given uncertainties in our ability to precisely age animals using skeletal and dental traits, and the considerable variation in the timing of key maturation events (especially the onset of estrous cycling in females), we decided to explore if sex differences were present among all sexed individuals (i.e., including the sexed animals with an estimated age between 5 and 10 years, n = 24). In this comparison the difference between females and males in δ^{56}Fe values neared the threshold for statistical significance ($t(12.15) = 1.97$, $p = 0.07$), whereas those for δ^{65}Cu values were far from significance ($W = 90$, $p = 0.30$). The effect size for δ^{56}Fe values was relatively high ($d = 0.83$), whereas for δ^{65}Cu values the shieh power was also high (0.76).

We also explored if there is a sex difference related to being raised in a captive compared to a wild environment. When examining captive versus wild chimpanzees, there was no observable difference in δ^{56}Fe values for either males or females. On the other hand, the only captive female chimpanzee we sampled had lower δ^{65}Cu values than other females, but we could not test if this was significant due to our sample size. For males, there was no observable difference in δ^{65}Cu values between captive and wild animals.

In bonobos (n = 3, see Figure 4.4.2), males had mean δ^{56}Fe and δ^{65}Cu values of -1.50 ± 0.38‰ and 0.61 ± 0.79‰, respectively. The one female had δ^{56}Fe and δ^{65}Cu values of -1.20‰ and 1.79‰, respectively. Overall, bonobos had lower δ^{56}Fe and higher δ^{65}Cu values relative to chimpanzees. We also observed that female bonobos had higher δ^{56}Fe and δ^{65}Cu values relative to males, however due to a small sample size, we were unable to test the statistical significance of these observations.

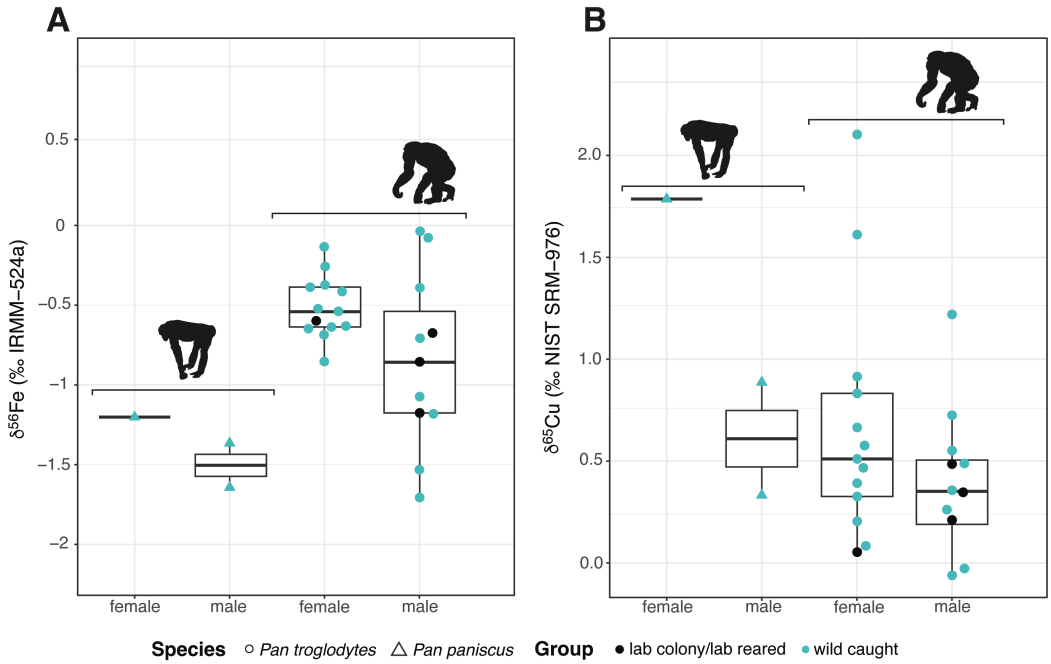

Figure 4.4.2. Boxplots depicting the median, upper, and lower quartiles between each sex (female, male) in chimpanzees (n = 24) and bonobos (n = 3) for (A) δ^{56}Fe values and (B) δ^{65}Cu values. Individuals of indeterminate sex (n = 2) and infants (n = 1) are not displayed here and were not included in statistical analyses.

4.5. Discussion

In this study, we present a refined method for analyzing Fe and Cu stable isotopes in bioapatite samples and explore if chimpanzees and bonobos can be used

as biologically meaningful analogs for hominin reproductive biology. On the first topic, we tested the existing protocol for bone and enamel presented in Jaouen et al. (2012). For the quantity of powdered bone sample needed to reliably measure Fe and Cu isotope compositions (~ 130 mg), we found that this protocol had premature elution of Cu and substantial breakthrough of Fe in the Zn fraction, suggesting that the 1.6 ml resin bed was overloaded (see Supporting Information 4.7.1. for details). Therefore, we adapted the protocol to better withstand larger sample quantities as well as to be more time and cost effective. We present a refined Fe and Cu isolation protocol that uses widely available Bio-Rad polypropylene columns, where the concentrated HCl volume was reduced by ~14% (from 0.85 liters to 0.73 liters), and the sample preparation time was reduced by ~37.5% (from 8 hours to 5 hours). This protocol has quantitative Cu and Fe recovery yields (> 98%) and elution curves (see Figure 4.7.1) that align well with previous methods, suggesting that its separation and collection of the targeted elements is at the high level needed for the isotopic analysis of the elements (Costas-Rodríguez et al., 2015; Lauwens et al., 2016; Maréchal et al., 1999; Sauzéat et al., 2021; Van Heghe et al., 2012).

With this method in hand, we turned to the following questions about Fe and Cu isotope variation in chimpanzees and bonobos. (1) Are there sex-related differences in δ^{56}Fe and δ^{65}Cu values in great apes? and (2) If there are sex-related isotope differences, does diet or female reproductive investment and/or estrous cycling contribute to these isotopic differences? We found little variation in δ^{56}Fe and

δ^{65}Cu values among geographic locations, suggesting that the patterns observed within our sample were unrelated to site of origin.

When examining sexually mature chimpanzees (i.e., those greater than ~ 10 years old), we found that the mean δ^{56}Fe and δ^{65}Cu values are higher in females relative to males (by 0.26‰ and 0.34‰, respectively). In the broader comparison that includes animals between 5 and 10 years old, we found the same pattern for both Fe and Cu isotopes, females had higher values than males (0.35‰ and 0.26‰, respectively). None of these comparisons met strict p-value cutoffs based on $\alpha = 0.05$ for statistical significance, yet when we consider the pattern of the broader comparison, δ^{56}Fe values were close to significance ($p = 0.07$) with a large effect size ($d = 0.83$), whereas δ^{65}Cu values were far from the threshold ($p = 0.3$). Given the relatively small sample sizes for each age class in the comparisons, we suspect the lack of significance for δ^{56}Fe values may be a Type II error, as the effect sizes for the statistical tests we performed were large. On the contrary, the pattern for the sex difference in δ^{65}Cu values diminishes when exploring a broader age class. Therefore, no substantial evidence suggests a sex difference in δ^{65}Cu values for chimpanzees. Our small sample of adult bonobos showed similar variations, with higher δ^{56}Fe and δ^{65}Cu values for females relative to males (by 0.30‰ and 1.2‰, respectively). This tentative sex difference in δ^{56}Fe values for chimpanzees and bonobos is consistent with that found in humans and rhesus macaques. The pattern in δ^{65}Cu values, however, is not; in fact, it is in the opposite direction than what has been reported previously (see Figure 4.2.1, Boucher et al., 2021; Jaouen & Balter, 2014; Jaouen et

al., 2012; Jaouen et al., 2017). In humans, there were significant differences for $\Delta^{56}Fe_{f\text{-}m}$ and $\Delta^{65}Cu_{f\text{-}m}$, where for humans as well as rhesus macaques, females had higher $\delta^{56}Fe$ values and lower $\delta^{65}Cu$ values.

Iron isotope differences between trophic positions

Chimpanzee males and females are known to differ in their dietary behavior in some regards and may also differ in their dietary requirements (see chapter 3). Mature male chimpanzees have been shown to eat more meat than females, which is known to have more bioavailable iron relative to plant foods (Tennie, Gilby and Mundry, 2009). Iron status, which is defined as amount of iron in iron stores e.g., blood serum ferritin or transferrin receptor saturation, has been shown to correlate with $\delta^{56}Fe$ values, where higher $\delta^{56}Fe$ values are related to lower iron status (Hotz et al., 2012). Chimpanzees have a primarily herbivorous diet, making it low in heme iron, which is more readily absorbed by the body than the non-heme iron in plant-foods (Vasconcelos & Grusak, 2006). Chimpanzees often supplement their diets with animal foods e.g., insect, primate and other small mammal meat, and geophagy of micronutrient rich soils or clay-infused water (Gerstner & Pruetz, 2022; Reynolds et al., 2019). In Budongo, Uganda, female chimpanzees have been shown to engage more in geophagy, specifically of iron-rich soils (Pebsworth et al., 2019).

Within food webs, $\delta^{56}Fe$ values decrease from plants, to herbivores, to carnivores. For $\delta^{56}Fe$ values, the isotope fractionation from plants to herbivores is -0.19‰ and from herbivores to carnivores is -0.51‰ (Jaouen et al., 2013). Given the

trophic fractionations reported here and using a simple linear mass balance model (see Supporting Information, Table 4.7.3), the lower mean δ^{56}Fe values observed in males would correspond to male diets that have 50 to 70% more meat than female diets. Male chimps consume slightly more animal products than females (5 to 10%, see Chapter 3), but this is far too little to explain such a sizeable δ^{56}Fe difference relative to females. A male diet with 10% more meat would only shift male δ^{56}Fe values by ~ -0.05‰ relative to females.

The potential impacts of geophagy are currently difficult to evaluate. If soils have higher δ^{56}Fe values than plants and Fe-deficient females engage in geophagy more than males, it could contribute to sex differences in Fe isotope values. Yet empirical studies at this point do not support these conjectures. Overall, we cannot explain the shared pattern of higher δ^{56}Fe values in female chimpanzees and bonobos with either a simple difference in trophic level related to sex differences in diet or a difference in the extent of geophagy between the sexes.

Iron isotope in light of the reproductive biology of *Pan*

Another possible mechanism relates to whether a species menstruates or reabsorbs their endometrial lining during the estrous cycle. Menstruating species, such as humans and rhesus macaques have bone δ^{56}Fe values that are higher (see Table 4.7.2). In mice, the opposite is observed, where bone δ^{56}Fe values are lower relative to males, suggesting high iron status and downregulated intestinal Fe absorption (Anoshkina et al., 2017; Hotz et al., 2012; Krayenbuehl et al., 2005). At the end of an estrous cycle, instead of menstruation, mice, along with most placental

mammals resorb their endometrial lining (Rudolph et al., 2012). Therefore, the lower δ^{56}Fe values in mice are consistent with the hypothesis that the sex difference is ascribed to greater Fe loss in females due to menstruation (Jaouen & Balter, 2014; Van Heghe et al., 2014; Van Heghe et al., 2012). Chimpanzees and bonobos appear to have no or minimal blood loss during menstruation. As noted above they do exhibit tumescence, but they resorb the blood within their estrous swellings after each cycle (Paoli et al., 2006; Rowell, 1963; Ryu et al., 2014). There is little reason to believe that there is Fe isotope fractionation during this process, and it is likely a closed system. Yet, despite minimal blood loss female chimpanzees and bonobos have higher δ^{56}Fe values than males, which is consistent with menstruating species (see Table 4.7.2).

While the topic has received minimal attention in the Fe literature, another way that all mammals, including chimpanzees and bonobos, lose Fe is by gestating, giving birth to, and nursing their young. We believe this is an important consideration when understanding sex-related differences in Fe fractionation. For females, the Fe losses that occur while growing their offspring, as well as the blood and placenta loss associated with birth, are high and the likelihood of anemia is much higher when gestating, where human females require ~1.0-7.5 mg Fe/day (Miller, 2016). The mean concentration (mg/L) of Fe in human breast milk has been found to be between 0.3-0.5 mg/L (Dorea, 2000), and thus is another substantial source of Fe loss.

In populations of wild chimpanzees, females have their first birth by 15 years old, and average ~ 6 offspring by the end of their lives at 45 to 50 years old (Atsalis

& Videan, 2009). In captive chimpanzees, females have first births much earlier, at around 10-11 years old, averaging around 7-8 offspring over their lifetime (Atsalis & Videan, 2009). Chimpanzees nurse their offspring for around 4 to 5 years, meaning that most of a female chimpanzees' life is spent either pregnant or nursing offspring, though the Fe concentration of chimpanzee breast milk is not yet known (Bădescu et al., 2017; Fahy et al., 2014; Power et al., 2015; Samuni, Tkaczynski, et al., 2020; Smith et al., 2010). Thus, Fe loss via reproductive investments (gestation, parturition, and nursing) might outweigh that from menstruation and be a principal driver of higher δ^{56}Fe values in females relative to male chimpanzees and bonobos and perhaps contribute to sex differences in Fe isotope values in other species too.

To explore this possibility, we compared captive and wild chimpanzees, as captive chimpanzees may have a higher reproductive investment, though the reproductive history of individuals in our study is unknown (Atsalis & Videan, 2009). We analyzed a small sample of captive chimpanzees (see Figure 4.4.2, n = 4) and did not observe a difference between wild vs. captive chimpanzees in δ^{56}Fe values for either sex. In order to more conclusively explore the effects of reproductive investment on Fe isotopes in chimpanzees, we would need to know the number of offspring and weaning age of offspring, as well as the Fe concentrations and δ^{56}Fe values in breast milk and the placenta/umbilical cord, all of which could be obtained for animals in captivity.

Cu isotope differences and the uncertainty of its source

The sex difference in δ^{65}Cu values is unlike that reported for reproductive age humans and rhesus macaques, where females have lower δ^{65}Cu values relative to males (Boucher et al., 2021; Jaouen & Balter, 2014; Jaouen et al., 2012; Jaouen et al., 2017). Specifically, the trend in δ^{65}Cu values for chimpanzees and bonobos most aligns with that of mice, where females have higher δ^{65}Cu values (Moynier et al., 2019; Moynier et al., 2022). In other species, Cu isotopes have been shown to vary based on diet, environmental context, and disease, which lead to higher variance in δ^{65}Cu values (see Figure 4.2.1; Jaouen et al., 2017). While we didn't find statistically significant δ^{65}Cu variation by place of origin, this might be due to the higher population level of Cu isotope variability. As noted above, the average turnover time for body Cu is approximately 2 months, so our sample of chimpanzees and bonobos may show greater individual volatility in Cu stores, resulting in high variance that obscures the detection of patterns related to location, diet or sex.

Within food webs, δ^{65}Cu values decrease from plants to herbivores and increase from herbivores to carnivores. The Cu isotope fractionation from plants to herbivores is -0.29‰ and from herbivores to carnivores is +1.16‰, with the range varying by geographic location (Jaouen et al., 2013). In humans, vegetarian females have lower δ^{65}Cu values than males (Van Heghe et al., 2012). Additionally, δ^{65}Cu values have been shown to be lower in body tissues affected by diseases (Costas-Rodríguez et al., 2016). While we cannot verify if any sampled individuals suffered from disease, we can explore if diet or environmental context affects the pattern observed for chimpanzees and bonobos.

As mentioned above, chimpanzees are primarily herbivorous, and Cu has been suggested to be more bioavailable in plant foods, with higher Cu absorption observed in primarily vegetarian diets relative to non-vegetarian diets (Hunt, 2003; Van Heghe et al., 2012). Since δ^{65}Cu values decrease from plants to herbivores, and increase from herbivores to carnivores, we explore the possibility of a diet effect. A recent study showed that mice fed a chimpanzee diet (fruits and vegetables) experienced upregulation of the gene controlling CP, leading to a reduction in the Fe-mediated oxidative stress associated with cognitive decline in non-human primates and humans (Kumar et al., 2023). Therefore, the pattern that we observe in chimpanzees could be related to the upregulation of CP, which is the dominant enzyme partitioning Cu in blood and reduces the free iron in the body. When CP is upregulated, it causes higher δ^{65}Cu values in blood, as ^{63}Cu is bound to the sulfur atoms of cysteine (Albarède, 2015; Selden et al., 2024). The upregulation of CP could affect body Cu status, which might affect the isotope values. This could explain why higher δ^{65}Cu values are observed for female chimpanzees and bonobos, but the mass balance of Cu in relation to Cu status and loss is less understood.

Another possible mechanism could be related to estrous cycling and reproductive investment, as for Fe isotopes. However, further studies are needed to explore Cu loss and fractionation due to menstruation, as shown for Fe (Jaouen & Balter, 2014; Van Heghe et al., 2013). The higher reproductive investment by females into their offspring could also be an important mechanism controlling Cu fractionation. Cu transport has been shown to increase during gestation and lactation,

where there is considerable transfer of Cu via CP to the fetus through the placenta and into breast milk through the mammary gland, which then has been shown to decrease during repeated treatment with estrogen (Costas-Rodríguez et al., 2019; Tapiero et al., 2003).Therefore, we suggest that future studies consider the reproductive investment of females that are sampled, and how this could contribute to additional Cu losses.

4.6. Conclusion

Overall, we demonstrate that δ^{56}Fe and δ^{65}Cu values can be reliably measured in the bone of chimpanzees and bonobos, opening the possibility of using great apes as models for hominins with minimal menstruation. In great apes, females have higher δ^{56}Fe values relative to males, though this isotopic difference was not significant, likely due to sample size limitations. While females were found to have higher δ^{65}Cu values relative to males as well, it is unclear what factors are contributing to this pattern. These patterns were not related to geographic origin or age class. We propose that two factors could be controlling sex-related differences in δ^{56}Fe values, (1) iron status and the upregulation/downregulation of iron, and (2) iron losses, which are related to species-specific differences in estrous cycling and reproductive investment, however additional studies are needed to parse this out, as well as explore what factors could be contributing to sex-related differences in δ^{65}Cu values for other species. At this time, what contributes to Cu status and loss in relation to estrous cycling and reproductive investment is not well understood. Overall, we suggest that chimpanzees and bonobos provide crucial insights into

understanding the evolutionary benefit of menstruation and menopause. We encourage future studies to consider the reproductive investment as well as the hormonal contraceptive use when analyzing sex-related differences in modern populations of humans and primates, as both will increase and decrease Fe and Cu status, potentially minimizing any observable differences in sex.

4.7. Supplementary Information

Supporting Information 4.7

Refining the Fe and Cu isolation protocol for bone

Bioapatite (a form of carbonate hydroxyapatite) is a calcium (Ca) and phosphate (PO_4)-rich material, with cationic substitutions including magnesium (Mg), and sodium (Na) that, along with Ca, introduce polyatomic interferences when analyzing Fe and Cu stable isotopes. Additionally, reference materials containing high amounts of Fe and phosphorus (P) have been shown to cause premature elution of Cu during isolation protocols, because there is competition between Fe and Cu for the chloride ions within the resin bed due to the occupation of resin sites by negatively charged phosphate (PO_4) species (Chapman et al., 2006). Therefore, using the same acid for the matrix and Cu elution in phosphate-rich materials can result in premature elution of Cu, and thus, there is not complete matrix separation nor the full recovery of Cu. Since the resin passage is known to fractionate Cu isotopes much more (~ 19%) between the first and last ml of Cu elution than observed in environmental samples, premature Cu elution and the incomplete collection of the entire Cu fraction

can result in an isotopically lighter sample (Blotevogel, 2017; Maréchal & Albarède, 2002; Maréchal et al., 1999). Therefore, the recovery target for Cu must be quantitative (95-100%). Typically, when working with phosphate-rich samples, the material is reduced to ash in a muffle furnace before being treating with hydrogen peroxide (H_2O_2), as a means of reducing the organic matter and preventing the resin from being overloaded (Boucher et al., 2021; Tas, 2000). However, combustion > 600°C can potentially fractionate Zn isotopes, so it is important to adapt the existing protocols to isolate Fe, Cu and Zn from bioapatite without pre-treatment via combustion (Toutain et al., 2008). In the present study, the digestion protocol was adapted to minimize non-endogenous isotope fractionation. Rather than reducing bone samples to ash, we treated each sample with 1ml of ultrapure 30% H_2O_2 at room temperature for 2 hours before adding 1ml of bidistilled 15.9N HNO_3 in a sealed beaker at 120°C for 1 hour. Then, the samples were evaporated to dryness at 110°C and re-dissolved in 1 ml of 7N HCl + 0.001% H_2O_2. Each sample then underwent the same column chromatography protocol a second time to effectively remove Ca, Mg, Na, and PO_4.

In the original Fe and Cu isolation protocol, quartz columns were found to be the most effective, however, they are expensive and easily broken/worn, therefore, we used the more cost-effective and accessible Bio-Rad polypropylene chromatography columns for this protocol. These columns can easily be acid-washed and rinsed with MQ H_2O to remove contamination and other trace metals. Additionally, we use much lower normality of acids to elute the elements of interest, which makes this protocol

faster, averaging ~ 4 to 5 hours rather than 7 to 9 hours. In order to ensure that the Fe and Cu yields were sufficient (> 98%) for the matrix of our samples, several experiments were performed using protocols that are currently available (Blotevogel et al., 2018; Boucher et al., 2021; Jaouen, 2012; Maréchal et al., 1999; Sauzéat et al., 2021; Van Heghe et al., 2012) and adapted to bioapatite. Since Fe and Cu are at trace levels in bone and teeth, a larger quantity of sample (> 100 mg) is needed to have 300 ppb of Cu and 50 ppb of Fe for successful measurements via Multiple Collector Inductively Coupled Plasma Mass Spectrometry (MC-ICP-MS).

We designed an experiment to ensure that the larger quantity of sample did not overload the resin bed, and then this protocol was optimized to have the steepest elution curves for each element (which correlates to % recovery). In this experiment, we isolated Fe, Cu and Zn from varying quantities of NIST SRM-1400 bone ash standard (80 mg, 100 mg, and 130 mg) with the respective resin beds of 1.6 ml, 2 ml and 2 ml (AG® MP-1, 100–200 μm dry mesh size). For the 80 mg sample, the protocol described in Maréchal et al. was used, adapted by Jaouen, where for blood and bone samples, 25 ml of 7N HCl + 0.001% H_2O_2 is used to elute Cu, 12 ml of 2N HCl + 0.001% H_2O_2 is used to elute Fe, and 12 ml of 0.5N HNO_3 is used to elute Zn (Jaouen, 2012; Maréchal et al., 1999). For the initial test, we increased the acid volume for each elution step, using 32 ml for Cu, 18 ml for Fe, and 14 ml for Zn. For the 130 mg bone ash standard, we used 4N HCl to elute Cu, rather than 7N HCl + 0.001% H_2O_2, as Cu is known to dissociate more effectively at lower concentrations of HCl (Blotevogel, 2017). A blank was analyzed alongside each sample and were all

found to be < 1 ppb for the elements of interest (^{56}Fe, ^{57}Fe, ^{63}Cu, ^{66}Zn) as well as the elements that introduce polyatomic or isobaric interferences (^{24}Mg, ^{27}Al, ^{31}P, ^{33}S, ^{43}Ca, ^{44}Ca, ^{47}Ti, ^{52}Cr, ^{55}Mn, ^{60}Ni, ^{88}Sr) on a Thermo Element XR high-resolution ICP-MS. For the 80 mg sample with 1.6 ml of resin, there was premature elution of Cu, and a bleedthrough found between Fe and Zn, which was suggestive of the resin being overloaded. Further, the yield was insufficient for Fe and Cu, ~66% and 74%, respectively, although the yield for Zn was ~97%. For the 100 mg sample with 2 ml resin bed, the yields were ~ 73% for Fe, ~84% for Cu, and ~93% for Zn. For the 130 mg with 2ml resin bed where Cu was eluted with 4N HCl, the yields were ~78% for Fe, ~100% for Cu, and ~100% for Zn, therefore we continued with this configuration.

When optimizing the isolation protocol, three iterations were performed, in order to ensure the complete recovery of the Fe and Cu. In the first iteration, a 133.4 mg sample of bone ash underwent digestion, then 9 ml of 7N HCl + 0.001% H_2O_2 for matrix elution, 16 ml of 4N HCl + 0.001% H_2O_2 for Cu elution, 18 ml of 0.7N HCl for Fe elution (as Fe is shown to dissociate more successfully at lower HCl concentrations), and 8 ml of 0.5N HNO_3 for Zn elution (Tremillon, 1967). We collected each 2 ml fraction to generate an elution curve and estimate the element recovery. Due to an instrumentation issue, the analysis of the samples for this iteration were inaccurate, therefore, we could not reliably estimate the yields.

Therefore, in the next iteration, we used 16 ml of 4N HCl + 0.001% H_2O_2 for Cu elution, 20 ml of 0.7N HCl for Fe elution, and 12 ml of 0.5N HNO_3 for Zn elution, with a 2 ml pre-conditioning step. The yields were 98% for Fe, 98.5% for Cu,

and 100% for Zn, where most of the Zn was found to elute in the first 6 ml. In the final method, in order to ensure the remaining ~2% of Cu and Fe was captured, we increased the elution volume for Cu to 20 ml and for Fe to 22 ml and reduced the elution volume for Zn to 10 ml (removing the pre-conditioning step). With this protocol, the yields were 100% for Cu, Fe, and Zn, suggesting that all elements of interest were successfully recovered. However, we found over the course of these iterations that the addition of a pre-conditioning step for Zn (2 ml 0.5N HNO_3), followed by an additional 7 ml yield more Zn than without this step.

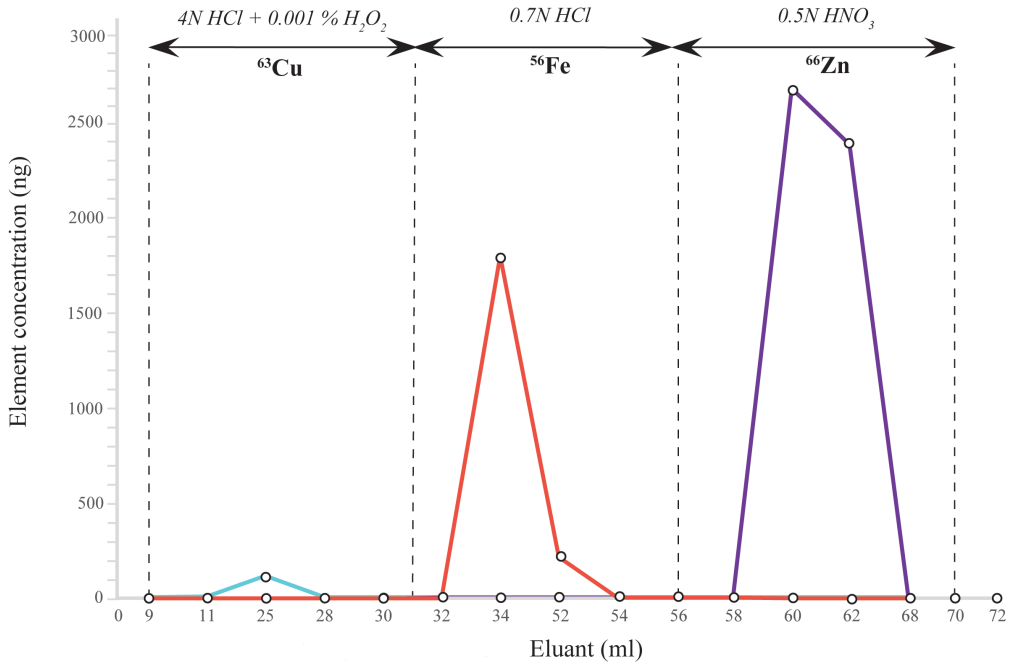

Figure 4.7.1. Elution curve for the isolation protocol of Fe and Cu, adapted for bioapatite. Elution curves of the NIST SRM-1400 bone ash standard (130 mg with 103 ng/g Cu, 2,520 ng/g Fe, and 3,575 ng/g Zn) on 2 ml of AG MP-1 resin. The concentrations were determined on the ThermoFisher Element XR High Resolution ICP-MS. Mean recovery are 98% for Cu, 102% for Fe, and 83% for Zn.

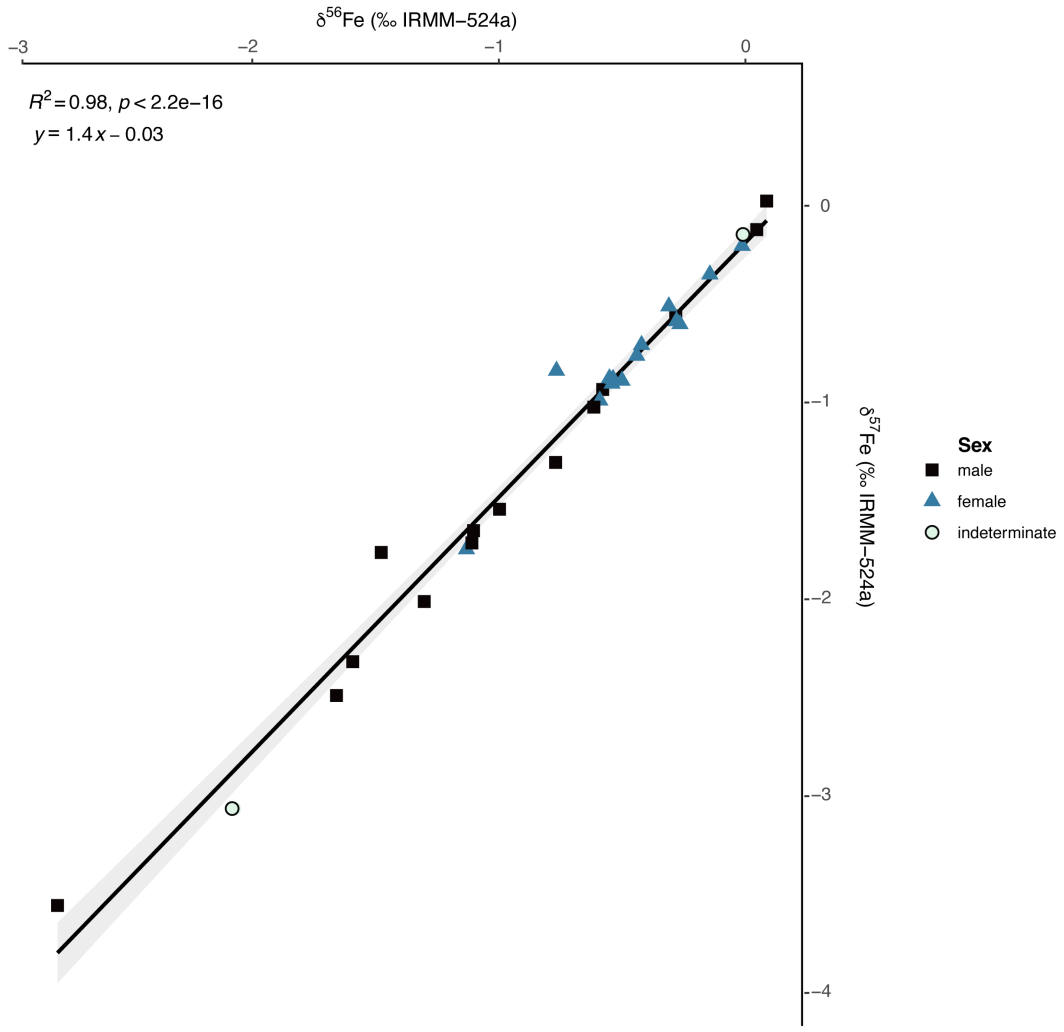

Figure 4.7.2. Fractionation line between isotopes, $\delta^{57}Fe$ vs. $\delta^{56}Fe$ (y = 1.4x - 0.03 , R^2 = 0.98) for samples.
All the samples fall on the theoretical mass-dependent fractionation lines.

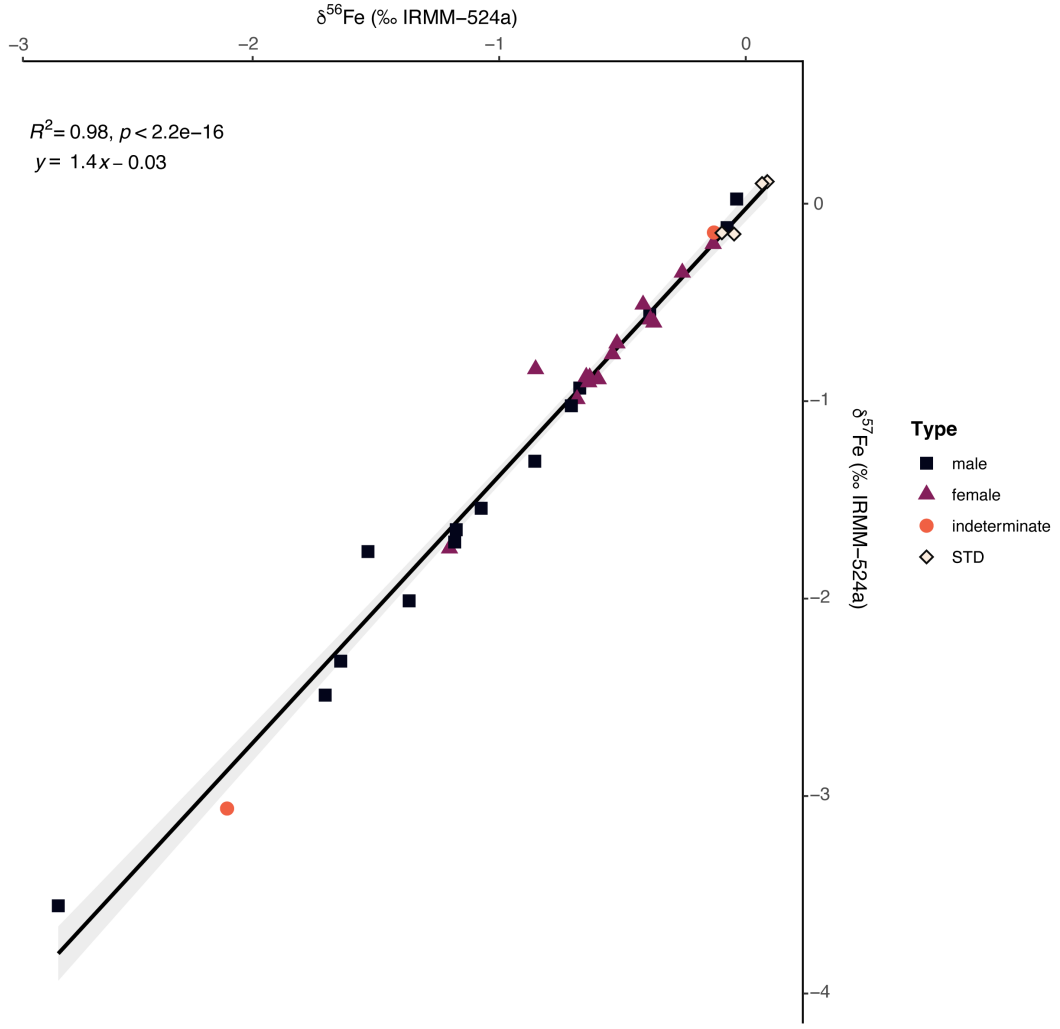

Figure 4.7.3. Fractionation line between isotopes, $\delta^{57}Fe$ vs. $\delta^{56}Fe$ (y = 1.4x - 0.03, R^2 = 0.98) for samples and standards.
All the samples and standards fall on the theoretical mass-dependent fractionation lines.

Table 4.7.1. Summary of all chimpanzees (*Pan troglodytes*, Sample ID No. 2401-2410 and 2414-2430) and bonobo samples (*Pan paniscus*, Sample ID No. 2411-2413) in this study (n = 30). Corrected $\delta^{56}Fe$, $\delta^{57}Fe$, and $\delta^{65}Cu$ values (in ‰) are included to 2 standard deviations (2σ) estimated from two replicate analyses, as well as Fe and Cu concentrations (in ppm). Samples where DNA analysis was performed are indicated (†). Note that the table contains information on two individuals that ultimately could not be sexed and one infant (*). These data are included here for completeness but were not used in any figures or statistical analyses.

ID	Origin Locality	Age Class	sex	$\delta^{56}Fe$	2σ	$\delta^{57}Fe$	[Fe] ppm	$\delta^{65}Cu$	2σ	[Cu] ppm
2415	Sakbayeme, Cameroon	ad	F	-0.54	0.1	-0.76	6.57	0.84	0.45	0.41
2417	Cameroon	ad	F	-0.64	0.15	-0.9	14.54	0.47	0.03	4.07

2418	Sakbayeme, Cameroon	ad	F†	-0.13	0.22	-0.2	15.68	1.62	0.16	0.28
2419	Sakbayeme, Cameroon	ad	F	-0.26	0.05	-0.35	28.55	0.67	0.02	4.7
2429	Lolodorf, Cameroon	ad	F†	-0.65	0.18	-0.88	6.81	0.92	0.11	12.24
2405	West Africa	adol	F	-0.52	0.19	-0.71	10.65	0.4	0.06	1.09
2410	Metet, Cameroon	subad	F	-0.85	0.19	-0.84	2404.44	0.52	0.01	0.96
2414	Efulan, Cameroon	subad	F†	-0.42	0.36	-0.51	21.42	0.33	0.23	0.47
2416	Efulan, Cameroon	subad	F†	-0.68	0.07	-0.99	18.77	0.58	0.18	1.35
2420	Sakbayeme, Cameroon	subad	F	-0.63	0.5	-0.88	19.48	0.21	0.06	3.26
2424	Sakbayeme, Cameroon	subad	F	-0.39	0.28	-0.59	12.96	0.09		0.18
2425	Sakbayeme, Sanaga Cameroon	subad	F	-0.37	0.53	-0.6	32.94	2.11	0.04	0.28
2403	West Africa	ad	M†	-0.39	0.27	-0.56	12.15	0.26	0.02	0.29
2421	Sakbayeme, Cameroon	ad	M	-0.71	0.01	-1.02	7.34	-0.06	0.00	1.57
2422	Sakbayeme, Cameroon	ad	M	-0.04	0.04	0.02	3.99	0.49	0.17	0.52
2423	Sakbayeme, Cameroon	ad	M	-1.53	0.05	-1.76	8.04	0.36	0.02	3.46
2426	Sakbayeme, Cameroon	ad	M	-0.08	0.3	-0.12	18.64	0.55		0.15
2427	Metet, Cameroon	ad	M†	-1.18	0.15	-1.71	14	0.73	0.2	0.29
2409	unknown	subad	M†	-1.07	0.08	-1.54	43.19	1.22	0.03	11.18
2402	unknown	subad	M†	-1.71	0.35	-2.49	16.04	-0.03	0.02	9.22
2408	lab colony	ad	F	-0.6	0.16	-0.89	47.36	0.06		0.11
2401	lab colony	ad	M	-0.86	0.45	-1.3	21.43	0.49		0.23
2406	lab colony	ad	M	-0.67	0.24	-0.93	12.83	0.21		0.24
2407	lab colony	ad	M	-1.17	0.18	-1.65	7.06	0.35		0.11
2412	Stanleyville, DRC	ad	F	-1.2	0.01	-1.75	10.65	1.79	0.38	0.19
2411	Stanleyville, DRC	ad	M	-1.37	0.07	-2.01	16.87	0.89	0.12	0.22
2413	Stanleyville, DRC	ad	M	-1.64	0.02	-2.32	2.33	0.33		0.17
2404	Ethiopia	inf*	M	-2.79	0.28	-3.56	73.76	0.13	0.16	3.85
2428	Lolodorf, Cameroon	adol*	? †	-0.13	0.14	-0.15	36.98	0.08	0.03	4.01
2430	unknown	adol*	? †	-2.1	0.04	-3.06	27.52	0.46	0.02	85.21

Table 4.7.2. Summary of published $\delta^{56}Fe$ and $\delta^{65}Cu$ values (in ‰).
Each letter corresponds to Figure 4.2.1, with references included below. Reference letters A to I have overt menstruation and reference letters J to L resorb their endometrial lining. In reproductive-age humans, there are significant differences for $\Delta^{56}Fe_{f\text{-}m}$ ($V = 133$, $p < 0.001$) and $\Delta^{65}Cu_{f\text{-}m}$ ($t(21) = -3.31$, $p = 0.003$).

				Mean				**Mean**						
				female				*male*						
Ref	**species**	**tissue**	**status**	**$\delta^{56}Fe$**	**2σ**	**$\delta^{65}Cu$**	**2σ**	**$\delta^{56}Fe$**	**2σ**	**$\delta^{65}Cu$**	**2σ**	**diet**	**$\Delta^{56}Fe_{f\text{-}m}$**	**$\Delta^{65}Cu_{f\text{-}m}$**
A (F. Albarede et al., 2011)	human	blood	reproductive	-2.58	0.18	0.01	0.16	-2.72	0.4	0.17	0.33	not specified	0.14	-0.16
B (K. Jaouen et al., 2013)	human	blood	reproductive	-2.65	0.33	-0.52	0.22	-2.63	0.44	-0.74	0.30	not specified	-0.02	0.22
B (K. Jaouen et al., 2013)	human	blood	post-reproductive	-2.60	0.48	-0.84	0.34	-	-	-	-	not specified	0.03	-0.10
C (Jaouen & Balter, 2014)	human	blood	post-reproductive	-2.59	0.42	0.71	0.54	-2.65	0.54	0.68	0.49	not specified	0.06	0.03
C (Jaouen & Balter, 2014)	human	blood	reproductive	-2.49	0.39	0.43	0.48	-2.72	0.36	0.67	0.36	not specified	0.23	-0.24
D (Van Heghe et al., 2013)	human	blood	reproductive	-2.62	0.37	-	-	-2.85	0.36	-	-	not specified	0.23	
E (Van Heghe et al., 2012)	human	blood	reproductive	-2.47	0.35	-0.51	0.46	-2.87	0.43	-0.07	0.52	vegetarian	0.40	-0.44
E (Van Heghe et al., 2012)	human	blood	reproductive	-2.65	0.22	-0.02	0.34	-2.99	0.48	-0.04	0.41	omnivore	0.34	0.02
F (Van Heghe et al., 2014)	human	blood	reproductive	-2.60	-	-0.25	-	-3.00	-	0.15	-	not specified	0.40	-0.40
F (Van Heghe et al., 2014)	human	blood	post-reproductive	-3.00	-	0.25	-	-	-	-	-	not specified	0.00	0.10
A (F. Albarede et al., 2011)	human	RBC	reproductive	-2.49	0.39	0.46	0.47	-2.72	0.36	0.67	0.36	not specified	0.23	-0.21
G (Jaouen et al., 2012)	human	bone	reproductive	-0.12	0.65	-0.20	0.25	-0.45	0.85	-0.11	0.16	omnivore, no fish	0.33	-0.09
H (Jaouen et al., 2017)	human	enamel	reproductive	-	-	0.26	0.2	-	-	0.27	0.23	omnivore, no fish		-0.01
H (Jaouen et al., 2017)	human	bone	reproductive	-	-	0.01	0.27	-	-	0.40	0.48	intermediate/omnivore		-0.39
H (Jaouen et al., 2017)	human	enamel	reproductive	-	-	0.12	0.27	-	-	0.29	0.33	intermediate/omnivore		-0.17

H (Jaouen et al., 2017)	human	enamel	reproductive	-	-	0.09	0.26	-	-	0.03	0.26	omnivore		0.06
I (Boucher et al., 2021)	rhesus macaque	bone	reproductive	-1.22	0.24	-2.44	0.09	-1.61	0.24	-1.04	0.09	omnivore	0.39	-1.40
I (Boucher et al., 2021)	rhesus macaque	tooth	reproductive	-0.92	0.24	-3.76	0.09	-1.21	0.24	-3.66	0.09	omnivore	0.29	-0.10
J (Balter et al., 2013)	mice	bone	reproductive	-0.93	0.28	0.06	-	-0.69	0.27	0.29	-	omnivore	-0.25	-0.23
J (Balter et al., 2013)	mice	blood	reproductive	-2.55	0.15	0.05	0.25	-2.49	0.12	-0.08	0.16	omnivore	-0.06	0.13
K (Moynier et al., 2022)	mice	RBC	reproductive	-	-	0.52	0.34	-	-	0.27	0.08	omnivore		0.25
L (Balter et al., 2013)	sheep	bone	reproductive	-1.30	0.21	0.25	0.07	-1.16	0.27	-0.01	0.13	herbivore	-0.14	0.25
L (Balter et al., 2013)	sheep	RBC	reproductive	-2.02	1.03	-0.56	0.13	-2.05	0.48	-0.66	0.45	herbivore	0.04	0.11

Table 4.7.3. The estimated mean $\delta^{56}Fe$ values for chimpanzees based on a linear mass-balance model (Faure, 2005).
We use the reported isotope fractionation between trophic level to extrapolate difference between males and females based on proportion of meat (%) in diet (Jaouen et al., 2013).

Diet type	$\Delta^{56}Fe$ (‰)	proportion of meat (%)	Mean $\delta^{56}Fe$(‰)
Plant	0	100%	-0.20
Herbivore	-0.2	100%	-0.20
Carnivore	-0.5	100%	-0.70
Male chimpanzee, omnivore	-0.25	55%	-0.45
Male chimpanzee, omnivore	-0.35	75%	-0.55
Female chimpanzee, herbivore	0	0%	-0.20
Male chimpanzee, omnivore	-0.05	10%	-0.25

4.8. References Cited

Adiguzel, D., & Celik-Ozenci, C. (2021). FoxO1 is a cell-specific core transcription factor for endometrial remodeling and homeostasis during menstrual cycle and early pregnancy. *Human Reproduction Update*, *27*(3), 570-583. https://doi.org/10.1093/humupd/dmaa060

Albarède, F. (2015). Metal Stable Isotopes in the Human Body: A Tribute of Geochemistry to Medicine. *Elements*, *11*(4), 265-269. https://doi.org/10.2113/gselements.11.4.265

Albarède, F., Télouk, P., & Balter, V. (2017). Medical Applications of Isotope Metallomics. *Reviews in Mineralogy and Geochemistry*, *82*(1), 851-885. https://doi.org/10.2138/rmg.2017.82.20

Albarede, F., Telouk, P., Blichert-Toft, J., Boyet, M., Agranier, A., & Nelson, B. (2004). Precise and accurate isotopic measurements using multiple-collector ICPMS [Article]. *Geochimica et Cosmochimica Acta*, *68*(12), 2725-2744. https://doi.org/10.1016/j.gca.2003.11.024

Albarede, F., Telouk, P., Lamboux, A., Jaouen, K., & Balter, V. (2011). Isotopic evidence of unaccounted for Fe and Cu erythropoietic pathways. *Metallomics*, *3*(9), 926-933.

Albarede, F., Telouk, P., Lamboux, A., Jaouen, K., & Balter, V. (2011). Isotopic evidence of unaccounted for Fe and Cu erythropoietic pathways. *Metallomics*, *3*(9), 926-933. https://doi.org/10.1039/c1mt00025j

Almécija, S., Hammond, A. S., Thompson, N. E., Pugh, K. D., Moyà-Solà, S., & Alba, D. M. (2021). Fossil apes and human evolution. *Science*, *372*(6542), eabb4363. https://doi.org/doi:10.1126/science.abb4363

Anoshkina, Y., Costas-Rodríguez, M., Speeckaert, M., Van Biesen, W., Delanghe, J., & Vanhaecke, F. (2017). Iron isotopic composition of blood serum in anemia of chronic kidney disease. *Metallomics*, *9*(5), 517-524.

Arredondo, M., & Núñez, M. T. (2005). Iron and copper metabolism. *Molecular Aspects of Medicine*, *26*(4-5), 313-327.

Atsalis, S., & Videan, E. (2009). Reproductive aging in captive and wild common chimpanzees: factors influencing the rate of follicular depletion. *American journal of primatology*, *71*(4), 271-282. https://doi.org/https://doi.org/10.1002/ajp.20650

Bădescu, I., Katzenberg, M. A., Watts, D. P., & Sellen, D. W. (2017). A novel fecal stable isotope approach to determine the timing of age-related feeding transitions in wild infant chimpanzees. *American journal of physical anthropology*, *162*(2), 285-299.

Balolia, K. L. (2015). The timing of spheno-occipital fusion in hominoids. *American journal of physical anthropology*, *156*(1), 135-140. https://doi.org/https://doi.org/10.1002/ajpa.22633

Balter, V., Lamboux, A., Zazzo, A., Telouk, P., Leverrier, Y., Marvel, J., Moloney, A. P., Monahan, F. J., Schmidt, O., & Albarede, F. (2013). Contrasting Cu, Fe, and Zn isotopic patterns in organs and body fluids of mice and sheep, with emphasis on cellular fractionation. *Metallomics*, *5*(11), 1470-1482. https://doi.org/10.1039/c3mt00151b

Blotevogel, S. (2017). *Study of elemental transfers and biogeochemical mechanisms in the soil-plant-wine continuum using isotopic and biochemical tracers* Université Paul Sabatier-Toulouse III].

Blotevogel, S., Oliva, P., Sobanska, S., Viers, J., Vezin, H., Audry, S., Prunier, J., Darrozes, J., Orgogozo, L., Courjault-Radé, P., & Schreck, E. (2018). The fate of Cu pesticides in vineyard soils: A case study using δ65Cu isotope ratios and EPR analysis. *Chemical Geology*, *477*, 35-46. https://doi.org/https://doi.org/10.1016/j.chemgeo.2017.11.032

Boesch, C., Kohou, G., Néné, H., & Vigilant, L. (2006). Male competition and paternity in wild chimpanzees of the Taï forest. *American Journal of Physical Anthropology: The Official Publication of the American Association of Physical Anthropologists*, *130*(1), 103-115.

Boessenkool, S., Hanghøj, K., Nistelberger, H. M., Der Sarkissian, C., Gondek, A. T., Orlando, L., Barrett, J. H., & Star, B. (2017). Combining bleach and mild predigestion improves ancient DNA recovery from bones. *Molecular Ecology Resources*, *17*(4), 742-751.

Bolter, D. R., & Zihlman, A. L. (2012). Skeletal development in Pan paniscus with comparisons to Pan troglodytes. *American journal of physical anthropology*, *147*(4), 629-636. https://doi.org/https://doi.org/10.1002/ajpa.22025

Boucher, R. D., Alavi, S. E., de Jong, H. N., Godfrey, L. V., & Vogel, E. R. (2021). Stable isotope evidence (Fe, Cu) suggests that sex, but not aging is recorded in rhesus macaque (Macaca mulatta) bone. *American journal of physical anthropology*.

Brimacombe, C. S., Kuykendall, K. L., & Nystrom, P. (2015). Epiphyseal fusion in Pan troglodytes relative to dental age. *American journal of physical anthropology*, *157*(1), 19-29. https://doi.org/https://doi.org/10.1002/ajpa.22684

Brimacombe, C. S., Kuykendall, K. L., & Nystrom, P. (2018). Epiphyseal fusion and dental development in Pan paniscus with comparisons with Pan troglodytes. *American journal of physical anthropology*, *167*(4), 903-913. https://doi.org/https://doi.org/10.1002/ajpa.23710

Catalini, L., & Fedder, J. (2020). Characteristics of the endometrium in menstruating species: lessons learned from the animal kingdom†. *Biology of Reproduction*, *102*(6), 1160-1169. https://doi.org/10.1093/biolre/ioaa029

Chamel, G., Gourlan, A. T., Télouk, P., Sayag, D., Milliard, V., Loiseau, C., Simon, M., Buff, S., & Ponce, F. (2017). Retrospective evaluation of blood copper stable isotopes ratio 65Cu/63Cu as a biomarker of cancer in dogs. *Veterinary and Comparative Oncology*, *15*(4), 1323-1332.

Chapman, J. B., Mason, T. F., Weiss, D. J., Coles, B. J., & Wilkinson, J. J. (2006). Chemical separation and isotopic variations of Cu and Zn from five geological reference materials. *Geostandards and Geoanalytical Research*, *30*(1), 5-16.

Cohen, J. (2013). *Statistical power analysis for the behavioral sciences*. Routledge.

Collins, M. J., Riley, M. S., Child, A. M., & Turner-Walker, G. (1995). A basic mathematical simulation of the chemical degradation of ancient collagen. *Journal of Archaeological Science*, *22*(2), 175-183.

Costas-Rodríguez, M., Anoshkina, Y., Lauwens, S., Van Vlierberghe, H., Delanghe, J., & Vanhaecke, F. (2015). Isotopic analysis of Cu in blood serum by multi-collector ICP-mass spectrometry: a new approach for the diagnosis and prognosis of liver cirrhosis? *Metallomics*, *7*(3), 491-498.

Costas-Rodríguez, M., Delanghe, J., & Vanhaecke, F. (2016). High-precision isotopic analysis of essential mineral elements in biomedicine: natural isotope ratio variations as potential diagnostic and/or prognostic markers. *TrAC Trends in Analytical Chemistry*, *76*, 182-193. https://doi.org/10.1016/j.trac.2015.10.008

Costas-Rodríguez, M., Van Campenhout, S., Hastuti, A. A., Devisscher, L., Van Vlierberghe, H., & Vanhaecke, F. (2019). Body distribution of stable copper isotopes during the progression of cholestatic liver disease induced by common bile duct ligation in mice. *Metallomics*, *11*(6), 1093-1103.

Dabney, J., Knapp, M., Glocke, I., Gansauge, M.-T., Weihmann, A., Nickel, B., Valdiosera, C., García, N., Pääbo, S., & Arsuaga, J.-L. (2013). Complete mitochondrial genome sequence of a Middle Pleistocene cave bear reconstructed from ultrashort DNA fragments. *Proceedings of the National Academy of Sciences*, *110*(39), 15758-15763.

de Flamingh, A., Coutu, A., Roca, A. L., & Malhi, R. S. (2020). Accurate sex identification of ancient elephant and other animal remains using low-coverage DNA shotgun sequencing data. *G3: Genes, Genomes, Genetics*, *10*(4), 1427-1432.

Deschner, T., & Boesch, C. (2007). Can the patterns of sexual swelling cycles in female Taï chimpanzees be explained by the cost-of-sexual-attraction hypothesis? *International Journal of Primatology*, *28*(2), 389-406.

Deschner, T., Heistermann, M., Hodges, K., & Boesch, C. (2004). Female sexual swelling size, timing of ovulation, and male behavior in wild West African chimpanzees. *Hormones and behavior*, *46*(2), 204-215.

Dorea, J. G. (2000). Iron and copper in human milk. *Nutrition*, *16*(3), 209-220. https://doi.org/https://doi.org/10.1016/S0899-9007(99)00287-7

Douglas, P. H., Hohmann, G., Murtagh, R., Thiessen-Bock, R., & Deschner, T. (2016). Mixed messages: wild female bonobos show high variability in the timing of ovulation in relation to sexual swelling patterns. *BMC Evolutionary Biology*, *16*(1), 140. https://doi.org/10.1186/s12862-016-0691-3

Emera, D., Romero, R., & Wagner, G. (2012). The evolution of menstruation: a new model for genetic assimilation: explaining molecular origins of maternal responses to fetal invasiveness. *BioEssays*, *34*(1), 26-35.

Fahy, G. E., Richards, M. P., Fuller, B. T., Deschner, T., Hublin, J. J., & Boesch, C. (2014). Stable nitrogen isotope analysis of dentine serial sections elucidate sex differences in weaning patterns of wild chimpanzees (Pan troglodytes). *American journal of physical anthropology*, *153*(4), 635-642.

Fehren-Schmitz, L., Jarman, C. L., Harkins, K. M., Kayser, M., Popp, B. N., & Skoglund, P. (2017). Genetic ancestry of Rapanui before and after European contact. *Current Biology*, *27*(20), 3209-3215. e3206.

Gerstner, K. F., & Pruetz, J. D. (2022). Wild Chimpanzee Welfare: A Focus on Nutrition, Foraging and Health to Inform Great Ape Welfare in the Wild and in Captivity. *Animals*, *12*(23), 3370. https://www.mdpi.com/2076-2615/12/23/3370

Gupta, S., Surti, N., Metterle, L., Chandra, A., & Agarwal, A. (2009). Antioxidants and female reproductive pathologies. *Archives of Medical Science*, *5*(1A), S151-S173.

Harvey, L. J., Armah, C. N., Dainty, J. R., Foxall, R. J., Lewis, D. J., Langford, N. J., & Fairweather-Tait, S. J. (2005). Impact of menstrual blood loss and diet on iron deficiency among women in the UK. *British Journal of Nutrition*, *94*(4), 557-564.

Hollander, M., Wolfe, D. A., & Chicken, E. (2013). *Nonparametric statistical methods* (Vol. 751). John Wiley & Sons.

Hotz, K., Krayenbuehl, P. A., & Walczyk, T. (2012). Mobilization of storage iron is reflected in the iron isotopic composition of blood in humans [Article]. *Journal of Biological Inorganic Chemistry*, *17*(2), 301-309. https://doi.org/10.1007/s00775-011-0851-2

Hunt, J. R. (2003). Bioavailability of iron, zinc, and other trace minerals from vegetarian diets. *The American journal of clinical nutrition*, *78*(3), 633S-639S.

Hunt, J. R., Zito, C. A., & Johnson, L. K. (2009). Body iron excretion by healthy men and women. *The American journal of clinical nutrition*, *89*(6), 1792-1798.

Ishikawa, A., Matsushita, H., Shimizu, S., Morita, N., Hanai, R., Sugiyama, S., Watanabe, K., & Wakatsuki, A. (2023). Impact of Menopause and the

Menstrual Cycle on Oxidative Stress in Japanese Women. *Journal of Clinical Medicine*, *12*(3), 829.

Jaouen, K. (2012). *Les isotopes des métaux de transition (Cu, Fe, Zn) au service de l'anthropologie* Ecole normale supérieure de lyon-ENS LYON].

Jaouen, K., & Balter, V. (2014). Menopause effect on blood Fe and Cu isotope compositions. *Am J Phys Anthropol*, *153*(2), 280-285. https://doi.org/10.1002/ajpa.22430

Jaouen, K., Balter, V., Herrscher, E., Lamboux, A., Telouk, P., & Albarede, F. (2012). Fe and Cu stable isotopes in archeological human bones and their relationship to sex. *Am J Phys Anthropol*, *148*(3), 334-340. https://doi.org/10.1002/ajpa.22053

Jaouen, K., Gibert, M., Lamboux, A., Telouk, P., Fourel, F., Albarede, F., Alekseev, A. N., Crubezy, E., & Balter, V. (2013). Is aging recorded in blood Cu and Zn isotope compositions? *Metallomics*, *5*(8), 1016-1024. https://doi.org/10.1039/c3mt00085k

Jaouen, K., Herrscher, E., & Balter, V. (2017). Copper and zinc isotope ratios in human bone and enamel. *Am J Phys Anthropol*, *162*(3), 491-500. https://doi.org/10.1002/ajpa.23132

Jaouen, K., & Pons, M.-L. (2016). Potential of non-traditional isotope studies for bioarchaeology. *Archaeological and Anthropological Sciences*, *9*(7), 1389-1404. https://doi.org/10.1007/s12520-016-0426-9

Jaouen, K., Pons, M.-L., & Balter, V. (2013). Iron, copper and zinc isotopic fractionation up mammal trophic chains. *Earth and Planetary Science Letters*, *374*, 164-172. https://doi.org/10.1016/j.epsl.2013.05.037

Johnstone, R. A., & Cant, M. A. (2019). Evolution of menopause. *Current Biology*, *29*(4), R112-R115. https://doi.org/https://doi.org/10.1016/j.cub.2018.12.048

Jónsson, H., Ginolhac, A., Schubert, M., Johnson, P. L., & Orlando, L. (2013). mapDamage2. 0: fast approximate Bayesian estimates of ancient DNA damage parameters. *bioinformatics*, *29*(13), 1682-1684.

Kander, M. C., Cui, Y., & Liu, Z. (2017). Gender difference in oxidative stress: a new look at the mechanisms for cardiovascular diseases. *Journal of cellular and molecular medicine*, *21*(5), 1024-1032.

Kapp, J. D., Green, R. E., & Shapiro, B. (2021). A fast and efficient single-stranded genomic library preparation method optimized for ancient DNA. *Journal of Heredity*, *112*(3), 241-249.

Krayenbuehl, P. A., Walczyk, T., Schoenberg, R., von Blanckenburg, F., & Schulthess, G. (2005). Hereditary hemochromatosis is reflected in the iron isotope composition of blood [Article]. *Blood*, *105*(10), 3812-3816. https://doi.org/10.1182/blood-2004-07-2807

Kumar, A., Pal, A., Singh, P., Rani, I., Tondolo, V., Rongioletti, M., & Squitti, R. (2023). Might Diet, APOE-APOA1 Axis, and Iron Metabolism Provide Clues About the Discrepancy in Alzheimer's Disease Occurrence Between Humans and Chimpanzees? A Bioinformatics-Based Re-Analysis of Gene Expression Data on Mice Fed with Human and Chimpanzee Diets. *Biological Trace Element Research*. https://doi.org/10.1007/s12011-023-03932-5

Lacreuse, A., Chennareddi, L., Gould, K. G., Hawkes, K., Wijayawardana, S. R., Chen, J., Easley, K. A., & Herndon, J. G. (2008). Menstrual cycles continue into advanced old age in the common chimpanzee (Pan troglodytes). *Biology of Reproduction*, *79*(3), 407-412.

Lauwens, S., Costas-Rodríguez, M., Van Vlierberghe, H., & Vanhaecke, F. (2016). Cu isotopic signature in blood serum of liver transplant patients: a follow-up study. *Scientific Reports*, *6*, 30683.

Li, H., & Durbin, R. (2009). Fast and accurate short read alignment with Burrows–Wheeler transform. *bioinformatics*, *25*(14), 1754-1760.

Liu, Y., Mao, X., Krause, J., & Fu, Q. (2021). Insights into human history from the first decade of ancient human genomics. *Science*, *373*(6562), 1479-1484. https://doi.org/doi:10.1126/science.abi8202

Llamas, B., Valverde, G., Fehren-Schmitz, L., Weyrich, L. S., Cooper, A., & Haak, W. (2017). From the field to the laboratory: Controlling DNA contamination in human ancient DNA research in the high-throughput sequencing era. *STAR: Science & Technology of Archaeological Research*, *3*(1), 1-14.

Maréchal, C., & Albarède, F. (2002). Ion-exchange fractionation of copper and zinc isotopes. *Geochimica et Cosmochimica Acta*, *66*(9), 1499-1509.

Maréchal, C. N., Telouk, P., & Albarède, F. (1999). Precise analysis of copper and zinc isotopic compositions by plasma-source mass spectrometry [Article]. *Chemical Geology*, *156*(1-4), 251-273. https://doi.org/10.1016/s0009-2541(98)00191-0

Marson, J., Meuris, S., Cooper, R. W., & Jouannet, P. (1991). Puberty in the Male Chimpanzee: Progressive Maturation of Semen Characteristics. *Biology of Reproduction*, *44*(3), 448-455. https://doi.org/10.1095/biolreprod44.3.448

Mathur, R., Titley, S., Hart, G., Wilson, M., Davignon, M., & Zlatos, C. (2009). The history of the United States cent revealed through copper isotope fractionation. *Journal of Archaeological Science*, *36*(2), 430-433. https://doi.org/https://doi.org/10.1016/j.jas.2008.09.029

Miller, E. M. (2016). The reproductive ecology of iron in women. *Am J Phys Anthropol*, *159*(Suppl 61), S172-195. https://doi.org/10.1002/ajpa.22907

Mittnik, A., Wang, C.-C., Svoboda, J., & Krause, J. (2016). A molecular approach to the sexing of the triple burial at the Upper Paleolithic Site of Dolní Věstonice. *PloS One*, *11*(10), e0163019.

Moynier, F., Creech, J., Dallas, J., & Le Borgne, M. (2019). Serum and brain natural copper stable isotopes in a mouse model of Alzheimer's disease. *Scientific Reports*, *9*(1), 1-7.

Moynier, F., Merland, A., Rigoussen, D., Moureau, J., Paquet, M., Mahan, B., & Borgne, M. L. (2022). Baseline distribution of stable copper isotope compositions of the brain and other organs in mice. *Metallomics*.

Paoli, T., Palagi, E., Tacconi, G., & Tarli, S. B. (2006). Perineal swelling, intermenstrual cycle, and female sexual behavior in bonobos (Pan paniscus). *American journal of primatology*, *68*(4), 333-347. https://doi.org/https://doi.org/10.1002/ajp.20228

Pebsworth, P. A., Hillier, S., Wendler, R., Glahn, R., Ta, C. A. K., Arnason, J. T., & Young, S. L. (2019). Geophagy among East African Chimpanzees: consumed soils provide protection from plant secondary compounds and bioavailable iron. *Environmental Geochemistry and Health*, *41*(6), 2911-2927. https://doi.org/10.1007/s10653-019-00366-8

Peltzer, A., Jäger, G., Herbig, A., Seitz, A., Kniep, C., Krause, J., & Nieselt, K. (2016). EAGER: efficient ancient genome reconstruction. *Genome biology*, *17*(1), 1-14.

Phillips, S. C., Johnson, J. E., Clyde, W. C., Setera, J. B., Maxbauer, D. P., Severmann, S., & Riedinger, N. (2017). Rock magnetic and geochemical evidence for authigenic magnetite formation via iron reduction in coal-bearing sediments offshore S himokita P eninsula, J apan (IODP S ite C0020). *Geochemistry, Geophysics, Geosystems*, *18*(6), 2076-2098.

Piña-Aguilar, R. E., López-Saucedo, J., Ruiz-Galaz, L. I., de Jesús Barroso-Padilla, J., Gallegos-Rivas, M. C., González-Ortega, C., & Gutiérrez-Gutiérrez, A. M. (2016). A human reproductive approach to the study of infertility in chimpanzees: An experience at Leon's Zoological Park, Mexico. Veterinary research forum,

Power, R. C., Salazar-García, D. C., Wittig, R. M., Freiberg, M., & Henry, A. G. (2015). Dental calculus evidence of Taï Forest Chimpanzee plant consumption and life history transitions. *Scientific Reports*, *5*(1), 1-13.

R Core Development Team. (2022). R: A Language and Environment for Statistical Computing. *R Foundation for Statistical Computing, Vienna, Austria*. https://www.R-project.org/

R Core Development Team. (2024). R: A language and environment for statistical computing. *R Foundation for Statistical Computing, Vienna, Austria*. URL https://www.R-project.org/

Reynolds, V., Pascual-Garrido, A., Lloyd, A. W., Lyons, P., & Hobaiter, C. (2019). Possible mineral contributions to the diet and health of wild chimpanzees in three East African forests. *American journal of primatology*, *81*(6), e22978. https://doi.org/https://doi.org/10.1002/ajp.22978

Rowell, T. (1963). Behaviour and female reproductive cycles of rhesus macaques. *Reproduction*, *6*(2), 193-203.

Rudolph, M., Döcke, W.-D., Müller, A., Menning, A., Röse, L., Zollner, T. M., & Gashaw, I. (2012). Induction of Overt Menstruation in Intact Mice. *PloS One*, *7*(3), e32922. https://doi.org/10.1371/journal.pone.0032922

Ryu, H., Hill, D. A., & Furuichi, T. (2014). Prolonged maximal sexual swelling in wild bonobos facilitates affiliative interactions between females. *Behaviour*, *152*.

Samuni, L., Tkaczynski, P., Deschner, T., Löhrrich, T., Wittig, R. M., & Crockford, C. (2020). Maternal effects on offspring growth indicate post-weaning juvenile dependence in chimpanzees (Pan troglodytes verus). *Frontiers in Zoology*, *17*(1), 1. https://doi.org/10.1186/s12983-019-0343-8

Sauzéat, L., Costas-Rodríguez, M., Albalat, E., Mattielli, N., Vanhaecke, F., & Balter, V. (2021). Inter-comparison of stable iron, copper and zinc isotopic compositions in six reference materials of biological origin. *Talanta*, *221*, 121576. https://doi.org/https://doi.org/10.1016/j.talanta.2020.121576

Sayers, K., Lovejoy, C. O., Emery, N. J., Clayton, N. S., Hunt, K. D., Laland, K. N., Brown, G. R., McGrew, W., Marchant, L. F., & Stanford, C. B. (2008). The chimpanzee has no clothes: a critical examination of Pan troglodytes in models of human evolution. *Current Anthropology*, *49*(1), 87-114.

Selden, C. R., Schilling, K., Godfrey, L., & Yee, N. (2024). Metal-binding amino acid ligands commonly found in metalloproteins differentially fractionate copper isotopes. *Scientific Reports*, *14*(1), 1902. https://doi.org/10.1038/s41598-024-52091-7

Sengupta, P., Dutta, S., & Chhikara, B. S. (2023). Genomes of extinct hominins and human reproductive evolution. *EXCLI journal*, *22*, 392.

Shieh, G., Jan, S.-l., & Randles, R. H. (2006). On power and sample size determinations for the Wilcoxon–Mann–Whitney test. *Journal of Nonparametric Statistics*, *18*(1), 33-43.

Smith, B. H., & Boesch, C. (2011). Mortality and the magnitude of the "wild effect" in chimpanzee tooth emergence. *Journal of human evolution*, *60*(1), 34-46.

Smith, T. D., Reynolds, R. L., Mano, N., Wood, B. J., Oladipupo, L., Hughes, G. K., Corbin, H. M., Taylor, J., Ufelle, A., Burrows, A. M., Durham, E., Vinyard, C. J., Cray, J. J., & DeLeon, V. B. (2021). Cranial synchondroses of primates at birth. *The Anatomical Record*, *304*(5), 1020-1053. https://doi.org/https://doi.org/10.1002/ar.24521

Smith, T. M., Smith, B. H., Reid, D. J., Siedel, H., Vigilant, L., Hublin, J.-J., & Boesch, C. (2010). Dental development of the Taï Forest chimpanzees revisited. *Journal of human evolution*, *58*(5), 363-373.

Sun, M., Archer, C., & Vance, D. (2021). New Methods for the Chemical Isolation and Stable Isotope Measurement of Multiple Transition Metals, with Application to the Earth Sciences. *Geostandards and Geoanalytical Research*, *45*(4), 643-658. https://doi.org/https://doi.org/10.1111/ggr.12402

Sykes, N., Spriggs, M., & Evin, A. (2019). Beyond curse or blessing: the opportunities and challenges of aDNA analysis. *World Archaeology*, *51*(4), 503-516. https://doi.org/10.1080/00438243.2019.1741970

Tapiero, H., Townsend, D. M., & Tew, K. D. (2003). Trace elements in human physiology and pathology. Copper. *J Biomedicine Pharmacotherapy*, *57*(9), 386-398.

Tas, A. C. (2000). Combustion synthesis of calcium phosphate bioceramic powders. *Journal of the European Ceramic Society*, *20*(14), 2389-2394. https://doi.org/https://doi.org/10.1016/S0955-2219(00)00129-1

Tennie, C., Gilby, I. C., & Mundry, R. (2009). The meat-scrap hypothesis: small quantities of meat may promote cooperative hunting in wild chimpanzees (Pan troglodytes). *Behavioral Ecology and Sociobiology, 63*(3), 421-431.

Thompson, M. E., Muller, M. N., & Wrangham, R. W. (2012). The energetics of lactation and the return to fecundity in wild chimpanzees. *Behavioral Ecology*, *23*(6), 1234-1241.

Timmermann, A., Yun, K.-S., Raia, P., Ruan, J., Mondanaro, A., Zeller, E., Zollikofer, C., Ponce de León, M., Lemmon, D., Willeit, M., & Ganopolski, A. (2022). Climate effects on archaic human habitats and species successions. *Nature*, *604*(7906), 495-501. https://doi.org/10.1038/s41586-022-04600-9

Toutain, J.-P., Sonke, J., Munoz, M., Nonell, A., Polvé, M., Viers, J., Freydier, R., Sortino, F., Joron, J.-L., & Sumarti, S. (2008). Evidence for Zn isotopic fractionation at Merapi volcano. *Chemical Geology*, *253*(1), 74-82. https://doi.org/https://doi.org/10.1016/j.chemgeo.2008.04.007

Tremillon, B. (1967). Separation on Ion-Exchange Resins In: Mir, Moscow.

Vahter, M., Berglund, M., & Åkesson, A. (2004). Toxic metals and the menopause. *British Menopause Society Journal*, *10*(2), 60-65.

Vallender, E. J., Hotchkiss, C. E., Lewis, A. D., Rogers, J., Stern, J. A., Peterson, S. M., Ferguson, B., & Sayers, K. (2023). Nonhuman primate genetic models for the study of rare diseases. *Orphanet Journal of Rare Diseases*, *18*(1), 20. https://doi.org/10.1186/s13023-023-02619-3

Van Heghe, L., Delanghe, J., Van Vlierberghe, H., & Vanhaecke, F. (2013). The relationship between the iron isotopic composition of human whole blood and iron status parameters. *Metallomics*, *5*(11), 1503-1509.

Van Heghe, L., Deltombe, O., Delanghe, J., Depypere, H., & Vanhaecke, F. (2014). The influence of menstrual blood loss and age on the isotopic composition of Cu, Fe and Zn in human whole blood. *Journal of Analytical Atomic Spectrometry*, *29*(3), 478-482.

Van Heghe, L., Engström, E., Rodushkin, I., Cloquet, C., & Vanhaecke, F. (2012). Isotopic analysis of the metabolically relevant transition metals Cu, Fe and Zn

in human blood from vegetarians and omnivores using multi-collector ICP-mass spectrometry. *Journal of Analytical Atomic Spectrometry*, *27*(8), 1327-1334.

Vasconcelos, M., & Grusak, M. A. (2006). Status and future developments involving plant iron in animal and human nutrition. *Iron Nutrition in Plants and Rhizospheric Microorganisms*, 1-22.

Walczyk, T., & von Blanckenburg, F. (2002). Natural iron isotope variations in human blood. *Science*, *295*(5562), 2065-2066. https://doi.org/10.1126/science.1069389

Walker, K. K., Walker, C. S., Goodall, J., & Pusey, A. E. (2018). Maturation is prolonged and variable in female chimpanzees. *Journal of human evolution*, *114*, 131-140.

Wallis, J. (1992). Chimpanzee genital swelling and its role in the pattern of sociosexual behavior. *American journal of primatology*, *28*(2), 101-113. https://doi.org/https://doi.org/10.1002/ajp.1350280203

Wang, W., Vilella, F., Alama, P., Moreno, I., Mignardi, M., Isakova, A., Pan, W., Simon, C., & Quake, S. R. (2020). Single-cell transcriptomic atlas of the human endometrium during the menstrual cycle. *Nature Medicine*, *26*(10), 1644-1653. https://doi.org/10.1038/s41591-020-1040-z

Wood, B. M., Negrey, J. D., Brown, J. L., Deschner, T., Thompson, M. E., Gunter, S., Mitani, J. C., Watts, D. P., & Langergraber, K. E. (2023). Demographic and hormonal evidence for menopause in wild chimpanzees. *Science*, *382*(6669), eadd5473. https://doi.org/doi:10.1126/science.add5473

Wu, L., Percak-Dennett, E. M., Beard, B. L., Roden, E. E., & Johnson, C. M. (2012). Stable iron isotope fractionation between aqueous Fe (II) and model Archean ocean Fe–Si coprecipitates and implications for iron isotope variations in the ancient rock record. *Geochimica et Cosmochimica Acta*, *84*, 14-28.

Zegkinoglou, N. N., Mathur, R., Kilias, S. P., Godfrey, L., Pletsas, V., Nomikou, P., & Zaronikola, N. (2023). Boiling-induced extreme Cu isotope fractionation in sulfide minerals forming by active hydrothermal diffusers at the Aegean Kolumbo volcano: Evidence from in situ isotope analysis. *Geology*, *51*(11), 1072-1076.

CHAPTER 5: Conclusion and Future Directions

This dissertation explored the possible applications of trace metal isotope (Sr, Zn, Fe, and Cu) analysis to living species of primates to address questions about human evolution. Each chapter highlights how trace metals can be used to answer questions of behavior, diet, and physiology, which has significant implications when considering their relationship to trends in the evolution of modern humans. This chapter will summarize some of the main conclusions from these studies, discuss the limitations, and consider the possible directions that future studies may take.

In Chapter 2, "Strontium isotopes track female dispersal in Taï chimpanzees," we assess the effectiveness of Sr isotope ratios in identifying female chimpanzee migration patterns. We were not able to determine the exact origins of female migrants. Still, we were able to significantly narrow the potential origin locales of migrating individuals and infer if they were local or non-local to the Taï chimpanzee project study area's range. We encourage the development and continued management of long-term field sites and the habituation of neighboring chimpanzee communities, as these study populations enable direct observations and monitoring of inter-group migration. By studying habituated populations of chimpanzees, we can improve conservation strategies and the management of wild primate populations, especially when considering how far females may travel to reach new territories. When considering the applications to human ancestors, Sr isotope ratios have potential in regions that are highly variable in their geology and, by extension, their Sr isotope ratios. For example, the East African rift, where the geology of the East

African rift is well-established and understood, including Sr isotope ratios in conjunction with other isotope systems (carbon, nitrogen, oxygen), can improve our current models of early human dispersal and migration patterns.

In Chapter 3, "Zinc isotope ratios ($\delta^{66}Zn$) suggest a sex difference in diet among wild chimpanzees (*Pan troglodytes verus*)", we explore if low levels of meat consumption could contribute to a change in trophic position in predominately frugivorous apes. In human evolution, a higher trophic position related to meat consumption (expensive tissue hypothesis) is thought to have triggered the increase in cranial volume in early human ancestors. However, the application of nitrogen-stable isotopes is limited in deep time due to diminished protein preservation over the past 50,000 years. In this project, we found that males had lower zinc isotope values, which is consistent with higher quantities of meat in their diets, although it could be related to meat consumed in both insect foraging and hunting. By including longitudinal observational data on hunting prowess, we can confirm higher instances of meat consumption in a couple of individuals where markedly lower zinc isotope values were observed (Riedel et al., 2020). A significant limitation within this study is related to the timing of tooth enamel formation, which occurs much more rapidly than in humans (Dean et al., 2023). As a result, constraining ontogenetic stages are much more complex, and it is crucial to consider the variation in enamel formation times when using zinc isotope ratios as a proxy for breastfeeding or post-weaned diet in hominin fossils. To successfully discern which layer of zinc was sampled and, thus, which ontogenetic stage is being sampled, we recommend future studies incorporate

histological analyses coupled with laser ablation-inductively coupled plasma-mass spectrometry (LA-ICPMS) (Dean et al., 2023; Smith et al., in review; Smith et al., 2021).

In Chapter 4, "How iron (Fe) and copper (Cu) isotopes relate to sex in great apes: a refined protocol for Fe and Cu isotope analysis in bone," we first adapt the existing column chromatography protocols for isolating Fe, Cu, and Zn to be better suited for the high sample volume, to use less concentrated acid, and is less time-intensive for bone samples (Maréchal et al., 1999; Jaouen, 2012; Boucher et al., 2021; Sauzéat et al., 2021). Then, we tested if sex-related differences in Fe and Cu stable isotopes exist, and if they do, what influences the variation between sexes in a museum-curated collection of wild and lab-reared chimpanzees and bonobos. We found that in the bone of reproductively mature chimpanzees (those greater than ten years old), the mean Fe and Cu isotope values are higher in females relative to males. Neither of the comparisons between sexes met the p-value cutoff when considering an $\alpha = 0.05$. However, since there was a relatively small sample size for each age class ($n < 10$), we suspect the lack of significance Fe isotope values may be a Type II error. Despite this, the sex difference in Fe isotope values is consistent with that found in humans and rhesus macaques, although, for Cu isotope values, it is in the opposite direction (Jaouen et al., 2012; Boucher et al., 2021; Moynier et al., 2022). Given the sex differences in diet observed for wild populations of chimpanzees (see Chapter 3) and the higher reproductive investment (see Chapter 4), we recommend that future

studies consider how these factors may influence sex-related differences in human ancestors.

As an undergraduate student, it was perplexing to find that most paleoanthropological studies omitted the sex-related differences in behavior and physiology that persist among most primate species. It is rare to find a primate example where the behavior and physiology are the same due to sexual dimorphism. Thus, it is crucial for research in human evolution to consider the sex-related differences in behavior and physiology when designing their research studies. The preceding chapters used great apes as a model for testing trace metal isotope analysis to address critical questions in the evolution of human dispersal patterns, diet, and physiology. In each chapter, we consider sex and age, as these are known to influence the behavior related to dispersal and diet and change the metabolism of trace metals. While we have demonstrated that Sr, Zn, Fe, and Cu isotopes can be successfully measured in the bioapatite of tooth enamel and bone, there are significant limitations in how these isotope systems can be applied in deep time when considering enamel formation times and the relative concentrations of these elements in tooth enamel. In the case of Sr isotope ratios and Zn isotope values, sufficient evidence suggests these are valuable tools that can be consistently applied in early human fossils (Copeland et al., 2011; Jaouen et al., 2022). However, it is equally vital to consider the ontogenetic stage and the timing of Sr and Zn deposition in each species analyzed. When considering Fe and Cu isotopes, we have shown that deep-time applications are unlikely, given the low level of Fe and Cu in tooth enamel. Still, there is potential to

address questions in bone samples from biologically relevant models to early human ancestors, such as chimpanzees and bonobos. With the findings presented in this dissertation, it is hoped that future paleoanthropologists will look to extant apes as models for testing the evolution of female dispersal patterns, meat consumption, menstruation, and decreased reproductive investment in modern humans. The new toolkit that this research offers will enable researchers to consider sex-related differences more deeply, especially in how the evolution of these differences contributes to higher oxidative stress levels and more instances of cardiovascular disease in post-menopausal women (Agarwal & Gupta, 2005; Ishikawa et al., 2023; Kander et al., 2017).

5.1. References Cited

Agarwal, A., & Gupta, S. (2005). Role of reactive oxygen species in female reproduction. Part I. Oxidative stress: a general overview. *Agro Food Industry Hi-Tech, 16*(1), 21-25.

Boucher, R. D., Alavi, S. E., de Jong, H. N., Godfrey, L. V., & Vogel, E. R. (2021). Stable isotope evidence (Fe, Cu) suggests that sex, but not aging is recorded in rhesus macaque (Macaca mulatta) bone. *American journal of physical anthropology*.

Copeland, S. R., Sponheimer, M., de Ruiter, D. J., Lee-Thorp, J. A., Codron, D., le Roux, P. J., . . . Richards, M. P. (2011). Strontium isotope evidence for landscape use by early hominins. *Nature, 474*(7349), 76.

Dean, M. C., Garrevoet, J., Van Malderen, S. J. M., Santos, F., Mirazón Lahr, M., Foley, R., & Le Cabec, A. (2023). The Distribution and Biogenic Origins of Zinc in the Mineralised Tooth Tissues of Modern and Fossil Hominoids: Implications for Life History, Diet and Taphonomy. *Biology, 12*(12), 1455.

Ishikawa, A., Matsushita, H., Shimizu, S., Morita, N., Hanai, R., Sugiyama, S., . . . Wakatsuki, A. (2023). Impact of Menopause and the Menstrual Cycle on Oxidative Stress in Japanese Women. *Journal of Clinical Medicine, 12*(3), 829.

Jaouen, K., Balter, V., Herrscher, E., Lamboux, A., Telouk, P., & Albarede, F. (2012). Fe and Cu stable isotopes in archeological human bones and their relationship to sex. *Am J Phys Anthropol, 148*(3), 334-340. doi:10.1002/ajpa.22053

Jaouen, K., Villalba-Mouco, V., Smith, G. M., Trost, M., Leichliter, J., Lüdecke, T., . . . Guiserix, D. (2022). A Neandertal dietary conundrum: Insights provided by tooth enamel Zn isotopes from Gabasa, Spain. *Proceedings of the National Academy of Sciences, 119*(43), e2109315119.

Kander, M. C., Cui, Y., & Liu, Z. (2017). Gender difference in oxidative stress: a new look at the mechanisms for cardiovascular diseases. *Journal of cellular and molecular medicine, 21*(5), 1024-1032.

Maréchal, C. N., Telouk, P., & Albarède, F. (1999). Precise analysis of copper and zinc isotopic compositions by plasma-source mass spectrometry. *Chemical Geology, 156*(1-4), 251-273. doi:10.1016/s0009-2541(98)00191-0

Moynier, F., Merland, A., Rigoussen, D., Moureau, J., Paquet, M., Mahan, B., & Borgne, M. L. (2022). Baseline distribution of stable copper isotope compositions of the brain and other organs in mice. *Metallomics*.

Riedel, J., Polansky, L., Wittig, R. M., & Boesch, C. (2020). Social rank overrides environmental and community fluctuations in determining meat access by female chimpanzees in the Taï National Park, Côte d'Ivoire. *PeerJ, 8*, e8283.

Sauzéat, L., Costas-Rodríguez, M., Albalat, E., Mattielli, N., Vanhaecke, F., & Balter, V. (2021). Inter-comparison of stable iron, copper and zinc isotopic compositions in six reference materials of biological origin. *Talanta, 221*, 121576. doi:https://doi.org/10.1016/j.talanta.2020.121576

Smith, T. M., Arora, M., Bharatiya, M., Leonard, N., Zhao, J.-x., & Austin, C. (in review). Brief Communication: Trace Element Patterns in Juvenile Wild Chimpanzees. *American Journal of Biological Anthropology*.

Smith, T. M., Cook, L., Dirks, W., Green, D. R., & Austin, C. (2021). Teeth reveal juvenile diet, health and neurotoxicant exposure retrospectively: What biological rhythms and chemical records tell us. *BioEssays, 43*(9), 2000298. doi:https://doi.org/10.1002/bies.202000298